Justus-Liebig-Universität Gießen

Fachbereich Medizin

Institut für Anatomie und Zellbiologie

Arbeitsgruppe

Viszerale Neurobiologie

Leiter: Prof. Dr. Wolfgang Kummer

Die Entdeckung und Charakterisierung der urethralen cholinergen chemosensorischen Zelle

Habilitationsschrift

zur Erlangung der Venia legendi

im Fach Anatomie und Zellbiologie im Fachbereich Medizin der Justus-Liebig-Universität Gießen

vorgelegt von

Dr. phil. nat. Klaus Oliver Deckmann

Gießen, 2021

„Das Experiment, dem nicht eine Theorie, d.h. eine Idee vorausgeht, verhält sich zur Naturforschung wie das Rasseln einer Kinderklapper zur Musik.“

Justus Freiherr von Liebig (1803 - 1873), deutscher Chemiker

Die nachfolgende Arbeit nimmt Bezug auf folgende Originalarbeiten:

I. **Deckmann K***, Filipski K*, Krasteva-Christ G, Fronius M, Althaus M, Rafiq A, Papadakis T, Renno L, Jurastow I, Wessels L, Wolff M, Schütz B, Weihe E, Chubanov V, Gudermann T, Klein J, Bschleipfer T, Kummer W. Bitter triggers acetylcholine release from polymodal urethral chemosensory cells and bladder reflexes. **Proc Natl Acad Sci U S A**. 2014;111(22):8287-92.

II. **Deckmann K**, Krasteva-Christ G, Rafiq A, Herden C, Wichmann J, Knauf S, Nassenstein C, Grevelding CG; Dorresteijn A, Chubanov V, Gudermann T, Bschleipfer T, Kummer W. Cholinergic urethral brush cells are widespread throughout placental mammals. **Int Immunopharmacol**. 2015 Nov;29(1):51-6.

III. **Deckmann K**, Rafiq A, Erdmann C, Illig C, Durschnabel M, Wess J, Weidner W, Bschleipfer T, Kummer W. Muscarinic receptors 2 and 5 regulate bitter response of urethral brush cells via negative feedback. **FASEB J**. 2018 Jun;32(6):2903-2910.

IV. Kandel C, Schmidt P, Perniss A, Keshavarz M, Scholz P, Osterloh S, Althaus M, Kummer W, **Deckmann K**. ENaC in Cholinergic Brush Cells. **Front Cell Dev Biol**. 2018 Aug 15;6:89.

V. Perniss A, Schmidt P, Soultanova A, Papadakis T, Dahlke K, Voigt A, Schütz B, Kummer W, **Deckmann K.** Development of epithelial cholinergic chemosensory cells of the urethra and trachea of mice. **Cell Tissue Res** 2021 Jul;385(1):21-35.

Relevante eigene Übersichtsartikel zum Thema:

VI. **Deckmann K**, Kummer W. Chemosensory epithelial cells in the urethra: sentinels of the urinary tract. **Histochem Cell Biol**. 2016 Dec;146(6):673-683.

VII. Kummer W, **Deckmann K**. Brush cells, the newly identified gatekeepers of the urinary tract. **Curr Opin Urol**. 2017 Mar;27(2):85-92

Inhaltsverzeichnis

Abbildungsverzeichnis

1 Einleitung

1.1 Ableitende Harnwege

Bei Menschen können die ableitenden Harnwege in zwei Teilbereiche gegliedert werden: den paarig angelegten oberen Harntrakt, gebildet aus Nierenbecken (Pelvis renalis) und Harnleitern (Ureter), und den unteren Harntrakt, bestehend aus der Blase (Vesica urinaria) und der Harnröhre (Urethra) (Abbildung 1.).

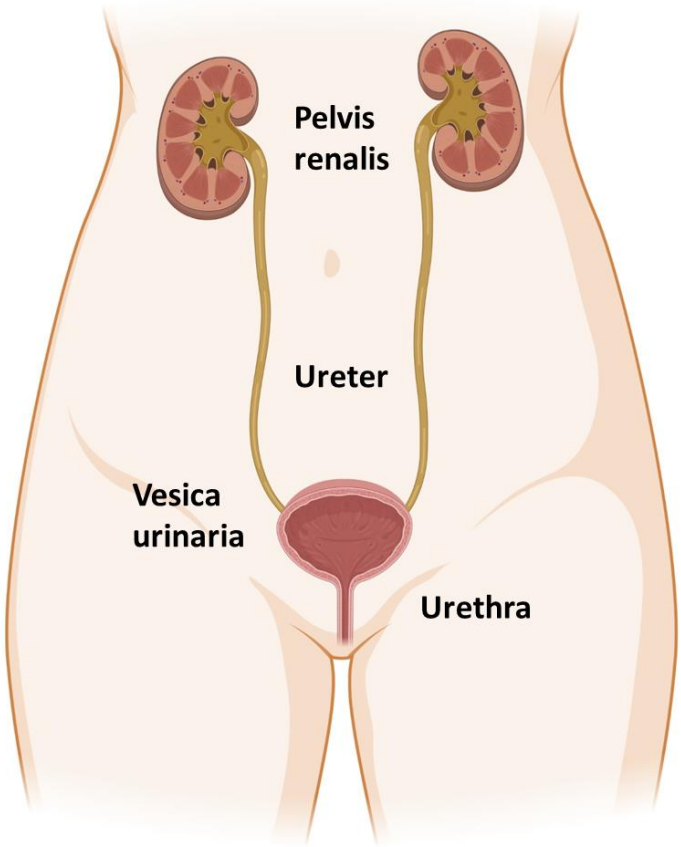

Abbildung 1. Die ableitenden Harnwege
Schematische Zeichnung der ableitenden Harnwege, bestehend aus Pelvis renalis, Ureter, Vesica urinaria und Urethra. Erstellt mit BioRender.com.

Ihre Hauptfunktion ist der Abtransport des Harns. Hierbei hat die Harnblase eine Sonderstellung als Sammel- und Speicherorgan des Harns [1-10]. Der Harn selbst wird in den beiden Nieren produziert und die ableitenden Harnwege haben keinen Einfluss mehr auf die Zusammensetzung des Harns.

Ausgekleidet sind die ableitenden Harnwege, mit Ausnahme der Urethra, mit einem mehrschichtigen Übergangsepithel, dem Urothel. Es besteht aus ca. 6 Zellreihen, die, insbesondere in der Blase, durch Dehnung im Zuge der Blasenfüllung an Höhe und Schichtung abnehmen, um eine Erhöhung des Fassungsvolumens zu ermöglichen. Das Urothel wird hauptsächlich aus drei Zelltypen gebildet: den auf der Basalmembran aufsitzenden Basalzellen, den Intermediärzellen und den gegen das Lumen ragenden Deckzellen. Diese sind die oberste Zellschicht im Urothel und bilden eine osmotische Barriere zwischen dem Urin und der interstitiellen Flüssigkeit. Die Auskleidung der Urethra unterscheidet sich hingegen von der einheitlichen Auskleidung der restlichen ableitenden Harnwege.

Die Urethra selbst bildet den letzten Abschnitt der ableitenden Harnwege, leitet den Harn nach außen und ist beim Mann ca. 20-25 cm, bei der Frau ca. 3-5 cm lang. Die Urethra des Mannes, beginnend in der Harnblase am Ostium urethrae internum, kann in zwei übergeordnete Abschnitte unterteilt werden: den im Becken liegenden pelvinen Teil und den im Penis liegenden penilen Teil, der mit dem Ostium urethrae externum endet [11]. Der pelvine Teil seinerseits besteht aus der Pars intramuralis, die noch innerhalb der Blasenwand liegt, gefolgt von der Pars prostatica, die durch die Prostata führt, und der im Diaphragma urogenitale gelegenen Pars intermedia (Pars membranacea). Der penile Teil bildet den letzten Abschnitt der männlichen Urethra und besteht aus der Pars spongiosa im Corpus spongiosum des Penis.

Die weibliche Urethra wird in einen proximalen und einen distalen Teil gegliedert. Vergleichbar wie beim Mann wird auch bei der Frau der sich in der Blasenwand befindende Teil Pars intramuralis genannt. Sie beginnt auch am Ostium urethrae internum etwa auf halber Höhe hinter der Symphyse und läuft dann parallel zu Vagina nach unten. Das letzte Stück der weiblichen Urethra ist als Crista urethralis vaginae als Auswölbung in der Wand der Vagina zu erkennen. Auch sie endet mit dem Ostium urethrae externum, welches sich im Fall der weiblichen Urethra im Vestibulum vaginae befindet [11].

Beim Mann ist nur der einige millimeterlange Übergangsbereich von Blase zu Urethra noch mit Urothel ausgekleidet. Der verhältnismäßig lange mittlere Teil der männlichen Urethra wird durch ein mehrschichtiges hochprismatisches Epithel gebildet, welches im Ausmündungsbereich in ein mehrschichtiges unverhorntes Plattenepithel übergeht [11]. Das Epithel der weiblichen Urethra besteht, vergleichbar mit dem des Mannes,

im Übergangsbereich von Blase zu Urethra noch aus Urothel. Dem Urothel schließt sich ein mehrschichtiges unverhorntes Plattenepithel an [11]. Im mehrschichtigen Epithel der männlichen und weiblichen Urethra befinden sich neben neuroendokrinen Zellen und nicht-cholinergen Bürstenzellen auch cholinerge chemosensorische Zellen, deren Entdeckung und Charakterisierung Gegenstand dieser Arbeit ist.

1.2 Die Urethra von Mäusen und Menschen

Sowohl in Menschen als auch in Mäusen verläuft die Urethra vom Ostium urethrae internum, welches am Harnblasendreieck (Trigonum vesicae) beginnt, bis zur äußeren Harnröhrenöffnung (Ostium urethrae externum oder Meatus urethrae). Die Urethra von männlichen Mäusen wird, vergleichbar zur männlichen menschlichen Urethra, auch in pelvine oder membranöse und penile Urethra eingeteilt. Der membranöse Teil ist dünn und befindet sich in direkter Nachbarschaft von Prostata, Bläschendrüse, Koagulationsdrüsen und den Samenleitern. Einen Unterschied bilden die periurethralen Drüsen. Diese münden beim Menschen in die penile Urethra (Pars spongiosa) und bei der Maus in die membranöse Urethra distal der Ausführungsgänge der Prostata. Im Gegensatz zum Menschen besitzen Nagetiere einen Penisknochen, das Os penis, der sich in unmittelbarer Nähe zur penilen Urethra befindet. Der strukturelle Aufbau der weiblichen Urethra ist bei Mäusen und Menschen vergleichbar. Auch bei Mäusen wird die weibliche Urethra in einen distalen und proximalen Teil gegliedert [12].

1.3 Muskelphysiologie der Miktion

Die Steuerung der Blasenfunktion und damit der Miktion ist ein komplexes Zusammenspiel verschiedener Muskeln und Steuerzentren [1-8, 10]. Die wichtigsten Muskeln sind der Detrusormuskel, Musculus detrusor vesicae, und die Sphinktere, der Musculus sphincter vesicae oder Musculus sphincter urethrea internus und der Musculus sphincter urethrea externus. Hierzu kommt noch in der Urethra eine dünne äußere Schicht aus ringförmiger glatter Muskulatur und eine zehnmal dickere innere Schicht aus glatter Längsmuskulatur [9, 13, 14]. Letztlich geht die Steuerung der Miktion mit der Steuerung der Muskulatur einher. Maßgeblich hierfür ist der aus glatter Muskulatur bestehende Detrusormuskel. Die Phosphorylierung der leichten Ketten des

Myosins (myosin regulatory light chain; MLC) ist für den Tonus der glatten Muskulatur verantwortlich. Phosphorylierung und der Muskeltonus nehmen zu, wenn die Aktivität der Myosin-Leichte-Ketten-Kinase (MLCK) überwiegt. Überwiegt hingegen die Aktivierung der Myosin-Leichte-Ketten-Phosphatase (MLCP), kommt es zur Dephosphorylierung von Myosin und somit zur Relaxation (Abbildung 2.). MCLP und MCLK arbeiten also gegensätzlich [10, 15]. Bei der Steuerung der Miktion nehmen Adrenozeptoren und muskarinische Acetylcholinrezeptoren (mAChR) eine zentrale Rolle ein. Sowohl Adrenozeptoren als auch mAChR sind an heterotrimere Guaninnukleotid-bindende Proteine (G-Proteine) gekoppelt. Eine solche Kopplung ist einer der häufigsten transmembranären Signaltransduktionsmechanismen und kann das Signal von Rezeptoren an verschiedenste Effektoren weiterleiten. Adrenozeptoren werden durch Adrenalin oder Noradrenalin aktiviert. Auf dem Musculus sphincter urethrea internus lokalisierte α-Adrenozeptoren sind an G-Proteine der G_q-Familie gekoppelt. G-Proteinen der G_q-Familie wird im Allgemeinen eine exzitatorische Wirkung zugeschrieben. Sie vermitteln ihre Wirkung über die Regulation von β-Isoformen der Phospholipase C (PLC) und werden deshalb auch als PLC-gekoppelte G-Proteine bezeichnet. PLC hydrolisiert Phosphatidylinositol-4,5-bisphosphat (PIP_2) zu Inositoltrisphosphat (IP_3) und Diacylglycerol (DAG). IP_3 bewirkt, durch die Bindung an den IP_3-Rezeptor, die Freisetzung von Calcium-Ionen aus dem sarkoplasmatischen Retikulum (SR). Im Falle der glatten Muskelzellen führt die Calciumfreisetzung zur Kontraktion, weil das freigesetzte Calcium an Calmodulin bindet, welches daraufhin mit der MLCK einen aktiven Komplex bildet. Die daraus resultierende Phosphorylierung der MLC führt zur Kontraktion, weil dadurch Aktin die Myosin-ATPase aktivieren kann [15].

Auf dem Detrusormuskel lokalisierte β-Adrenozeptoren sind zwar auch an G-Proteine gekoppelt, allerdings sind sie mit G-Proteinen der G_S-Familie verbunden. Hierbei handelt es sich um G-Proteine, die durch die Aktivierung der Adenylatcyclase ihre Wirkung entfalten. Hierdurch wird die Konzentration von cAMP im Cytosol erhöht, was zur Aktivierung der Proteinkinase A führt. Deshalb werden sie auch als G-Proteine mit cAMP-abhängigen Reaktionen bezeichnet. Die Proteinase A steigert die Aktivität der MLCP, welche für die Relaxation der Muskelzellen verantwortlich ist (Abbildung 2.). Adrenorezeptoren nehmen daher eine zentrale Rolle in der Füllphase ein (Abbildung 3.).

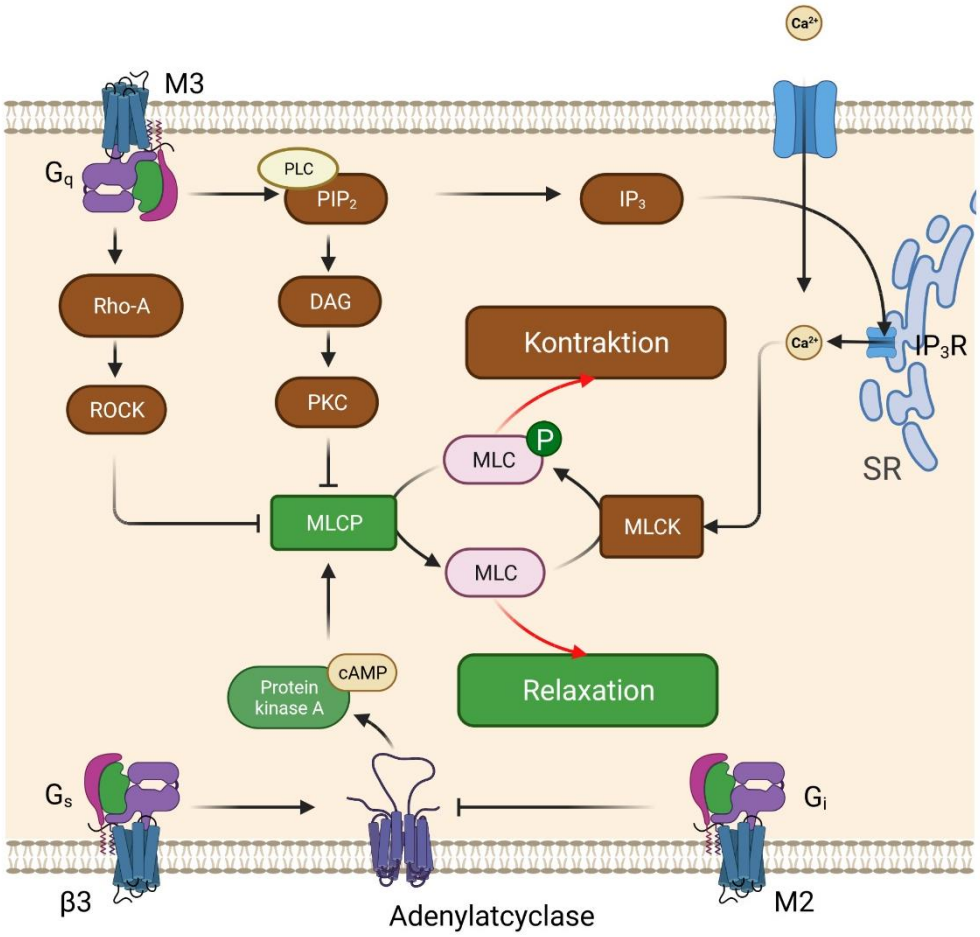

Abbildung 2. Intrazelluläre Signalwege der Detrusorkontraktionen und –relaxation
Aktivierung von M3 führt zur intrazellulärem Ca^{2+}-Freisetzung und zum Ca^{2+}-Einstrom. Dies trägt zu Kontraktionen bei. Die Aktivierung von M2 hemmt die Adenylatcyclase und reduziert die β3-adrenerge Rezeptor-vermittelte Relaxation. Rho-A = Ras-Homologenfamilie A; ROCK = Rho-Kinase; PLC = Phospholipase C; DAG = Diacylglycerin; PKC = Proteinkinase C; PKA = Proteinkinase A; MLC = leichte Myosinkette; IP_3 = Inositoltrisphosphat; IP_3R = IP_3-Rezeptor; PIP_2 = Phosphatidylinositol-4,5-bisphosphat; SR = sarkoplasmatisches Retikulum; MLCK = Myosin-Leichte-Ketten-Kinase; MLCP = Myosin-Leichte-Ketten-Phosphatase; heterotrimere Guaninnukleotid-bindende Proteine (G-Proteine): G_q = Gq-Familie (exitatorisch); G_S = GS-Familie (Adenylatcyclase aktivieren); G_i = G_i-Familie (Adenylatcyclase inhibierend); β3 = Adrenozeptoren β3; M3 = muskarinischer Acetylcholinrezeptor 3; M5 = muskarinischer Acetylcholinrezeptor 5; nach [10]; Erstellt mit BioRender.com**.**

MAChR hingegen sind für die Miktion von entscheidender Bedeutung. MAChR können in 5 Unterklassen (M1-M5) einteilen werden. Die fünf Unterklassen werden durch fünf verschiedene Gene kodiert und können auch aufgrund ihrer Lokalisation im Körper und ihrer molekularen und pharmakologischen Eigenschaften unterschieden werden [16]. Bei Steuerung der Miktion stehen M2 und M3 im Focus (Abbildung 2.). M1- und M3-Rezeptoren sind G_q-Protein gekoppelt. Über M5-Rezeptoren ist wenig bekannt.

Es wird aber davon ausgegangen, dass auch sie einen ähnlichen Mechanismus wie M1- und M3-Rezeptoren haben. M2 und M4 sind G_i-Protein gebunden. Bei der Familie der G_i-Proteine handelt es sich um inhibitorische G-Proteine. Sie entfalten ihre Wirkung durch die Hemmung der Adenylatcyclase und stellen somit Gegenspieler der G-Proteine der G_s-Familie dar (Abbildung 2.) [17-21].

1.4 Steuerung der Miktion

Die Regulation der Miktion erfolgt auf mehreren Ebenen und über verschiedene Nerven [1-8]. Auf Blasenebene ist zunächst die Kontraktionssteuerung des Detrusormuskels von Relevanz. Diese erfolgt durch das Rückenmark und dem angeschlossenen Plexus hypogastricus inferior. Hinzu kommt die Steuerung der beteiligten Sphinktere durch vegetative und somatische Nerven [2, 10, 22, 23]. Die vegetative Innervation erfolgt parasympathisch über die Nervi pelvici splanchnici und sympathisch über die Nervi hypogastrici. Beides läuft über den Plexus hypogastricus inferior. Die somatische Innervation kommt aus dem Nervus pudendus [2, 4, 5, 10, 22-27]. Die übergeordnete Regulation erfolgt durch das pontine Miktionszentrum, das im Hirnstramm lokalisiert und Teil der Formatio reticularis ist. Das pontine Miktionszentrum wird vom periaquäduktalen Grau gesteuert. Dieses wird seinerseits durch übergeordnete Blasenzentren des Di- und Telencephalons beeinflusst. Von größter Relevanz sind hierbei das frontale Blasenzentrum, subkortikale Regelmechanismen, die parahippocampale Strukturen mit einbeziehen, und der anteriorer Cingulus im Zusammenspiel mit dem supplementärmotorischen Kortex [2, 10, 28-42].

Die Steuerung der Miktion beinhaltet zwei Phasen, die Füllungsphase (Abbildung 3.) und die Miktion selbst (Abbildung 4.). Während der Füllungsphase ist die Blase unter physiologischen Bedingungen in Richtung Urethra verschlossen und kann durch den in den Nieren produzierten Harn über die Ureteren gefüllt werden.

In dieser Phase ist der aus glatter Muskulatur bestehende Musculus sphincter urethrea internus sowie die glatte Muskulatur der Urethra durch die Freisetzung von Noradrenalin aus postganglionären sympathischen Fasern des aus dem Plexus hypogastricus entspringenden Nervus hypogastricus über α-Adrenozeptoren kontrahiert [1-8, 10, 43, 44].

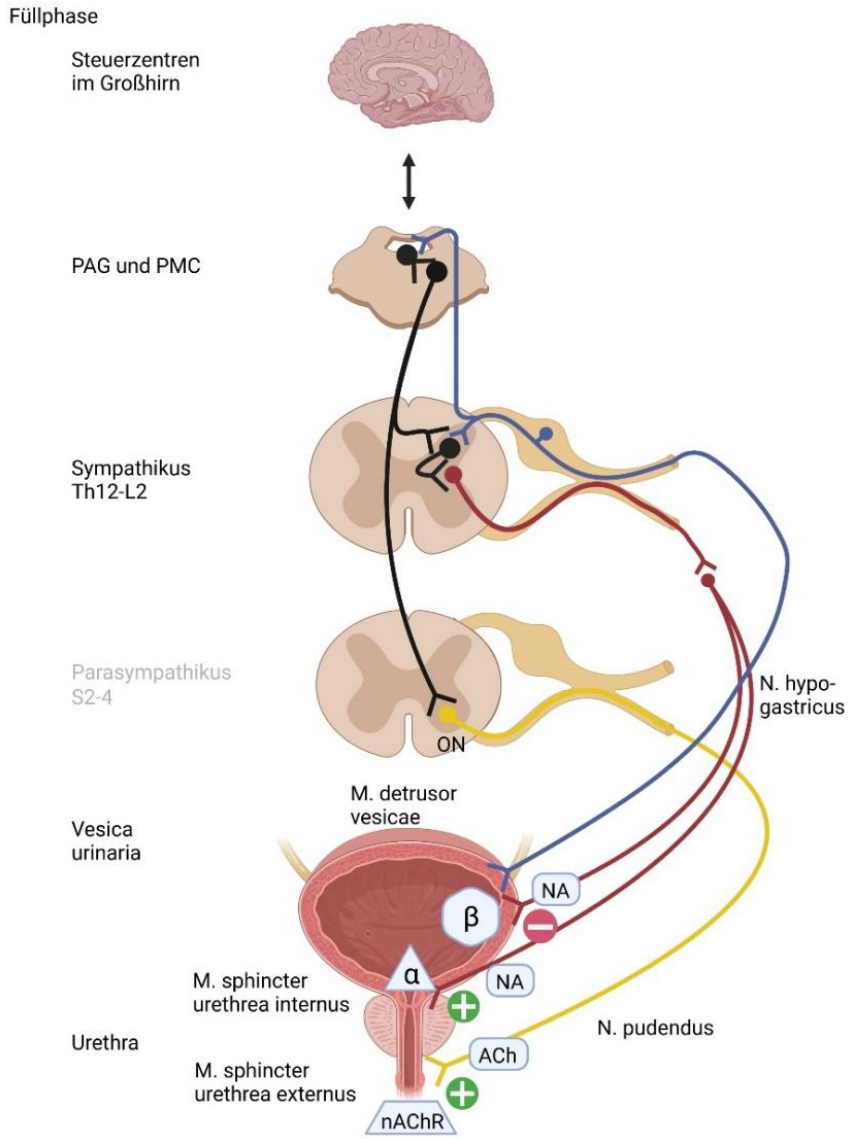

Abbildung 3. Innervation der Harnblase und ihrer Sphinkteren während der Füllphase
Schematische Darstellung der Innervation während der Füllphase. Die Blase ist in Richtung Urethra verschlossen und kann gefüllt werden. Der aus glatter Muskulatur bestehende M. sphincter urethrea internus wird durch Noradrenalin (NA) aus sympathischen Fasern des aus dem Plexus hypogastricus (nicht dargestellt) entspringenden N. hypogastricus über seine α-Adrenozeptoren (α) kontrahiert. Parallel halten sympathische Fasern durch Noradrenalin (NA) über die Bindung an β-Adrenozeptoren (β) auf dem M. detrusor vesicae diesen entspannt. Zeitgleich erfolgt auch die Aktivierung des aus quergestreifter Muskulatur aufgebauten M. sphincter urethrae externus über nikotinische Acetylcholinrezeptoren (nAChR) durch den N. pudendus. Die Wandspannung wird durch aufsteigende Kollaterale über das periaquäduktale Grau (PAG) an das pontine Miktionszentrum (PMC) weitergeleitet, welches durch absteigende Bahnen mit dem sakralen parasympathischen Miktionszentrum bzw. sympathischen Miktionszentrum des Thorakolumbalmarks interagiert. Die übergeordnete Steuerung der Miktion erfolgt durch das frontale Blasenzentrum und weitere Hirnstrukturen. ON = Onuf-Kern; Blau = sensible; Gelb = somatomotorisch; Rot = sympathisch; Erstellt mit biorender.com

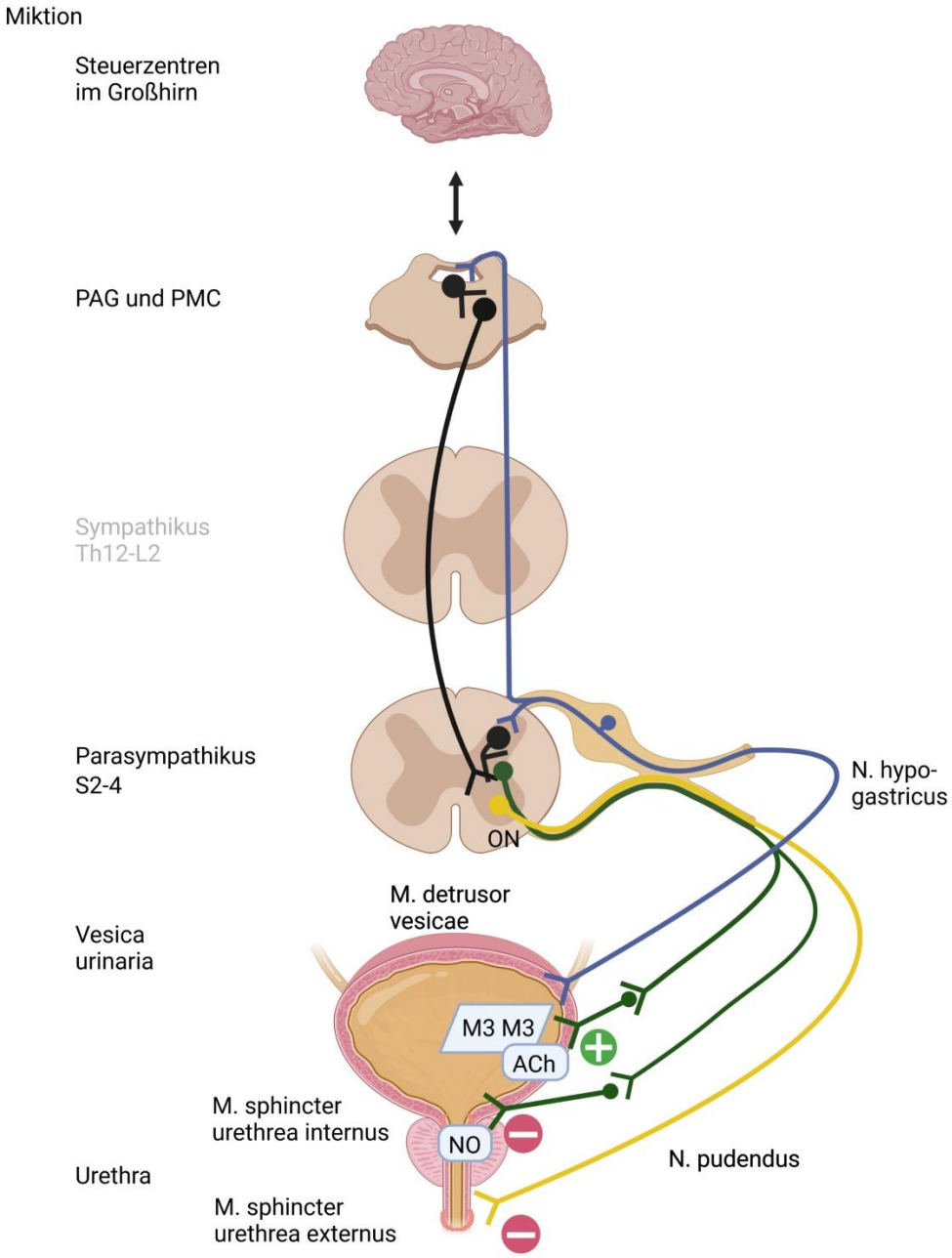

Abbildung 4. Innervation der Harnblase und ihrer Sphinkteren während der Miktion
Schematische Darstellung der Innervation während der Miktion. Die Steigerung der Wandspannung führt zur Reduktion der sympathischen Aktivität und Aktivierung des parasympathischen Nn. pelvici splanchnici. Acetylcholin (ACh) wird freigesetzt und bindet an M2- und M3-Rezeptoren (M2, M3) auf dem M. detrusor vesicae. Parallel erfolgt die Hemmung des M. sphincter urethrea internus, durch Stickstoffmonoxid (NO), und das Ausbleiben der Aktivierung des M. sphincter urethrea exsternus was eine Erschlaffung der Sphinktere zur Folge hat. Die übergeordnete Steuerung der Miktion erfolgt durch Die übergeordnete Steuerung der Miktion erfolgt durch das frontale Blasenzentrum und weitere Hirnstrukturen. ON = Onuf-Kern; Blau = sensible; Gelb = somatomotorisch; Grün = parasympathisch; Erstellt mit biorender.com

Parallel halten sympathische Fasern mit gleichem Ursprung durch Noradrenalinfreisetzung über die Bindung an β-Adrenozeptoren auf dem Musculus detrusor vesicae diesen entspannt [1-8, 10, 43]. Somit unterstützt die Aktivierung des Sympathikus einen Verschluss der Harnblase. Zeitgleich erfolgt auch die Aktivierung des aus quergestreifter Muskulatur aufgebauten Musculus sphincter urethrae externus über nikotinische Acetylcholinrezeptoren (nAChR) durch den Nervus pudendus, die Zellkörper der dafür verantwortlichen Neurone befinden sich im Onuf-Kern (Nucleus Onuf) des Rückenmarks [2, 4, 5, 10, 22-27].

Die Steuerung und Aktivierung der Miktion erfolgt unter physiologischen Bedingungen über die Blasenfüllung. Die autonome Kontraktionssteuerung des Detrusormuskels führt zunächst durch intrinsische Mechanismen dazu, dass bei steigender Harnmenge die Relaxation des Detrusormuskels steigt. Hierdurch ist es möglich, dass trotz zunehmenden Blasenvolumens der Blasendruck zunächst konstant niedrig bleibt. Dies ermöglicht die Füllung der Blase. Aber bei immer weiter steigender Harnmenge, erhöhen sich allmählich auch der intravesikuläre Druck und dadurch die Wandspannung. Dies wird durch sensible Fasern in der Blasenwand wahrgenommen und an das Rückenmark weitergeleitet [1-6, 10, 22, 23, 45-47]. Hierbei sei zu bemerken, dass das Urothel eine wichtige Rolle bei der Signalwahrnehmung und Signalweiterleitung spielt. Die Expression verschiedener Rezeptoren [17, 48-61] ermöglicht es dem Urothel, eine Vielzahl von „sensorischen Inputs“ wahrzunehmen und auf diese zu reagieren. Hierzu gehören neben der erhöhten Dehnung während der Blasenfüllung auch lösliche Faktoren oder freigesetzte Mediatoren/Peptide/Transmitter aus Nerven, Entzündungszellen oder Blutgefäßen [62-65]. Die afferenten Signale nehmen zu, bis sie schließlich einen Schwellenwert erreichen, um einen Miktionsreflex auszulösen. Die Steigerung der Wandspannung führt zur Reduzierung sympathischer Aktivität und zur Aktivierung von parasympathischen Neuronen im Sakralmark. Die Aktivierung dieser efferenten Nerven induziert die Blasenentleerung [1-6, 10, 22, 23, 45-47]. Es wird Acetylcholin (ACh) aus dem postganglionären Fasern der parasympathischen Nervi pelvici splanchnici freigesetzt. ACh bindet an M2- und M3-Rezeptoren auf dem Detrusormuskel. Die Aktivierung der an G_q-Protein gekoppelten M3-Rezeptoren führt direkt zur Kontraktion des Muskels [2, 10, 43, 66-69]. Die Aktivierung der M2-Rezeptoren hingegen führt zur Aktivierung der gekoppelten G_i-Proteine. Dies führt zu

einer indirekten Kontraktion. Durch die Aktivierung G_i-Proteine wird die Aktivität der durch β-Adrenozeptoren induzierten Adenylatcyclase reduziert und somit die Relaxation aufgehoben. Zeitgleich erfolgt die parasympathische koordinierte Relaxation des Musculus sphincter urethrae internus und der glatte Muskulatur der Urethra, durch die Freisetzung von Stickstoffmonoxid, was eine Erschlaffung des Sphinkters und der glatten Muskulatur der Urethra zur Folge hat [2, 9, 43, 70-74]. Dies ermöglicht die Miktion. Somit sorgt die Aktivierung des Parasympathikus über eine Erregung der Blasenwandmuskulatur für eine Entleerung der Harnblase. Da die Miktion aber willkürlich gesteuert werden kann, muss zunächst eine Freigabe durch die übergeordneten Regulationszentren erfolgen. Steigende Wandspannung wird durch aufsteigende Kollaterale über das periaquäduktale Grau an das pontine Miktionszentrum der Formatio reticularis weitergeleitet, welches die Freigabe oder Hemmung von Miktion durch absteigende Bahnen zum sakralen parasympathischen Miktionszentrum bzw. sympathischen Miktionszentrum des Thorakolumbalmarks steuert. Die Steuerung des pontinen Miktionszentrums erfolgt durch das periaquäduktale Grau [2, 28, 38, 41, 42]. Dieses wiederrum wird übergeordnet gesteuert durch das frontale Blasenzentrum (Regelkreislauf: Thalamus/Insula/vorderer Gyrus cinguli/Gyrus frontalis superior medialis) [2, 28-38], subkortikale Mechanismen, die parahippocampale Strukturen mit einbeziehen [2, 10, 39] und dem anterioren Cingulus im Zusammenspeil mit dem supplementärmotorische Kortex [2]. An der Steuerung scheinen aber auch der Hypothalamus [2, 37], die Basalganglien, der parietale Kortex, das limbischen System und das Kleinhirn beteiligt zu sein [2, 40]. Bemerkenswert hierbei ist, dass die Blasenentleerung über das vegetative Nervensystem abläuft, aber über höhere Zentren willkürlich gesteuert wird. Es ist einer der seltenen Fälle, dass eine willkürliche Kontrolle über vegetative Steuerzentren erfolgt [17-21].

1.5 Geschmackswahrnehmung

Die klassische Geschmackswahrnehmung findet über die oropharyngealen Geschmacksknospen statt. Bitter, süß, umami, salzig, sauer und fettig sind die sechs Geschmacksqualitäten, die von Geschmacksknospen erkannt werden [75-77]. Eine Geschmacksknospe besteht aus 50 bis 100 einzelnen Zellen und ist aus

verschiedenen Zelltypen aufgebaut [77]. Diese werden an Hand von ultrastrukturellen Eigenschaften, Proteinexpressionsprofilen und ihren unterschiedlichen Funktionen bzw. Eigenschaften in Geschmackszellen des Typs I bis III und Basalzellen eingeteilt. Typ-I-Geschmackszellen haben eine unterstützende Funktion und verschiedene Eigenschaften, die auch Gliazellen aufweisen. Zudem konnte gezeigt werden, dass Typ-I-Geschmackszellen auf Salz reagieren [78]. Typ-III-Geschmackszellen sind für die Wahrnehmung von sauer und salzig wichtig [79-86]. Basalzellen sind die Vorläuferzellen, die sich in Geschmackszellen differenzieren [87]. In Typ-II-Geschmackszellen in den oropharyngealen Geschmacksknospen wird die Wahrnehmung von bitter, süß und umami durch die kanonische Geschmackstransduktionskaskade vermittelt.

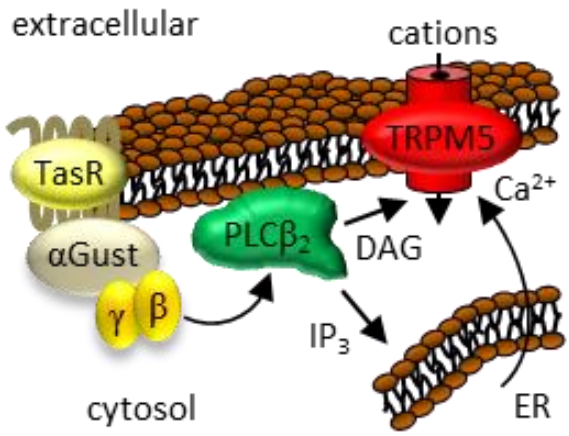

Abbildung 5. Geschmackstransduktionskaskade
Schematische Darstellung der aus Geschmacksknospen bekannten kanonischen Geschmackstransduktionskaskade. Geschmacksrezeptoren (TasR), das geschmacksspezifische G-Protein α-Gustducin, die Phospholipase Cβ2 (PLCβ2), der Kationenkanal TRPM5 (transient receptor potential cation channel, subfamily M, member 5), DAG, Diacylglycerin; ER, endoplasmatisches Retikulum; IP_3, Inositoltrisphosphat; [I].

Hierzu zählen die G-Protein-gekoppelten Geschmacksrezeptoren (TasR), die geschmacksspezifische G-Protein α-Untereinheit α-Gustducin, die Phospholipase Cβ2 (PLCβ2) und der Kationenkanal TRPM5 (transient receptor potential cation channel, subfamily M, member 5) [75] (Abbildung 5.). Lange Zeit ging man davon aus, dass jeder Geschmacksmodalität (bitter, süß und umami) einer Untergruppe von Geschmackszellen zugeordnet ist und sich die jeweiligen Geschmacksmodalitäten gegenseitig ausschließen. Beispielsweise würde eine süßempfindliche Typ-II-Zelle

Süßrezeptoren exprimieren, aber nicht Bitter- oder Umami-Rezeptoren und umgekehrt [87]. Dies scheint für Typ-II-Geschmackszellen auch der Fall zu sein. Kürzlich wurde aber nachgewiesen, dass eine Subpopulation von Typ-III-Geschmackszellen, sogenannte BR-(broadly responsive)-Geschmackszellen, einen polymodalen Charakter aufweisen und auf mehrere Stimuli (bitter, süß, sauer und umami) reagieren [79].

Die Tas1R-Familie hat nur drei Mitglieder (Tas1R1, Tas1R2 und Tas1R3). Süße Verbindungen werden durch das Tas1R2/Tas1R3-Heterodimer erkannt, während das Tas1R1/Tas1R3-Heterodimer einen Umami (z.B. Glutamat)-Rezeptor darstellt [88-91]. Hierbei sei zu erwähnen, dass einige Studien dafür sprechen, dass an der Wahrnehmung von Umami auch metabotrope Glutamat-Rezeptoren (mGluR), vor allem der mGluR-4 und mGluR-1, die in Geschmackszellen exprimiert werden, beteiligt sind [92-96] und es zur Wahrnehmung von süß einen alternativen Tas1R-unabhängigen Signalweg gibt [97].

Die Wahrnehmung von Bittersubstanzen erfolgt über die Tas2R-Familie. Sie besitzt je nach Spezies ca. 40 Mitglieder [98-101]. In den Typ-II-Geschmackszellen der Geschmacksknospe führt die Stimulation der Geschmacksrezeptoren zur Aktivierung der angeschlossenen kanonischen Geschmackstransduktionskaskade. An die oben genannten Rezeptoren sind heterotrimere G-Proteine gekoppelt. Im nicht aktivierten Zustand sind die G-Proteine, bestehend aus α-Gustducin und einem βγ-Dimer, fest mit Guanosindiphosphat (GDP) verbunden. Kommt es zur Aktivierung am Geschmacksrezeptor wird GDP durch Guanosintriphosphat (GTP) ersetzt und das G-Protein zerfällt. Das βγ-Dimer aktiviert PLCβ2, dies führt zur Spaltung von PIP_2 in IP_3 und DAG. IP_3 aktiviert IP_3-Rezeptoren des Typs 3. Die Aktivierung dieser im ER lokalisierten Calciumkanäle, führt zum Ausstrom von Calcium-Ionen aus dem ER. In Folge wird die intrazelluläre Calciumkonzentration ($[Ca^{2+}]_i$) erhöht und der Ionenkanal TRPM5 geöffnet und die Zelle depolarisiert. In Typ-II-Geschmackszellen führt die Depolarisation zur Freisetzung des in diesem Fall als Transmitter dienenden Adenosintriphosphat (ATP) über Hemikanäle, wie den spannungsgesteuerten ATP-Freisetzungskanal CALHM1 (calcium homeostasis modulator 1), der erforderlich für die Wahrnehmung von süß, bitter und umami ist [75, 102-105]. Dies führt zu Aktivierung von Typ-III-Geschmackszellen, die neben ihrer Rolle als Detektoren für sauer und salzig auch eine Funktion als präsynaptische Mediatorzellen zur

Weiterleitung der Signale von Typ-II-Geschmackszellen haben [87] und zu direkten Erregung von sensorischen Nervenfasern über Kanalsynapsen (channel synapses)[104, 106-110].

Andere Klassen von G-Protein-gekoppelten Rezeptoren sprechen auf kurz- und langkettige Fettsäuren an [75]. Im Gegensatz dazu öffnen Säuren (Protonen) und Salze (Natriumchlorid) Ionenkanäle, was direkt zu einer Depolarisation der Geschmackszelle führt. Als Kandidaten für saure Geschmacksrezeptoren wurden nichtselektive Kationenkanäle vorgeschlagen, die durch die Proteine PKD2L1 (polycystic kidney disease 2-like 1) und PKD2L3 (polycystic kidney disease 2-like 3) gebildet werden [75, 84, 111, 112]. Allerdings zeigten Knockout-Maus-Experimenten, dass diese Tiere nur eine verringerte, nicht aber eine ausbleibende Reaktion auf pH-Wert-Veränderungen haben [113, 114]. Knockout-Maus-Experimenten mit Tieren ohne funktionellem OTOP1 (Otopetrin 1) hingegen zeigen keine Reaktion auf Veränderungen des pH-Wertes [115, 116]. Deshalb wird davon ausgegangen, dass der Ionenkanal OTOP1 primär für die Wahrnehmung der Geschmacksqualität sauer verantwortlich ist [117].

Frühere Studien haben gezeigt, dass Amilorid-sensitive NaCl-Antworten in einem Zelltyp auftreten, der weder eine Typ II- noch Typ III-Zelle ist [118, 119], aber möglicherweise Typ I-Zellen [78] oder ein einzigartiger Zelltyp [120]. Ein Ionenkanal, der auch in Typ-I-Geschmackszellen vorhanden ist und von dem angenommen wird, dass er die Salzwahrnehmung vermittelt, ist der Amilorid-sensitive epitheliale Natriumkanal ENaC (epithelial Na-channel; auch SCNN1: sodium channel non-neuronal 1) [118, 121-125]. ENaC ist üblicherweise ein Heteromer, aufgebaut aus den drei Untereinheiten α, β und γ [126]. Die drei Untereinheiten werden durch die Gene *Scnn1a, Scnn1b und Scnn1c* codiert. Der Mensch hat noch eine vierte Untereinheit (δ), deren Funktion aber noch nicht geklärt werden konnte [127]. Allerdings scheint auch eine ENaC bzw. nicht amilorid-sensitive Perzeption von salzig möglich [122]. Zudem gibt es Hinweise, dass die Salzwahrnehmung auch über Typ-III-Geschmackszellen erfolgen könnte [79, 82, 128]. Hierfür sprechen Expressions- sowie Funktionsanalysen, die auch gegen die rein ENaC-vermittelte Wahrnehmung von Salz sprechen [129]. Hierbei wurde α-ENaC hauptsächlich in Geschmackszellen vom Typ III gefunden. β-ENaC hingegen wurde hauptsächlich in Typ-I- und einigen Typ-II-Zellen gefunden.

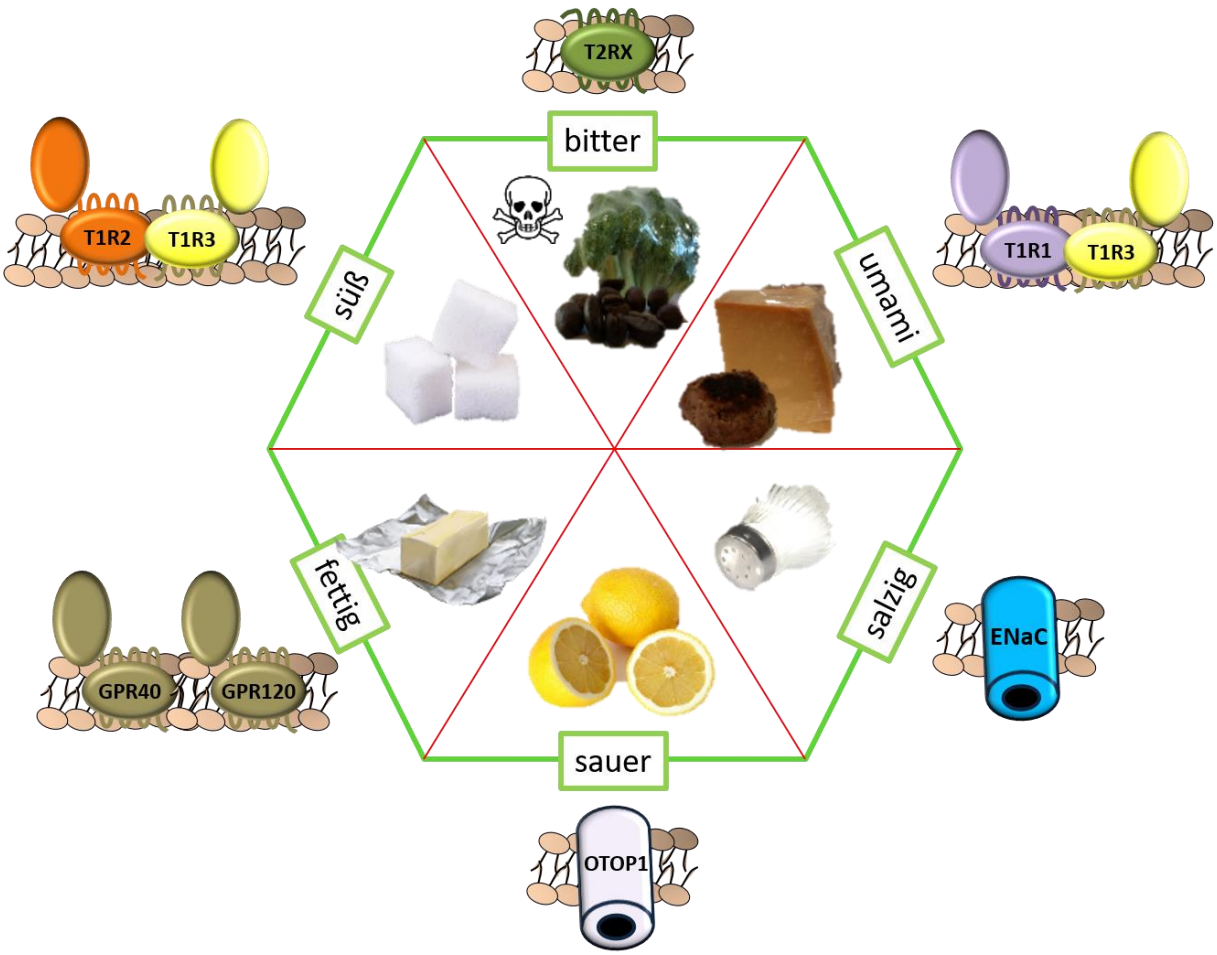

Abbildung 6. Geschmackswahrnehmung
Die Geschmackswahrnehmung der sechs Geschmacksqualitäten (süß, bitter, umami, fettig, sauer und salzig) erfolgt durch spezifische Rezeptoren. Süße Verbindungen werden primär durch das Tas1R2/Tas1R3-Heterodimer erkannt, während das Tas1R1/Tas1R3-Heterodimer einen Umami (z.B. Glutamat)-Rezeptor darstellt. Die Wahrnehmung von Bittersubstanzen erfolgt über die Tas2R-Familie. Salzwahrnehmung erfolgt über den amilorid-sensitiven epithelialen Natriumkanal ENaC und Sauerwahrnehmung erfolgt über OTOP1. Die Wahrnehmung von Fett wird mit CD36, GPR40 und GPR120 in Verbindung gebracht. Adaptiert aus [75].

γ-ENaC wurde hauptsächlich in Typ-II-Zellen gefunden, mit geringen Mengen in Typ-III- und Typ-I-Zellen. Interessanterweise exprimierte keine einzige Geschmackszelle sowohl α-ENaC als auch β-ENaC [120, 129]. Folgerichtig wäre die Ausbildung eines funktionstüchtigen Heteromers in Geschmackszellen nicht möglich. α-ENaC scheint für die funktionelle Integrität des Ionenkanals essenziell, da die amilorid-sensitiven Reaktionen im Knockout aufgehoben werden. Eine mögliche Erklärung besteht darin, dass Typ-I-Zellen möglicherweise niedrige Mengen an α-ENaC und γ-ENaC unterhalb

des Detektionslevels exprimieren. Diese würden sich dann mit β-ENaC verbinden und einen funktionellen Kanal in Typ-I-Zellen bilden. Eine weitere Möglichkeit wäre die aus Experimenten bekannte Ausbildung amilorid-sensitiver Homomere aus ENaCα-Untereinheiten [130, 131]. Die Wahrnehmung von Fett scheint durch eine Kombination von Somatosensorik und Gustatorik zu erfolgen. Früher ging man davon aus, dass die Wahrnehmung von Fett nur über seine Textur und somit somatosensorisch erfolgt [75]. Es konnten aber spezifische Membranrezeptoren, wie CD36 (cluster of differentiation 36; auch FAT: fatty acid translocase), GPR40 (G-protein coupled receptor 40; auch FFAR1: Free fatty acid receptor 1) oder GPR120 (G-protein coupled receptor 120; auch FFAR4: Free fatty acid receptor 4), die für den Nachweis von Fettsäuren essentiell sind, in Sinneszellen in den Geschmacksknospen nachgewiesen werden [132-136] und zudem gezeigt werden, dass freie Fettsäuren Sinneszellen in den Geschmacksknospen stimulieren [132, 137, 138]. Somit kann auch fettig als eine weitere Geschmacksqualität angesehen werden [139]. Eine Übersicht, welche Rezeptoren bzw. Proteine oder Mechanismen zur Wahrnehmung der sechs Geschmacksqualitäten verwendet werden, wird in der Abbildung 6. gezeigt.

1.6 Chemosensorische Wächterzellen

Bei Säugetieren enthalten die Schleimhäute der Atemwege und des Magen-Darm-Trakts spezielle solitäre Epithelzellen mit flaschenähnlicher Gestalt. Aufgrund ihres charakteristischen Bürstensaums am apikalen Ende aus Mikrovilli werden sie als "Bürstenzellen” bezeichnet [140-143].

Mittels Antikörpernachweis wurde Villin, ein Strukturprotein dieser Mikrovilli, als ein charakteristischer Marker für diese Bürstenzellen definiert [140]. Neuere Daten weisen allerdings daraufhin, dass es sich auch um das Strukturprotein Advillin handeln könnte. Somit wäre die Markierung eine Folge einer Kreuzreaktivität der verwendeten Antikörper [144]. Ursprünglich wurde dieser Zelltyp allein aufgrund seiner charakteristischen Ultrastruktur identifiziert. Rhodin und Dalhamn beschrieben 1956 erstmals mittels Elektronenmikroskopie im Trachealepithel der Ratte einen seltenen Zelltyp ohne Flimmerhärchen, statt dessen mit bürstenartigen Fortsätzen, die sie veranlassten, diese Zelle als „Bürstenzelle“ zu bezeichnen [141]. Zellen mit ähnlicher, wenn nicht völlig identischer Ultrastruktur, wurden an verschiedenen Stellen der

oberen Atemwege und im Magen-Darm-Trakt gefunden [140, 145-149]. Sowohl aus historisch gewachsenen als auch aus morphologischen Gründen werden diese Zellen in unterschiedlichen anatomischen Organsystemen unterschiedlich benannt. Im Darm etablierte sich die Nomenklatur "tuft (Büschel)" oder "tuft cells (Büschelzellen)" [150, 151]. In den oberen Atemwegen werden diese Zellen bevorzugt als „solitäre chemosensorische Zellen“ bezeichnet [152, 153]. Erste Hinweise auf ihre chemosensorische Funktion ergaben sich aus dem immunhistochemischen Nachweis des geschmacksspezifischen G-Proteins α-Gustducin in diesen Zellen [147, 152]. In der Zwischenzeit zeigten strukturelle, histochemische und Einzelzellsequenzierungsdaten mehrere einzigartige charakteristische Merkmale, die unterschiedliche Zellpopulationen innerhalb und zwischen Organen definieren [154-158]. Neben α-Gustducin wurden auch andere Komponenten der kanonischen Geschmackstransduktionskaskade (siehe 1.3.) in den Bürstenzellen der Atemwege und des Magen-Darm-Traktes identifiziert. Hemmung von Komponenten der Geschmackstransduktionskaskade, wie zum Beispiel die Hemmung von PLCβ2 oder TRPM5, oder die genetische Deletion von TRPM5 schwächte die Reaktion von Bürstenzellen auf bittere Reize ab [159-162]. Bei genetischer Deletion von TRPM5 geht im Infektionsmodell mit Helminthen der natürliche Abwehrmechanismus des Magen-Darm-Trakts gegen Würmer verloren [151]. Dies legt nahe, dass die Rezeptoren und Transduktionsmechanismen in Typ-II-Geschmackszellen und extraoralen chemosensorischen Zellen sehr ähnlich sind. Allerdings ist zu bemerken, dass während Typ-II-Geschmackszellen ATP als primären Botenstoff verwenden, zumindest Bürstenzellen der Atemwege ACh als Botenstoff nutzen. Hierzu exprimieren sie das ACh synthetisierende Enzym Cholinacetyltransferase (ChAT) [155, 162, 163]. Ein weiterer eindeutig identifizierter Bürstenzellmarker ist DCLK1 (Doublecortin-like kinase 1; Synonym: Doublecortin and CaM kinase-like 1 [DCAMKL1]) [164-168]. Inzwischen ist bekannt, dass diese Zellen mit Hilfe verschiedener Rezeptoren und der kanonischen Geschmackstransduktionskaskade mögliche Schadstoffe, wie "bittere" Bakterienprodukte, virulenz-assoziierte Formyl-Peptide oder Helminthen, in der Schleimhautflüssigkeit detektieren und gezielt protektive Mechanismen, wie den Verschluss von Gängen, die in benachbarte Kompartimente führen (Vomeronasalorgan), Atemreflexe, tracheale mukoziliäre Reinigung (mucociliary clearance), neurogene Entzündungen oder Typ-2-Immunantworten [140-143, 151-

153, 155, 157, 161, 162, 167, 169-171], einleiten, um das weitere Eindringen der potenziell schädlichen Substanzen zu verhindern. Hierzu setzen sie nach Stimulation ACh frei, um benachbarte sensorische Nervenendigungen und andere Zellen durch cholinerge Signalübertragung zu beeinflussen [155, 162, 163]. Deshalb wird Bürstenzellen eine Rolle als Wächterzellen zugesprochen. Sie sind besonders häufig an anatomischen Eintrittsstellen in den Körper, wie den oberen Atemwegen (Eingang in die gesamten Atemwege) [160, 172], in der Tuba auditiva (Eingang zum Mittelohr) [149], Nasenöffnung des Ductus vomeronasalis [161], Gallenblase, Gallen- und Pankreasgang (Verbindung von Darm zu Leber und Gallenblase bzw. Bauchspeicheldrüse), dem Gastrointestinaltrakt [140, 145, 173-175], der Konjunktiva [176] und dem gingivalen Saumepithel [177] zu finden. Bürstenzellen konnten auch im Thymus detektiert werden [178]. Alle diese Zellen sind eng miteinander verwandt, obwohl es organspezifische Unterschiede gibt [77, 157, 179, 180]. Entsprechend ihrer Wächterfunktion nimmt die Anzahl der Bürstenzellen mit zunehmendem Abstand von Eingang, zumindest in den Atemwegen, ab. In der Maus gibt zahlreiche Bürstenzellen in der Nase und fast keine mehr in den intrapulmonalen Atemwegen [181]. Dies weist auf ein allgemeines Prinzip hin, bei dem chemosensorische Wächterzellen im Eingangsbereich zur äußeren Umgebung oder inneren Körperoberflächen mit bakterieller Besiedlung vorkommen und entscheidende Elemente des angeborenen mukosalen Immunsystems darstellen [164, 181-185]. Vor diesem Hintergrund war ein ähnliches bürstenzellbasierendes Wächtersystem in den Harnwegen zu erwarten.

1.7 Die solitären Zellen der Urethra

Im Urethralepithel befinden sich neuroendokrine Zellen. Hierbei handelt es sich um solitäre Zellen, die morphologisch durch elektronenmikroskopisch sichtbare Vesikel im basalen Zellbereich charakterisiert sind. Diese auch als Paraneurone bezeichneten Zellen können durch die Expression von Tryptophanhydroxylase (Synthese von Serotonin), Chromogranin A (sekretorisches Vesikelprotein) und Protein Gene Product 9.5 (neuronaler Marker) molekular identifiziert werden [62, 186-202]. Sie wurden erstmals 1951 von Feyrter in der Urethra beschrieben. Feyrter bezeichnete sie als „Helle Zellen“ aufgrund ihres „chromophoben“ Charakters in Standardfärbungen [203, 204]. Durch Formaldehydbehandlung fluoreszieren diese Zellen aufgrund des Amins

Serotonin, genauso wie die enterochromaffinen Zellen des Magen-Darm-Traktes, gelb und werden mit chromsalzhaltigen Lösungen schwarz gefärbt [205, 206]. Deshalb wurden sie früher auch als urethrale chromaffine Zellen bezeichnet [191, 192, 207-209]. Ein weiterer bislang unbekannter solitärer Zelltyp ist Gegenstand dieser Arbeit.

1.8 Klinische Relevanz dieser Arbeit

Davon ausgehend, dass es sich bei dem bislang unbekannten solitären Zelltyp auch um eine chemosensorische Wächterzelle handelt, die als Abwehrmechanismus die Miktion beeinflusst, gibt zwei klinisch relevante Aspekte, die in direkter Verbindung mit dieser Arbeit stehen: Harnwegsinfekte und das Syndrom der überaktive Blase.

1.8.1 Das Syndrom der überaktive Blase

Das Syndrom der überaktiven Blase (auch hyperaktive Blase, früher: Reizblase oder nervöse Reizblase; overactive bladder (OAB) syndrome) ist eine häufige funktionelle Störung der Blasenfunktion, die etwa 12–16% der Bevölkerung in den westlichen Ländern und Millionen von Menschen weltweit betrifft [210-213]. Diese funktionelle Störung hat keine bekannte organpathologische Grundlage. Betroffene leiden unter ständigem Harndrang und überdurchschnittlich häufiger Blasenentleerung (Polyurie); hierbei handelt es sich meist um die häufige Abgabe kleiner Urinmengen (Pollakisurie). Dies ist oft mit Harninkontinenz und oder nächtlichem Harnlassen (Nykturie) assoziiert [213-217]. Die Ursachen für das OAB-Syndrom sind multifaktoriell und bislang noch nicht vollständig geklärt [218]. Mit einem OAB-Syndrom ist oftmals, aber nicht zwingend, eine fehlerhafte Steuerung und damit einhergehend eine fehlerhafte Kontraktion und somit eine messbare Überaktivität des Detrusormuskels, d.h. eine Detrusorhyperaktivität verbunden. Während der Füllungsphase ist der Detrusormuskel normalerweise entspannt und die Blase kann sich ausdehnen. Bei Betroffenen ist dies nicht der Fall. Der Detrusormuskel kontrahiert bei Menschen mit OAB-Syndrom schon in der Füllungsphase, auch wenn keine oder nur kleine Mengen Urin in der Blase vorhanden sind. Das Zusammenziehen löst Harndrang aus, der von den Betroffenen meist nicht unterdrückt werden kann. Das OAB-Syndrom wird derzeit häufig mit Antagonisten von mAChR behandelt [43, 69, 219-221]. In Deutschland zugelassene Substanzen sind Darifenacin (M3-Rezeptor-Antagonist), Fesoterodin (M2/3-Rezeptor-

Antagonist), Oxybutinin (M1/2/3-Rezeptor-Antagonist), Propiverin (M2/3-Rezeptor-Antagonist), Solifenacin (M3-Rezeptor-Antagonist), Tolterodin (M2/3-Rezeptor-Antagonist), Trospiumchlorid (M2/3-Rezeptor-Antagonist; Keine ZNS-Nebenwirkung) [219, 222-250]. Die zugrunde liegende Idee hierbei ist, dass während der Füllphase durch die Blockade der mAChR des Detrusormuskels die pathophysiologischen Kontraktionen gehemmt werden [247]. Ein weiteres Leitsymptom der OAB ist der imperative Harndrang, welches auch durch die Therapie mit Antimuskarinika gelindert wird [247, 251]. Die Grundlage dieses Symthome ist wohl auch eine Kontraktion des Detrusormuskels bereits in der Füllphase. Weil Antimuskarinika sowohl zur Linderung der Polyurie als auch zur Linderung des imperativen Harndrangs führen, muss unter pathophysiologischen Bedingungen ACh auch in der Füllphase freigesetzt werden. Unter physiologisch Bedingungen wird in der Füllphase allerdings kein ACh aus den parasympathischen Nerven, die den Detrusormuskel innervieren, freigesetzt [252]. Eine mögliche Erklärung hierfür ist, dass es noch eine weitere nicht-neuronale Quelle für ACh gibt. Eine pathologische Steigerung der ACh Freisetzung aus dieser nicht-neuronalen ACh-Quelle stellt eine mögliche Erklärung für die Detrusorüberaktivität dar.

1.8.2 Harnwegsinfekte

Die ableitenden Harnwege und somit auch die Urethra sind aber nicht nur einfache muskuläre Röhren zur Speicherung und Abgabe von Harn. Aufgrund ihrer direkten Verbindung zur Außenwelt stellen sie eine potentielle Eintrittspforte für toxische Substanzen und Mikroben dar [253].

Harnwegsinfekte (urinary tract infection; UTI) gehören zu den häufigsten bakteriellen Infektionen weltweit und werden multifaktoriell in ihrer Entstehung beeinflusst [254, 255]. Zu UTI zählen Infektionen der Urethra (Urethritis), der Blase (Zystitis), des Ureters (Ureteritis) und der Nieren (Pyelonephritis). Angesichts der Häufigkeit der Erkrankung ist es von entscheidender Wichtigkeit, mehr über die Grundlagen der Bakterien-Wirt-Beziehung und die Mechanismen im Körper zu erfahren, die sich bei einer UTI abspielen. Dieses Verständnis könnte später die Grundlage für neue alternative Therapien und Therapieansatzpunkte bilden. Hauptauslöser von Entzündungen im Urogenitaltrakt sind durch Bakterien verursachte UTI. Für UTI ist ein aszendierender Verlauf typisch. Die Keime gelangen durch Schmierinfektion zur

äußeren Harnröhrenöffnung und wandern die Urethra hinauf in die Harnblase oder bis in die Niere, wo sie zu einer Zystitis bzw. Pyelonephritis führen. *Uropathogene Escherichia coli* (UPEC) sind für 75 bis 95% der UTI weltweit verantwortlich [256, 257]. Sie gehören zur Familie der Enterobakterien. Sie sind gerade, sporenlose, gramnegative Bakterien, die unter fakultativ anaeroben Bedingungen wachsen. Es ist bekannt, dass Bakterien bitterrezeptoraktivierende Substanzen produzieren und sezernieren [159, 258, 259]. In bakteriellen Biofilmen können solche Substanzen eine Konzentration von bis zu 600 µM erreichen [260]. Biofilme werden unter anderem von gramnegativen Bakterien wie *Pseudomonas aeruginosa* produziert, die für den größten Teil der katheterassoziierten Harnwegsinfekte verantwortlich sind [261]. Der Glutamatmetabolismus unterstützt das pathogene Potential von *Proteus mirabilis* im Harnwegsbereich [262], und freie Aminosäuren (“umami”) erleichtern das Bakterienwachstum im Urin [263].

2 Zielsetzung dieser Arbeit

Ausgehend von der Hypothese, dass es an verschiedenen Eingängen in den Körper chemosensorische Zellen mit Wächterfunktion gibt, war es Ziel dieser Arbeit zu klären, ob es in der Urethra neben den bereits bekannten neuroendokrinen Zellen noch einen weiteren bürstenzell-ähnlichen Zelltyp gibt. Folgende initiale Hypothese wurde im Rahmen dieser Forschungsarbeit adressiert:

1. **Es gibt Bürstenzellen im Epithel der Urethra → [I]**

Nach der Entdeckung der „urethralen Bürstenzellen (UBC)“ folgte die Charakterisierung dieser erstmals identifizierten Zellen. Da bei Bürstenzellen des Respirationstraktes eine morphologische und molekulare Ähnlichkeit zu Geschmackszellen festgestellt werden konnte, fokussierte sich die initiale Charakterisierung der neuendeckten UBC auf die Hypothese, dass es sich auch hier um chemosensorische Wächterzellen handelt, die mittels Geschmacksrezeptoren und Elementen der Geschmackssignaltransduktionskaskade entscheidend an der Detektion und Abwehr von eindringenden Noxen und Keimen beteiligt sind.
Der Name „urethrale Bürstenzelle“ wurde aufgrund ihrer hohen Ähnlichkeit zu Bürstenzellen, die bereits aus dem Respirationstrakt, dem Magen-Darm-Trakt und den Gallenwegen bekannt waren, gewählt. Im Laufe der Arbeit stellte sich heraus, dass es sich bei den urethralen Bürstenzellen aber um mindestens zwei unterschiedliche Zellpopulationen handelt.
UBC oder urethrale cholinerge chemosensorische Zellen (UCCC), die Gegenstand dieser Arbeit sind, definiert durch die Expression von Advillin bzw. Villin, ChAT und der Geschmackstransduktionskaskade und weiteren Bürstenzellmarkern, werden im Folgenden als UCCC oder aus historisch gewachsenen Gründen als UBC bezeichnet.
Die zweite Population ist zwar mittels Antikörpern gegen Villin markierbar, hat aber weder ChAT noch die Komponenten der Geschmackstransduktionskaskade. Es handelt sich daher um nicht-cholinerge Bürstenzellen.
Die Charakterisierung von UCCC wurde im Rahmen dieser Forschungsarbeit mittels folgender Hypothesen durchgeführt (Die Ziffern verweisen auf die zugehörigen Original- und Übersichtsarbeiten).

2. **UCCC exprimieren Elemente der Geschmackswahrnehmung → [I], [IV]**
3. **UCCC sind polymodale Chemosensoren → [I], [IV]**
4. **UCCC verwenden Acetylcholin als Botenstoff für parakrine und autokrine Signalübertragungen → [I], [III]**
5. **UCCC lösen neuronale Reflexe aus → [I]**
6. **UCCC sind in verschiedenen Säugetierspezies präsent → [I], [II]**
7. **UCCC entstehen postnatal und es gibt einen geschlechtsspezifischen Unterschied in der Entwicklung → [V]**
8. **Das Protein MyD88 und Toll-like Rezeptoren haben einen Einfluss auf die Entwicklung von UCCC → [V]**
9. **UCCC sind chemosensorische Wächterzellen, initiieren Abwehrmechanismen und beeinflussen die Miktion → [I], [III-VII]**

3 Ergebnisse und Diskussion

3.1 Es gibt Bürstenzellen im Epithel der Urethra

I. **Deckmann K***, Filipski K*, Krasteva-Christ G, Fronius M, Althaus M, Rafiq A, Papadakis T, Renno L, Jurastow I, Wessels L, Wolff M, Schütz B, Weihe E, Chubanov V, Gudermann T, Klein J, Bschleipfer T, Kummer W. Bitter triggers acetylcholine release from polymodal urethral chemosensory cells and bladder reflexes. **Proc Natl Acad Sci U S A**. 2014;111(22):8287-92.

Um initial zu klären, ob es urethrale Bürstenzellen gibt, wurden zwei unabhängig erzeugte Reporter-Mausstämme [264, 265] verwendet. Hierbei handelt es sich um ChAT-eGFP-Mausstämme. In diesen gentechnisch veränderten Mausstämmen ist hinter einem zusätzlichen artifiziell ins Genom der Mäuse eingebrachten Promotor des ChAT-Gens das Gen eines grünfluoreszierenden Proteins (eGFP) eingefügt. Hierdurch wird in diesen Reporter-Mausstämmen in jeder Zelle, in der ChAT exprimiert wird, auch das über Fluoreszenz detektierbare eGFP exprimiert. Beim Screening von Gewebeschnitten und Gesamtgewebepräparaten (whole mounts) der Urethra und des restlichen Urogenitaltrakts dieser ChAT-Reporter-Mausstämme konnten erstmals solitäre ChAT-positive Zellen im Epithel der Urethra identifiziert werden. Die ChAT-eGFP^{+}-Zellen waren aber nur im Epithel der Urethra, nicht im Epithel des Nierenbeckens, des Harnleiters, der Harnblase oder des Beckensegments des Vas deferens zu finden (Abbildung 7.). Zudem konnten diese Zellen bei männlichen Mäusen in den Ausführungsgängen der Prostata, Bläschendrüse, Koagulationsdrüsen sowie bei männlichen und weiblichen Mäusen in den Ausführungsgängen der periurethralen Drüsen jeweils in der Nähe der Öffnung zur Urethra, nicht aber in den Drüsen selbst, gefunden werden. Die Form der Zellen variiert von der typischen flaschenartigen Struktur, bekannt von den trachealen Bürstenzellen, mit einer breiten Basis an der Basalmembran und einer länglichen Spitze, die Richtung Lumen reicht, bis hin zu komplexeren Morphologien mit schlanken Fußfortsätzen, die direkt auf die Basallamina reichen oder sich ihr schräg annähern. Es konnten auch Zellen mit horizontal ausgerichtetem Zellkörper identifiziert werden, bei denen unklar bleibt, ob sie Kontakt zum Lumen der Urethra haben (Abbildung 8.).

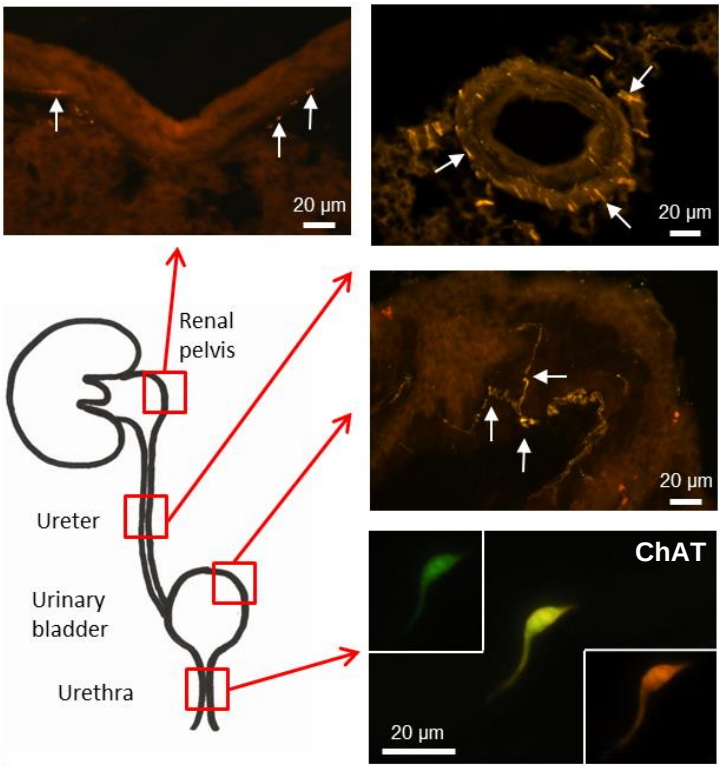

Abbildung 7. Cholinerge Epithelzellen in der Urethra
Gewebeschnitte der Urethra und des restlichen Urogenitaltrakts von ChAT-eGFP-Mäusen. Solitäre ChAT-eGFP^{+}-Zellen konnten nur im Epithel der Urethra identifiziert werden. Sie wurden nicht im Epithel des Nierenbeckens, des Harnleiters, der Harnblase gefunden. Das eGFP-Signal (grün) wurde mittels Cy3-konjugiertem Antikörper (orange) verstärkt. In allen anderen Teilen der Harnwege wurden cholinerge Nervenfasern (Pfeile) durch Antikörpermarkierung sichtbar. Hierbei wurden jedoch keine ChAT-eGFP-exprimierenden Epithelzellen sichtbar; [l].

Bei den Bürstenzellen handelt es sich nicht um neuroendokrine Zellen. Dies konnte anhand von Doppelmarkierungen mit Antikörpern gegen spezifische Marker von neuroendokrinen Zellen - Serotonin (Produkt der Tryptophanhydroxylase), Chromogranin A (sekretorisches Vesikelprotein) oder Protein Gene Product 9.5 (neuronaler Marker) – und Antikörpern gegen Bürstenzellmarker (Villin) oder Marker für cholinerge Bürstenzellen (ChAT) ermittelt werden. Ob urethrale Bürstenzellen Villin, Advillin oder beides exprimieren, ist zurzeit nicht eindeutig geklärt. Bei beiden Proteinen handelt es sich um Mikrovillusstrukturproteine mit einer sehr hohen Ähnlichkeit. Daher können Kreuzreaktivitäten der verwendeten Antikörper nicht endgültig ausgeschlossen werden. Daten aus Bürstenzellpopulationen des Gastrointestinaltrakts weisen auf eine Expression von Advillin hin [144].

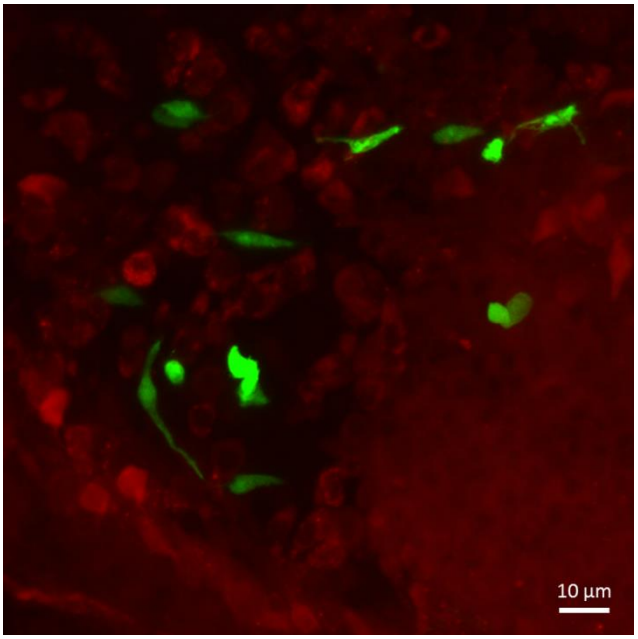

Abbildung 8. Morphologie der urethralen ChAT-eGFP$^+$-Zellen
Gewebeschnitt der Urethra einer ChAT-eGFP-Maus zur Darstellung der komplexen Morphologie der urethralen ChAT-eGFP$^+$-Epithelzellen (grün). Die Aufnahme wurde mittels Z-Stack erstellte, überlagerte und auf eine Z-Ebene reduzierte. Die Form der Zellen variiert von der typischen flaschenartigen Struktur mit einer breiten Basis und einer länglichen Spitze, die Richtung Lumen reicht, bis hin zu komplexeren Morphologien mit schlanken Fußfortsätzen. Es sind auch Zellen mit horizontal ausgerichtetem Zellkörper zusehen. Autofluoreszenz des Urethraepithels ist in Rot sichtbar. Die Aufnahme wurde mit einem Konfokalen-Laser-Scanning-Mikroskops aufgenommen.

Es wurden zwei Villin-immunreaktive Zellpopulationen identifiziert: cholinerge und nicht-cholinerge Bürstenzellen (Abbildung 9.). Solitäre chemosensorische Zellen waren bis dato aus verschiedenen Organsystemen bekannt. Sie konnten unter anderem im respiratorischen und im Gastrointestinal-Trakt identifiziert werden. Bislang unbekannt war, dass es solche Zellen auch in der Urethra gibt. Wahrscheinlich blieben sie aufgrund ihrer anatomischen Beschränkung auf das Eintrittsportal in den Urogenitaltrakt (d.h. die Harnröhre und die Drüsengänge, die sich in diesen öffnen) unentdeckt, da sich frühere Suchen auf die zentralen Organe des Urogenitaltraktes (Blase, Niere, Gebärmutter und Prostata) konzentrierten [140]. Somit konnte erstmals gezeigt werden, dass es urethrale Bürstenzellen bzw. solitäre cholinerge Zellen in der Urethra gibt.

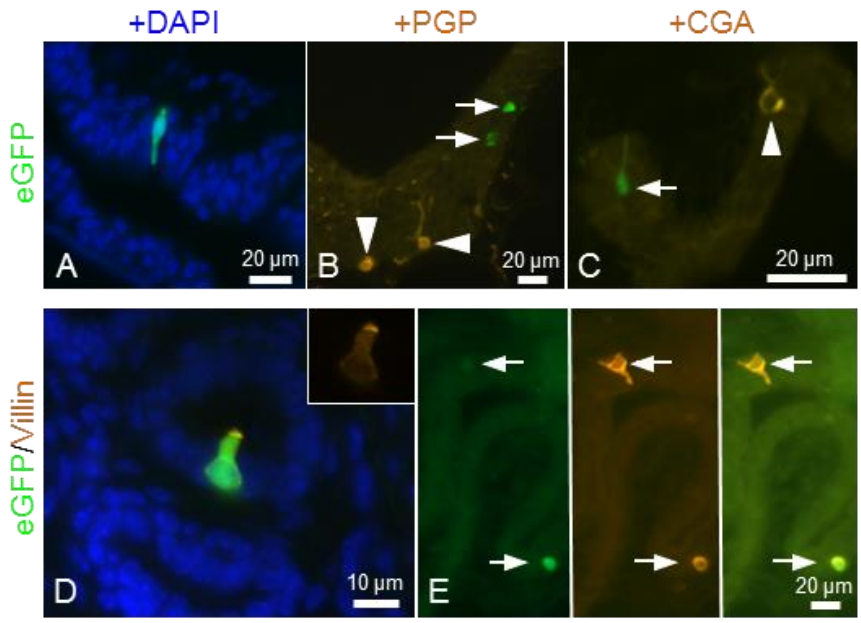

Abbildung 9. Cholinerge Epithelzellen sind keine neuroendokrinen Zellen
Immunfluoreszenzbilder muriner Urethrae von ChAT-eGFP-Mäusen. (A) Eine ChAT-eGFP-Zelle erstreckt sich durch die Epithelschicht der Urethra. Kerne wurden mit DAPI gegengefärbt. (B) ChAT-eGFP-Zellen (Pfeile) unterscheiden sich von Protein gene product 9.5 (PGP)-immunreaktiven neuroendokrinen Zellen (Pfeilspitzen). (C) Die ChAT-eGFP-Zelle (Pfeil) zeigt keine Immunreaktivität bei Antikörpern gegen den neuroendokrinen Zellmarker Chromogranin A (CGA). Die Pfeilspitze zeigt eine CGA^+ neuroendokrine Zelle. (D). Die flaschenförmige ChAT-eGFP$^+$-Zelle ist immunreaktiv für den Bürstenzellmarker Villin. (Insert) Färbung mit Antikörpern gegen Villin, zeigt die Konzentration von mikrovillösem Protein am apikalen Zellpol. EGFP (grün), Villin-Immunreaktivität (orange) und Zellkerne (DAPI; blau) (E) Villin$^+$-Zelle ist nicht $ChAT^+$ (oberer Pfeile). Eine weitere Zelle ist doppelt positiv (unterer Pfeil); [I].

3.2 UCCC exprimieren Elemente der Geschmackswahrnehmung

I. **Deckmann K***, Filipski K*, Krasteva-Christ G, Fronius M, Althaus M, Rafiq A, Papadakis T, Renno L, Jurastow I, Wessels L, Wolff M, Schütz B, Weihe E, Chubanov V, Gudermann T, Klein J, Bschleipfer T, Kummer W. Bitter triggers acetylcholine release from polymodal urethral chemosensory cells and bladder reflexes. **Proc Natl Acad Sci U S A**. 2014;111(22):8287-92.

IV. Kandel C, Schmidt P, Perniss A, Keshavarz M, Scholz P, Osterloh S, Althaus M, Kummer W, **Deckmann K**. ENaC in Cholinergic Brush Cells. **Front Cell Dev Biol.** 2018 Aug 15;6:89.

Wie in chemosensorischen Zellen des Respirations- bzw. Magen-Darm-Traktes, können auch in UCCC Elemente der kanonischen Geschmackstransduktionskaskade nachgewiesen werden. Sie exprimieren α-Gustducin, PLCβ2 und TRPM5. Hierbei

zeigte sich auch, dass die ChAT-eGFP- und TRPM5-Immunmarkierung nahezu 1:1 übereinstimmen. Ein vergleichbares Bild zeigte sich auch bei DCLK1, einem anderen Marker für Bürstenzellen (Abbildung 10.).

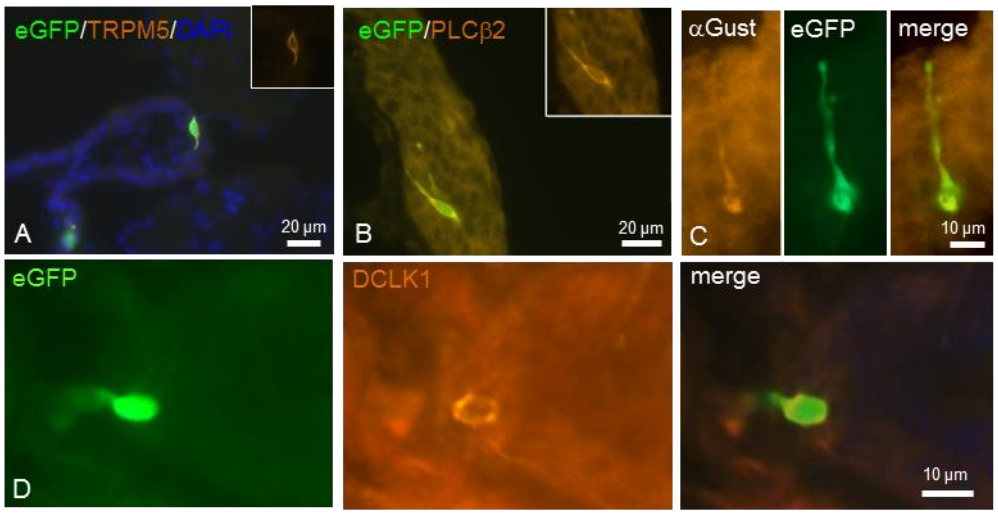

Abbildung 10. ChAT-eGFP$^+$-Zellen der Urethra exprimieren Elemente der Geschmackstransduktionskaskade und den Bürstenzellmarker DCLK1
Immunfluoreszenzbilder muriner Urethrae von ChAT-eGFP-Mäusen. (A) ChAT-eGFP$^+$-Zellen (grün) und werden durch Antikörper gegen TRPM5 (orange) markiert; Kerne sind mit DAPI blau markiert. (B) Eine ChAT-eGFP$^+$-Zelle ist immunmarkiert für PLCβ2 (B), (C) α-Gustducin (αGust); [I]; (D) bzw. DCLK1.

Die Mehrheit der ChAT-eGFP$^+$-Zellen war PLCβ2$^+$ und ein Drittel war α-Gustducin$^+$. Dieses unvollständige Kolokalisationsmuster ist mit der Beobachtung kongruent, dass es verschiedene Subpopulationen von Bürstenzellen in der Urethra gibt, einschließlich cholinerger/TRPM5$^+$ und nicht-cholinerger Villin$^+$, meist TRPM5$^-$, Zellen. RT-PCR-Analyse von isolierten UCCC ergab eine mRNA-Expression der Geschmacksrezeptoren Tas1R1 und Tas1R3, zuständig für die Wahrnehmung von Umami, sowie die Expression des Bittergeschmacksrezeptors Tas2R108, zu dessen Liganden der Bitterstoff Denatonium zählt. Tas2R119 und Tas2R105, dessen Ligand Cycloheximid ist, hingegen konnten nicht nachgewiesen werden. RT-PCR-Analysen von isolierten UCCC zeigten auch eine mRNA-Expression der für die ENaC Untereinheiten kodierenden Gene *Scnn1a, Scnn1b* und *Scnn1g* (Abbildung 11.).

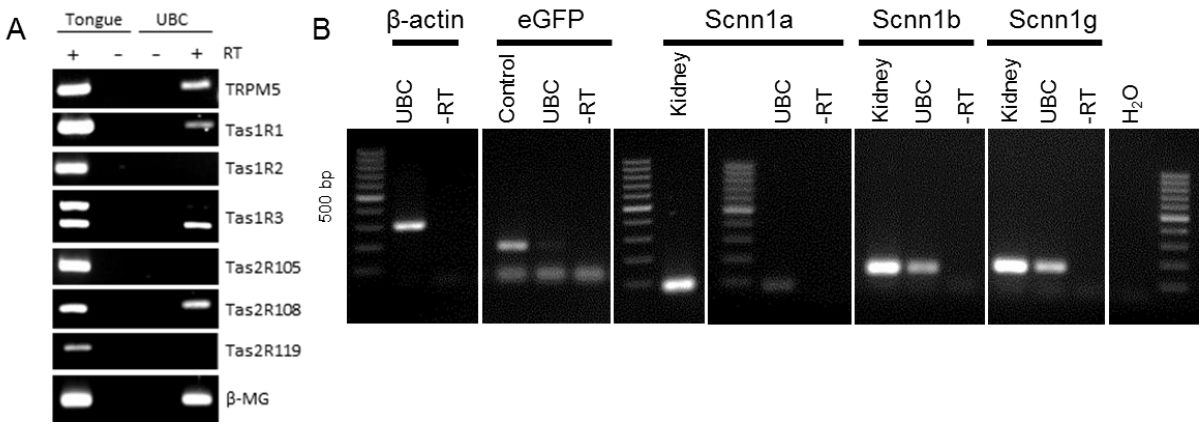

Abbildung 11. UCCC exprimieren verschiedene Proteine zur Wahrnehmung von Geschmacksqualitäten.
RT-PCR von isolierten UBC/UCCC (A) Nachweis von Geschmacksrezeptoren und *Trpm5*. Zunge fungiert als Positivkontrolle; *β2-Mikroglobulin* (β-MG) als Housekeeping-Gen; (B) Nachweis von *Scnn1a, b, g* und *eGFP*; Niere fungiert als Positivkontrolle. *β-Aktin* als Housekeeping-Gen; [I; IV].

Immunhistochemische Untersuchungen in ENaCα-Reportermäusen (Scnn1a/tdTomato-Reportermäusen) stützen die Ergebnisse, da sie eine Kolokalisation der ENaCα-Untereinheit und TRPM5 zeigten. Allerdings wiesen nicht alle UCCC eine Expression der ENaCα-Untereinheit auf (Abbildung 12.).

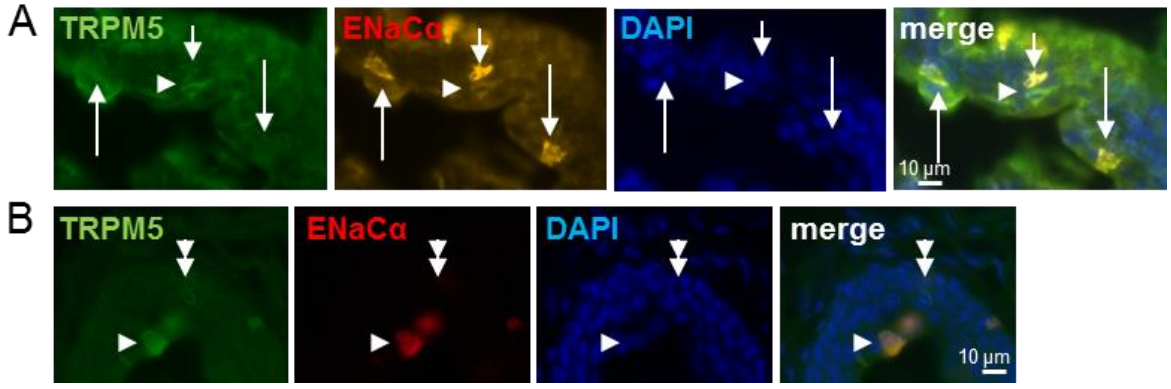

Abbildung 12. UCCC exprimieren ENaCα
(A, B) In Gefrierschnitten der Urethra von ENaCα-Reportermäusen (orange oder rot) wurden UCCC mittels Antikörper gegen TRPM5 markiert (grün) und Zellkerne mittels DAPI (blau) gefärbt. Mehrere Epithelzellen exprimieren nur ENaCα (Pfeile in A). Mindestens zwei von ihnen (lange Pfeile in A) sind Deckzellen des Urothels, gemessen an ihrer Form und Position. Die Pfeilspitzen zeigen auf ENaCα-(orange) und TRPM5-(grün) doppelt positive Zellen, die doppelte Pfeilspitze zeigt auf eine TRPM5-immunreaktive Zelle, die keine ENaCα-Markierung aufweist; [IV].

Diese Beobachtungen lassen vermuten, dass nur eine Subpopulation von UCCC ENaCα exprimiert. Ein auffälliges Merkmal von UCCC ist die Koexpression von Geschmacksrezeptoren der Tas1R- und Tas2R-Familien. In ähnlicher Weise exprimieren einzelne nasale chemosensorische Zellen Tas1R3 gemeinsam mit Tas2R5 und Tas2R8 [266]. Diese Situation steht im Gegensatz zur oropharyngealen Gustation in Typ-II-Geschmackszellen, bei der Tas1R- und Tas2R-Rezeptoren nicht coexprimiert werden [99, 266]. Dies hat zur Folge, dass 83% der Typ-II-Geschmackszellen in den Geschmacksknospen der Papilla vallata von Mäusen auf nur eine einzige Geschmacksqualität reagieren [267] und sich die jeweiligen Geschmacksmodalitäten gegenseitig ausschließen [87]. Eine Subpopulation von Typ-III-Geschmackszellen, sogenannte BR (broadly responsive) – Geschmackszellen, weist hingegen einen polymodalen Charakter auf [79]. Demnach konnte gezeigt werden, dass die neu entdeckten, solitären, cholinergen Zellen potenzielle Chemosensoren sind.

3.3 UCCC sind polymodale Chemosensoren

I. **Deckmann K***, Filipski K*, Krasteva-Christ G, Fronius M, Althaus M, Rafiq A, Papadakis T, Renno L, Jurastow I, Wessels L, Wolff M, Schütz B, Weihe E, Chubanov V, Gudermann T, Klein J, Bschleipfer T, Kummer W. Bitter triggers acetylcholine release from polymodal urethral chemosensory cells and bladder reflexes. **Proc Natl Acad Sci U S A**. 2014;111(22):8287-92.

IV. Kandel C, Schmidt P, Perniss A, Keshavarz M, Scholz P, Osterloh S, Althaus M, Kummer W, **Deckmann K**. ENaC in Cholinergic Brush Cells. **Front Cell Dev Biol.** 2018 Aug 15;6:89.

Anhand der intrazellulären Calcium-Konzentration wurde die Reaktion von isolierten UCCC auf verschiedene Substanzen gemessen. Hierbei zeigte sich, dass UCCC entsprechend ihrem Rezeptorprofil auf verschiedene Substanzen mit einer Erhöhung der intrazellulären Calcium-Konzentration reagieren. UCCC reagieren auf die Bittersubstanz Denatonium, Mononatrium L-Glutamat (Umami), NaCl (salzig) und ATP. Außerdem reagieren UCCC auf hitzeinaktivierte UPEC (Abbildung 13.). Interessanterweise zeigen UCCC hierbei ein polymodales Antwortverhalten (Abbildung 14.).

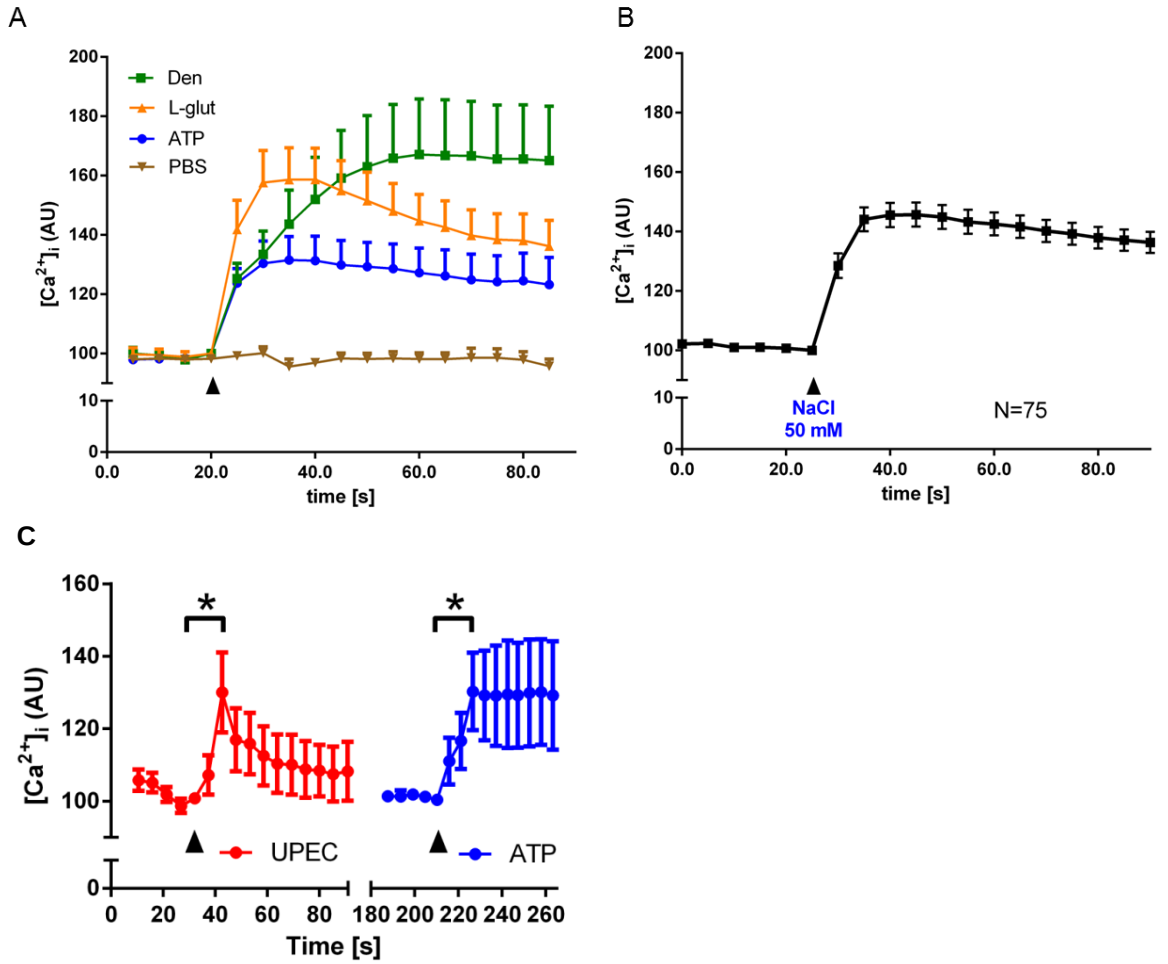

Abbildung 13. UCCC reagieren auf verschiedene Geschmacksqualitäten und UPEC
Bestimmung der intrazellulären Calciumkonzentration ($[Ca^{2+}]_i$) von isolierten, vereinzelten ChAT$^+$-Zellen (UCCC) aus ChAT-eGFP-Mäusen nach Applikation verschiedener Substanzen mittels kontinuierlichen Konfokale Laserscanning-Aufnahmen der Intensität der Fluoreszenz des Calciumindikators Calcium Orange. Alle Substanzen wurden unter kontinuierlichem Fluss in der Kammer hinzugefügt, so dass die angegebenen Konzentrationen anfänglich erreicht waren und dann ausgewaschen wurden. (A) UCCC reagieren auf ATP (0.5 mM) Denatonium (25 mM) und Mononatrium L-Gutamat (25 mM) (N=32) (B) UCCC reagieren auf NaCl (50 mM) (N=75). (C) UCCC reagieren auf hitzeinaktivierte UPEC (2-5x10^7 koloniebildenden Einheiten) im vergleichbaren Umfang wie auf ATP (0.5 mM). Die y-Achse zeigt arbiträre Einheiten (arbitrary unit; AU), die mit der $[Ca^{2+}]_i$ korrelieren. Die Graphen zeigen Mittelwert und SEM. *p<0,05, gepaarter t-Test; [I; IV].

Somit konnten wir zeigen, dass eine beträchtliche Anzahl von auf Denatonium ansprechenden UCCC auch auf Mononatrium L-Glutamat reagiert. In Bezug auf die oropharyngeale Gustation spiegeln diese Substanzen einen aversiven (Denatonium: Bitter) und einen attraktiven (Mononatriumglutamat: Umami) Stimulus wider und werden üblicherweise von verschiedenen Zellpopulationen wahrgenommen, die

immer noch als Subtypen von Typ-II-Geschmackszellen angesehen werden [75]. Die vorliegenden Daten zeigen, dass in UCCC offenbar ein breiteres Spektrum an Substanzen bzw. Geschmacksqualitäten wahrgenommen wird [78]. Interessant ist hierbei die kürzlich entdeckten „broad responsive“-Geschmackszellen, die dem Typ III zugeordnet wurden. Diese Zellen reagieren sowohl auf bitter, süß, umami und sauer Stimuli und weisen daher auch einen polymodalen Charakter auf [79]. Dies ist ein Hinweis darauf, das UCCC möglicherweise eine nähere Verwandtschaft zu Typ-III-Geschmackszellen als zu Typ-II-Geschmackszellen aufweisen könnten. Dagegen spricht allerdings das unterschiedliche Profil der Signalkaskaden beider Zelltypen.

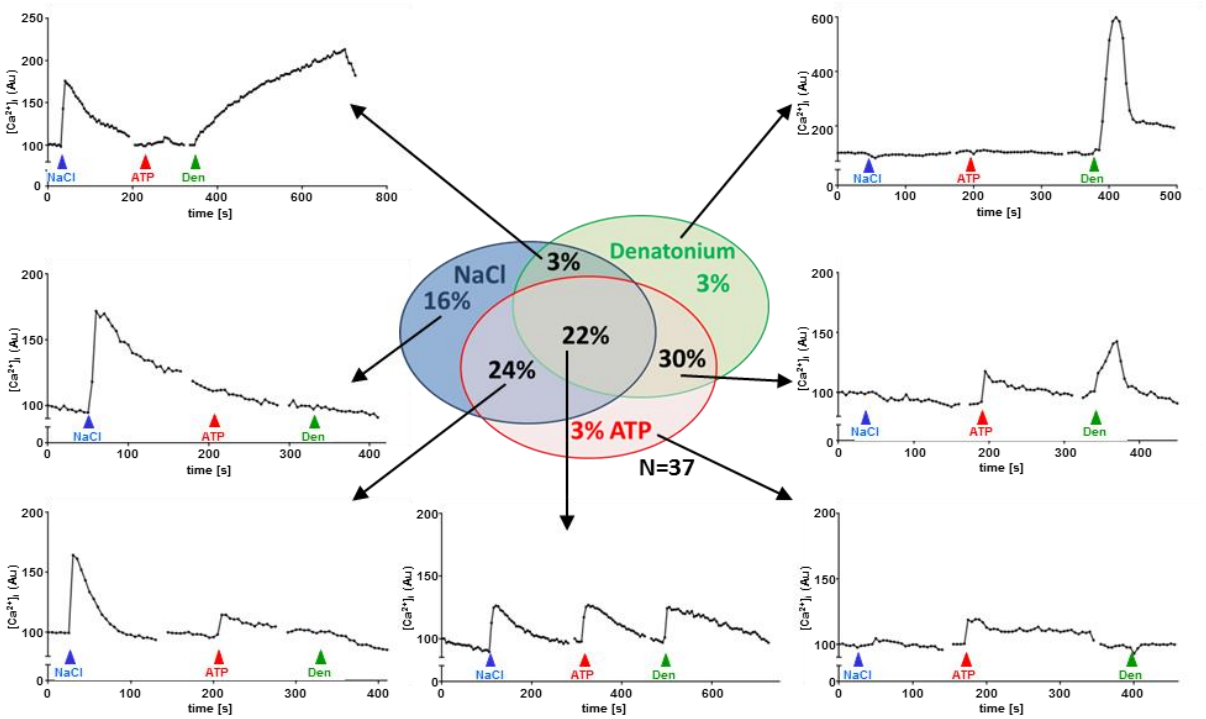

Abbildung 14. UCCC sind polymodal
Antwortverhalten von isolierten UCCC (N=37) auf sequenzielle Stimulation mit NaCl (50 mM) Denatonium (25 mM) und ATP (0.5 mM). Bestimmt wurde die intrazelluläre Calciumkonzentration ($[Ca^{2+}]_i$) von isolierten, vereinzelten $ChAT^+$-Zellen (UCCC) aus ChAT-eGFP-Mäusen mittels kontinuierlichen konfokalen Laserscanning-Aufnahmen der Intensität der Fluoreszenz des Calciumindikators Calcium Orange. Alle Substanzen wurden unter kontinuierlichem Fluss in der Kammer hinzugefügt, so dass die angegebenen Konzentrationen anfänglich erreicht und dann ausgewaschen wurden. Die Sequenz der Stimuli wurde zwischen den Experimenten geändert. Graphen zeigen repräsentative Aufnahmen von einzelnen $ChAT^+$-Zellen. Die y-Achse zeigt arbiträre Einheiten (arbitrary unit; AU), die mit $[Ca^{2+}]_i$ korrelieren; [IV].

Letztlich untermauern die bisherigen Ergebnisse den polymodalen Charakter von UCCC. Dieser polymodale Charakter und damit die Möglichkeit zur Aktivierung durch Substanzen, die in der oropharyngealen Gustation als aversiv, und anderen Substanzen, die als attraktiv wahrgenommen werden, stellt keinesfalls einen Widerspruch dar, da alle detektierten Substanzen ein potentielles Gefahrensignal in der Urethra darstellen. Dies lässt sich dahingehend erklären, dass Bakterien einerseits in der oropharyngealen Gustation als aversiv wahrgenommene bitterrezeptoraktivierende Substanzen produzieren und sezernieren [65, 125, 126] und andererseits freie Aminosäuren ("umami"), die in der oropharyngealen Gustation als attraktiv wahrgenommen, das Bakterienwachstum im Urin erleichtern [130] bzw. der Glutamatmetabolismus das pathogene Potential von Bakterien wie *Proteus mirabilis* im Harnwegsbereich unterstützt [129].
Da weitere Unterscheidungskriterien fehlen, interpretieren wir die vielfältigen Kombinationen der Reaktion auf verschiedene chemosensorische Stimuli und der Genexpression verwandter Signalkomponenten als phänotypische Variation von breit aufgestellten polymodalen chemosensorischen Zellen (Subpopulation), anstatt mehrere klar getrennte Zelltypen zu definieren. Hierdurch war es möglich zu zeigen, dass die neuendeckten urethrale cholinergen Zellen mittels Chemosensorik verschiedene Substanzen wahrnehmen und daher als polymodale UCCC bezeichnet werden können.

3.4 UCCC verwenden Acetylcholin als Botenstoff für parakrine und autokrine Signalübertragungen

I. **Deckmann K***, Filipski K*, Krasteva-Christ G, Fronius M, Althaus M, Rafiq A, Papadakis T, Renno L, Jurastow I, Wessels L, Wolff M, Schütz B, Weihe E, Chubanov V, Gudermann T, Klein J, Bschleipfer T, Kummer W. Bitter triggers acetylcholine release from polymodal urethral chemosensory cells and bladder reflexes. **Proc Natl Acad Sci U S A**. 2014;111(22):8287-92.

III. **Deckmann K**, Rafiq A, Erdmann C, Illig C, Durschnabel M, Wess J, Weidner W, Bschleipfer T, Kummer W. Muscarinic receptors 2 and 5 regulate bitter response of urethral brush cells via negative feedback. **FASEB J**. 2018 Jun;32(6):2903-2910.

Das Konzept der UCCC als chemosensorische Wächterzelle, die die chemische Zusammensetzung der Flüssigkeit auf der Schleimhautoberfläche überwacht und

lokale oder reflexive Reaktionen als protektive Maßnahmen induziert, impliziert eine stimulusinduzierte Signalübertragung an benachbarte Zellen. Aufgrund der Expression des ACh synthetisierenden Enzyms ChAT in UCCC wurde ACh als potenzieller Botenstoff untersucht. Hierbei konnte gezeigt werden, dass der Überstand von isolierten Zellen der Harnröhre mehr ACh enthält, wenn die Zellen mit Denatonium stimuliert wurden (Abbildung 15.).

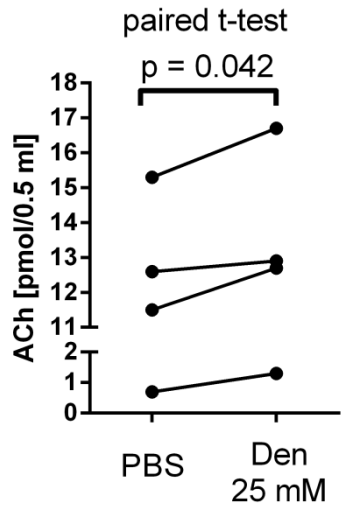

Abbildung 15. Denatonium führt zur ACh-Freisetzung aus isolierten Zellen der Urethra. ACh-Konzentration im Überstand von isolierten Zellen der Urethra nach 5 min Exposition gegenüber PBS (Kontrolle) oder Denatonium. Die Urethrae wurden aus vier Wildtypmäusen (C57BL/6) entnommen und die Zellen vereinzelt und isoliert. Aus einer Harnröhre erhaltene Zellen wurden auf 4 Kammern einer 24-Well-Kulturplatte ausgesät. Jeweils zwei Kammern wurden 5 min lang mit Denatonium (25 mM) bzw. PBS inkubiert. Anschließend wurden die Überstande (0,5 ml) entnommen, gefriergetrocknet und der ACh-Gehalt mittels HPLC (High Performance Liquid Chromatography) und elektrochemischer Detektion bestimmt. Die Werte der beiden Kammern mit gleicher Behandlung aus demselben Tier wurden gepoolt. Isolate von einer Harnröhre wurden als gepaarte Daten behandelt; p-Werte wurden mit einem gepaarten t-Test berechnet; [l].

Des Weiteren konnte ein Anstieg der intrazellulären Calcium-Konzentration in isolierten Zellen der Urethra nach Stimulation mit Denatonium nur beobachtet werden, wenn sie sich in der Nähe von UCCC befanden. In Anwesenheit von Blockern für die mAChR und nAChR blieb dieser Anstieg auch in Anwesenheit der UCCC aus. Die Experimente zeigen somit, dass die Menge an ACh, die bei Stimulation durch einen Bitterstoff freigesetzt wird, ausreicht, um parakrine Effekte zu induzieren.

Interessanterweise zeigten UCCC selbst bei der Stimulation mit Denatonium in Anwesenheit von Blockern für die mAChR und nAChR ein erhöhtes Antwortverhalten

(Abbildung 16.). Diese verstärkte Antwort von UCCC auf Stimulation nach Anwendung einer nAChR/mAChR-Blockermischung zeigt, dass ACh als Sekretionsprodukt der UCCC die Sensitivität der UCCC auf autokrine Weise reguliert.

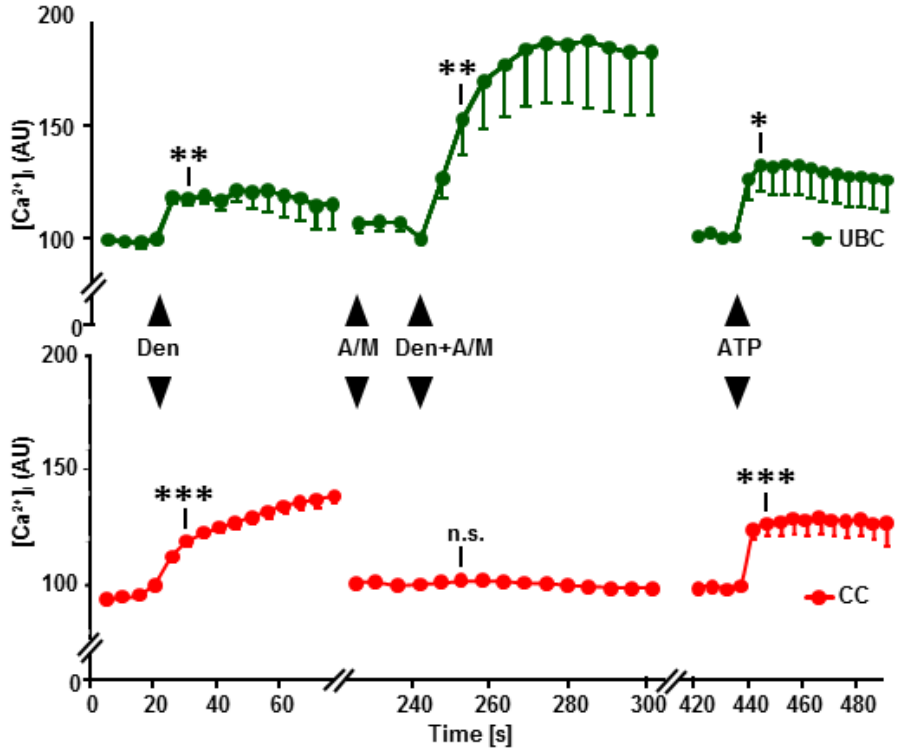

Abbildung 16. UCCC nutzen ACh zur parakrinen Signalübertragung
Parallele Bestimmung der $[Ca^{2+}]_i$ im gleichen Sichtfeld von isolierten urethralen $eGFP^+$-(UBC/UCCC; n=13; oben) und $eGFP^-$- (CC; n=74; unten) Epithelzellen mittels kontinuierlichen konfokalen Laserscanning-Aufnahmen der Intensität der Fluoreszenz des Calciumindikators Calcium Orange. Alle Substanzen wurden unter kontinuierlichem Fluss in der Kammer hinzugefügt, so dass die angegebenen Konzentrationen anfänglich erreicht und dann ausgewaschen wurden. Beide Zelltypen reagieren auf Denatonium (Den; 25 mM) mit einem Anstieg der intrazellulären Ca^{2+}-Konzentration. In Anwesenheit von cholinergen Blockern (Atropin und Mecamylamin; A+M) geht diese Reaktion in $eGFP^-$-Zellen verloren, bleibt aber in $eGFP^+$-Zellen bestehen. Reaktion auf ATP zeigt die Lebensfähigkeit der Zellen am Ende des Experiments. Die y-Achse zeigt arbiträre Einheiten (arbitrary unit; AU), die mit $[Ca^{2+}]_i$ korrelieren; *p<0,05; **p<0,01; ***p<0,001, gepaarter t-Test verglichen mit Wert unmittelbar vor der Substanzapplikation; [I].

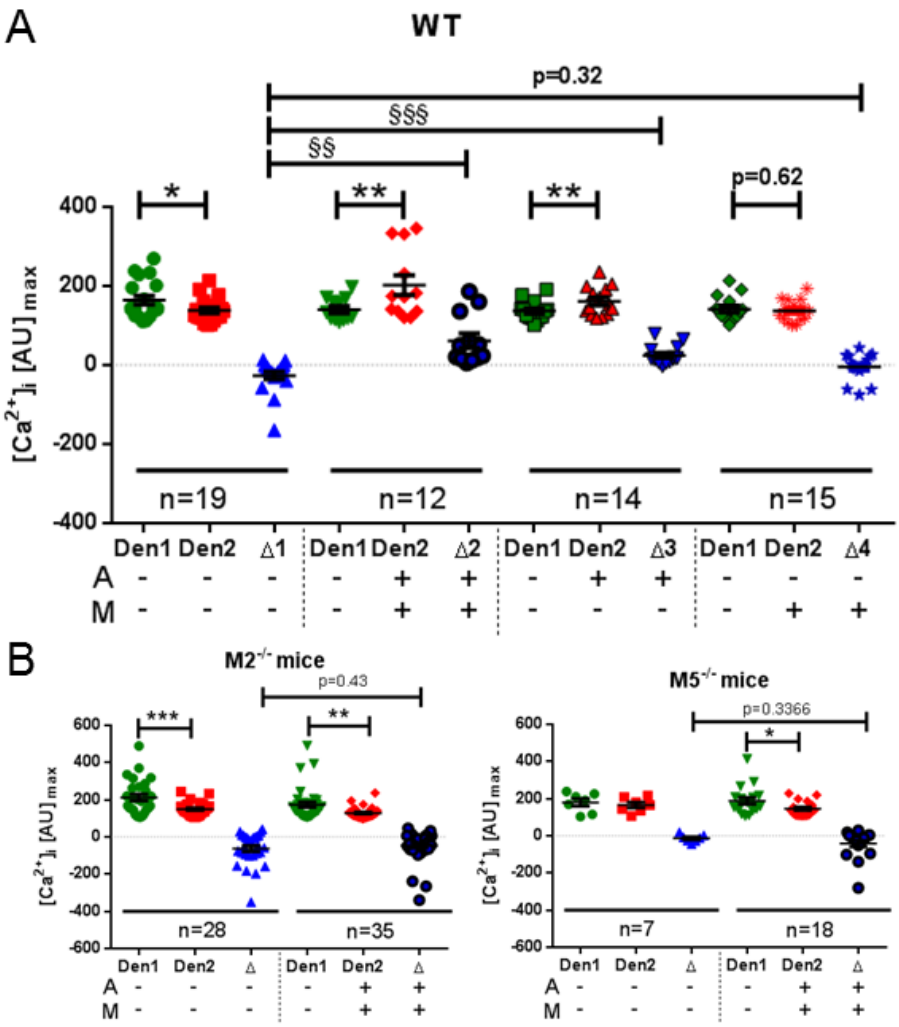

Abbildung 17. UCCC nutzen ACh für einen durch M2- und M5-Rezeptoren vermittelten autokrinen negativen Rückkopplungsmechanismus

Antwortverhalten von isolierten UCCC auf repetitive Stimulation mit Denatonium (25 mM) in Anwesenheit und ohne den mAChR-Blocker Atropin (A; 2 µM) und/oder den nAChR-Blocker Mecamylamin (M; 20 µM)). Bestimmt wurde die intrazelluläre Calciumkonzentration ($[Ca^{2+}]_i$) von einzelnen isolierten, vereinzelten UCCC aus (A) WT-Mäusen und (B) M2-Rezeptor-KO-Mäuse ($M2^{-/-}$) und M5-Rezeptor-KO-Mäuse ($M5^{-/-}$) mittels kontinuierlichen Konfokale Laserscanning-Aufnahmen der Intensität der Fluoreszenz des Calciumindikators Calcium Orange. Die Isolation erfolgte durch magnetgekoppelten TRPM5-Antikörper. Alle Substanzen wurden unter kontinuierlichem Fluss in der Kammer hinzugefügt, so dass die angegebenen Konzentrationen anfänglich erreicht und dann ausgewaschen wurden. Dargestellt sind Spitzenwerte der intrazellulären Calciumkonzentrationen nach Stimulation. Den1 = erste Stimulation, Den2 = zweite Stimulation; Δ = Den2-Den1. Die y-Achse zeigt arbiträre Einheiten (arbitrary unit; AU), die mit $[Ca^{2+}]_i$ korrelieren. Die Werte wurden analysiert mit einem gepaarter t-Test bzw. einer einfaktoriellen ANOVA und Dunnett´s multiplem Vergleichstest; *p<0,05; §§/**p<0,01; §§§/***p<0,001; [III].

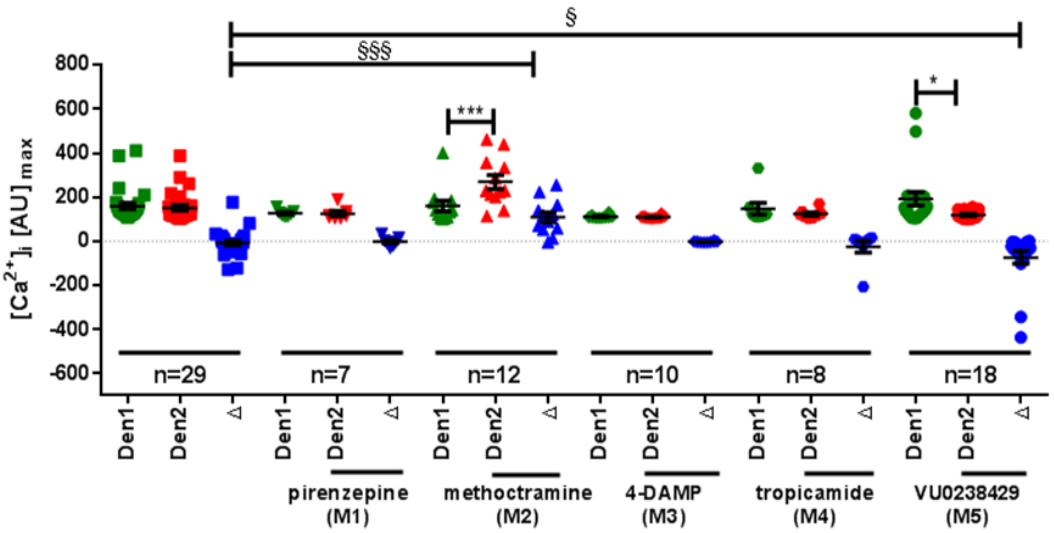

Abbildung 18. Auswirkungen von selektiver pharmakologischer Intervention von muskarinischen Rezeptoren auf die Antwort von UCCC zu bitterem Reiz.
Antwortverhalten von isolierten UCCC auf repetitive Stimulation mit Denatonium (25 mM) in Anwesenheit und ohne verschiedene mAChR-Blocker. Bestimmt wurde die intrazelluläre Calciumkonzentration ($[Ca^{2+}]_i$) von einzelnen isolierten, vereinzelten $ChAT^+$-Zellen (UCCC) aus ChAT-eGFP-Mäusen mittels kontinuierlichen Konfokale Laserscanning-Aufnahmen der Intensität der Fluoreszenz des Calciumindikators Calcium Orange. Alle Substanzen wurden unter kontinuierlichem Fluss in der Kammer hinzugefügt, so dass die angegebenen Konzentrationen anfänglich erreicht und dann ausgewaschen wurden. Dargestellt sind Spitzenwerte der intrazelluären Calciumkonzentrationen nach Stimulation. Den1 = erste Stimulation, Den2 = zweite Stimulation; Δ = Den2-Den1. Die Wirkstoffkonzentrationen waren wie folgt: Denatonium (Den1 und Den2; 25 mM), Pirenzepin (0,001 mM; M1-Rezeptorinhibitor), Methoctramin (0,001 mM; M2-Rezeptorinhibitor), 4-DAMP (0,001 mM; M3-Rezeptorinhibitor), Tropicamid (0,001 mM; M4-Rezeptorinhibitor), und VU 0238429 (0,005 mM; positiv allosterischer Modulator des M5-Rezeptors) Die y-Achse zeigt arbiträre Einheiten (arbitrary unit; AU), die mit $[Ca^{2+}]_i$ korrelieren. Die Werte wurden analysiert mittels einfaktorieller ANOVA und Dunnett´s multiplen Vergleichstest. §§/*p<0,05; §§§/***p<0,001; [III].

Dieses erhöhte Antwortverhalten konnte auf einen cholinergen autokrinen negativen Rückkopplungsmechanismus zurückgeführt werden (Abbildung 17.A). Inhibitor- und Knockout-Maus-Experimente ergaben, dass M2- und M5-Rezeptoren eine entscheidende Rolle bei der autokrinen negativen Regulation von UCCC spielen (Abbildung 17.B und 18.).

Interessanterweise wird in den komplex regulierten Geschmacksknospen auch ein über mAChR reguliertes autokrines cholinerges Signal verwendet, um die gustatorischen Signalweiterleitung zu beeinflussen. Allerdings wirkt der autokrine Mechanismus in Geschmacksknospen, im Gegensatz zum Mechanismus in UCCC,

über M3-Rezeptoren und führt eher zur Verstärkung als zur Abschwächung des gustatorischen Signals [268].

In cholinergen Neuronen findet man häufiger autokrine negative Rückkopplungsschleifen, die über den M2-Rezeptor reguliert werden, so zum Beispiel in Neurone des Striatums [269], in α-Motoneuronen [270] und postganglionären parasympathischen Neuronen [271]. Bei parasympathischen cholinergen Neuronen kann auch der M4-Rezeptor als Autorezeptor dienen, der die ACh-Freisetzung hemmt. Er ist auch der dominante, wenn auch nicht der einzige Rezeptor, mit dieser Funktion in der Harnblase der Maus [272]. Beide, M2- und M4-Rezeptoren, wirken typischerweise über G_i-Proteine und die nachgeschaltete Hemmung der Adenylatcyclaseaktivität und spannungsaktivierte Ca^{2+}-Kanäle [273]. Dies passt sehr gut zu den von uns erhobenen Daten, dass der M2-Rezeptor eine Hemmung auf den durch einen bitteren Stimulus ausgelösten Anstieg von $[Ca^{2+}]_i$ in UCCC bewirkt.

Der M5-Rezeptor ist jedoch im Allgemeinen eher mit einer Zunahme von $[Ca^{2+}]_i$ assoziiert [273, 274] und erhöht dementsprechend die Aktivität von primären afferenten Neuronen im Rückenmark, spinalen glutamatergen Interneuronen und Somatodendriten von Neuronen der Substantia nigra [273, 275, 276]. Dieses steht in klarem Gegensatz zu der dämpfenden Wirkung auf stimuliertes $[Ca^{2+}]_i$, die in UCCC beobachtet wird. Dennoch ist ein durch den M5-Rezeptor vermittelte Hemmung auch in anderen Bereichen bekannt, zum Beispiel in dopaminergen Nervenendigungen des Striatums [274]. Die zugrundeliegenden Signalwege sind aber noch unbekannt. Zusammengenommen konnte gezeigt werden, dass UCCC nach Stimulation ACh freisetzen, das sowohl als autokriner als auch als parakriner Botenstoff fungiert.

3.5 UCCC lösen neuronale Reflexe aus

I. **Deckmann K***, Filipski K*, Krasteva-Christ G, Fronius M, Althaus M, Rafiq A, Papadakis T, Renno L, Jurastow I, Wessels L, Wolff M, Schütz B, Weihe E, Chubanov V, Gudermann T, Klein J, Bschleipfer T, Kummer W. Bitter triggers acetylcholine release from polymodal urethral chemosensory cells and bladder reflexes. **Proc Natl Acad Sci U S A**. 2014;111(22):8287-92.

Eine Wächterzelle, die nach Erkennung von potenziell schädlichen Substanzen keine Abwehrreaktionen einleiten kann, ist sprichwörtlich ein zahnloser Tiger. Eine mögliche Abwehrreaktion, die UCCC initiieren könnte, wären Miktionen zum Ausspülen der

eindringenden Bedrohungen. Hierzu müssten UCCC sensorische Nervenfasern stimulieren. Da UCCC den Botenstoff ACh freisetzen, liegt die Vermutung nahe, dass sensorische Nervenfasern mit cholinergen Rezeptoren als Empfänger des Signalstoffes dienen. Immunhistochemische Untersuchungen und Verwendung einer Reportermaus zeigten, dass Nervenfasern mit Expression der nAChR Untereinheit α3 ein dichtes Netzwerk unterhalb des urethralen Epithels bilden, in es eintreten und, vergleichbar wie bei den chemosensorischen Zellen in der Trachea [155], in unmittelbarer Umgebung von UCCC zu finden sind (Abbildung 19.A).

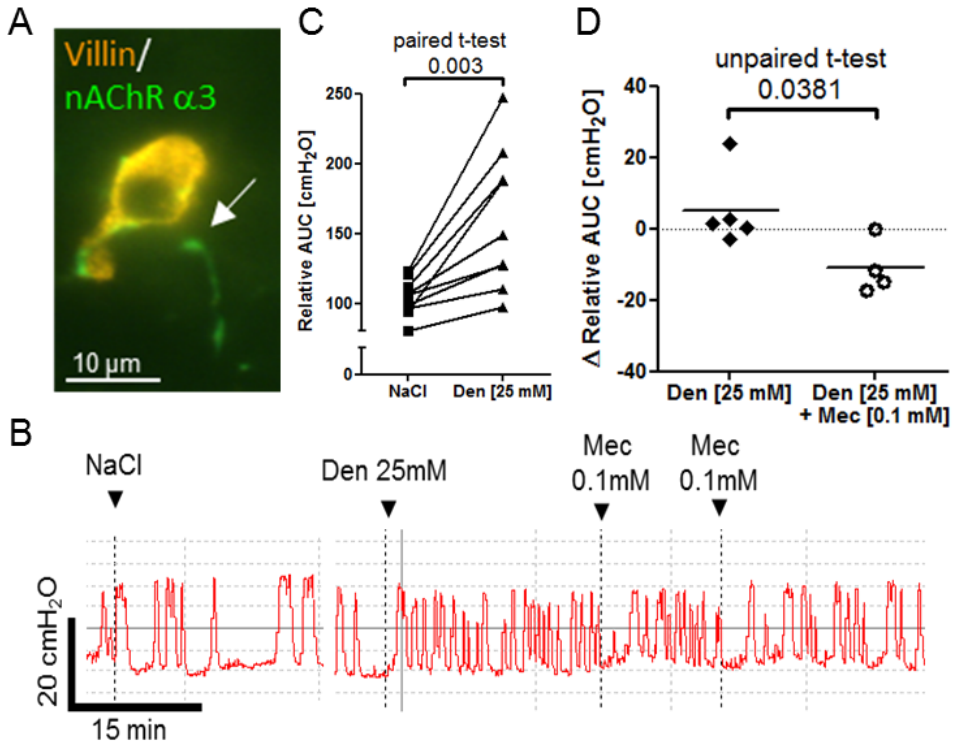

Abbildung 19. Sensible Nervenfasern reichen an UCCC heran und lösen reflektorische Blasenaktivierung bei Applikation einer Bittersubstanz aus
(A) Eine sensorische Nervenfaser, die eGFP unter der Kontrolle des Promotors der α3-Untereinheit des Nikotinrezeptors exprimiert (Pfeil), stellt Kontakt mit einer Villin-immunreaktiven Zelle im urethralen Epithel her. (B) Zystometrische Aufzeichnungen von anästhesierten Ratten. Dargestellt ist der intravesikuläre Druck, der durch die Kontraktion und der damit einhergehenden Miktion beeinflusst wird. Intraurethrale Stimulation mit Denatonium erhöht die Detrusoraktivität im Vergleich zu physiologischer Kochsalzlösung (NaCl), diese Stimulation wird durch Mecamylamin (Mec) vermindert. (C-D) Detrusoraktivität von anästhesierten Ratten quantifiziert als „Area under the Curve“ (AUC); [l].

Um herauszufinden, ob die Stimulation von UCCC die Detrusoraktivität und somit das Miktionsverhalten beeinflusst, wurden urodynamische Untersuchungen durchgeführt.

Diese Untersuchungen sind ausschließlich in vivo durchführbar, da hierzu ein funktionierender Miktionsreflexbogen vorhanden sein muss. Eine Stimulation von UCCC in vitro oder am toten Tier würde nicht zu einer Fortleitung der Information über die sensorischen Fasern zum Rückenmark führen. Es käme somit nicht zur Umschaltung auf Fasern, welche wieder zurück zur Blase führen (Efferenzen), und in Folge bliebe die Kontraktion der Blasenmuskulatur im Sinne einer Miktion aus. Um urodynamische Untersuchungen durchführen zu können, wurde zunächst ein Katheter in den Blasendom der zu untersuchenden Tiere implantiert. Hierüber konnte die Blase mit physiologischer Kochsalzlösung gefüllt werden. Hatte die Blase einen entsprechenden Füllstand erreicht, wurde eine Miktion ausgelöst. Miktionen, d.h. zur Entleerung führende Kontraktionen des Blasenmuskels, wurden als Druckerhöhung innerhalb der Blase über ein Manometer detektiert (Blasendruckmessung = Cystomanometrie, CMM). Durch die gleichmäßige Füllung der Blase über eine Perfusionspumpe ergab sich ein gleichmäßiges Miktionsmuster (Abbildung 20.). Dieses Muster wurde durch Denatonium charakteristisch verändert. Die Applikation von Substanzen erfolgte über einen intraurethral eingeführten Katheter. Diese Untersuchung kann prinzipiell im wachen Zustand der Tiere oder aber in Narkose durchgeführt werden. Da während der CMM eine Substanzapplikation intraurethral erfolgte, wurde sie in Narkose durchgeführt. Als Narkotikum wurde Urethan verwendet, da es bei cystomanometrischen Untersuchungen am Nager, im Gegensatz zu zahlreichen anderen Narkoseschemata, den Miktionsreflex nicht unterdrückt [277, 278]. Die CMM bei der urethananästhesierten Maus ist jedoch äußerst schwierig, da Mäuse hierbei häufig eine Blasenatonie entwickeln, welche eine Überlaufblase zur Folge hat. Messungen sind somit in der Regel an der urethannarkotisieren Maus nicht möglich. Mäuse haben darüber hinaus ein deutlich erhöhtes Letalitätsrisiko bei Urethannarkosen [279]. Deshalb wurden für die urodynamischen Untersuchungen urethananästhesierte Ratten verwendet. Ziel der Untersuchungen war es zu ermitteln, inwiefern eine intraurethrale Stimulation mit dem UCCC-stimulierenden Bitterstoff Denatonium zu einer reflektorischen Veränderung der Detrusoraktivität und somit zu einer Veränderung des Miktionsverhaltens führt. Es konnte gezeigt werden, dass die intraurethrale Stimulation mit Denatonium zur Erhöhung der Detrusoraktivität führt und somit zum reflexiven Auslösen einer Miktion. Dies erfolgte im Konzentrationsbereich,

der auch zur Stimulation von UCCC führte. Durch die lokale Applikation eines nikotinergen Blockers wurde die Detrusorantwort signifikant reduziert (Abbildung 19.).

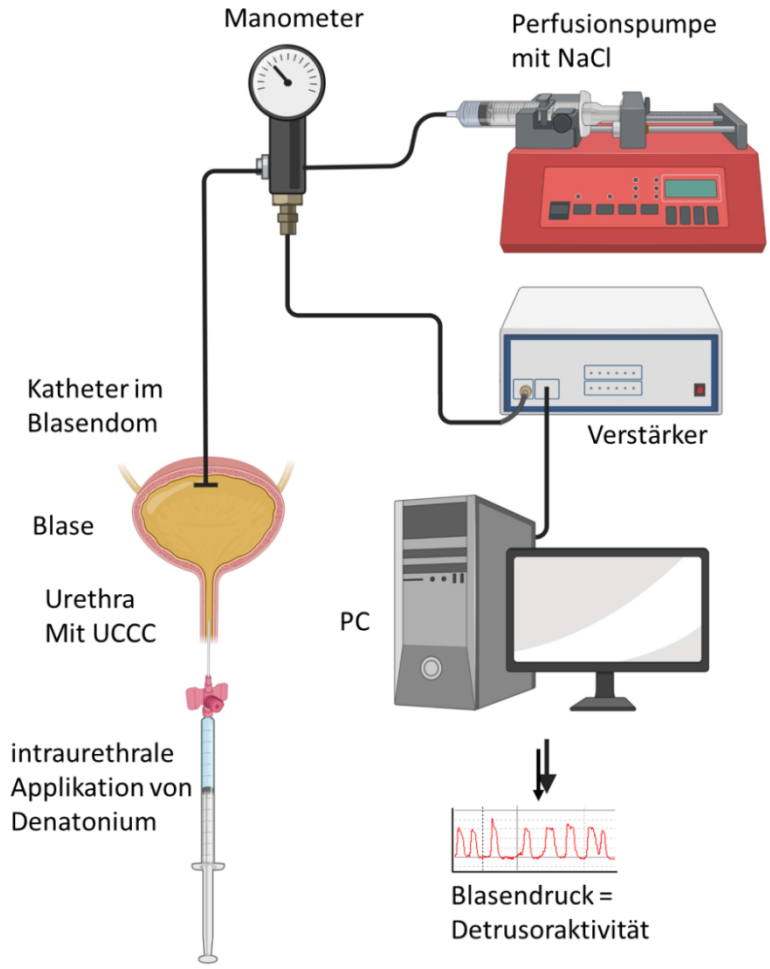

Abbildung 20. Aufbau einer urodynamischen Messstation
Zur urodynamischen Untersuchung wurde ein Katheter in den Blasendom der zu untersuchenden Ratten implantiert. Hierüber konnte die Blase gleichmäßig mit physiologischer Kochsalzlösung über eine Perfusionspumpe gefüllt werden. Miktionen, d.h. zur Blasenentleerung führende Kontraktionen des Blasenmuskels, wurden als Druckerhöhung innerhalb der Blase über ein Manometer detektiert. Die Applikation von Substanzen (Denatonium) erfolgte über einen intraurethral eingeführten Katheter. Erstellt mit BioRender.com

Daraus lässt sich schließen, dass diese Reflexaktivierung abhängig von einer cholinergen nikotinrezeptorabhängigen Signalweiterleitung von UCCC auf sensorische Nervenfasern ist. Die Einleitung der Miktion wird als protektive Maßnahme interpretiert, da es zum Auswaschen von potentiell schädlichen Stoffen führt. Nichtsdestotrotz wurde der denatonium-induzierte Anstieg der Detrusoraktivität nicht vollständig durch den nAChR-Inhibitor Mecamylamin aufgehoben. Hierfür könnte es

mehrere Erklärungen geben. Möglicherweise könnte ein zusätzlicher exzitatorisch wirkender mAChR beteiligt sein. Interessanterweise ist bekannt, dass mAChR von afferenten Neuronen der Harnwege exprimiert werden [280]. Eine weitere Möglichkeit wäre die zusätzliche Beteiligung eines Cotransmitters wie ATP. ATP wird von Geschmackszellen verwendet, um Informationen an afferente Fasern in Geschmacksknospen zu übertragen [102]. Eine andere Erklärung wäre ein unzureichender Zugang von intraluminal appliziertem Mecamylamin zur basolateral gelegenen Kommunikationsstelle zwischen chemosensorischen Zellen und Nervenfasern, da Epithelien der unteren Harnwege eine außerordentlich dichte Barriere bilden [281]. Zusammenfassend konnte gezeigt werden, dass die intraurethrale Applikation eines UCCC-stimulierenden Bitterstoffes zur Einleitung einer als protektiv interpretierten Miktionen führt.

3.6 UCCC sind in verschiedenen Säugetierspezies präsent

I. **Deckmann K***, Filipski K*, Krasteva-Christ G, Fronius M, Althaus M, Rafiq A, Papadakis T, Renno L, Jurastow I, Wessels L, Wolff M, Schütz B, Weihe E, Chubanov V, Gudermann T, Klein J, Bschleipfer T, Kummer W. Bitter triggers acetylcholine release from polymodal urethral chemosensory cells and bladder reflexes. **Proc Natl Acad Sci U S A**. 2014;111(22):8287-92.

II. **Deckmann K,** Krasteva-Christ G, Rafiq A, Herden C, Wichmann J, Knauf S, Nassenstein C, Grevelding CG; Dorresteijn A, Chubanov V, Gudermann T, Bschleipfer T, Kummer W. Cholinergic urethral brush cells are widespread throughout placental mammals**. Int Immunopharmacol**. 2015 Nov;29(1):51-6**.**

Initial wurden UCCC in Mäusen mit Hilfe von ChAT-eGFP-Reportertieren entdeckt. Mit der Frage einer medizinischen Übertragbarkeit der Befunde und versuchsspezifischer Faktoren wurde ihr Vorkommen anschließend in Menschen und Ratten nachgewiesen. Während dieser Arbeit stellte sich die Frage, ob UCCC auch in anderen Säugetieren vorkommen. Um dies zu klären, wurden in 11 weiteren Säugetierarten aus 5 verschiedenen Ordnungen mittels Antikörper gegen Bürstenzellmarker nach UCCC gesucht. In der Ordnung der Nagetiere (Rodentia) wurden neben den Mäusen (*Mus musculus*) und Ratten (*Rattus norvegicus*) Hamster (*Mesocricetus auratus*) und Meerschweinchen (*Cavia porcellus*) untersucht. In der Ordnung der Primaten (Primates) wurden neben Menschen (*Homo sapiens sapiens*), Javaneraffen (*Macaca fascicularis*) und Weißbüschelaffen (*Callithrix jacchus*) untersucht. In der Ordnung der

Fleischfresser (Carnivora) umfasste die Untersuchung Hunde (*Canis lupus familiaris*), Katzen (*Felis catus*) und den Dachs (*Meles meles*). In der Ordnung der Paarhufer (Artiodactyla) waren es Schweine (*Sus scrofa domestica*), Rinder (*Bos taurus*) und Rotwild (*Capreolus capreolus*), und in der Ordnung der Unpaarhufer (Perissodactyla) wurde in den Harnröhren von Pferden (*Equus ferus caballus*) mittels Antikörper gegen Bürstenzellmarker nach UCCC gesucht (Abbildung 21.).

Mit den verwendeten Markern konnten in allen untersuchten Spezies solitäre Zellen in der Urethra identifiziert werden. Diese Daten weisen darauf hin, dass UCCC innerhalb der Säugetiere weitverbreitet sind und sich vor mehr als 64,5 Millionen Jahren entwickelt haben müssten.

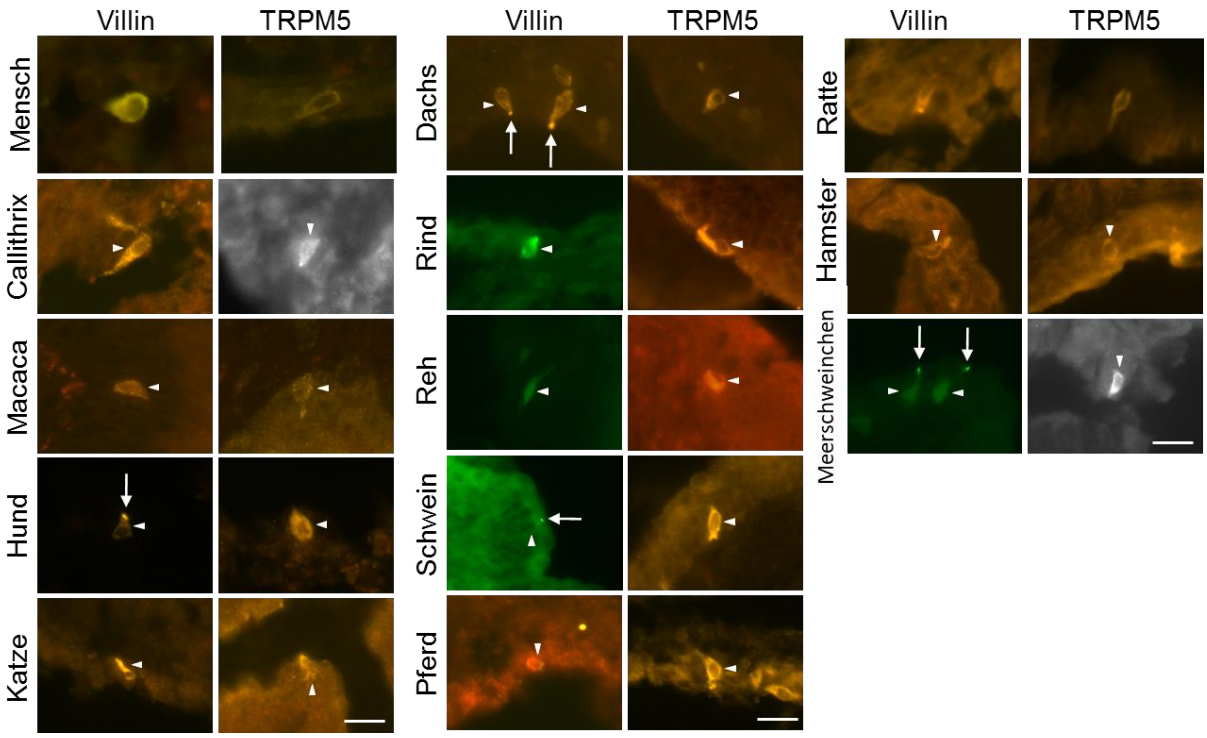

Abbildung 21. UCCC in 13 verschiedene Säugetierarten
Immunhistochemische Markierung von urethralen Epithelzellen mit Antikörpern gegen den Bürstenzellmarker Villin und Antikörpern gegen den UCCC-Marker TRPM5; [I; II].

3.7 UCCC entstehen postnatal und es gibt einen geschlechtsspezifischen Unterschied in der Entwicklung

V. Perniss A, Schmidt P, Soultanova A, Dahlke K, Voigt A, Kummer W, **Deckmann K**. Postnatal development of epithelial cholinergic chemosensory cells of the urethra, trachea and thymus of mice. **Cell Tissue Res** 2021 Jul;385(1):21-35.

Neben der evolutionären Entwicklung wurde auch die postnatale Entwicklung der UCCC in Mäusen untersucht. Hierbei zeigte sich ein Sexualdimorphismus. Bei männlichen Mäusen traten UCCC erstmals zwischen 6 bis 10 Tagen nach der Geburt auf (Postnatal 6-10; P6-10), bei weiblichen Mäusen erst zwischen Tag 11 und 20 nach Geburt (P11-20). Bei beiden Geschlechtern wurden maximale UCCC-Zahlen im Zeitraum zwischen P40 und P220 erreicht und die Anzahl ging danach zurück. Junge (P6-P40) männliche Mäuse hatten zunächst signifikant höhere UCCC-Zahlen als gleichaltrige weibliche Mäuse, was durch das frühere Auftreten der UCCC erklärt werden kann. Bemerkenswerterweise zeigte sich ein gegenteiliges Bild in älteren (P40+) Tieren (Abbildung 22.). Diese Daten zeigen, dass es bei der Entwicklung von UCCC einen Geschlechtsdimorphismus gibt.

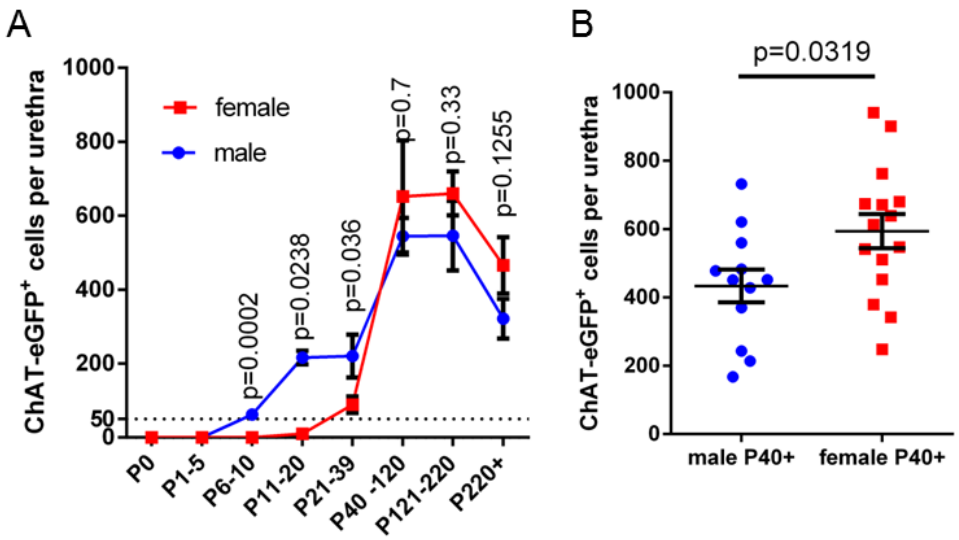

Abbildung 22. Postnatale Entwicklung von UCCC
(A) Anzahl der ChAT-eGFP⁺-Zellen pro Urethra, ermittelt in “whole-mount” Präparaten von weiblichen und männlichen Mäusen an verschiedenen Zeitpunkten während der Entwicklung. (B) Anzahl von ChAT-eGFP⁺ Zellen pro Harnröhre in Tieren P40+, kumulierte Daten der drei ältesten Altersgruppen (männlich N=26, weiblich N=21); [V].

3.8 Das Protein MyD88 und Toll-like-Rezeptoren haben einen Einfluss auf die Entwicklung von UCCC

V. Perniss A, Schmidt P, Soultanova A, Papadakis T, Dahlke K, Voigt A, Schütz B, Kummer W, Deckmann K. Development of epithelial cholinergic chemosensory cells of the urethra and trachea of mice. **Cell Tissue Res** 2021 Jul;385(1):21-35.

Da UCCC als Wächterzellen gegen potentiell schädliche Substanzen und Eindringlinge wie Bakterien fungieren, wurde untersucht, ob die Expression von Rezeptoren und Signalwegen, die zur Bakteriendetektion genutzt werden, einen Einfluss auf die UCCC-Entwicklung haben.

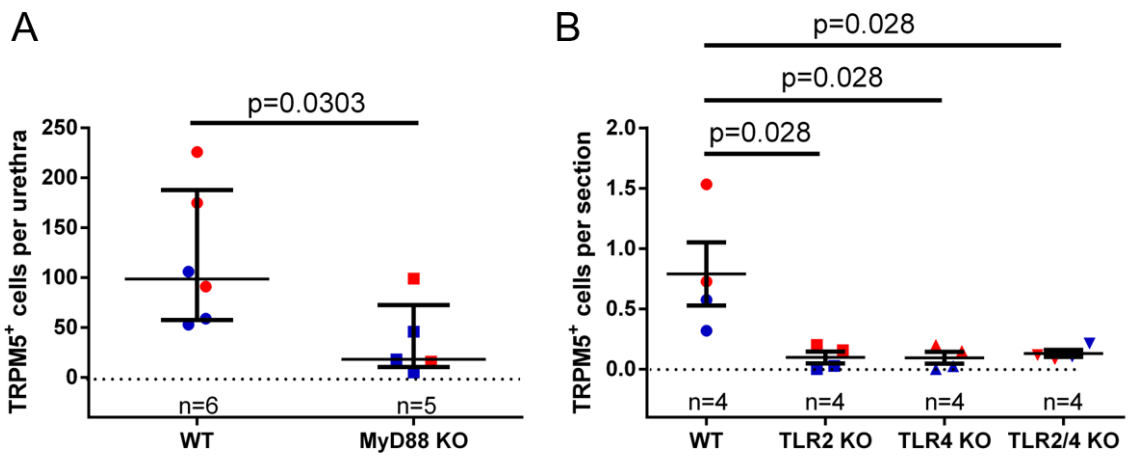

Abbildung 23. UCCC in MyD88-KO-, TLR2-KO-, TLR4-KO- und TLR2/4-KO-Mäusen
(A) Quantitative Analyse von TRPM5$^+$-Zellen pro Urethra, gezählt in "whole-mount" Präparaten von weiblichen und männlichen MyD88-KO- und WT-Mäusen. (B) Anzahl von TRPM5$^+$-Zellen in Schnitten der Urethrae von TLR-WT-, TLR2-KO-, TLR4-KO- und TLR2/4-KO-Mäusen. Jeder Datenpunkt repräsentiert die durchschnittliche Anzahl von Zellen aus 20 Schnitten von einem Tier. Balken und Fehlerbalken zeigen Mittelwert und SEM. Blau: männliche Tiere, Rot: weibliche Tiere. Alle untersuchten Tiere waren erwachsen (> 12 Wochen). P-Werte wurden mit dem Mann-Whitney-Test berechnet; [V].

Deshalb wurden der Einfluss der Deletion der Toll-like-Rezeptoren (TLR) 2 und 4 sowie MyD88 untersucht. MyD88 ist an der nachgeschaltete Signalkaskade aller TLRs mit Ausnahme von TLR3 beteiligt [282]. TLR2 und TLR4 wurden aufgrund ihrer Rolle bei der Erkennung von bakteriellen Lipopeptiden und Lipoteichonsäuren von grampositiven Bakterien (TLR2) und Lipopolysaccharid von gramnegativen Bakterien

(TLR4) ausgewählt [283, 284]. Die Untersuchungen zeigten, dass sowohl in Urethrae von MyD88-defizienten als auch in Urethrae von TLR2- und TLR4-defizienten Mäusen signifikant weniger UCCC zu finden sind (Abbildung 23.).

3.9 UCCC sind chemosensorische Wächterzellen, initiieren Abwehrmechanismen und beeinflussen die Miktion

I. **Deckmann K***, Filipski K*, Krasteva-Christ G, Fronius M, Althaus M, Rafiq A, Papadakis T, Renno L, Jurastow I, Wessels L, Wolff M, Schütz B, Weihe E, Chubanov V, Gudermann T, Klein J, Bschleipfer T, Kummer W. Bitter triggers acetylcholine release from polymodal urethral chemosensory cells and bladder reflexes. **Proc Natl Acad Sci U S A**. 2014;111(22):8287-92.

III. **Deckmann K**, Rafiq A, Erdmann C, Illig C, Durschnabel M, Wess J, Weidner W, Bschleipfer T, Kummer W. Muscarinic receptors 2 and 5 regulate bitter response of urethral brush cells via negative feedback. **FASEB J**. 2018 Jun;32(6):2903-2910.

IV. Kandel C, Schmidt P, Perniss A, Keshavarz M, Scholz P, Osterloh S, Althaus M, Kummer W, **Deckmann K**. ENaC in Cholinergic Brush Cells. **Front Cell Dev Biol.** 2018 Aug 15;6:89.

VI. **Deckmann K,** Kummer W. Chemosensory epithelial cells in the urethra: sentinels of the urinary tract. **Histochem Cell Biol.** 2016 Dec; 146(6):673-683.

VII. Kummer W**, Deckmann K.** Brush cells, the newly identified gatekeepers of the urinary tract. **Curr Opin Urol.** 2017 Mar; 27(2):85-92

Alle unsere Ergebnisse weisen darauf hin, dass es sich bei UCCC um Wächterzellen handelt, die mittels Geschmacksrezeptoren und Elementen der Geschmackssignaltransduktionskaskade entscheidend an der Detektion und Abwehr von eindringender Noxen und Keime beteiligt sind. Sie bestätigen das Konzept der UCCC als chemosensorische „Sentinel“-Zelle, die die chemische Zusammensetzung der Flüssigkeit auf der Schleimhautoberfläche überwacht und durch ACh-Freisetzung lokale oder reflexive Abwehrmechanismen induziert. Hierbei zeigten sich verschiedenen Subpopulationen, die über ein jeweiliges Rezeptorrepertoire verfügen, um verschiedene potenziell gefährliche Stoffe wie zum Beispiel Bitterstoffe, Umami, Salz und bakterielle Metabolite wahrzunehmen.

Hierzu sei erwähnt, dass bei der oropharyngealen Geschmackswahrnehmung bitter einen aversiven Reiz und umami einen lohnenden Reiz darstellt, was die Frage nach der möglichen funktionellen Bedeutung der Wahrnehmung beider Eigenschaften durch eine einzelne Zelle aufwirft. Im Gegensatz dazu stellen diese Eigenschaften auf anderen Schleimhautoberflächen, wie der Harnröhrenschleimhaut, einen potenziell schädlichen (aversiven) Gehalt dar. Bakterien produzieren und sezernieren bitterrezeptoraktivierende Substanzen [159, 258, 259]. In Biofilmen können solche Substanzen aus dem gramnegativen Bakterium *Pseudomonas aeruginosa*, einem der vorherrschenden verursachenden Mikroorganismen bei katheterassoziierten Harnwegsinfektionen [261], Konzentrationen von bis zu 600 µM erreichen [260]. Andererseits ist der Glutamatstoffwechsel positiv mit dem pathogenen Potenzial von *Proteus mirabilis* im Harntrakt verknüpft [262] und freie Aminosäuren (d.h. umami) fördern das Bakterienwachstum im Urin [263]. Daher kann die Bitter/Umami-Polymodalität chemosensorischer Zellen dazu dienen, das Spektrum für die Erkennung potenziell gefährlicher Stoffe im Harnröhrenlumen zu erweitern. Interessanterweise reagieren diese chemosensorischen Zellen auf hitzeinaktivierte UPEC, die Hauptursache für eine Harnwegsinfektion [256]. UCCC werden demnach als Wachposten der unteren Harnwege interpretiert, dessen Aufgabe die Überwachung der Schleimhautoberfläche und die Detektion potenziell gefährliche Inhalte ist. Die Hauptfunktion der UCCC scheint also im Schutz vor aufsteigenden Harnwegsinfektionen zu liegen. Hierfür ist eine Lokalisation am Eingang in den Urogenitaltrakt besonders sinnvoll.

Die physiologische Bedeutung der Reaktion von UCCC auf Salz bleibt ungewiss. UCCC-stimulierende Salzkonzentrationen können im Urin von erwachsenen Mäusen während Wassermangels oder hoher Salzaufnahme durchaus erreicht werden [285]. Bedrohliche bakterielle Infektionen sind jedoch in der Regel nicht mit erhöhten Salzkonzentrationen verbunden. Somit könnte ENaCα in UCCC eine andere Funktion haben als die Überwachung der luminalen NaCl-Konzentration. ENaC ist auch ein mechanosensitiver Ionenkanal, der auf Scherkräfte reagiert [286, 287]. Deshalb ist es denkbar, dass eine ENaC exprimierende UCCC an Messung des Urinflusses beteiligt sind. Diese Theorie wird dadurch gestützt, dass Scherkräfte auf die gesamte Zelle wirken, was die Expression von ENaC im gesamten Epithel und nicht nur an der Membran, die ins Lumen reicht, erklären würde.

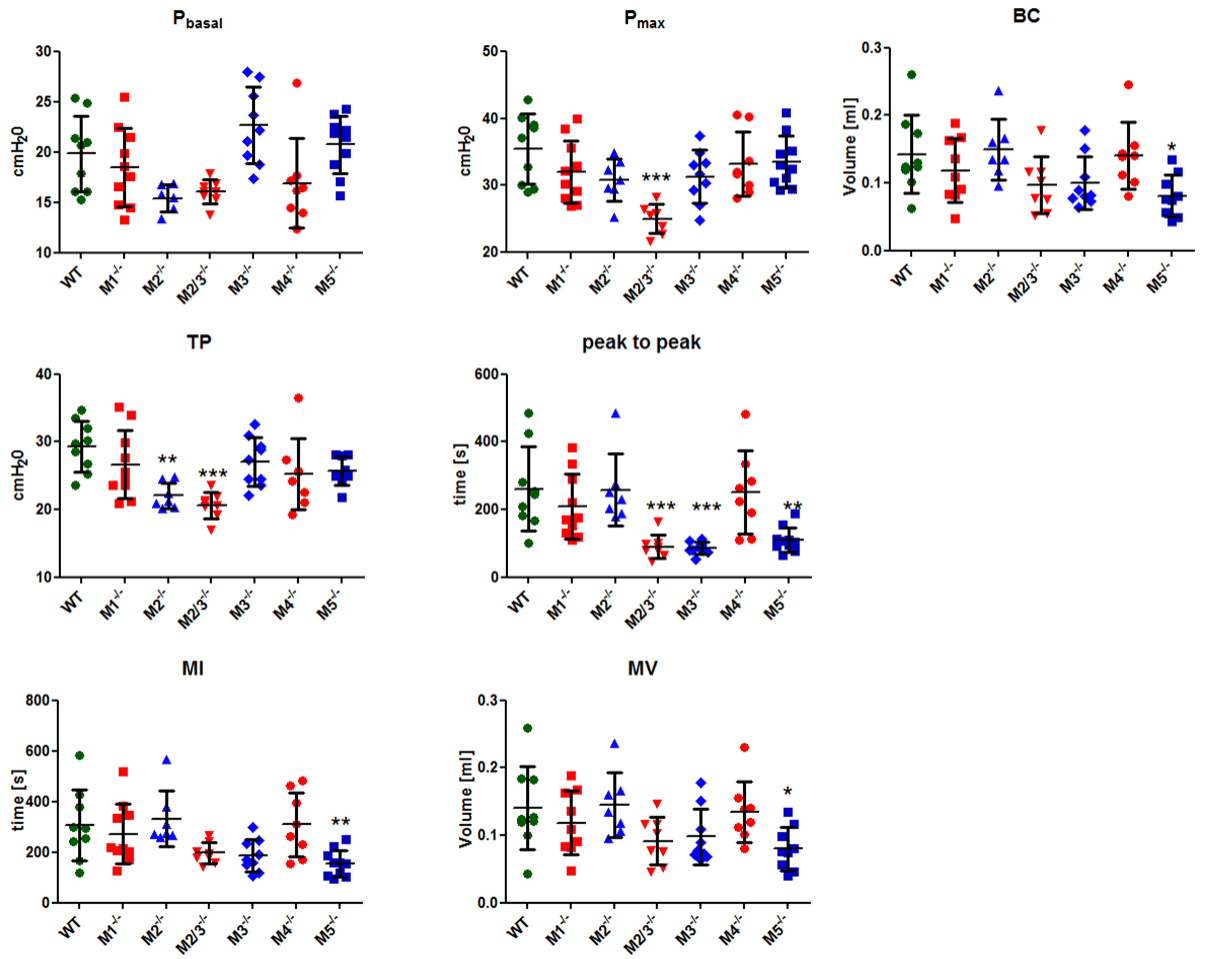

Abbildung 24. Urodynamische Messungen in M1–5-defizienten Mäusen
Zystometrie wurde durchgeführt bei wachen, sich frei bewegenden Mäusen. Die Infusion der Kochsalzlösung erfolgte über einen Katheter im Blasendom direkt in die Blase mit einer Geschwindigkeit von 1,5 ml/h. Nach einer Stabilisierungsphase von 15–30 min wurden der intravesikale Druck und die Miktion kontinuierlich aufgezeichnet. Analysiert wurden das Basaldruckniveau (Pbase), der maximale Detrusordruck während Miktion (Pmax), Schwellendruck (TP), Blasenkapazität (BC), Zeitintervall zwischen 2 Druckspitzen (PP), Miktionsintervall (MI), Miktionsvolumen (MV) und Residualvolumen (RV). Zur statistischen Auswertung der zystometrischen Parameter zwischen den jeweiligen Mausstämmen wurde eine 1-faktorielle ANOVA, gefolgt von einem Mehrfachvergleichstest nach Dunnett, verwendet; *p<0,05, **p<0,01, ***p, 0,001; [III].

Die als Abwehrmechanismus initiierte Miktion würde demnach die Scherkräfte in der Urethra erhöhen und somit ENaC-vermittelt den von UCCC eingeleiteten Schutzreflex amplifizieren. Dafür spricht auch die Beobachtung, dass die Effizienz der Harnblasenentleerung über einen sensorischen Rückkopplungsmechanismus in der

Urethra kontrolliert wird. In der Urethra sind solche „Durchflusssensoren“ zwar physiologisch gut charakterisiert, ihre anatomische Lokalisation wurde aber noch nicht gefunden [288-290].

Allerdings zeigen unsere Experimente auch eine mögliche andere Seite von UCCC. UCCC regulieren sich selbst über einen durch M2- und M5-Rezeptoren vermittelten cholinergen autokrinen negativer Rückkopplungsmechanismus. Tiere mit ungehemmten UCCC zeigen Symptome einer überaktiven Blase (Abbildung 24.). Ein OAB-Syndrom geht oft mit einer fehlerhaften Steuerung und mit einer Detrusorhyperaktivität einher. Eine solche fehlerhafte Steuerung könnte auch durch eine Fehlaktivierung oder Überaktivität von UCCC hervorgerufen werden und Ursache einer Detrusorhyperaktivität sein. Interessanterweise wird das OAB-Syndrom mit Antagonisten von mAChR behandelt [69]. Hierbei kommen primär M2 bzw. M3-Rezeptor selektive Antimuskarinika [219, 222-250] zum Einsatz, was in Anbetracht der Rolle dieser Rezeptoren während der Miktion auch sinnvoll ist. In Bezug auf überaktive UCCC als Auslöser von OAB sind Antimuskarinika mit hemmender Wirkung auf den M2-Rezeptor nach unseren Erkenntnissen auch nützlich. Da aber auch der M5-Rezeptor hierbei eine zentrale Rolle zu spielen scheint, wäre dieser ein weiterer selektive angreifbarer Ansatzpunkt zur Therapie.

Eine selektive zu Beeinflussung des M5-Rezeptors mittels einem Medikaments, welchen die Blut-Hirnschranke nicht passieren kann, um mögliche Nebenwirkungen des hauptsächlich im ZNS exprimierten Rezeptors [273, 275, 276] zu vermeiden, stellt somit eine vielversprechende therapeutische Option dar.

Zusammenfassen konnte ein bislang unbekannter Zelltyp in der Urethra identifiziert werden. Diese UCCC sind Wächterzellen am Eingang des Urogenitaltraktes, die über klassische Geschmacksrezeptoren die chemische Zusammensetzung des Flüssigkeitsfilms auf der Schleimhautoberfläche auf das Vorhandensein potenziell schädlicher Substanzen, einschließlich bakterieller Produkte, prüfen und daraufhin ACh freisetzen, dass über Nervenfasern reflektorische Abwehrreaktionen einleitet.

4 Zusammenfassung

Die ableitenden Harnwege sind nicht nur einfache muskuläre Röhren zur Speicherung und Abgabe von Harn. Aufgrund ihrer direkten Verbindung zur Außenwelt stellen sie eine potentielle Eintrittspforte für toxische Substanzen und Mikroben dar. Im mehrschichtigen Epithel der Urethra befinden sich verschiedene solitäre Zelltypen: neuroendokrine Zellen, nicht-cholinerge Bürstenzellen und cholinerge chemosensorische Zellen (Abbildung 25.).

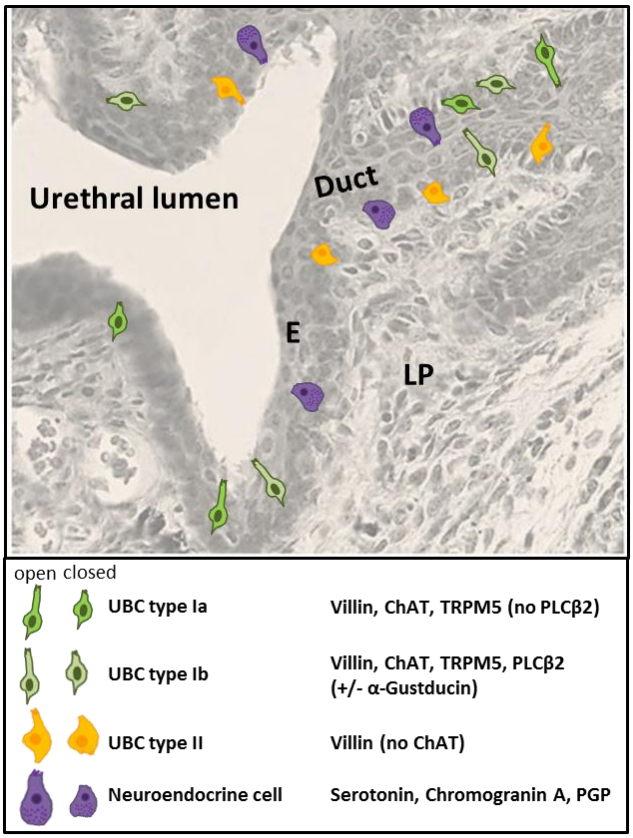

Abbildung 25. Übersicht der verschiedenen solitären Epithelzellen der Urethra
Mögliche chemosensorische Epithelzelltypen in der Harnröhre und Ausführungsgängen der Harnröhrendrüsen, ein ursprünglicher mit Hämatoxylin-Eosin gefärbter Abschnitt wurde als Hintergrundbild genommen. Chemosensorische Eigenschaften wurden validiert für UCCC (UBC Typ I), die in zwei Subpopulationen (Ia und Ib) unterteilt werden können. Unterscheidungsmerkmal ist die Immunreaktivität gegenüber Antikörpern gegen die Phospholipase Cβ2 (PLCβ2). Eine chemosensorische Funktion von nicht-cholinergen solitären villin-immunreaktive Zellen (UBC Typ II) und serotonergen neuroendokrinen Zellen mit basal gelegenen sekretorischen Vesikeln istGegenstand aktueller Forschung. E = Epithel, LP = Lamina propria, PGP = Proteingenprodukt 9.5; [VI].

Die Entdeckung und Charakterisierung dieser urethralen cholinergen chemosensorischen Zellen (UCCC) ist Gegenstand dieser Arbeit (Abbildung 26.).

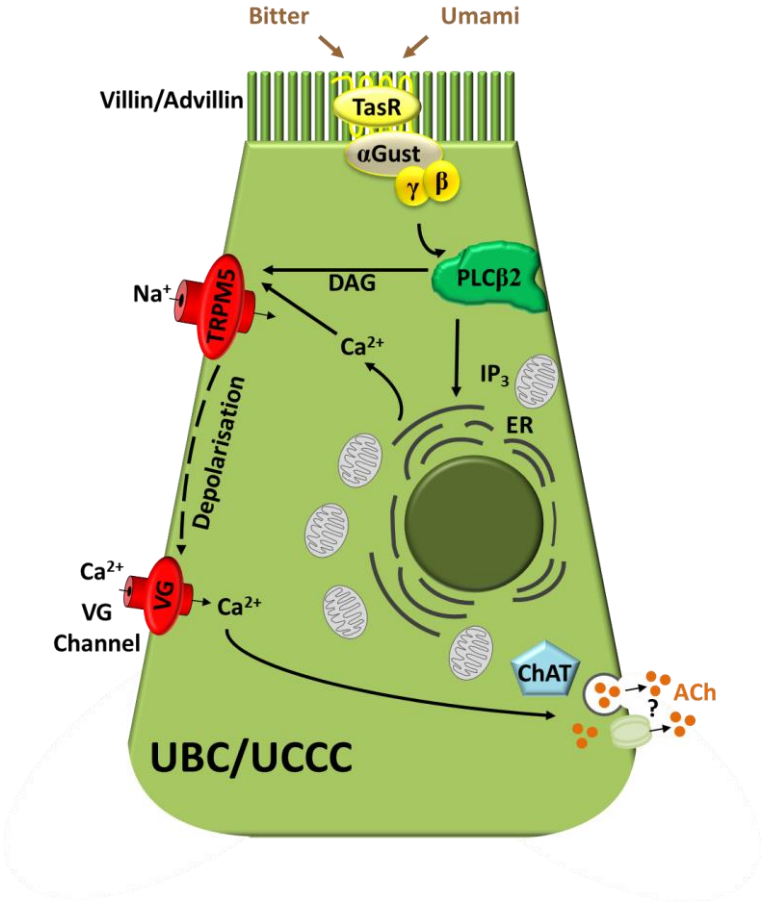

Abbildung 26. Schematische Zeichnung einer UBC/UCCC
Elemente der Geschmackstransduktionskaskade in UCCC/UBC. Geschmacksrezeptoren (TasR) werden am apikalen Ende in der Nähe des dort lokalisierten Büschels aus Advillin bzw. Villin antizipiert. Die nachgeschaltete Kaskade beinhaltet die Aktivierung von Phospholipase Cβ2 (PLCβ2) durch die β- und γ-Untereinheit des an die TasR gekoppelten G-Proteins, Bildung von Inositol-Tris-Phosphat (IP_3) und Diacylglycerin (DAG) mit anschließender Freisetzung von Calcium aus dem endoplasmatischen Retikulum (ER) und der Öffnung des Kationenkanals TRPM5, was zur Depolarisation der Zelle führt. Dies führt schließlich zur Öffnung von spannungsgesteuerten (VG) Calciumkanälen. Dies wiederum löst die Freisetzung von Acetylcholin (ACh), entweder durch vesikuläre Exozytose oder durch Hemikanäle, aus. αGust = G-Protein α-Untereinheit α-Gustducin; ChAT-Cholinacetyltransferase; [VI].

Nach der Entdeckung der UCCC in Mäusen konnte die Präsenz von UCCC in 14 weiteren Säugetierspezies aus 5 verschiedenen Ordnungen nachgewiesen werden [154, 291]. Es folgte die Charakterisierung dieser erstmals identifizierten Zellen. Sie zeigen eine hohe Ähnlichkeit zu solitären cholinergen chemosensorischen Zellen des Respirationstraktes, des Magen-Darm-Traktes und der Gallenwege, obgleich diese

Zellen nicht identisch sind. Da insbesondere bei den solitären cholinergen chemosensorischen Zellen des Respirationstraktes bereits vor Jahren eine morphologische und molekulare Ähnlichkeit zu Geschmackszellen festgestellt werden konnte, fokussierte die Charakterisierung der solitären urethralen Zelle auf die Hypothese, dass es sich auch hier um chemosensorische Wächterzellen handelt, die mittels Geschmacksrezeptoren und Elementen der Geschmackssignaltransduktionskaskade entscheidend zur Detektion und Abwehr eindringender Noxen und Keime beitragen.

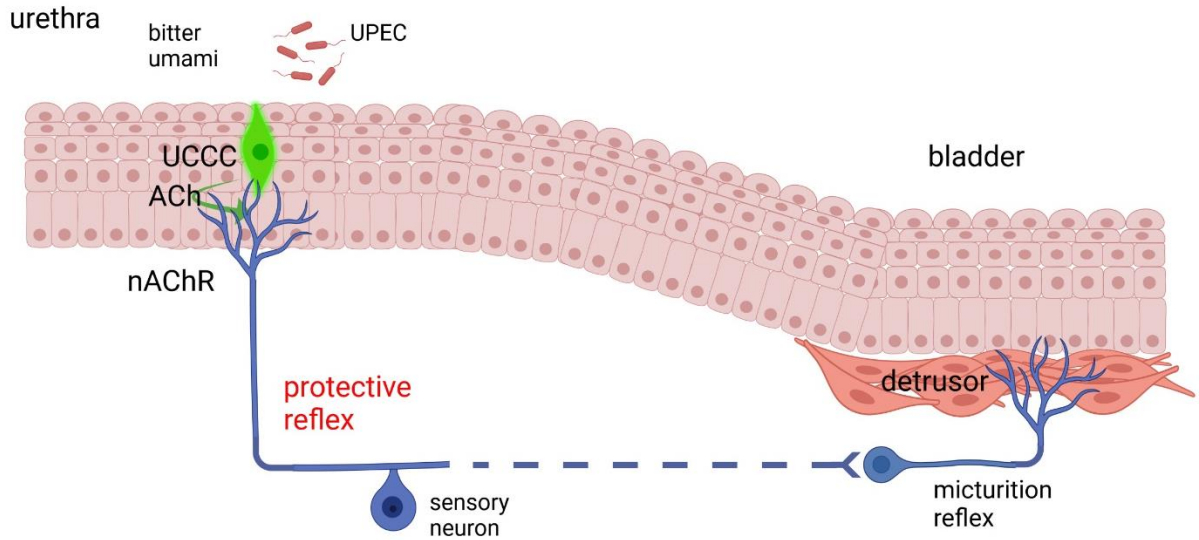

Abbildung 27. Schematische Darstellung des protektiven Wirkungsmechanismus von UBC/UCCC
Die Aktivierung der UCCC/UBC durch potenziell schädliche Substanzen oder Bakterien (Substanzen mit Bitterstoffcharakter, Umami oder Bakterien wie UPEC) führt zur Freisetzung von ACh. ACh löst über nAChR den Miktionsreflex und somit eine Blasendetrusorkontraktion nach; [VII].

Der Nachweis der ChAT in diesen Zellen resultierte in der Bezeichnung *urethral cholinergic chemosensory cell*. UCCC wurden als solitäre im Epithel der Urethra vorkommende Zellen identifiziert, wohingegen Harnblase, Ureter und Nierenbecken keine UCCC enthalten. UCCC exprimieren verschiedene Geschmacksrezeptoren aus der Tas1R (süß und umami) und Tas2R-Familie (bitter) und Elemente der Geschmackssignaltransduktionskaskade. PLCβ2, α-Gust und TRPM5 wurden von uns als UCCC-spezifische, aber in variabler Ausprägung exprimierte Marker identifiziert

(Abbildung 26.). Verschiedenste extern applizierte Substanzen, wie zum Beispiel Bitterstoffe, Umami, Salz und bakterielle Metabolite, führen zur Aktivierung der UCCC [154, 292]. Dies resultiert in einer Freisetzung von ACh und einer nachgeschalteten Erregung von sensorischen Nervenendigungen, die an die UCCC herantreten. Die Kommunikation von UCCC mit Nerven und benachbarten Zellen mittels ACh kann durch die Blockade von cholinergen Rezeptoren unterbunden werden. Die Erregung der sensorischen Nervenendigungen durch das von UCCC freigesetzte ACh löst wiederum schützende Reflexe aus. Im Falle der Urethra wird eine Blasenentleerung getriggert, die zur Spülung der Harnröhre führt [154] (Abbildung 27.).

Zudem konnten autoregulatorische Mechanismen entschlüsselt werden. Diese über die M2- und M5-Rezeptoren vermittelten Rückkopplungsmechanismen modulieren die Antwort der UCCC auf Stimulation [293] (Abbildung 29.). Dies hat möglicherweise eine klinische Relevanz für das Syndrom der überaktiven Blase. Diese geht oft mit einer Detrusorhyperaktivität einher. Diese könnte auch durch eine Fehlaktivierung oder Überaktivität von UCCC hervorgerufen werde, da UCCC die Miktion beeinflussen und durch einen über M2- und M5-Rezeptoren vermittelten negativen Rückkopplungsmechanismus reguliert werden. Des Weiteren wurden Erkenntnisse über die postnatale Entwicklung von UCCC gesammelt. Hierbei konnte gezeigt werden, dass es einen Sexualdimorphismus gibt. UCCC erscheinen in männlichen Tieren früher als in weiblichen Tieren. Später überwiegt die Anzahl der UCCC aber in weiblichen Tieren. Außerdem konnte gezeigt werden, dass die Entwicklung von UCCC durch die Toll-like-Rezeptoren 2 und 4 und MyD88, dem Signalkaskadenprotein aller Toll-like Rezeptoren mit Ausnahme des Toll-like-Rezeptors 3, beeinflusst wird.

Dementsprechend handelt es sich bei UCCC um Wächterzellen, die mittels Geschmacksrezeptoren und Elementen der Geschmackssignaltransduktionskaskade entscheidend an der Detektion und Abwehr von eindringenden Noxen und Keimen beteiligt sind. Sie sind chemosensorische „Sentinel“-Zellen, deren verschiedene Subpopulationen über ein jeweiliges Rezeptorrepertoire verfügt, um verschiedene Stoffe von den einige auch auch potenziell gefährliche sein könnten wie zum Beispiel Bitterstoffe, Umami, Salz und bakterielle Metabolite wahrzunehmen. Dies hilft bei der Überwachung der chemischen Zusammensetzung der Flüssigkeit auf der Schleimhautoberfläche. Als protektive Maßnahmen induzieren sie lokale oder reflexive Reaktionen via ACh.

Zusammenfassend konnte ein neuer Zelltyp, die urethrale cholinerge chemosensorische Zelle, entdeckt und initial charakterisiert werden

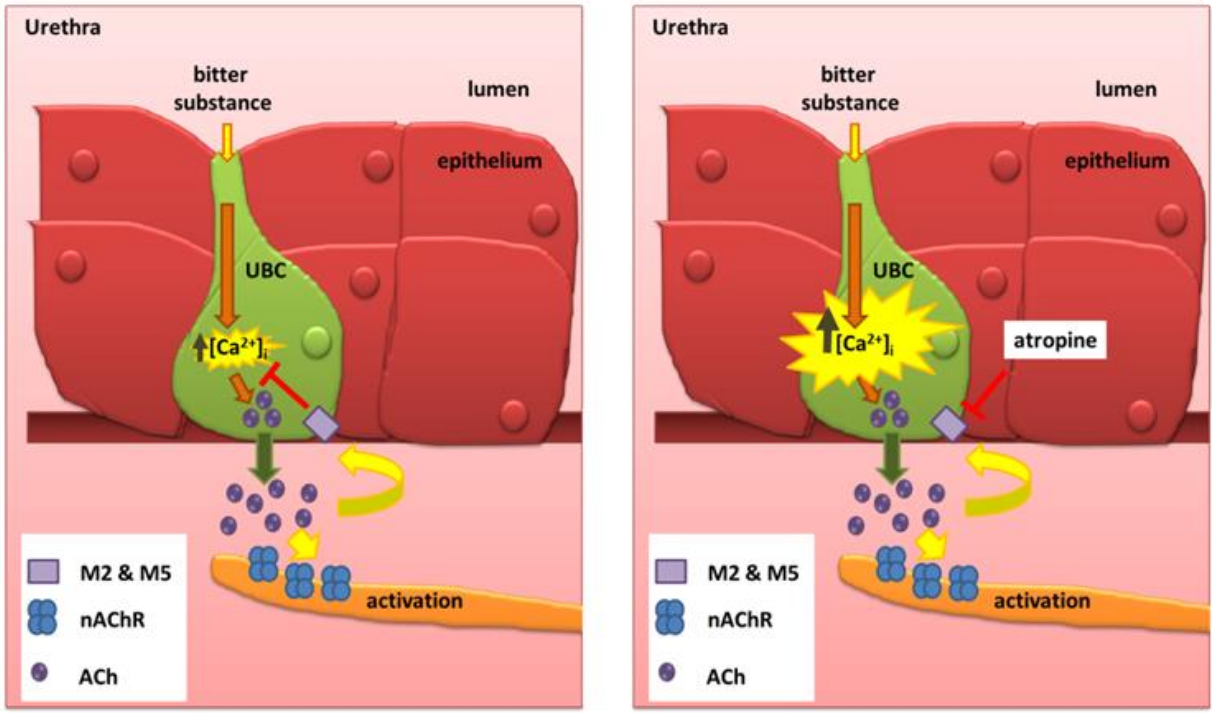

Abbildung 28. Schematische Darstellung des negativen Rückkopplungsmechanismus
Die Aktivierung einer kanonischen Geschmackstransduktionskaskade in UCCC/UBCs führt zu einem Anstieg von $[Ca^{2+}]_i$, gefolgt von einer ACh-Freisetzung. Die Reaktion von UCCC wird über einen durch M2- und M5-Rezeptoren vermittelten cholinergen negativen autokrinen Rückkopplungsmechanismus abgedämpft; [III].

5 Literaturverzeichnis

1. de Groat, W.C. and N. Yoshimura, *Afferent nerve regulation of bladder function in health and disease.* Handb Exp Pharmacol, 2009(194): p. 91-138.
2. de Groat, W.C., D. Griffiths, and N. Yoshimura, *Neural control of the lower urinary tract.* Compr Physiol, 2015. **5**(1): p. 327-96.
3. De Groat, W.C., *Spinal cord projections and neuropeptides in visceral afferent neurons.* Prog Brain Res, 1986. **67**: p. 165-87.
4. Birder, L., et al., *Neural control of the lower urinary tract: peripheral and spinal mechanisms.* Neurourol Urodyn, 2010. **29**(1): p. 128-39.
5. Birder, L.A., *Nervous network for lower urinary tract function.* Int J Urol, 2013. **20**(1): p. 4-12.
6. Kanai, A. and K.E. Andersson, *Bladder afferent signaling: recent findings.* J Urol, 2010. **183**(4): p. 1288-95.
7. Andersson, K.E., *Detrusor myocyte activity and afferent signaling.* Neurourol Urodyn, 2010. **29**(1): p. 97-106.
8. Janig, W. and J.F. Morrison, *Functional properties of spinal visceral afferents supplying abdominal and pelvic organs, with special emphasis on visceral nociception.* Prog Brain Res, 1986. **67**: p. 87-114.
9. Karnup, S., *Spinal interneurons of the lower urinary tract circuits.* Auton Neurosci, 2021. **235**: p. 102861.
10. de Groat, W.C. and N. Yoshimura, *Anatomy and physiology of the lower urinary tract.* Handb Clin Neurol, 2015. **130**: p. 61-108.
11. Benninghoff, A.D.D., *Anatomie : Makroskopische Anatomie, Histologie, Embryologie, Zellbiologie*. 2008, München: Elsevier, Urban & Fischer.
12. Treuting, P.M.D.S.M.M.K.S., *Comparative anatomy and histology : a mouse, rat, and human atlas*. 2018.
13. Huisman, A.B., *Aspects on the anatomy of the female urethra with special relation to urinary continence.* Contrib Gynecol Obstet, 1983. **10**: p. 1-31.
14. Keegan, K.A., D.K. Nanigian, and A.R. Stone, *Female urethral stricture disease.* Curr Urol Rep, 2008. **9**(5): p. 419-23.
15. Mizuno, Y., et al., *Myosin light chain kinase activation and calcium sensitization in smooth muscle in vivo.* Am J Physiol Cell Physiol, 2008. **295**(2): p. C358-64.
16. Caulfield, M.P. and N.J. Birdsall, *International Union of Pharmacology. XVII. Classification of muscarinic acetylcholine receptors.* Pharmacol Rev, 1998. **50**(2): p. 279-90.
17. Chess-Williams, R., *Muscarinic receptors of the urinary bladder: detrusor, urothelial and prejunctional.* Auton Autacoid Pharmacol, 2002. **22**(3): p. 133-45.
18. Duc, N.M., H.R. Kim, and K.Y. Chung, *Structural mechanism of G protein activation by G protein-coupled receptor.* Eur J Pharmacol, 2015. **763**(Pt B): p. 214-22.
19. Neves, S.R., P.T. Ram, and R. Iyengar, *G protein pathways.* Science, 2002. **296**(5573): p. 1636-9.
20. Murthy, K.S., *Signaling for contraction and relaxation in smooth muscle of the gut.* Annu Rev Physiol, 2006. **68**: p. 345-74.

21. Michel, M.C. and W. Vrydag, *Alpha1-, alpha2- and beta-adrenoceptors in the urinary bladder, urethra and prostate.* Br J Pharmacol, 2006. **147 Suppl 2**: p. S88-119.
22. de Groat, W.C., et al., *Neural control of the urethra.* Scand J Urol Nephrol Suppl, 2001(207): p. 35-43; discussion 106-25.
23. Yoshimura, N. and W.C. de Groat, *Neural control of the lower urinary tract.* Int J Urol, 1997. **4**(2): p. 111-25.
24. de Groat, W.C. and N. Yoshimura, *Mechanisms underlying the recovery of lower urinary tract function following spinal cord injury.* Prog Brain Res, 2006. **152**: p. 59-84.
25. Barber, M.D., et al., *Innervation of the female levator ani muscles.* Am J Obstet Gynecol, 2002. **187**(1): p. 64-71.
26. Pierce, L.M., et al., *Innervation of the levator ani muscles in the female squirrel monkey.* Am J Obstet Gynecol, 2003. **188**(5): p. 1141-7.
27. Thor, K.B. and W.C. de Groat, *Neural control of the female urethral and anal rhabdosphincters and pelvic floor muscles.* Am J Physiol Regul Integr Comp Physiol, 2010. **299**(2): p. R416-38.
28. Griffiths, D., *Neural control of micturition in humans: a working model.* Nat Rev Urol, 2015. **12**(12): p. 695-705.
29. Athwal, B.S., et al., *Brain responses to changes in bladder volume and urge to void in healthy men.* Brain, 2001. **124**(Pt 2): p. 369-77.
30. Hofmann, T., et al., *TRPM5 is a voltage-modulated and Ca(2+)-activated monovalent selective cation channel.* Curr Biol, 2003. **13**(13): p. 1153-8.
31. Craig, A.D., *Interoception: the sense of the physiological condition of the body.* Curr Opin Neurobiol, 2003. **13**(4): p. 500-5.
32. Craig, A.D., *How do you feel? Interoception: the sense of the physiological condition of the body.* Nat Rev Neurosci, 2002. **3**(8): p. 655-66.
33. Griffiths, D., et al., *Brain control of normal and overactive bladder.* J Urol, 2005. **174**(5): p. 1862-7.
34. Griffiths, D. and S.D. Tadic, *Bladder control, urgency, and urge incontinence: evidence from functional brain imaging.* Neurourol Urodyn, 2008. **27**(6): p. 466-74.
35. DasGupta, R., R.B. Kavia, and C.J. Fowler, *Cerebral mechanisms and voiding function.* BJU Int, 2007. **99**(4): p. 731-4.
36. Kavia, R.B., R. Dasgupta, and C.J. Fowler, *Functional imaging and the central control of the bladder.* J Comp Neurol, 2005. **493**(1): p. 27-32.
37. Holstege, G., *Micturition and the soul.* J Comp Neurol, 2005. **493**(1): p. 15-20.
38. Fowler, C.J., D. Griffiths, and W.C. de Groat, *The neural control of micturition.* Nat Rev Neurosci, 2008. **9**(6): p. 453-66.
39. Tadic, S.D., et al., *Brain responses to bladder filling in older women without urgency incontinence.* Neurourol Urodyn, 2013. **32**(5): p. 435-40.
40. Zhang, H., et al., *An fMRI study of the role of suprapontine brain structures in the voluntary voiding control induced by pelvic floor contraction.* Neuroimage, 2005. **24**(1): p. 174-80.
41. Griffiths, D.J. and C.J. Fowler, *The micturition switch and its forebrain influences.* Acta Physiol (Oxf), 2013. **207**(1): p. 93-109.
42. Blok, B.F., A.T. Willemsen, and G. Holstege, *A PET study on brain control of micturition in humans.* Brain, 1997. **120 (Pt 1)**: p. 111-21.

43. Andersson, K.E. and A. Arner, *Urinary bladder contraction and relaxation: physiology and pathophysiology.* Physiol Rev, 2004. **84**(3): p. 935-86.
44. Keast, J.R., M. Kawatani, and W.C. De Groat, *Sympathetic modulation of cholinergic transmission in cat vesical ganglia is mediated by alpha 1- and alpha 2-adrenoceptors.* Am J Physiol, 1990. **258**(1 Pt 2): p. R44-50.
45. Xu, D., et al., *Pharmacological Inhibition of mPGES-1 Selectively Suppresses PGE2 and Relieves Fever and Pain.*, in *Presented at the 10th International Conference on Bioactive Lipids in Cancer, Inflammation and Related Diseases*. 2007: Montreal, Canada.
46. Jung, S.Y., et al., *Urethral afferent nerve activity affects the micturition reflex; implication for the relationship between stress incontinence and detrusor instability.* J Urol, 1999. **162**(1): p. 204-12.
47. de Groat, W.C. and C. Wickens, *Organization of the neural switching circuitry underlying reflex micturition.* Acta Physiol (Oxf), 2013. **207**(1): p. 66-84.
48. Beckel, J.M. and L.A. Birder, *Differential expression and function of nicotinic acetylcholine receptors in the urinary bladder epithelium of the rat.* J Physiol, 2012. **590**(6): p. 1465-80.
49. Beckel, J.M., et al., *Expression of functional nicotinic acetylcholine receptors in rat urinary bladder epithelial cells.* Am J Physiol Renal Physiol, 2006. **290**(1): p. F103-10.
50. Chopra, B., et al., *Expression and function of bradykinin B1 and B2 receptors in normal and inflamed rat urinary bladder urothelium.* J Physiol, 2005. **562**(Pt 3): p. 859-71.
51. Chopra, B., et al., *Expression and function of rat urothelial P2Y receptors.* Am J Physiol Renal Physiol, 2008. **294**(4): p. F821-9.
52. Birder, L.A., et al., *Adrenergic- and capsaicin-evoked nitric oxide release from urothelium and afferent nerves in urinary bladder.* Am J Physiol, 1998. **275**(2): p. F226-9.
53. Birder, L.A., et al., *Beta-adrenoceptor agonists stimulate endothelial nitric oxide synthase in rat urinary bladder urothelial cells.* J Neurosci, 2002. **22**(18): p. 8063-70.
54. Birder, L.A., et al., *Feline interstitial cystitis results in mechanical hypersensitivity and altered ATP release from bladder urothelium.* Am J Physiol Renal Physiol, 2003. **285**(3): p. F423-9.
55. Birder, L. and K.E. Andersson, *Urothelial signaling.* Physiol Rev, 2013. **93**(2): p. 653-80.
56. Burnstock, G., *Purine-mediated signalling in pain and visceral perception.* Trends Pharmacol Sci, 2001. **22**(4): p. 182-8.
57. Carattino, M.D., S. Sheng, and T.R. Kleyman, *Mutations in the pore region modify epithelial sodium channel gating by shear stress.* J Biol Chem, 2005. **280**(6): p. 4393-401.
58. Uchiyama, T. and R. Chess-Williams, *Muscarinic receptor subtypes of the bladder and gastrointestinal tract.* J Smooth Muscle Res, 2004. **40**(6): p. 237-47.
59. Everaerts, W., et al., *Inhibition of the cation channel TRPV4 improves bladder function in mice and rats with cyclophosphamide-induced cystitis.* Proc Natl Acad Sci U S A, 2010. **107**(44): p. 19084-9.
60. Ossovskaya, V.S. and N.W. Bunnett, *Protease-activated receptors: contribution to physiology and disease.* Physiol Rev, 2004. **84**(2): p. 579-621.

61. Birder, L.A., et al., *Vanilloid receptor expression suggests a sensory role for urinary bladder epithelial cells.* Proc Natl Acad Sci U S A, 2001. **98**(23): p. 13396-401.
62. Hashimoto, Y., et al., *Scanning electron microscopic observation of apical sites of open-type paraneurons in the stomach, intestine and urethra.* Arch Histol Cytol, 1999. **62**(2): p. 181-9.
63. LaBerge, J., et al., *Expression of corticotropin-releasing factor and CRF receptors in micturition pathways after cyclophosphamide-induced cystitis.* Am J Physiol Regul Integr Comp Physiol, 2006. **291**(3): p. R692-703.
64. Apodaca, G., *The uroepithelium: not just a passive barrier.* Traffic, 2004. **5**(3): p. 117-28.
65. Birder, L.A. and W.C. de Groat, *Mechanisms of disease: involvement of the urothelium in bladder dysfunction.* Nat Clin Pract Urol, 2007. **4**(1): p. 46-54.
66. Matsui, M., et al., *Multiple functional defects in peripheral autonomic organs in mice lacking muscarinic acetylcholine receptor gene for the M3 subtype.* Proc Natl Acad Sci U S A, 2000. **97**(17): p. 9579-84.
67. Matsui, M., et al., *Mice lacking M2 and M3 muscarinic acetylcholine receptors are devoid of cholinergic smooth muscle contractions but still viable.* J Neurosci, 2002. **22**(24): p. 10627-32.
68. Andersson, K.E., *Detrusor contraction--Focus on muscarinic receptors.* Scand J Urol Nephrol Suppl, 2004(215): p. 54-7.
69. Andersson, K.E., *Antimuscarinics for treatment of overactive bladder.* Lancet Neurol, 2004. **3**(1): p. 46-53.
70. Andersson, K.E. and A.J. Wein, *Pharmacology of the lower urinary tract: basis for current and future treatments of urinary incontinence.* Pharmacol Rev, 2004. **56**(4): p. 581-631.
71. Andersson, K.E., et al., *Electrically-induced, nerve-mediated relaxation of rabbit urethra involves nitric oxide.* J Urol, 1992. **147**(1): p. 253-9.
72. Claßen, J.S., Alfons, *Interventionelle Neurophysiologie*. 2013, Stuttgart: Thieme.
73. Burnett, A.L., et al., *Urinary bladder-urethral sphincter dysfunction in mice with targeted disruption of neuronal nitric oxide synthase models idiopathic voiding disorders in humans.* Nat Med, 1997. **3**(5): p. 571-4.
74. Ho, K.M., et al., *Co-localization of carbon monoxide and nitric oxide synthesizing enzymes in the human urethral sphincter.* J Urol, 1999. **161**(6): p. 1968-72.
75. Chaudhari, N. and S.D. Roper, *The cell biology of taste.* J Cell Biol, 2010. **190**(3): p. 285-96.
76. Sclafani, A., *The sixth taste?* Appetite, 2004. **43**(1): p. 1-3.
77. Finger, T.E. and S.C. Kinnamon, *Taste isn't just for taste buds anymore.* F1000 Biol Rep, 2011. **3**: p. 20.
78. Vandenbeuch, A., T.R. Clapp, and S.C. Kinnamon, *Amiloride-sensitive channels in type I fungiform taste cells in mouse.* BMC Neurosci, 2008. **9**: p. 1.
79. Dutta Banik, D., et al., *A subset of broadly responsive Type III taste cells contribute to the detection of bitter, sweet and umami stimuli.* PLoS Genet, 2020. **16**(8): p. e1008925.
80. Chang, R.B., H. Waters, and E.R. Liman, *A proton current drives action potentials in genetically identified sour taste cells.* Proc Natl Acad Sci U S A, 2010. **107**(51): p. 22320-5.

81. Ye, W., et al., *The K+ channel KIR2.1 functions in tandem with proton influx to mediate sour taste transduction.* Proc Natl Acad Sci U S A, 2016. **113**(2): p. E229-38.
82. Lewandowski, B.C., et al., *Amiloride-Insensitive Salt Taste Is Mediated by Two Populations of Type III Taste Cells with Distinct Transduction Mechanisms.* J Neurosci, 2016. **36**(6): p. 1942-53.
83. Huang, Y.A., et al., *Presynaptic (Type III) cells in mouse taste buds sense sour (acid) taste.* J Physiol, 2008. **586**(12): p. 2903-12.
84. Huang, A.L., et al., *The cells and logic for mammalian sour taste detection.* Nature, 2006. **442**(7105): p. 934-8.
85. Kataoka, S., et al., *The candidate sour taste receptor, PKD2L1, is expressed by type III taste cells in the mouse.* Chem Senses, 2008. **33**(3): p. 243-54.
86. Oka, Y., et al., *High salt recruits aversive taste pathways.* Nature, 2013. **494**(7438): p. 472-5.
87. Gravina, S.A., G.L. Yep, and M. Khan, *Human biology of taste.* Ann Saudi Med, 2013. **33**(3): p. 217-22.
88. Nelson, G., et al., *An amino-acid taste receptor.* Nature, 2002. **416**(6877): p. 199-202.
89. Nelson, G., et al., *Mammalian sweet taste receptors.* Cell, 2001. **106**(3): p. 381-90.
90. Zhao, G.Q., et al., *The receptors for mammalian sweet and umami taste.* Cell, 2003. **115**(3): p. 255-66.
91. Zhang, Y., et al., *Coding of sweet, bitter, and umami tastes: different receptor cells sharing similar signaling pathways.* Cell, 2003. **112**(3): p. 293-301.
92. Chaudhari, N., A.M. Landin, and S.D. Roper, *A metabotropic glutamate receptor variant functions as a taste receptor.* Nat Neurosci, 2000. **3**(2): p. 113-9.
93. Yasumatsu, K., et al., *Involvement of multiple taste receptors in umami taste: analysis of gustatory nerve responses in metabotropic glutamate receptor 4 knockout mice.* J Physiol, 2015. **593**(4): p. 1021-34.
94. Kusuhara, Y., et al., *Taste responses in mice lacking taste receptor subunit T1R1.* J Physiol, 2013. **591**(7): p. 1967-85.
95. Toyono, T., et al., *Expression of metabotropic glutamate receptor group I in rat gustatory papillae.* Cell Tissue Res, 2003. **313**(1): p. 29-35.
96. Nakashima, K., et al., *Behavioral responses to glutamate receptor agonists and antagonists implicate the involvement of brain-expressed mGluR4 and mGluR1 in taste transduction for umami in mice.* Physiol Behav, 2012. **105**(3): p. 709-19.
97. Yee, K.K., et al., *Glucose transporters and ATP-gated K+ (KATP) metabolic sensors are present in type 1 taste receptor 3 (T1r3)-expressing taste cells.* Proc Natl Acad Sci U S A, 2011. **108**(13): p. 5431-6.
98. Chandrashekar, J., et al., *T2Rs function as bitter taste receptors.* Cell, 2000. **100**(6): p. 703-11.
99. Adler, E., et al., *A novel family of mammalian taste receptors.* Cell, 2000. **100**(6): p. 693-702.
100. Matsunami, H., J.P. Montmayeur, and L.B. Buck, *A family of candidate taste receptors in human and mouse.* Nature, 2000. **404**(6778): p. 601-4.
101. Bachmanov, A.A. and G.K. Beauchamp, *Taste receptor genes.* Annu Rev Nutr, 2007. **27**: p. 389-414.

102. Finger, T.E., et al., *ATP signaling is crucial for communication from taste buds to gustatory nerves.* Science, 2005. **310**(5753): p. 1495-9.
103. Huang, Y.J., et al., *The role of pannexin 1 hemichannels in ATP release and cell-cell communication in mouse taste buds.* Proc Natl Acad Sci U S A, 2007. **104**(15): p. 6436-41.
104. Taruno, A., et al., *CALHM1 ion channel mediates purinergic neurotransmission of sweet, bitter and umami tastes.* Nature, 2013. **495**(7440): p. 223-6.
105. Vandenbeuch, A., C.B. Anderson, and S.C. Kinnamon, *Mice Lacking Pannexin 1 Release ATP and Respond Normally to All Taste Qualities.* Chem Senses, 2015. **40**(7): p. 461-7.
106. Taruno, A., et al., *Taste transduction and channel synapses in taste buds.* Pflugers Arch, 2021. **473**(1): p. 3-13.
107. Ma, Z., et al., *CALHM3 Is Essential for Rapid Ion Channel-Mediated Purinergic Neurotransmission of GPCR-Mediated Tastes.* Neuron, 2018. **98**(3): p. 547-561 e10.
108. Kashio, M., et al., *CALHM1/CALHM3 channel is intrinsically sorted to the basolateral membrane of epithelial cells including taste cells.* Sci Rep, 2019. **9**(1): p. 2681.
109. Demura, K., et al., *Cryo-EM structures of calcium homeostasis modulator channels in diverse oligomeric assemblies.* Sci Adv, 2020. **6**(29): p. eaba8105.
110. Romanov, R.A., et al., *Chemical synapses without synaptic vesicles: Purinergic neurotransmission through a CALHM1 channel-mitochondrial signaling complex.* Sci Signal, 2018. **11**(529).
111. Ishimaru, Y., et al., *Transient receptor potential family members PKD1L3 and PKD2L1 form a candidate sour taste receptor.* Proc Natl Acad Sci U S A, 2006. **103**(33): p. 12569-74.
112. LopezJimenez, N.D., et al., *Two members of the TRPP family of ion channels, Pkd1l3 and Pkd2l1, are co-expressed in a subset of taste receptor cells.* J Neurochem, 2006. **98**(1): p. 68-77.
113. Horio, N., et al., *Sour taste responses in mice lacking PKD channels.* PLoS One, 2011. **6**(5): p. e20007.
114. Nelson, T.M., et al., *Taste function in mice with a targeted mutation of the pkd1l3 gene.* Chem Senses, 2010. **35**(7): p. 565-77.
115. Teng, B., et al., *Cellular and Neural Responses to Sour Stimuli Require the Proton Channel Otop1.* Curr Biol, 2019. **29**(21): p. 3647-3656 e5.
116. Zhang, J., et al., *Sour Sensing from the Tongue to the Brain.* Cell, 2019. **179**(2): p. 392-402 e15.
117. Tu, Y.H., et al., *An evolutionarily conserved gene family encodes proton-selective ion channels.* Science, 2018. **359**(6379): p. 1047-1050.
118. Chandrashekar, J., et al., *The cells and peripheral representation of sodium taste in mice.* Nature, 2010. **464**(7286): p. 297-301.
119. Roebber, J.K., S.D. Roper, and N. Chaudhari, *The Role of the Anion in Salt (NaCl) Detection by Mouse Taste Buds.* J Neurosci, 2019. **39**(32): p. 6224-6232.
120. Vandenbeuch, A. and S.C. Kinnamon, *Is the Amiloride-Sensitive Na+ Channel in Taste Cells Really ENaC?* Chem Senses, 2020. **45**(4): p. 233-234.
121. Lindemann, B., *Receptors and transduction in taste.* Nature, 2001. **413**(6852): p. 219-25.

122. Heck, G.L., S. Mierson, and J.A. DeSimone, *Salt taste transduction occurs through an amiloride-sensitive sodium transport pathway.* Science, 1984. **223**(4634): p. 403-5.
123. Lin, W., et al., *Epithelial Na+ channel subunits in rat taste cells: localization and regulation by aldosterone.* J Comp Neurol, 1999. **405**(3): p. 406-20.
124. Avenet, P. and B. Lindemann, *Amiloride-blockable sodium currents in isolated taste receptor cells.* J Membr Biol, 1988. **105**(3): p. 245-55.
125. Lindemann, B., et al., *Occurrence of ENaC subunit mRNA and immunocytochemistry of the channel subunits in taste buds of the rat vallate papilla.* Ann N Y Acad Sci, 1998. **855**: p. 116-27.
126. Canessa, C.M., A.M. Merillat, and B.C. Rossier, *Membrane topology of the epithelial sodium channel in intact cells.* Am J Physiol, 1994. **267**(6 Pt 1): p. C1682-90.
127. Giraldez, T., et al., *The epithelial sodium channel delta-subunit: new notes for an old song.* Am J Physiol Renal Physiol, 2012. **303**(3): p. F328-38.
128. Larson, E.D., et al., *Function, Innervation, and Neurotransmitter Signaling in Mice Lacking Type-II Taste Cells.* eNeuro, 2020. **7**(1).
129. Lossow, K., et al., *Segregated Expression of ENaC Subunits in Taste Cells.* Chem Senses, 2020. **45**(4): p. 235-248.
130. Canessa, C.M., et al., *Amiloride-sensitive epithelial Na+ channel is made of three homologous subunits.* Nature, 1994. **367**(6462): p. 463-7.
131. Baldin, J.P., D. Barth, and M. Fronius, *Epithelial Na(+) Channel (ENaC) Formed by One or Two Subunits Forms Functional Channels That Respond to Shear Force.* Front Physiol, 2020. **11**: p. 141.
132. Laugerette, F., et al., *CD36 involvement in orosensory detection of dietary lipids, spontaneous fat preference, and digestive secretions.* J Clin Invest, 2005. **115**(11): p. 3177-84.
133. Cartoni, C., et al., *Taste preference for fatty acids is mediated by GPR40 and GPR120.* J Neurosci, 2010. **30**(25): p. 8376-82.
134. Besnard, P., P. Passilly-Degrace, and N.A. Khan, *Taste of Fat: A Sixth Taste Modality?* Physiol Rev, 2016. **96**(1): p. 151-76.
135. Besnard, P., *Lipids and obesity: Also a matter of taste?* Rev Endocr Metab Disord, 2016. **17**(2): p. 159-70.
136. Sclafani, A., K. Ackroff, and N.A. Abumrad, *CD36 gene deletion reduces fat preference and intake but not post-oral fat conditioning in mice.* Am J Physiol Regul Integr Comp Physiol, 2007. **293**(5): p. R1823-32.
137. Gilbertson, T.A., *Gustatory mechanisms for the detection of fat.* Curr Opin Neurobiol, 1998. **8**(4): p. 447-52.
138. Gilbertson, T.A., et al., *Fatty acid responses in taste cells from obesity-prone and -resistant rats.* Physiol Behav, 2005. **86**(5): p. 681-90.
139. Mattes, R.D., *Is there a fatty acid taste?* Annu Rev Nutr, 2009. **29**: p. 305-27.
140. Hofer, D. and D. Drenckhahn, *Identification of brush cells in the alimentary and respiratory system by antibodies to villin and fimbrin.* Histochemistry, 1992. **98**(4): p. 237-42.
141. Rhodin, J. and T. Dalhamn, *Electron microscopy of the tracheal ciliated mucosa in rat.* Z Zellforsch Mikrosk Anat, 1956. **44**(4): p. 345-412.
142. Luciano, L., E. Reale, and H. Ruska, *[On a "chemoreceptive" sensory cell in the tachea of the rat].* Z Zellforsch Mikrosk Anat, 1968. **85**(3): p. 350-75.

143. Sbarbati, A. and F. Osculati, *A new fate for old cells: brush cells and related elements.* J Anat, 2005. **206**(4): p. 349-58.
144. Ruppert, A.L., et al., *Advillin is a tuft cell marker in the mouse alimentary tract.* J Mol Histol, 2020. **51**(4): p. 421-435.
145. Luciano, L., M. Castellucci, and E. Reale, *The brush cells of the common bile duct of the rat. This section, freeze-fracture and scanning electron microscopy.* Cell Tissue Res, 1981. **218**(2): p. 403-20.
146. Luciano, L. and E. Reale, *Brush cells of the mouse gallbladder. A correlative light- and electron-microscopical study.* Cell Tissue Res, 1990. **262**(2): p. 339-49.
147. Hofer, D. and D. Drenckhahn, *Cytoskeletal markers allowing discrimination between brush cells and other epithelial cells of the gut including enteroendocrine cells.* Histochem Cell Biol, 1996. **105**(5): p. 405-12.
148. Hansen, A. and T.E. Finger, *Is TrpM5 a reliable marker for chemosensory cells? Multiple types of microvillous cells in the main olfactory epithelium of mice.* BMC Neurosci, 2008. **9**: p. 115.
149. Krasteva, G., et al., *Cholinergic chemosensory cells in the auditory tube.* Histochem Cell Biol, 2012. **137**(4): p. 483-97.
150. Isomaki, A.M., *A new cell type (tuft cell) in the gastrointestinal mucosa of the rat. A transmission and scanning electron microscopic study.* Acta Pathol Microbiol Scand A, 1973: p. Suppl 240:1-35.
151. Howitt, M.R., et al., *Tuft cells, taste-chemosensory cells, orchestrate parasite type 2 immunity in the gut.* Science, 2016. **351**(6279): p. 1329-33.
152. Finger, T.E., et al., *Solitary chemoreceptor cells in the nasal cavity serve as sentinels of respiration.* Proc Natl Acad Sci U S A, 2003. **100**(15): p. 8981-6.
153. Lin, W., et al., *TRPM5-expressing solitary chemosensory cells respond to odorous irritants.* J Neurophysiol, 2008. **99**(3): p. 1451-60.
154. Deckmann, K., et al., *Bitter triggers acetylcholine release from polymodal urethral chemosensory cells and bladder reflexes.* Proc Natl Acad Sci U S A, 2014. **111**(22): p. 8287-92.
155. Krasteva, G., et al., *Cholinergic chemosensory cells in the trachea regulate breathing.* Proc Natl Acad Sci U S A, 2011. **108**(23): p. 9478-83.
156. Montoro, D.T., et al., *A revised airway epithelial hierarchy includes CFTR-expressing ionocytes.* Nature, 2018. **560**(7718): p. 319-324.
157. Nadjsombati, M.S., et al., *Detection of Succinate by Intestinal Tuft Cells Triggers a Type 2 Innate Immune Circuit.* Immunity, 2018. **49**(1): p. 33-41 e7.
158. Yamamoto, Y., et al., *Immunohistochemical characterization of brush cells in the rat larynx.* J Mol Histol, 2018. **49**(1): p. 63-73.
159. Tizzano, M., et al., *Nasal chemosensory cells use bitter taste signaling to detect irritants and bacterial signals.* Proc Natl Acad Sci U S A, 2010. **107**(7): p. 3210-5.
160. Gulbransen, B.D., et al., *Nasal solitary chemoreceptor cell responses to bitter and trigeminal stimulants in vitro.* J Neurophysiol, 2008. **99**(6): p. 2929-37.
161. Ogura, T., et al., *Chemoreception regulates chemical access to mouse vomeronasal organ: role of solitary chemosensory cells.* PLoS One, 2010. **5**(7): p. e11924.
162. Saunders, C.J., et al., *Cholinergic neurotransmission links solitary chemosensory cells to nasal inflammation.* Proc Natl Acad Sci U S A, 2014. **111**(16): p. 6075-80.

163. Ogura, T., et al., *Cholinergic microvillous cells in the mouse main olfactory epithelium and effect of acetylcholine on olfactory sensory neurons and supporting cells.* J Neurophysiol, 2011. **106**(3): p. 1274-87.
164. Middelhoff, M., et al., *Dclk1-expressing tuft cells: critical modulators of the intestinal niche?* Am J Physiol Gastrointest Liver Physiol, 2017. **313**(4): p. G285-G299.
165. Gerbe, F., et al., *DCAMKL-1 expression identifies Tuft cells rather than stem cells in the adult mouse intestinal epithelium.* Gastroenterology, 2009. **137**(6): p. 2179-80; author reply 2180-1.
166. Saqui-Salces, M., et al., *Gastric tuft cells express DCLK1 and are expanded in hyperplasia.* Histochem Cell Biol, 2011. **136**(2): p. 191-204.
167. Bankova, L.G., et al., *The cysteinyl leukotriene 3 receptor regulates expansion of IL-25-producing airway brush cells leading to type 2 inflammation.* Sci Immunol, 2018. **3**(28).
168. Perniss, A., et al., *Development of epithelial cholinergic chemosensory cells of the urethra and trachea of mice.* Cell Tissue Res, 2021.
169. Perniss, A., et al., *Chemosensory Cell-Derived Acetylcholine Drives Tracheal Mucociliary Clearance in Response to Virulence-Associated Formyl Peptides.* Immunity, 2020. **52**(4): p. 683-699 e11.
170. Gerbe, F., et al., *Intestinal epithelial tuft cells initiate type 2 mucosal immunity to helminth parasites.* Nature, 2016. **529**(7585): p. 226-30.
171. Krasteva, G., et al., *Cholinergic brush cells in the trachea mediate respiratory responses to quorum sensing molecules.* Life Sci, 2012. **91**(21-22): p. 992-6.
172. Saunders, C.J., S.D. Reynolds, and T.E. Finger, *Chemosensory brush cells of the trachea. A stable population in a dynamic epithelium.* Am J Respir Cell Mol Biol, 2013. **49**(2): p. 190-6.
173. Weyrauch, K.D. and B. Schnorr, *[Ultrastructure of the epithelium of the major pancreatic duct in sheep].* Acta Anat (Basel), 1976. **96**(2): p. 232-47.
174. Luciano, L. and E. Reale, *A new morphological aspect of the brush cells of the mouse gallbladder epithelium.* Cell Tissue Res, 1979. **201**(1): p. 37-44.
175. Schutz, B., et al., *Chemical coding and chemosensory properties of cholinergic brush cells in the mouse gastrointestinal and biliary tract.* Front Physiol, 2015. **6**: p. 87.
176. Wiederhold, S., et al., *A novel cholinergic epithelial cell with chemosensory traits in the murine conjunctiva.* Int Immunopharmacol, 2015.
177. Zheng, X., et al., *Gingival solitary chemosensory cells are immune sentinels for periodontitis.* Nat Commun, 2019. **10**(1): p. 4496.
178. Panneck, A.R., et al., *Cholinergic epithelial cell with chemosensory traits in murine thymic medulla.* Cell Tissue Res, 2014. **358**(3): p. 737-48.
179. O'Leary, C.E., C. Schneider, and R.M. Locksley, *Tuft Cells-Systemically Dispersed Sensory Epithelia Integrating Immune and Neural Circuitry.* Annu Rev Immunol, 2019. **37**: p. 47-72.
180. Pan, J., et al., *Acetylcholine From Tuft Cells: The Updated Insights Beyond Its Immune and Chemosensory Functions.* Front Cell Dev Biol, 2020. **8**: p. 606.
181. Krasteva, G. and W. Kummer, *"Tasting" the airway lining fluid.* Histochem Cell Biol, 2012. **138**(3): p. 365-83.
182. Tizzano, M. and T.E. Finger, *Chemosensors in the nose: guardians of the airways.* Physiology (Bethesda), 2013. **28**(1): p. 51-60.

183. Kummer, W. and K. Deckmann, *Brush cells, the newly identified gatekeepers of the urinary tract.* Curr Opin Urol, 2017. **27**(2): p. 85-92.
184. Schneider, C., C.E. O'Leary, and R.M. Locksley, *Regulation of immune responses by tuft cells.* Nat Rev Immunol, 2019.
185. Deckmann, K. and W. Kummer, *Chemosensory epithelial cells in the urethra: sentinels of the urinary tract.* Histochem Cell Biol, 2016. **146**(6): p. 673-683.
186. Andersson, K.E., *Urethral afferent signalling: role of 5-HT paraneurons.* Acta Physiol (Oxf), 2018. **222**(2).
187. Birder, L.A. and F.A. Kullmann, *Role of neurogenic inflammation in local communication in the visceral mucosa.* Semin Immunopathol, 2018. **40**(3): p. 261-279.
188. Czaja, K., et al., *Neuroendocrine cells in the female urogenital tract of the pig, and their immunohistochemical characterization.* Acta Anat (Basel), 1996. **157**(1): p. 11-9.
189. Fujita, T., *Taste cells in the gut and on the tongue. Their common, paraneuronal features.* Physiol Behav, 1991. **49**(5): p. 883-5.
190. Fujita, T., T. Kanno, and S. Kobayashi, *The Paraneuron*. 1988.
191. Hanyu, S., et al., *Distribution of serotonin-immunoreactive paraneurons in the lower urinary tract of dogs.* Am J Anat, 1987. **180**(4): p. 349-56.
192. Iwanaga, T., et al., *Topographical relation between serotonin-containing paraneurons and peptidergic neurons in the intestine and urethra.* Biol Signals, 1994. **3**(5): p. 259-70.
193. Kullmann, F.A., et al., *Serotonergic paraneurones in the female mouse urethral epithelium and their potential role in peripheral sensory information processing.* Acta Physiol (Oxf), 2018. **222**(2).
194. Kullmann, F.A., et al., *Inflammation and Tissue Remodeling in the Bladder and Urethra in Feline Interstitial Cystitis.* Front Syst Neurosci, 2018. **12**: p. 13.
195. Tamaki, M., et al., *Calcitonin gene-related peptide (CGRP)-immunoreactive nerve terminals in the whole mount preparations of the dog urethra.* Arch Histol Cytol, 1992. **55**(1): p. 1-11.
196. Vittoria, A., et al., *Immunocytochemistry of paraneurons in the female urethra of the horse, cattle, sheep, and pig.* Anat Rec, 1992. **233**(1): p. 18-24.
197. Vittoria, A., et al., *Serotonin-, somatostatin- and chromogranin A-containing cells of the urethro-prostatic complex in the sheep. An immunocytochemical and immunofluorescent study.* J Anat, 1990. **171**: p. 169-78.
198. Aumuller, G., et al., *Regional distribution of neuroendocrine cells in the urogenital duct system of the male rat.* Prostate, 2012. **72**(3): p. 326-37.
199. Aumuller, G., et al., *Neurogenic origin of human prostate endocrine cells.* Urology, 1999. **53**(5): p. 1041-8.
200. Aumuller, G., et al., *Semiquantitative morphology of human prostatic development and regional distribution of prostatic neuroendocrine cells.* Prostate, 2001. **46**(2): p. 108-15.
201. Kummer, W., K.S. Lips, and U. Pfeil, *The epithelial cholinergic system of the airways.* Histochem Cell Biol, 2008. **130**(2): p. 219-34.
202. Szczyrba, J., et al., *Neuroendocrine Cells of the Prostate Derive from the Neural Crest.* J Biol Chem, 2017. **292**(5): p. 2021-2031.
203. Feyrter, F., *[Pathology of the urogenital system of light cells].* Virchows Arch Pathol Anat Physiol Klin Med, 1951. **320**(6): p. 564-76.

204. Feyrter, F., *[The urogenital light-cell system of man].* Z Mikrosk Anat Forsch, 1951. **57**(3): p. 324-44.
205. Falck, B., C. Owman, and N.O. Sjostrand, *Peripherally Located Adrenergic Neurons Innervating the Vas Deferens and the Seminal Vesicle of the Guinea-Pig.* Experientia, 1965. **21**: p. 98-100.
206. Owman, C., T. Owman, and N.O. Sjoberg, *Short adrenergic neurons innervating the female urethra of the cat.* Experientia, 1971. **27**(3): p. 313-5.
207. Dixon, J.S., J.A. Gosling, and D.R. Ramsdale, *Urethral chromaffin cells. A light and electron microscopic study.* Z Zellforsch Mikrosk Anat, 1973. **138**(3): p. 397-406.
208. Fetissof, F., et al., *Endocrine cells in the prostate gland, urothelium and Brenner tumors. Immunohistological and ultrastructural studies.* Virchows Arch B Cell Pathol Incl Mol Pathol, 1983. **42**(1): p. 53-64.
209. Ramsdale, D.R., *Further observations on urethral chromaffin cells: an electron microscopic study.* Cell Tissue Res, 1974. **148**(4): p. 499-504.
210. Milsom, I., et al., *How widespread are the symptoms of an overactive bladder and how are they managed? A population-based prevalence study.* BJU Int, 2001. **87**(9): p. 760-6.
211. Irwin, D.E., et al., *Impact of overactive bladder symptoms on employment, social interactions and emotional well-being in six European countries.* BJU Int, 2006. **97**(1): p. 96-100.
212. Irwin, D.E., et al., *Population-based survey of urinary incontinence, overactive bladder, and other lower urinary tract symptoms in five countries: results of the EPIC study.* Eur Urol, 2006. **50**(6): p. 1306-14; discussion 1314-5.
213. Stewart, W.F., et al., *Prevalence and burden of overactive bladder in the United States.* World J Urol, 2003. **20**(6): p. 327-36.
214. Abrams, P.C., L.; Khoury, S.; Wein A.; J. *Incontinence : 5th International Consultation on Incontinence, Paris, February 2012*. 2012. [Paris]: ICUD-EAU.
215. Abrams, P., et al., *The standardisation of terminology of lower urinary tract function: report from the Standardisation Sub-committee of the International Continence Society.* Neurourol Urodyn, 2002. **21**(2): p. 167-78.
216. Abrams, P., et al., *The standardisation of terminology in lower urinary tract function: report from the standardisation sub-committee of the International Continence Society.* Urology, 2003. **61**(1): p. 37-49.
217. Abrams, P., *Describing bladder storage function: overactive bladder syndrome and detrusor overactivity.* Urology, 2003. **62**(5 Suppl 2): p. 28-37; discussion 40-2.
218. Bschleipfer, T., *Epidemiologie und Ätiologie der Blasenüberaktivität.* Referateband der Deutschen Kontinenz Gesellschaft, 22. Kongress der DKG und 71. Seminar des Arbeitskreises urologische Funktionsdiagnostik und Urologie der Frau, 2010: p. 107-110 (nicht PubMed gelistet).
219. Abrams, P. and K.E. Andersson, *Muscarinic receptor antagonists for overactive bladder.* BJU Int, 2007. **100**(5): p. 987-1006.
220. Andersson, K.E., et al., *Pharmacological treatment of overactive bladder: report from the International Consultation on Incontinence.* Curr Opin Urol, 2009. **19**(4): p. 380-94.
221. Wiedemann, A., et al., *[Urinary incontinence in geriatric patients: pharmacological Therapy].* Aktuelle Urol, 2019. **50**(4): p. 424-440.

222. Palmtag, H.G., M.; Heidler, H., *Urodynamik Fort- und Weiterbildungskommission der Deutschen Urologen, Arbeitskreis Urologische Funktionsdiagnostik und Urologie der Frau*. 2004, Berlin Heidelberg New York: springer.
223. Nabi, G., et al., *Anticholinergic drugs versus placebo for overactive bladder syndrome in adults.* Cochrane Database Syst Rev, 2006(4): p. CD003781.
224. Junemann, K.P., et al., *Propiverine versus tolterodine: efficacy and tolerability in patients with overactive bladder.* Eur Urol, 2005. **48**(3): p. 478-82.
225. Rai, B.P., et al., *Anticholinergic drugs versus non-drug active therapies for non-neurogenic overactive bladder syndrome in adults.* Cochrane Database Syst Rev, 2012. **12**: p. CD003193.
226. Hay-Smith, J., et al., *Which anticholinergic drug for overactive bladder symptoms in adults.* Cochrane Database Syst Rev, 2005(3): p. CD005429.
227. Alhasso, A.A., et al., *Anticholinergic drugs versus non-drug active therapies for overactive bladder syndrome in adults.* Cochrane Database Syst Rev, 2006(4): p. CD003193.
228. Abrams, P., et al., *Twelve-month treatment of overactive bladder: efficacy and tolerability of tolterodine.* Drugs Aging, 2001. **18**(7): p. 551-60.
229. Giannantoni, A., et al., *New frontiers in intravesical therapies and drug delivery.* Eur Urol, 2006. **50**(6): p. 1183-93; discussion 1193.
230. Di Stasi, S.M., et al., *Intravesical electromotive administration of oxybutynin in patients with detrusor hyperreflexia unresponsive to standard anticholinergic regimens.* J Urol, 2001. **165**(2): p. 491-8.
231. Chapple, C.R., et al., *The effects of antimuscarinic treatments in overactive bladder: an update of a systematic review and meta-analysis.* Eur Urol, 2008. **54**(3): p. 543-62.
232. Chapple, C., et al., *The effects of antimuscarinic treatments in overactive bladder: a systematic review and meta-analysis.* Eur Urol, 2005. **48**(1): p. 5-26.
233. Chapple, C.R., et al., *Treatment outcomes in the STAR study: a subanalysis of solifenacin 5 mg and tolterodine ER 4 mg.* Eur Urol, 2007. **52**(4): p. 1195-203.
234. Athanasopoulos, A., et al., *Combination treatment with an alpha-blocker plus an anticholinergic for bladder outlet obstruction: a prospective, randomized, controlled study.* J Urol, 2003. **169**(6): p. 2253-6.
235. Daly, D.M., et al., *The inhibitory role of acetylcholine and muscarinic receptors in bladder afferent activity.* Eur Urol, 2010. **58**(1): p. 22-8; discussion 31-2.
236. Hay-Smith, J., et al., *Anticholinergic drugs versus placebo for overactive bladder syndrome in adults.* Cochrane Database Syst Rev, 2002(3): p. CD003781.
237. Nordling, J., *[Anticholinergic drugs versus non-drug treatment of overactive bladder syndrome in adults. A survey of a Cochrane review].* Ugeskr Laeger, 2007. **169**(50): p. 4345-7.
238. Abrams, P., *Evidence for the efficacy and safety of tolterodine in the treatment of overactive bladder.* Expert Opin Pharmacother, 2001. **2**(10): p. 1685-701.
239. Abrams, P., *Tolterodine : A Viewpoint by Paul Abrams.* Drugs, 1998. **55**(6): p. 821.
240. Abrams, P., et al., *Tolterodine, a new antimuscarinic agent: as effective but better tolerated than oxybutynin in patients with an overactive bladder.* Br J Urol, 1998. **81**(6): p. 801-10.

241. Abrams, P., et al., *Safety and tolerability of tolterodine for the treatment of overactive bladder in men with bladder outlet obstruction.* J Urol, 2006. **175**(3 Pt 1): p. 999-1004; discussion 1004.
242. Appell, R.A., et al., *Treatment of overactive bladder: long-term tolerability and efficacy of tolterodine.* World J Urol, 2001. **19**(2): p. 141-7.
243. Chapple, C., et al., *Tolterodine treatment improves storage symptoms suggestive of overactive bladder in men treated with alpha-blockers.* Eur Urol, 2009. **56**(3): p. 534-41.
244. Chapple, C.R., et al., *Efficacy and safety of tolterodine extended-release in men with overactive bladder symptoms treated with an alpha-blocker: effect of baseline prostate-specific antigen concentration.* BJU Int, 2010. **106**(9): p. 1332-8.
245. Chapple, C.R., T. Yamanishi, and R. Chess-Williams, *Muscarinic receptor subtypes and management of the overactive bladder.* Urology, 2002. **60**(5 Suppl 1): p. 82-8; discussion 88-9.
246. Dmochowski, R., et al., *Efficacy and tolerability of tolterodine extended release in male and female patients with overactive bladder.* Eur Urol, 2007. **51**(4): p. 1054-64; discussion 1064.
247. Kim, Y., et al., *Antimuscarinic agents exhibit local inhibitory effects on muscarinic receptors in bladder-afferent pathways.* Urology, 2005. **65**(2): p. 238-42.
248. Rentzhog, L., et al., *Efficacy and safety of tolterodine in patients with detrusor instability: a dose-ranging study.* Br J Urol, 1998. **81**(1): p. 42-8.
249. Roehrborn, C.G., et al., *Efficacy and tolerability of tolterodine extended-release in men with overactive bladder and urgency urinary incontinence.* BJU Int, 2006. **97**(5): p. 1003-6.
250. Yamanishi, T., C.R. Chapple, and R. Chess-Williams, *Which muscarinic receptor is important in the bladder?* World J Urol, 2001. **19**(5): p. 299-306.
251. Finney, S.M., et al., *Antimuscarinic drugs in detrusor overactivity and the overactive bladder syndrome: motor or sensory actions?* BJU Int, 2006. **98**(3): p. 503-7.
252. Kim, U.K. and D. Drayna, *Genetics of individual differences in bitter taste perception: lessons from the PTC gene.* Clin Genet, 2005. **67**(4): p. 275-80.
253. Chromek, M., *The role of the antimicrobial peptide cathelicidin in renal diseases.* Pediatr Nephrol, 2015. **30**(8): p. 1225-32.
254. Stamm, W.E. and S.R. Norrby, *Urinary tract infections: disease panorama and challenges.* J Infect Dis, 2001. **183 Suppl 1**: p. S1-4.
255. Flores-Mireles, A.L., et al., *Urinary tract infections: epidemiology, mechanisms of infection and treatment options.* Nat Rev Microbiol, 2015. **13**(5): p. 269-84.
256. Ulett, G.C., et al., *Uropathogenic Escherichia coli virulence and innate immune responses during urinary tract infection.* Curr Opin Microbiol, 2013. **16**(1): p. 100-7.
257. Kline, K.A. and A.L. Lewis, *Gram-Positive Uropathogens, Polymicrobial Urinary Tract Infection, and the Emerging Microbiota of the Urinary Tract.* Microbiol Spectr, 2016. **4**(2).
258. Hettinger, T.P., B.K. Formaker, and M.E. Frank, *Cycloheximide: no ordinary bitter stimulus.* Behav Brain Res, 2007. **180**(1): p. 4-17.
259. Lee, R.J., et al., *T2R38 taste receptor polymorphisms underlie susceptibility to upper respiratory infection.* J Clin Invest, 2012. **122**(11): p. 4145-59.

260. Charlton, T.S., et al., *A novel and sensitive method for the quantification of N-3-oxoacyl homoserine lactones using gas chromatography-mass spectrometry: application to a model bacterial biofilm.* Environ Microbiol, 2000. **2**(5): p. 530-41.
261. Shuman, E.K. and C.E. Chenoweth, *Recognition and prevention of healthcare-associated urinary tract infections in the intensive care unit.* Crit Care Med, 2010. **38**(8 Suppl): p. S373-9.
262. Pearson, M.M., et al., *Transcriptome of Proteus mirabilis in the murine urinary tract: virulence and nitrogen assimilation gene expression.* Infect Immun, 2011. **79**(7): p. 2619-31.
263. Aubron, C., et al., *Changes in urine composition after trauma facilitate bacterial growth.* BMC Infect Dis, 2012. **12**: p. 330.
264. Tallini, Y.N., et al., *BAC transgenic mice express enhanced green fluorescent protein in central and peripheral cholinergic neurons.* Physiol Genomics, 2006. **27**(3): p. 391-7.
265. von Engelhardt, J., et al., *Functional characterization of intrinsic cholinergic interneurons in the cortex.* J Neurosci, 2007. **27**(21): p. 5633-42.
266. Ohmoto, M., et al., *Genetic tracing of the gustatory and trigeminal neural pathways originating from T1R3-expressing taste receptor cells and solitary chemoreceptor cells.* Mol Cell Neurosci, 2008. **38**(4): p. 505-17.
267. Tomchik, S.M., et al., *Breadth of tuning and taste coding in mammalian taste buds.* J Neurosci, 2007. **27**(40): p. 10840-8.
268. Dando, R. and S.D. Roper, *Acetylcholine is released from taste cells, enhancing taste signalling.* J Physiol, 2012. **590**(Pt 13): p. 3009-17.
269. Mohr, F., et al., *Dysfunctional Presynaptic M2 Receptors in the Presence of Chronically High Acetylcholine Levels: Data from the PRiMA Knockout Mouse.* PLoS One, 2015. **10**(10): p. e0141136.
270. Oliveira, L., M.A. Timoteo, and P. Correia-de-Sa, *Modulation by adenosine of both muscarinic M1-facilitation and M2-inhibition of [3H]-acetylcholine release from the rat motor nerve terminals.* Eur J Neurosci, 2002. **15**(11): p. 1728-36.
271. Fryer, A.D. and J. Maclagan, *Muscarinic inhibitory receptors in pulmonary parasympathetic nerves in the guinea-pig.* Br J Pharmacol, 1984. **83**(4): p. 973-8.
272. Zhou, H., et al., *Heterogeneity of release-inhibiting muscarinic autoreceptors in heart atria and urinary bladder: a study with M(2)- and M(4)-receptor-deficient mice.* Naunyn Schmiedebergs Arch Pharmacol, 2002. **365**(2): p. 112-22.
273. Wess, J., *Molecular biology of muscarinic acetylcholine receptors.* Crit Rev Neurobiol, 1996. **10**(1): p. 69-99.
274. Forster, G.L., et al., *M5 muscarinic receptors are required for prolonged accumbal dopamine release after electrical stimulation of the pons in mice.* J Neurosci, 2002. **22**(1): p. RC190.
275. Foster, D.J., et al., *M5 receptor activation produces opposing physiological outcomes in dopamine neurons depending on the receptor's location.* J Neurosci, 2014. **34**(9): p. 3253-62.
276. Chen, S.R., et al., *Differential regulation of primary afferent input to spinal cord by muscarinic receptor subtypes delineated using knockout mice.* J Biol Chem, 2014. **289**(20): p. 14321-30.
277. Andersson, K.E., R. Soler, and C. Fullhase, *Rodent models for urodynamic investigation.* Neurourol Urodyn, 2012. **30**(5): p. 636-46.

278. De Wachter, S., *Afferent signaling from the bladder: species differences evident from extracellular recordings of pelvic and hypogastric nerves.* Neurourol Urodyn, 2011. **30**(5): p. 647-52.
279. Lemack, G.E., et al., *Physiologic sequelae of partial infravesical obstruction in the mouse: role of inducible nitric oxide synthase.* J Urol, 1999. **161**(3): p. 1015-22.
280. Nandigama, R., et al., *Muscarinic acetylcholine receptor subtypes expressed by mouse bladder afferent neurons.* Neuroscience, 2010. **168**(3): p. 842-50.
281. Khandelwal, P., S.N. Abraham, and G. Apodaca, *Cell biology and physiology of the uroepithelium.* Am J Physiol Renal Physiol, 2009. **297**(6): p. F1477-501.
282. Wang, J.Q., et al., *Toll-Like Receptors and Cancer: MYD88 Mutation and Inflammation.* Front Immunol, 2014. **5**: p. 367.
283. Irvine, K.L., et al., *The molecular basis for recognition of bacterial ligands at equine TLR2, TLR1 and TLR6.* Vet Res, 2013. **44**: p. 50.
284. Park, B.S., et al., *The structural basis of lipopolysaccharide recognition by the TLR4-MD-2 complex.* Nature, 2009. **458**(7242): p. 1191-5.
285. Li, X.C., Y. Shao, and J.L. Zhuo, *AT1a receptor signaling is required for basal and water deprivation-induced urine concentration in AT1a receptor-deficient mice.* Am J Physiol Renal Physiol, 2012. **303**(5): p. F746-56.
286. Althaus, M., et al., *Mechano-sensitivity of epithelial sodium channels (ENaCs): laminar shear stress increases ion channel open probability.* FASEB J, 2007. **21**(10): p. 2389-99.
287. Guo, D., et al., *Role of epithelial Na+ channels in endothelial function.* J Cell Sci, 2016. **129**(2): p. 290-7.
288. Peng, C.W., et al., *Role of pudendal afferents in voiding efficiency in the rat.* Am J Physiol Regul Integr Comp Physiol, 2008. **294**(2): p. R660-72.
289. Todd, J.K., *Afferent Impulses in the Pudendal Nerves of the Cat.* Q J Exp Physiol Cogn Med Sci, 1964. **49**: p. 258-67.
290. Danziger, Z.C. and W.M. Grill, *Dynamics of the sensory response to urethral flow over multiple time scales in rat.* J Physiol, 2015. **593**(15): p. 3351-71.
291. Deckmann, K., et al., *Cholinergic urethral brush cells are widespread throughout placental mammals.* Int Immunopharmacol, 2015. **29**(1): p. 51-6.
292. Kandel, C., et al., *ENaC in Cholinergic Brush Cells.* Front Cell Dev Biol, 2018. **6**: p. 89.
293. Deckmann, K., et al., *Muscarinic receptors 2 and 5 regulate bitter response of urethral brush cells via negative feedback.* FASEB J, 2018. **32**(6): p. 2903-2910.

6 Publikationsübersicht

Orignalarbeiten

I. **Deckmann K***, Filipski K*, Krasteva-Christ G, Fronius M, Althaus M, Rafiq A, Papadakis T, Renno L, Jurastow I, Wessels L, Wolff M, Schütz B, Weihe E, Chubanov V, Gudermann T, Klein J, Bschleipfer T, Kummer W. Bitter triggers acetylcholine release from polymodal urethral chemosensory cells and bladder reflexes. **Proc Natl Acad Sci U S A**. 2014;111(22):8287-92.

II. **Deckmann K**, Krasteva-Christ G, Rafiq A, Herden C, Wichmann J, Knauf S, Nassenstein C, Grevelding CG; Dorresteijn A, Chubanov V, Gudermann T, Bschleipfer T, Kummer W. Cholinergic urethral brush cells are widespread throughout placental mammals. **Int Immunopharmacol**. 2015 Nov;29(1):51-6.

III. **Deckmann K**, Rafiq A, Erdmann C, Illig C, Durschnabel M, Wess J, Weidner W, Bschleipfer T, Kummer W. Muscarinic receptors 2 and 5 regulate bitter response of urethral brush cells via negative feedback. **FASEB J**. 2018, Jan 17:fj201700582R. Epub 2018 Jan 17

IV. Kandel C, Schmidt P, Perniss A, Keshavarz M, Scholz P, Osterloh S, Althaus M, Kummer W, **Deckmann K**. ENaC in Cholinergic Brush Cells. **Front Cell Dev Biol**. 2018 Aug 15;6:89. doi: 10.3389/fcell.2018.00089. eCollection 2018.

V. Perniss A*, Schmidt P*, Soultanova A, Papadakis T, Dahlke K, Voigt A, Schütz B, Kummer W, **Deckmann K**. Development of epithelial cholinergic chemosensory cells of the urethra and trachea of mice. **Cell Tissue Res** 2021 Jul;385(1):21-35.

Übersichtsarbeiten

VI. **Deckmann K**, Kummer W. Chemosensory epithelial cells in the urethra: sentinels of the urinary tract. **Histochem Cell Biol**. 2016 Dec; 146(6):673-683.

VII. Kummer W, **Deckmann K**. Brush cells, the newly identified gatekeepers of the urinary tract. **Curr Opin Urol**. 2017 Mar; 27(2):85-92.

7 Publikationen

PNAS

Bitter triggers acetylcholine release from polymodal urethral chemosensory cells and bladder reflexes

Klaus Deckmann[a,1], Katharina Filipski[a,1], Gabriela Krasteva-Christ[a,b], Martin Fronius[c,d], Mike Althaus[d], Amir Rafiq[a], Tamara Papadakis[a], Liane Renno[a], Innokentij Jurastow[a], Lars Wessels[a], Miriam Wolff[a], Burkhard Schütz[e], Eberhard Weihe[b,e], Vladimir Chubanov[f], Thomas Gudermann[b,f], Jochen Klein[g], Thomas Bschleipfer[h,2], and Wolfgang Kummer[a,b,2,3]

[a]Institute of Anatomy and Cell Biology, Justus-Liebig University, 35385 Giessen, Germany; [b]German Center for Lung Research, 35392 Giessen, Germany; [c]Department of Physiology, University of Otago, 9016 Dunedin, New Zealand; [d]Institute of Animal Physiology, Justus-Liebig University, 35392 Giessen, Germany; [e]Institute of Anatomy and Cell Biology, Philipps University, 35037 Marburg, Germany; [f]Walter-Straub Institute for Pharmacology and Toxicology, Ludwig-Maximilian University, 80336 Munich, Germany; [g]Department of Pharmacology, School of Pharmacy, Goethe University Frankfurt, 60438 Frankfurt am Main, Germany; and [h]Department of Urology, Pediatric Urology, and Andrology, Justus-Liebig University, 35392 Giessen, Germany

Edited by Scott J. Hultgren, Washington University School of Medicine, St. Louis, MO, and approved April 22, 2014 (received for review February 10, 2014)

Chemosensory cells in the mucosal surface of the respiratory tract ("brush cells") use the canonical taste transduction cascade to detect potentially hazardous content and trigger local protective and aversive respiratory reflexes on stimulation. So far, the urogenital tract has been considered to lack this cell type. Here we report the presence of a previously unidentified cholinergic, polymodal chemosensory cell in the mammalian urethra, the potential portal of entry for bacteria and harmful substances into the urogenital system, but not in further centrally located parts of the urinary tract, such as the bladder, ureter, and renal pelvis. Urethral brush cells express bitter and umami taste receptors and downstream components of the taste transduction cascade; respond to stimulation with bitter (denatonium), umami (monosodium glutamate), and uropathogenic *Escherichia coli*; and release acetylcholine to communicate with other cells. They are approached by sensory nerve fibers expressing nicotinic acetylcholine receptors, and intraurethral application of denatonium reflexively increases activity of the bladder detrusor muscle in anesthetized rats. We propose a concept of urinary bladder control involving a previously unidentified cholinergic chemosensory cell monitoring the chemical composition of the urethral luminal microenvironment for potential hazardous content.

Mucosal surfaces of the mammalian respiratory and gastrointestinal tract contain solitary epithelial cells with characteristic microvilli at their tip, from which the name "brush cells" derives (1–3). In the respiratory tract, these brush cells serve as sentinels, using the canonical taste transduction cascade to monitor the mucosal lining fluid for potential harmful substances, such as "bitter" bacterial products, and evoking reflexes aimed at combating further ingression of such compounds, such as closure of ducts leading into adjacent compartments (vomeronasal organ) or respiratory reflexes (4–7).

In line with such a sentinel function, brush cell abundance decreases with increasing distance to the opening to the outside world, being numerous in the nose and nearly absent in the intrapulmonary airways. Physiologically, the urinary tract allows passage in only one direction to release urine, but ascending infection by uropathogenic bacteria is not uncommon and is a major risk factor in fatal kidney disease and male infertility (8, 9). We hypothesized that the urogenital tract also may be equipped with chemosensory sentinel cells that monitor the lumen for potential hazardous content.

Results

Brush Cells Are Positioned at the Portal of Entry into the Urinary Tract. The majority of chemosensory brush cells of the mouse airways use acetylcholine as a signaling molecule and can be readily identified in mice expressing GFP driven by the promoter of the acetylcholine-synthesizing enzyme choline acetyltransferase (ChAT-eGFP mice) (4, 6). On screening of tissue sections and whole-mount preparations of the urogenital tract of two independently generated ChAT-eGFP mouse strains (10, 11), we observed solitary ChAT-eGFP$^+$ cells in the epithelium of the urethra, but not in the epithelial linings of the renal pelvis, ureter, urinary bladder, and pelvic segment of the vas deferens (Fig. 1 and Fig. S1). The total numbers of such urethral cells did not differ significantly between male and female animals (mean ± SD, 379 ± 99 and 551 ± 253, respectively, $P = 0.26$, t test; $n = 6$ for each sex). In male prostate, coagulating, and seminal glands and in both male and female paraurethral glands, these cells are located in the excretory ducts close to the opening into the urethra, but not in the glandular bodies themselves (Fig. S2). These cells vary in shape from the typical flask-like structure of tracheal brush cells, with a broad base at the basement membrane and an elongated tip reaching the lumen, to more complex morphologies with slender foot processes reaching the basal lamina directly or in an oblique course (Figs. 2 and 3). Horizontally oriented cell bodies with unclear connections to the luminal surface are seen as well (Fig. 3 *A* and *B*).

Double-labeling procedures revealed that these cells are distinct from the previously known urethral neuroendocrine cell population (12, 13) expressing protein gene product 9.5, serotonin, and chromogranin A (Fig. 2 *B* and *C* and Table S1). In

Significance

We report the presence of a previously unidentified cholinergic, polymodal chemosensory cell in the mammalian urethra, the potential portal of entry for bacteria and harmful substances into the urogenital system. These cells exhibit structural markers of respiratory chemosensory cells ("brush cells"). They use the classical taste transduction cascade to detect potential hazardous compounds (bitter, umami, uropathogenic bacteria) and release acetylcholine in response. They lie next to sensory nerve fibers that carry acetylcholine receptors, and placing a bitter compound in the urethra enhances activity of the bladder detrusor muscle. Thus, monitoring of urethral content is linked to bladder control via a previously unrecognized cell type.

Author contributions: K.D., G.K.-C., T.B., and W.K. designed research; K.D., K.F., G.K.-C., M.F., M.A., A.R., T.P., L.R., I.J., L.W., M.W., J.K., T.B., and W.K. performed research; B.S., E.W., V.C., and T.G. contributed new reagents/analytic tools; K.D., K.F., G.K.-C., M.F., J.K., T.B., and W.K. analyzed data; and K.D., K.F., M.F., T.B., and W.K. wrote the paper.

The authors declare no conflict of interest.

This article is a PNAS Direct Submission.

[1]K.D. and K.F. contributed equally to this work.

[2]T.B. and W.K. contributed equally to this work.

[3]To whom correspondence should be addressed. E-mail: wolfgang.kummer@anatomie.med.uni-giessen.de.

This article contains supporting information online at www.pnas.org/lookup/suppl/doi:10.1073/pnas.1402436111/-/DCSupplemental.

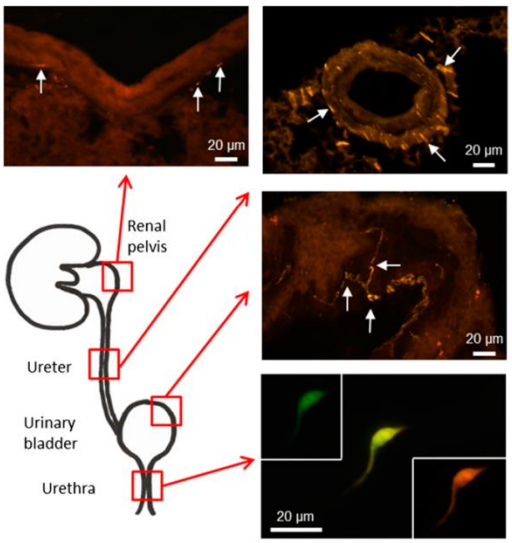

Fig. 1. Cholinergic eGFP-expressing epithelial cells are restricted to the urethra in the urinary tract. Visualization of GFP was enhanced by application of a chicken anti-eGFP antibody, followed by Cy3-conjugated anti-chicken Ig. GFP and Cy3 channels are shown separately and also in the merged image for the slender epithelia cell in the urethra. In all other parts of the urinary system, cholinergic nerve fibers (arrows) were visualized by this procedure, but no ChAT-eGFP–expressing epithelial cells were seen.

contrast to these neuroendocrine cells, nearly all (>90%) urethral ChAT-eGFP$^+$ cells express villin (Fig. 2*D* and Table S2) and at the ultrastructural level exhibit a tuft of apical microvilli and additional basolateral microvilli (Fig. 2 *F* and *G*), the defining features of respiratory and gastrointestinal brush cells (14). A significant additional population of urethral villin-positive cells (≥50%) lacked ChAT-eGFP fluorescence (Fig. 2*E* and Table S2), indicative of the presence of distinct populations of cholinergic and noncholinergic urethral brush cells.

Cholinergic Urethral Brush Cells Use the Canonical Taste Transduction Cascade to Detect Bitter Substances. Respiratory chemosensory brush cells express elements of the canonical taste transduction cascade, including the taste-specific G protein α-gustducin, phospholipase $C_{\beta 2}$ (PLCβ2), and the transient potential receptor cation channel melanostatin 5 (TRPM5) (5, 6, 15–17). These proteins are also expressed in urethras from ChAT-eGFP and WT mice (Fig. 3 *A–D*). ChAT-eGFP and TRPM5 immunolabeling matched nearly 1:1 (Fig. 3*A* and Table S3), and the majority of ChAT-eGFP$^+$ cells exhibited PLCβ2 immunoreactivity (Fig. 3*B*), although an additional PLCβ2$^+$/ChAT-eGFP$^-$ cell population exists (Table S3 and Fig. S3 *A* and *B*). Clear α-gustducin immunolabeling was observed in approximately one-third of ChAT-eGFP$^+$ cells (Fig. 3*C*, Table S3, and Fig. S3*A*). These incomplete colocalization patterns argue for the presence of subpopulations of urethral brush cells, including cholinergic/TRPM5$^+$ and noncholinergic cells, mostly TRPM5$^-$ cells.

Accordingly, TRPM5 antibody, different from that used for immunolabeling and directed against an extracellular domain, served to isolate the presumptive cholinergic chemosensory cells for RT-PCR analysis. This analysis revealed mRNA expression of the bitter taste receptor Tas2R108 (for which denatonium is a ligand), but not of Tas2R105 (for which cycloheximide is a ligand) or of Tas2R119 (Fig. 4*A*). Cellular responses in intracellular calcium concentration ($[Ca^{2+}]_i$) to unspecific (e.g., ATP) and gustatory stimuli were recorded from dissociated cells identified by ChAT-eGFP fluorescence and from cells isolated from WT and ChAT-eGFP mice via the TRPM5 antibody conjugated to magnetic beads. Consistent with detection of Tas2R108 mRNA, denatonium caused a dose-dependent (2.5–25 mM) increase in $[Ca^{2+}]_i$ in the majority of cells tested (45/49; 92%) (Fig. 4 *B* and *C*). Although TPRM5 itself is a monovalent-specific cation channel activated by Ca^{2+} rather than a Ca^{2+} channel itself (18), its inhibition by triphenylphosphine oxide (TPPO) is known to significantly reduce the tastant-induced rise in $[Ca^{2+}]_i$ in mouse taste bud cells (19); we found that this action applies to denatonium responses in urethral cells as well (Fig. 4*D*). In whole-cell patch-clamp recordings, denatonium caused activation of a delayed and long-lasting inward current in 15 of 21 cells (Fig. 4*E*).

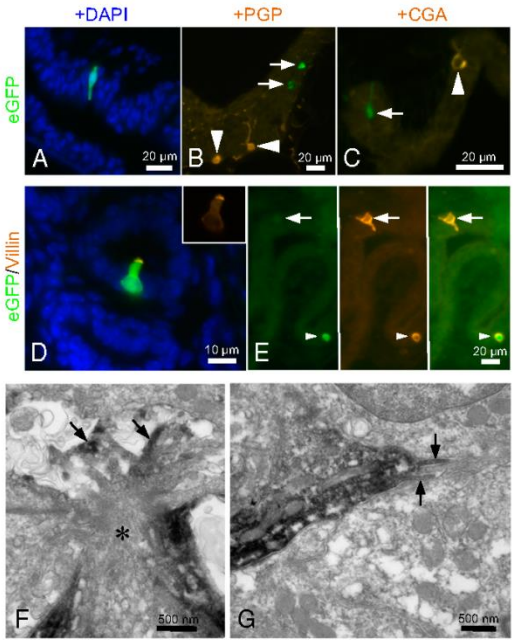

Fig. 2. A cholinergic epithelial cell of the urethra is a brush cell, not a neuroendocrine cell. (*A*) Male penile urethra. A slender ChAT-eGFP cell extends through the epithelial layer. Nuclei are counterstained with DAPI. (*B*) Female urethra. ChAT-eGFP cells (arrows) are distinct from protein gene product 9.5 (PGP)-immunoreactive neuroendocrine cells (arrowheads). (*C*) Male urethra. The ChAT-eGFP cell (arrow) does not express the neuroendocrine cell marker chromogranin A (CGA). The arrowhead indicates a CGA$^+$ neuroendocrine cell. (*D*) Male urethra, colliculus seminalis. Merged image showing eGFP (green), villin immunoreactivity (orange), and cell nuclei (DAPI; blue). The flask-shaped ChAT-eGFP cell is immunoreactive for the brush cell marker villin. (*Inset*) Villin only, showing the concentration of this microvillous protein at the apical cell pole. (*E*) Male urethra. Another villin$^+$ brush cell is not ChAT+ (arrows). Arrowheads indicate double-positive cells. (*F*) Female urethra, pre-embedding ultrastructural eGFP immunolabeling. The apical region of the eGFP-immunoreactive cell (asterisk) exhibits characteristic brush cell features, with numerous filaments, tubulovesicular structures, and microvilli (arrows) projecting into the lumen. In this particular case, the microvilli extend into an intercellular cavity in the upper layer of the epithelium that had no visible connection to the urethral lumen. (*G*) Same cell as depicted in *F* exhibiting lateral microvilli (arrows), another brush cell feature.

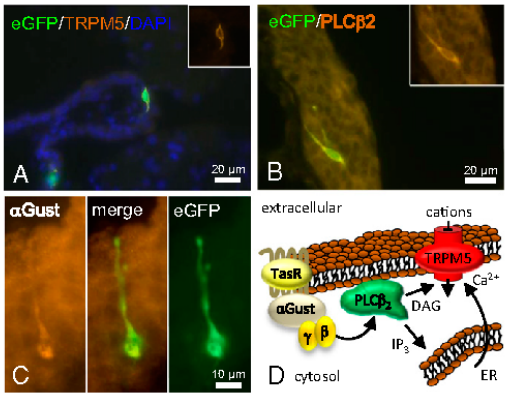

Fig. 3. Cholinergic urethral brush cells express components of the canonical taste transduction cascade. (*A*) Male urethra. ChAT-eGFP (green) and TRPM5 (orange) are expressed by the same cell; nuclei are labeled in blue with DAPI. (*B*) Female urethra. An obliquely oriented ChAT-eGFP cell is immunolabeled for PLCβ2. In this section plane, no connection of this cell to the urethral lumen is visible. (*C*) Male urethra, diverticular region. α-Gustducin (αGust)$^+$ ChAT-eGFP cell extending a slender process toward the lumen. (*D*) Schematic drawing of the canonical transduction cascade known from taste buds (based upon information published in ref. 49) depicting the position and role of α-gustducin, PLCβ2, and TRPM5 in this process. DAG, diacylglycerol; ER, endoplasmic reticulum; IP_3, inositol trisphosphate; TasR, taste receptor.

In addition, immediate and highly reversible currents were triggered by short, repetitive pulses of denatonium (Fig. S4).

Cholinergic Urethral Brush Cells Are Polymodal Chemosensors. Tas1R family members (Tas1R1–3) participate in sweet and umami (free L-amino acids) perception. Isolated urethral cholinergic chemosensory cells expressed mRNAs coding for Tas1R1 and Tas1R3, whereas Tas1R2 expression was not detected (Fig. 4*A*). Tas1R1–Tas1R3 coexpression yields an umami receptor (20). Accordingly, urethral brush cells responded with increases in $[Ca^{2+}]_i$ to monosodium glutamate (umami, 25 mM; 90%; 38/42 cells) in addition to denatonium and ATP (0.5 mM; 91%; 43/47 cells). The majority of cells (86%; 36/42) responded to both the bitter receptor agonist denatonium and glutamate, exhibiting properties of a polymodal (bitter/umami) chemosensor (Fig. 4*F*).

Notably, not all bitter substances triggered responses in urethral brush cells. In line with the lack of detectable Tas2R105 mRNA in urethral brush cells (Fig. 4*A*), cycloheximide, a Tas2R105 agonist, did not evoke changes in $[Ca^{2+}]_i$ at a concentration of 0.1 mM (Fig. 4*G*), which is known to stimulate a $[Ca^{2+}]_i$ increase in Tas2R105-transfected cells (21). In addition to synthetic bitter and umami stimuli, heat-inactivated uropathogenic *Escherichia coli* (strain CFT073; 2–5 × 10^7 cfu) also triggered a rise in $[Ca^{2+}]_i$ (Fig. 4*H*). Tas1R2–Tas1R3 coexpression yields a sweet receptor (22). Consistent with the absence of detectable Tas1R2 mRNA in urethral brush cells (Fig. 4*A*), the artificial sweetener saccharin (5 mM) did not trigger a $[Ca^{2+}]_i$ response in urethral brush cells (Fig. 4*G*).

Urethral Brush Cells Use Acetylcholine for Stimulus-Induced Paracrine Signaling. The concept of brush cells serving as chemosensory sentinels monitoring the chemical composition of mucosal surface fluids and initiating local or reflexive responses implies stimulus-induced signaling to neighboring cells. In view of these cells' ChAT expression, we tested for acetylcholine as a potential messenger released by urethral brush cells. Acetylcholine content in the supernatant (0.5 mL) of isolated urethral cells was increased by an average of 0.875 pmol (from a baseline of 10.0 pmol) in response to stimulation with denatonium (25 mM, 5 min) (Fig. 5*A*). In our experiments, we noted a rise in $[Ca^{2+}]_i$ in response to denatonium in non–GFP-expressing cells when situated in the vicinity of ChAT-eGFP$^+$ cells, but not in isolated cells resting on coverslips devoid of ChAT-eGFP cells (Fig. S5). Such cells express functional acetylcholine receptors; administration of 25 μM acetylcholine together with the esterase inhibitor physostigmine (5 μM) evoked a rise in $[Ca^{2+}]_i$ in eGFP cells that was sensitive to a cholinergic blocker mixture (2 μM atropine and 20 μM mecamylamine) (Fig. 5*B*). In the presence of the same cholinergic blockers, denatonium still evoked a rise in $[Ca^{2+}]_i$, even at a slightly enhanced level, in ChAT-eGFP cells, but no longer in eGFP cells, demonstrating stimulus-evoked cholinergic signaling between chemosensory cells and surrounding cells (Fig. 5*C*).

Sensory Nerve Fibers Approach Urethral Brush Cells and Elicit Reflex Bladder Activation on Urethral Bitter Substance Application. Cholinergic chemosensory cells of the respiratory tract are approached by cholinoceptive sensory nerve fibers that initiate protective respiratory reflexes (4–6). The dominant nicotinic acetylcholine receptor (nAChR) subtype of viscerosensory neurons contains the α3 subunit, and such neurons project to the murine lower urinary tract (23). Using a GFP reporter mouse strain for this promoter (24), we identified a dense nerve fiber network immediately underneath and partially penetrating into the urethral epithelium, coming into contact with villin-positive brush cells (Fig. 6*A*). Because urethral sensory nerve fibers are known to be linked to the micturition reflex and to coordinate muscle constriction of the bladder and urethra (25), we assessed for reflex coupling between urethral bitter sensing and detrusor activity. The mouse urethra is too small to allow simultaneous cystometric recording of intravesical pressure and urethral manipulation, and thus rat is the model of choice for this purpose (26).

We first validated by immunohistochemistry the occurrence of solitary villin-, α-gustducin–, PLCβ2-, TRPM5-, and ChAT-immunoreactive cells in the urethral mucosa of rats (Fig. 6*B*). Notably, such cells were also detected in two human urethral specimens obtained during prostatectomy (Fig. 6*B*), demonstrating that their occurrence is not restricted to rodents. Continuous filling of the bladder with saline solution (0.04 mL/min) through a catheter inserted into the bladder dome simulated natural bladder filling in fast motion and caused cycles of rising intravesical pressure and micturition in urethane-anesthetized rats. Urethral instillation of saline solution (0.9%; 50 μL) through the external urethral orifice augmented pressure rises only slightly, but a single dose of denatonium (25 mM; 50 μL) significantly increased detrusor activity far beyond the first micturition, causing washout or a drastic dilution of urethral content (Fig. 6 *C* and *D*). Lower denatonium concentrations (2.5–12.5 mM; $n = 2$ each) had no obvious effect, resembling the effectiveness of denatonium on $[Ca^{2+}]_i$ rises in isolated urethral chemosensory cells. Intraurethral administration of the general nicotinic receptor blocker mecamylamine (10^{-4} M) significantly reduced the denatonium-induced increase in detrusor activity, although the activity did not completely return to baseline (Fig. 6 *C* and *E*). When administered before denatonium, mecamylamine also did not completely block the denatonium-induced rise in detrusor activity ($n = 2$).

Discussion

Up to now, solitary chemosensory or brush cells have been identified in the respiratory and gastrointestinal tracts, but not in any other mammalian organ system. Likely owing due to their anatomic restriction to the portal of entry into the urogenital tract (i.e., the urethra and glandular ducts opening into it), these chemosensory cells have escaped detection in previous searches for urogenital brush cells that focused on more centrally located organs, including the kidney, uterus, and prostate gland, before the sentinel function of solitary chemosensory cells had been proposed (14). Coexpression patterns of various components of

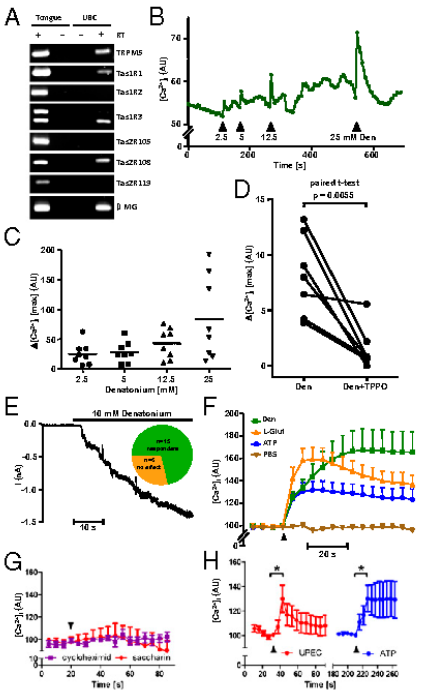

Fig. 4. Urethral cholinergic brush cells are polymodal chemosensors. (*A*) RT-PCR, agarose gel. Urethral brush cells (UBCs) were isolated by magnetic beads coated with TRPM5 antibody. Tongue, positive control; β2-microglobulin (β-MG), housekeeping gene; +/− RT, aliquots processed with/without reverse transcription. (*B* and *C*) Dose-dependent increase in $[Ca^{2+}]_i$ in dissociated UBC in response to the Tas2R108 agonist denatonium. All drugs were added under continuous flow in the chamber, so that indicated concentrations were reached initially and then washed out. (*B*) Confocal laser scanning recording of changes in Calcium Orange fluorescence in a single cholinergic (eGFP$^+$) brush cell. The *y* axis depicts arbitrary units (AU) correlating to $[Ca^{2+}]_i$. (*C*) The *y* axis depicts maximum $[Ca^{2+}]_i$ increases in eight cholinergic cells in response to increasing denatonium concentrations. (*D*) Same technique as in *B* and *C*. Shown are maximum $[Ca^{2+}]_i$ increases evoked by 25 mM denatonium before and after application of the TRPM5 inhibitor TPPO (0.25 mM) in seven cholinergic brush cells. (*E*) Whole-cell patch-clamp recording, with membrane potential clamped to −60 mV. Increased inward current was observed in 15 of 21 cells (responders). (*F*–*H*) Same technique as in *B*–*D*. (*F*) Superimposed calcium increases in 32 polymodal cells that responded to all three stimuli (0.5 mM ATP, 25 mM denatonium, and 25 mM L-glutamate). (*G*) In contrast, dissociated cells did not respond to the Tas2R105 agonist cycloheximide (Cyc; 0.1 mM) or to the artificial sweetener saccharin (Sac; 5 mM). (*H*) Heat-inactivated uropathogenic *E. coli* (UPEC; 2–5 × 10^7 cfu) induced $[Ca^{2+}]_i$ increase to the same extent as ATP. Graphs depict mean and SEM. *$P < 0.05$, paired *t* test.

the taste transduction cascade and ChAT-eGFP suggest the presence of more than one chemosensory cell type in the urethra, including a cholinergic type using PLCβ2 and TRPM5, proteins essential for oropharyngeal bitter and umami perception (27), for downstream signaling. Consistent with our $[Ca^{2+}]_i$ measurements, this signaling pathway involves Gβγ stimulation of PLCβ2 with subsequent release of Ca^{2+} from intracellular stores (28).

The role of the taste-specific Gα protein α-gustducin (29), which is expected to activate a phosphodiesterase, is less clear (28). In taste buds, α-gustducin is inconsistently coexpressed with T1R1–3, particularly in the posterior tongue (30), and its genetic ablation diminishes, but does not abrogate, bitter and umami gustation (31, 32). Similarly, the vast majority (≥90%) of cholinergic urethral brush cells respond to bitter (denatonium) and umami (L-glutamate), but only approximately one-third coexpress α-gustducin.

A striking feature of cholinergic/TRPM5$^+$ urethral chemosensory cells is the coexpression of taste receptors of the Tas1R and Tas2R families and the resulting polymodal response to both bitter and umami stimuli. Similarly, solitary nasal chemosensory cells coexpress Tas1R3 with Tas2R5 and Tas2R8 (33); however, although the responses of these cells to bitter stimuli are well documented (34), whether they also respond to umami remains to be established. This situation is in contrast to oropharyngeal gustation, where Tas1R and Tas2R receptors are not coexpressed in taste buds (33, 35), and 83% of receptor cells in murine vallate papillae respond to only a single taste quality, which provides a basis for taste coding in taste buds (36).

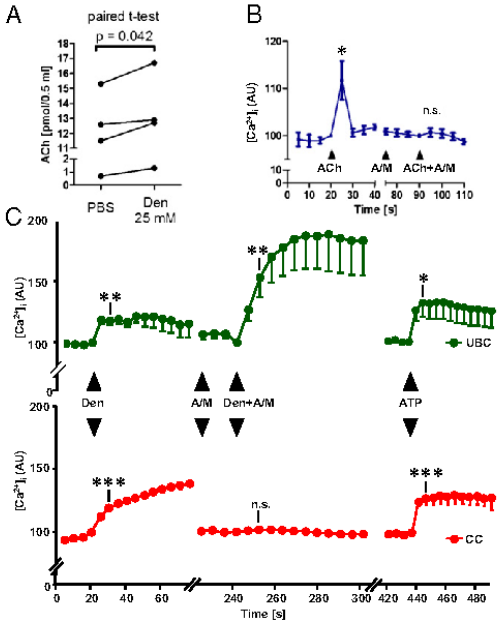

Fig. 5. Urethral brush cells release acetylcholine. (*A*) Acetylcholine (Ach) content in the supernatant (0.5 mL) of isolated urethral cells after a 5-min exposure to PBS (control) or denatonium. Isolates from one urethra are treated as paired data. (*B*) Calcium recordings from eight eGFP$^-$ urethral cells located on coverslips that did not contain eGFP$^+$ cells. In the continuous presence of the acetylcholine esterase inhibitor physostigmine (5 μM), acetylcholine (25 μM) evokes an increase in $[Ca^{2+}]_i$ that is sensitive to a mixture (A+M) of muscarinic (2 μM atropine) and nicotinic (20 μM mecamylamine) acetylcholine receptor blockers. (*C*) Parallel $[Ca^{2+}]_i$ recordings from eGFP$^+$ ($n = 13$, *Upper*) and eGFP$^-$ ($n = 74$; *Lower*) isolated urethral cells located in their vicinity (same field of view during confocal laser scanning recording) on the coverslip. Both cell types respond to denatonium (Den; 25 mM) with a $[Ca^{2+}]_i$ increase. This responsiveness is lost in eGFP$^-$ cells, but persists (even at enhanced levels; $P = 0.04$, paired *t* test) in eGFP$^+$ cells after pretreatment with cholinergic blockers (A+M; *A*), demonstrating denatonium-evoked cholinergic signaling from eGFP$^+$ to eGFP$^-$ cells. Response to the nongustatory stimulus ATP demonstrates the viability of cells at the end of the experiment. n.s., nonsignificant. *$P < 0.05$; **$P < 0.01$; ***$P < 0.001$, paired *t* test compared with value immediately before substance application.

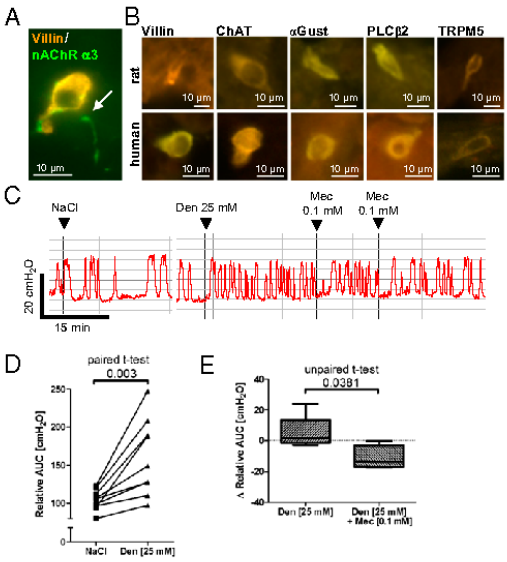

Fig. 6. Sensory nerve fibers approach urethral brush cells and elicit reflex bladder activation on application of a bitter substance. (*A*) A sensory nerve fiber expressing eGFP under the control of the nicotinic receptor α3-subunit (arrow) establishes contact with a villin-immunoreactive brush cell in the mouse urethra. (*B*) Immunolabeling. Solitary epithelial cells with immunoreactivity to brush cell markers, taste transduction cascade components, and ChAT in rat and human urethral epithelium. (*C–E*) Cystometric recordings from urethane-anesthesized rats. The bladder was continuously filled with saline (0.04 mL/min), causing a rise in intravesical pressure and initiating detrusor contraction and micturition. (*C*) Original recording of a single experiment showing that urethral instillation of denatonium increases detrusor activity compared with saline application, which is diminished by the nicotinic blocker mecamylamine (Mec). (*D* and *E*) Detrusor activity quantified as AUC. (*D*) Denatonium increases detrusor activity. AUC was determined over a period of 18–36 min in each condition, in nine experiments. (*E*) First, recordings were made after stimulation with a single dose of denatonium for a minimum of 18 min, with AUC/min as the baseline value. AUC/min decreased after application of mecamylamine, but increased over time when no additional compound was applied.

In oropharyngeal gustation, bitter represents an aversive stimulus and umami represents a rewarding stimulus, raising the question as to the possible functional meaning of sensing of both qualities by a single cell. In contrast, on other mucosal surfaces, such as the urethral lining, these qualities represent potentially harmful (aversive) content. Bacteria produce and secrete bitter receptor-activating substances (5, 37, 38). In biofilms, such substances from the Gram-negative bacterium *Pseudomonas aeruginosa*, one of the predominant causative microorganisms in catheter-associated urinary tract infection (39), can reach concentrations as high as 600 μM (40). On the other hand, glutamate metabolism is positively linked to the pathogenic potential of *Proteus mirabilis* in the urinary tract (41), and free amino acids (i.e., umami) facilitate bacterial growth in urine (42). Thus, the bitter/umami polymodality of chemosensory cells may serve to broaden the spectrum for recognition of potential hazardous material in the urethral lumen. Most importantly, these chemosensory cells responded to heat-inactivated uropathogenic *E. coli*, the primary cause of urinary tract infection (43).

Acetylcholine, a secretory product of these cells, may alter sensitivity of this process in an autocrine manner, as demonstrated by the enhanced tastant response after application of a muscarinic/nicotinic receptor blocker mixture. In the more complex lingual taste buds, autocrine cholinergic signaling enhances taste signaling via muscarinic receptors (44). Our cell culture experiments revealed that the amount of acetylcholine released on bitter stimulation is also sufficient to induce paracrine effects. In situ, these cholinergic cells, like those in the trachea (6), are directly approached by sensory nerve fibers expressing the nicotinic acetylcholine receptor α3 subunit, and luminal denatonium evoked reflex activation of the detrusor muscle at a concentration that stimulated urethral chemosensory cells. This reflex activation was sensitive to local application of a nicotinic receptor blocker, demonstrating the involvement of cholinergic, nicotinic transmission from chemosensory cells to sensory nerve fibers. Nonetheless, the denatonium-induced increase in detrusor activity was not entirely abrogated, possibly owing to (*i*) additional involvement of excitatory muscarinic acetylcholine receptors that are also expressed by urinary tract afferent neurons (45); (*ii*) additional involvement of a cotransmitter, such as ATP, which transmits information from taste cells to afferent fibers in taste buds (46); or (*iii*) insufficient access of intraluminally applied mecamylamine to the basolaterally located communication site between chemosensory cells and nerve fibers, as lower urinary tract epithelia form an extraordinary tight barrier (47).

In conclusion, we propose a concept of urinary bladder control involving a previously unidentified cholinergic chemosensory cell monitoring the chemical composition of the urethral luminal microenvironment for potential hazardous content.

Materials and Methods

Animals. Two independently generated ChAT$^{(BAC)}$-eGFP mice were provided by M. Kotlikoff (Cornell University), and H. Monyer (University of Heidelberg) (10, 11). Tg(*Chrna3*-EGFP)BZ135Gsat mice with eGFP driven by the nAChR α3β4α5 cluster were provided by I. Ibanez-Tallon (MDC Molecular Medicine) (24). C57BL/6 mice were obtained from The Jackson Laboratory. Male Clr:WI Wistar rats were obtained from Charles River Deutschland. All animals were housed under standard laboratory conditions (12 h dark, 12 h light). Mice were killed by inhalation of an overdose of isoflurane (Abbott) and exsanguination. The experiments were approved by the local authorities (Rp Giessen, Germany; reference nos. A9/2011, A11/2011, A60/2012, A61/2012, and 12/2013).

Cell Isolation. Urethrae were dissected, cut into small pieces, and enzymatically digested in dispase (2 mg/mL; Sigma-Aldrich) for 30 min in HBSS (Invitrogen) and 5 min in trypsin/PBS (1:1, Invitrogen) at 37 °C. After centrifugation (60 × *g*, 5 min) and mechanical dissociation, cells were resuspended in PBS and separated through a cell strainer (70 μM; BD Bioscience). Chemosensory cells were identified by either eGFP or a rabbit polyclonal TRPM5-antibody (ab72151, 1:125; Abcam) directed against an extracellular domain. Cells were incubated for 1 h at 37 °C with this primary antibody, followed by a 1-h incubation with FITC-conjugated donkey anti-rabbit IgG (1:125; Millipore) at 37 °C. The same procedure, but using Cy5-conjugated donkey anti-rabbit IgG (1:400; Dianova), was also applied to cells isolated from ChAT-eGFP mice. As observed in the immunohistochemistry of tissue sections (Table S3), TRPM5 labeling and eGFP expression matched nearly 1:1. For subsequent RT-PCR analysis (primer sequences given in Table S4), chemosensory cells were isolated by incubating dissociated urethra first with the TRPM5 antibody as described above and then with magnetic beads (Invitrogen) coated with goat anti-rabbit IgG (H+L) (PI65-6100; Invitrogen), followed by harvesting by magnetic cell separation.

Measurement of Intracellular Calcium Concentration. Isolated cells were loaded with fluorescent calcium indicator Calcium Orange AM (3 μL) in Tyrode III solution (297 μL; 8 mM $CaCl_2$, 130 mM NaCl, 5 mM KCl, 1 mM $MgCl_2$, 10 mM Hepes, 10 mM glucose, 10 mM pyruvic acid, and 5 mM $NaHCO_3$) according to the manufacturer's protocol (Invitrogen) and then plated on coverslips for 30–60 min at 37 °C. Intracellular calcium concentration was analyzed with a confocal laser scanning microscope (Zeiss LSM 710; 561-nm wavelength generated by a DPSS 561-10 laser) during continuous superfusion (3 mL/min) with Tyrode solution. Fluorescence intensities at the start of the recording period were set arbitrarily at 100%. Test stimuli and concentrations were adenosine 5′-triphosphate bis(Tris) salt dihydrate (ATP, 0.5 mM; Sigma-Aldrich), cycloheximide (0.1 mM; Sigma-Aldrich), denatonium benzoate (25 mM; Molekula), L-glutamic acid monosodium salt monohydrate (L-glutamate, 25 mM; Sigma-Aldrich),

PHYSIOLOGY

saccharin (5 mM; Fluka), acetylcholine chloride (25 μM; Sigma-Aldrich), and heat-inactivated uropathogenic *E. coli* [UPEC strain CFT073 (NCBI: AE014075, NC_004431), ~2–5 × 10^7 cfu, provided by T. Chakraborty, JLU Giessen]. Inhibitors were TPPO (0.25 mM, Sigma-Aldrich), eserine hemisulfate (10 μM; Sigma-Aldrich), mecamylamine hydrochloride (0.02 mM; Sigma-Aldrich), and atropine sulfate (0.002 mM; RBI). Data are presented as mean ± SEM and were analyzed by the two-tailed paired *t* test.

Patch-Clamp Rrecordings. Cells were isolated from ChAT-eGFP mice as described for $[Ca^{2+}]_i$ recordings, and eGFP-expressing cells were identified with a fluorescence microscope (Zeiss Axiovert 10). The bath solution consisted of 140 mM NaCl, 4.5 mM KCl, 2.5 mM $CaCl_2$, 1 mM MgCl, 10 mM Hepes, and 5 mM D-glucose (pH 7.4). The pipette solution consisted of 10 mM NaCl, 18 mM KCl, 92 mM K-gluconate, 0.5 mM $MgCl_2$, 1 mM EDTA, and 10 mM Hepes (pH 7.2). The liquid junction potential was absorbed with the clamped voltage, producing an effective membrane potential of –60 mV. The bath solution included appropriate amounts of mannitol to compensate for osmotic changes or different concentrations of denatonium (1–25 mM), applied by a pressure-driven perfusion system. Transmembrane currents were amplified (EPC 9; Heka Electronics) and recorded continuously (sampled with 10 kHz, filtered with 3 kHz) with Pulse 8.77 software (Heka Electronics).

Urodynamic Measurement. Rats were anesthetized by an s.c. injection of urethane (1.2 g/kg) at 1 h before surgery and maintained under anesthesia during the surgical preparation while on a heating pad (37 °C). A catheter (PE 50; Intramedic) was inserted into the bladder dome and connected to a pressure transducer and an infusion pump. Saline solution at room temperature was infused into the bladder at a rate of 0.04 mL/min. After a stabilization phase of 15–30 min, the intravesical bladder pressure was recorded continuously, and 50 μL of test stimuli were delivered into the urethral external orifice via a 0.9 × 25 mm cannula (Braun Vasofix G22) mounted on a 100-μL pipette. For final data analysis, areas under the curve (AUC) of equal time periods before and after stimulation were compared; data are presented as AUC/min. The urodynamic recording sessions took 3–4 h for each animal.

Fluorescence microscopy and immunohistochemistry, pre-embedding immunohistochemistry, and EM, RT-PCR, and acetylcholine measurements were performed as described previously (6, 48), with minor modifications. More details are provided in *SI Materials and Methods*.

ACKNOWLEDGMENTS. We thank M. Bodenbenner and K. Michael for technical assistance. This work was supported by the LOEWE Program of the State of Hesse (Non-neuronal Cholinergic Systems, project A5, to W.K. and T.B.) and the Deutsche Forschungsgemeinschaft (T.G. and V.C.). This study was awarded the Eugen-Rehfisch Prize of the Forum Urodynamicum.

1. Rhodin J, Dalhamn T (1956) Electron microscopy of the tracheal ciliated mucosa in rat. *Z Zellforsch Mikrosk Anat* 44(4):345–412.
2. Luciano L, Reale E, Ruska H (1968) [On a glycogen containing brusc cell in the rectum of the rat.] *Z Zellforsch Mikrosk Anat* 91(1):153–158. German.
3. Sbarbati A, Osculati F (2005) A new fate for old cells: Brush cells and related elements. *J Anat* 206(4):349–358.
4. Ogura T, Krosnowski K, Zhang L, Bekkerman M, Lin W (2010) Chemoreception regulates chemical access to mouse vomeronasal organ: Role of solitary chemosensory cells. *PLoS ONE* 5(7):e11924.
5. Tizzano M, et al. (2010) Nasal chemosensory cells use bitter taste signaling to detect irritants and bacterial signals. *Proc Natl Acad Sci USA* 107(7):3210–3215.
6. Krasteva G, et al. (2011) Cholinergic chemosensory cells in the trachea regulate breathing. *Proc Natl Acad Sci USA* 108(23):9478–9483.
7. Krasteva G, Canning BJ, Papadakis T, Kummer W (2012) Cholinergic brush cells in the trachea mediate respiratory responses to quorum sensing molecules. *Life Sci* 91(21-22):992–996.
8. Bhushan S, et al. (2009) Testicular innate immune defense against bacteria. *Mol Cell Endocrinol* 306(1-2):37–44.
9. Roberts JA (1991) Etiology and pathophysiology of pyelonephritis. *Am J Kidney Dis* 17(1):1–9.
10. Tallini YN, et al. (2006) BAC transgenic mice express enhanced green fluorescent protein in central and peripheral cholinergic neurons. *Physiol Genomics* 27(3):391–397.
11. von Engelhardt J, Eliava M, Meyer AH, Rozov A, Monyer H (2007) Functional characterization of intrinsic cholinergic interneurons in the cortex. *J Neurosci* 27(21):5633–5642.
12. Vittoria A, Cocca T, La Mura E, Cecio A (1992) Immunocytochemistry of paraneurons in the female urethra of the horse, cattle, sheep, and pig. *Anat Rec* 233(1):18–24.
13. Aumüller G, et al. (2012) Regional distribution of neuroendocrine cells in the urogenital duct system of the male rat. *Prostate* 72(3):326–337.
14. Höfer D, Drenckhahn D (1992) Identification of brush cells in the alimentary and respiratory system by antibodies to villin and fimbrin. *Histochemistry* 98(4):237–242.
15. Finger TE, et al. (2003) Solitary chemoreceptor cells in the nasal cavity serve as sentinels of respiration. *Proc Natl Acad Sci USA* 100(15):8981–8986.
16. Kaske S, et al. (2007) TRPM5, a taste-signaling transient receptor potential ion-channel, is a ubiquitous signaling component in chemosensory cells. *BMC Neurosci* 8:49.
17. Pérez CA, Margolskee RF, Kinnamon SC, Ogura T (2003) Making sense with TRP channels: Store-operated calcium entry and the ion channel Trpm5 in taste receptor cells. *Cell Calcium* 33(5-6):541–549.
18. Hofmann T, Chubanov V, Gudermann T, Montell C (2003) TRPM5 is a voltage-modulated and Ca(2+)-activated monovalent selective cation channel. *Curr Biol* 13(13):1153–1158.
19. Palmer RK, et al. (2010) Triphenylphosphine oxide is a potent and selective inhibitor of the transient receptor potential melastatin-5 ion channel. *Assay Drug Dev Technol* 8(6):703–713.
20. Li X, et al. (2002) Human receptors for sweet and umami taste. *Proc Natl Acad Sci USA* 99(7):4692–4696.
21. Chandrashekar J, et al. (2000) T2Rs function as bitter taste receptors. *Cell* 100(6):703–711.
22. Nelson G, et al. (2001) Mammalian sweet taste receptors. *Cell* 106(3):381–390.
23. Nandigama R, et al. (2013) Expression of nicotinic acetylcholine receptor subunit mRNA in mouse bladder afferent neurons. *Neuroscience* 229:27–35.
24. Frahm S, et al. (2011) Aversion to nicotine is regulated by the balanced activity of β4 and α5 nicotinic receptor subunits in the medial habenula. *Neuron* 70(3):522–535.
25. Jung SY, et al. (1999) Urethral afferent nerve activity affects the micturition reflex: Implication for the relationship between stress incontinence and detrusor instability. *J Urol* 162(1):204–212.
26. Andersson KE, Soler R, Füllhase C (2011) Rodent models for urodynamic investigation. *Neurourol Urodyn* 30(5):636–646.
27. Zhang Y, et al. (2003) Coding of sweet, bitter, and umami tastes: Different receptor cells sharing similar signaling pathways. *Cell* 112(3):293–301.
28. Kinnamon SC (2012) Taste receptor signalling—from tongues to lungs. *Acta Physiol (Oxf)* 204(2):158–168.
29. McLaughlin SK, McKinnon PJ, Margolskee RF (1992) Gustducin is a taste cell-specific G protein closely related to the transducins. *Nature* 357(6379):563–569.
30. Kim MR, et al. (2003) Regional expression patterns of taste receptors and gustducin in the mouse tongue. *Biochem Biophys Res Commun* 312(2):500–506.
31. Wong GT, Gannon KS, Margolskee RF (1996) Transduction of bitter and sweet taste by gustducin. *Nature* 381(6585):796–800.
32. Glendinning JI, et al. (2005) Contribution of alpha-gustducin to taste-guided licking responses of mice. *Chem Senses* 30(4):299–316.
33. Ohmoto M, Matsumoto I, Yasuoka A, Yoshihara Y, Abe K (2008) Genetic tracing of the gustatory and trigeminal neural pathways originating from T1R3-expressing taste receptor cells and solitary chemoreceptor cells. *Mol Cell Neurosci* 38(4):505–517.
34. Gulbransen BD, Clapp TR, Finger TE, Kinnamon SC (2008) Nasal solitary chemoreceptor cell responses to bitter and trigeminal stimulants in vitro. *J Neurophysiol* 99(6):2929–2937.
35. Adler E, et al. (2000) A novel family of mammalian taste receptors. *Cell* 100(6):693–702.
36. Tomchik SM, Berg S, Kim JW, Chaudhari N, Roper SD (2007) Breadth of tuning and taste coding in mammalian taste buds. *J Neurosci* 27(40):10840–10848.
37. Hettinger TP, Formaker BK, Frank ME (2007) Cycloheximide: No ordinary bitter stimulus. *Behav Brain Res* 180(1):4–17.
38. Lee RJ, et al. (2012) T2R38 taste receptor polymorphisms underlie susceptibility to upper respiratory infection. *J Clin Invest* 122(11):4145–4159.
39. Shuman EK, Chenoweth CE (2010) Recognition and prevention of healthcare-associated urinary tract infections in the intensive care unit. *Crit Care Med* 38(8, Suppl):S373–S379.
40. Charlton TS, et al. (2000) A novel and sensitive method for the quantification of N-3-oxoacyl homoserine lactones using gas chromatography-mass spectrometry: Application to a model bacterial biofilm. *Environ Microbiol* 2(5):530–541.
41. Pearson MM, Yep A, Smith SN, Mobley HL (2011) Transcriptome of *Proteus mirabilis* in the murine urinary tract: Virulence and nitrogen assimilation gene expression. *Infect Immun* 79(7):2619–2631.
42. Aubron C, et al. (2012) Changes in urine composition after trauma facilitate bacterial growth. *BMC Infect Dis* 12:330.
43. Ulett GC, et al. (2013) Uropathogenic *Escherichia coli* virulence and innate immune responses during urinary tract infection. *Curr Opin Microbiol* 16(1):100–107.
44. Dando R, Roper SD (2012) Acetylcholine is released from taste cells, enhancing taste signalling. *J Physiol* 590(Pt 13):3009–3017.
45. Nandigama R, et al. (2010) Muscarinic acetylcholine receptor subtypes expressed by mouse bladder afferent neurons. *Neuroscience* 168(3):842–850.
46. Finger TE, et al. (2005) ATP signaling is crucial for communication from taste buds to gustatory nerves. *Science* 310(5753):1495–1499.
47. Khandelwal P, Abraham SN, Apodaca G (2009) Cell biology and physiology of the uroepithelium. *Am J Physiol Renal Physiol* 297(6):F1477–F1501.
48. Mohr F, Zimmermann M, Klein J (2013) Mice heterozygous for AChE are more sensitive to AChE inhibitors but do not respond to BuChE inhibition. *Neuropharmacology* 67:37–45.
49. Behrens M, Meyerhof W (2011) Gustatory and extragustatory functions of mammalian taste receptors. *Physiol Behav* 105(1):4–13.

International Immunopharmacology 29 (2015) 51–56

Contents lists available at ScienceDirect

International Immunopharmacology

journal homepage: www.elsevier.com/locate/intimp

Cholinergic urethral brush cells are widespread throughout placental mammals

Klaus Deckmann [a,*], Gabriela Krasteva-Christ [a,b,k], Amir Rafiq [a], Christine Herden [c], Judy Wichmann [b,d,e,f], Sascha Knauf [b,d,e,f], Christina Nassenstein [a,b], Christoph G. Grevelding [g], Adriaan Dorresteijn [h], Vladimir Chubanov [i], Thomas Gudermann [b,i], Thomas Bschleipfer [j], Wolfgang Kummer [a,b]

[a] Institute for Anatomy and Cell Biology, Justus-Liebig-University, 35385 Giessen, Germany
[b] German Center for Lung Research (DZL), Germany
[c] Institute of Veterinary Pathology, Justus-Liebig-University Giessen, 35392 Giessen, Germany
[d] Pathology Unit, German Primate Center, Leibniz-Institute for Primate Research, 37077 Goettingen, Germany
[e] Fraunhofer Institute for Toxicology and Experimental Medicine, 30625 Hannover, Germany
[f] Biomedical Research in Endstage and Obstructive Lung Disease (BREATH), 30625 Hannover , Germany
[g] BFS, Institute for Parasitology, Justus-Liebig-University, 35392 Giessen, Germany
[h] Institute for General Zoology and Developmental Biology, Justus-Liebig-University, 35385 Giessen, Germany
[i] Walter-Straub-Institute for Pharmacology and Toxicology, Ludwig-Maximilians-University, 80336 Munich, Germany
[j] Department of Urology, Pediatric Urology and Andrology, Klinikum Weiden, 92637 Weiden, Germany
[k] Institute for Anatomy and Cell Biology, Julius-Maximilians-University Wuerzburg, Koellikerstrasse 6, 97070 Wuerzburg, Germany

ARTICLE INFO

Article history:
Received 4 March 2015
Received in revised form 20 May 2015
Accepted 21 May 2015
Available online 1 June 2015

Keywords:
Chemosensory
Acetylcholine
Urethra
Placental mammals

ABSTRACT

We previously identified a population of cholinergic epithelial cells in murine, human and rat urethrae that exhibits a structural marker of brush cells (villin) and expresses components of the canonical taste transduction signaling cascade (α-gustducin, phospholipase Cβ2 (PLCβ2), transient receptor potential cation channel melanostatin 5 (TRPM5)). These cells serve as sentinels, monitoring the chemical composition of the luminal content for potentially hazardous compounds such as bacteria, and initiate protective reflexes counteracting further ingression. In order to elucidate cross-species conservation of the urethral chemosensory pathway we investigated the occurrence and molecular make-up of urethral brush cells in placental mammals. We screened 11 additional species, at least one in each of the five mammalian taxonomic units primates, carnivora, perissodactyla, artiodactyla and rodentia, for immunohistochemical labeling of the acetylcholine synthesizing enzyme, choline acetyltransferase (ChAT), villin, and taste cascade components (α-gustducin, PLCβ2, TRPM5). Corresponding to findings in previously investigated species, urethral epithelial cells with brush cell shape were immunolabeled in all 11 mammals. In 8 species, immunoreactivities against all marker proteins and ChAT were observed, and double-labeling immunofluorescence confirmed the cholinergic nature of villin-positive and chemosensory (TRPM5-positive) cells. In cat and horse, these cells were not labeled by the ChAT antiserum used in this study, and unspecific reactions of the secondary antiserum precluded conclusions about ChAT-expression in the bovine epithelium. These data indicate that urethral brush cells are widespread throughout the mammalian kingdom and evolved not later than about 64.5 million years ago.

1. Introduction

Mucosal surfaces of the mammalian lower respiratory and gastrointestinal tract contain solitary epithelial cells with a characteristic flask-like shaped and a tuft of blunt, stiff microvilli at their apical tip, from which the name "brush cells" derived [1–4]. The actin-binding protein villin is a structural marker protein within these microvilli [1]. In the upper respiratory tract, cells with similar shape and functional characteristics carry phenotypically different microvilli and are often referred to as "solitary chemosensory cells" [5,6]. In the respiratory tract, these cells serve as sentinels, using the canonical taste transduction cascade to monitor the mucosal lining fluid for potential harmful substances, such as "bitter" bacterial products. In response, they evoke reflexes aimed at combating further ingression of such compounds, such as closure of ducts leading into adjacent compartments (vomeronasal organ) or respiratory reflexes [7–9]. In mice, acetylcholine is synthesized and released by these cells and serves as an important mediator in initiating these protective reflexes [7,10,11]. In line with the proposed sentinel function, brush cell abundance decreases with increasing distance to the opening to the outside world, being numerous in the nose and nearly absent in the intrapulmonary airways [12].

Based on this sentinel concept, we have predicted and validated the presence of such previously unrecognized cells in the urethral epithelium

* Corresponding author. Tel.: +49 641 9947014.
E-mail address: Klaus-Deckmann@gmx.de (K. Deckmann).

http://dx.doi.org/10.1016/j.intimp.2015.05.038
1567-5769/

("urethral brush cells" = UBC) and in the very distal portions of the glandular (e.g. prostate) excretory ducts opening into the urethra, but neither deeper within the glands nor elsewhere in the urinary tract (bladder, ureter, renal pelvis) [13]. Like in the airways, these cells express components of the canonical bitter and umami taste transduction signaling cascade, such as the G-protein α-gustducin, phospholipase Cβ2 (PLCβ2), transient potential receptor cation channel melanostatin 5 (TRPM5) [5,8,10,14–16] and taste receptors of the Tas1R and Tas2R families [13].

Physiologically, the urinary tract allows passage in only one direction to release urine, but ascending infection by uropathogenic bacteria is not uncommon and is a major risk factor in fatal kidney disease and male infertility [17,18]. In response to various potential hazardous substances, including uropathogenic *Escherichia coli* (UPEC), UBC release acetylcholine to excite sensory nerve fibers eliciting a protective reflex, i.e. micturition which flushes the urethral content [13]. We have put forward the concept that this cell serves as a sentinel at the entrance to the urogenital tract to monitor and to prevent the ascent of potential hazardous content, mainly bacteria [13].

In mice, structurally similar cholinergic epithelial cells expressing components of the taste transduction cascade have been identified in the gastrointestinal tract including the gallbladder [19,20], the auditory tube [21], and the thymic medulla [22]. Hence, it is tempting to assume the presence of a general surveillance system constituting of cholinergic epithelial cells monitoring the chemical composition of their immediate surroundings and releasing acetylcholine upon stimulation to initiate appropriate defense mechanisms in the presence of hazardous compounds. It has to be taken into account, however, that this concept is nearly entirely based on experiments conducted in rodents, specifically mice and rats, and even between these closely related species some marked differences are known. In the rat, brush cells are found in the lung alveoli (type III alveolar cells), whereas they are absent at this location in mice (reviewed in [12]). Their cholinergic phenotype has been primarily shown for mice [7,9,11,19,22,23], where additional populations of non-cholinergic brush cells also exist in trachea and urethra [10,13], and beyond that evidence for acetylcholine synthesis has been provided for rat bronchi as well as rat and human urethra by means of choline acetyltransferase (ChAT) antibodies [13,24].

Hence, we set out to determine the occurrence of cholinergic UBC in the mammalian kingdom. Previously, we have identified UBC in the murine, human, and rat urethrae [13]. Here, we investigated 11 additional species, at least one in each of the five mammalian taxonomic units primates, carnivora, perissodactyla, artiodactyla and rodentia (Fig. 1). To this end, immunohistochemistry was performed using antibodies directed against ChAT, against a characteristic structural marker of cholinergic brush cells (villin), and against components of the canonical taste transduction signaling cascade (α-gustducin, PLCβ2, TRPM5).

2. Material and methods

2.1. Animals

All specimens were taken from animals that were sacrificed in the context of approved experiments addressing other organ systems (guinea pig, golden hamster) or were obtained from the local slaughterhouse (pig), at routine autopsy at the Institute of Veterinary Pathology at the Justus-Liebig-University Giessen (horse, cattle, dog, cat), or provided by local huntsmen (red deer, badger).

Urethras from cynomolgus monkeys (*Macaca fascicularis*, N = 2 males) and common marmosets (*Callithrix jacchus*, N = 1 female and 4 males) were provided by the German Primate Center GmbH (Goettingen, Germany). Samples originate from animals that were breed at the German Primate Center. Housing conditions at the German Primate Center fulfilled German and European regulations: national animal protection act (§7-9/TierSchG/7833-3) and European Parliament and European Council Directive on the protection of animals used for scientific purposes (2010/63/EU). In addition animal husbandry and usage fulfilled the requirements according to the "Guide for the care and use of laboratory animals" (US National Research Council). Genital healthy animals were humanely euthanized because of non-infection related animal welfare reasons (e.g. trauma) or were post mortem examined due to the study design of other experiments. Organs were exclusively sampled during post mortem examination. The Animal Welfare and Ethics Committee of the German Primate Center approved the use of samples for this study. Urethrae of horses (*Equus ferus caballus*, N = 1 female and N = 2 males), dogs (*Canis lupus familiaris*, N = 2 females and N = 2 males), cats (*Felis catus*, N = 1 female and N = 2 male) and cattle (*Bos taurus*, N = 2 females and N = 3 males) were collected in the Institute of Veterinary Pathology in Giessen during routine necropsies; where urethrae were redundant remains. We

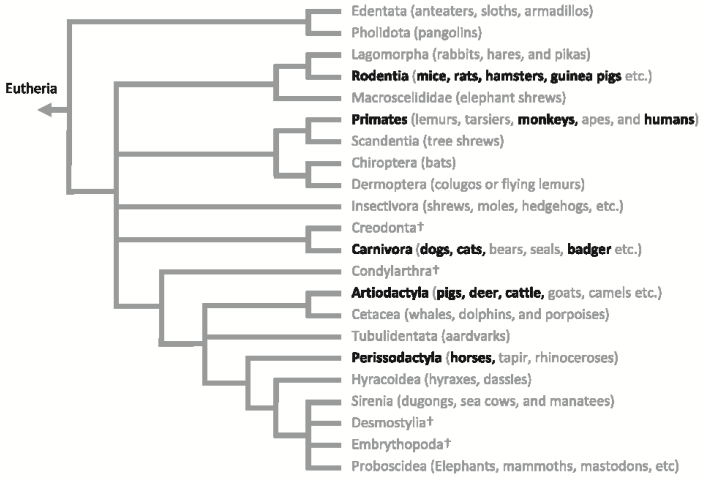

Fig. 1. Phylogenetic tree of eutheria. The depicted topology and branch lengths illustrate the relationships among the species. Analyzed taxonomic units and related species are written in bold type. Extinct taxa are labeled with †. Adapted from tree of life web project [26].

obtained urethrae from three odd-toed ungulates: one male and one female haflinger and one male warmblood, urethrae from four different dogs of both genders (two male mongrels, a female pug and a female boxer), urethrae of three European shorthairs (cats) of both genders, and five specimens of cattle (one male and one female Limousin cattle, one male and one female Holstein Friesians, and one male Charolais cattle).

Urethrae of pigs (*Sus scrofa domestica*, N = 3 females N = 3 males), were obtained from a local slaughterhouse; where urethrae were redundant remains. Urethrea of a European badger (*Meles meles*, N = 1 male) and three red deers (*Capreolus capreolus*, N = 1 female and N = 2 males), were provided by local huntsmen, tissues were redundant remains of animals shot. Guinea pigs (*Cavia porcellus*, N = 2 females) were sacrificed to obtain material for education; experiments were approved by the Regional Council of Giessen (Regierungspraesidium Giessen: V54-19 c 20/15 c GI 20/10 A11/2013), all urethrae were redundant remains. Urethrae of six golden hamsters (*Mesocricetus auratus*) of both genders were redundant remains in another experiment approved by the Regional Council of Giessen (Regierungspraesidium Giessen: V54-19 c 20/15 c GI 18/10).

2.2. Immunohistochemistry

Urethrae from all investigated animals were dissected immediately after sacrifice of the animals except for pigs where urethrae were available for dissection after the routine processing at the slaughterhouse which lasted approximately up to 15 min. Specimens were immersion fixed by either 4% paraformaldehyde or 2% paraformaldehyde/15% saturated picric acid in 0.1 M phosphate buffer. The duration of fixation differed from tissue to tissue. After fixation, tissue was washed, frozen, and sectioned as described previously [10]. Sections were processed for routine single- and double-labeling immunofluorescence as described earlier [10]. Each primary antibody was applied to 4–18 tissue sections from every individual animal. For single-labeling immunofluorescence, we used the following primary antibodies: goat anti-ChAT (AB144P, 1:500 dilution; Chemicon), rabbit anti-α-gustducin (sc-395, 1:1000; Santa Cruz Biotechnology), rabbit anti-PLCβ2 (sc-206, 1:1200; Santa Cruz Biotechnology), rabbit anti-TPRM5 (1:500-2000) [14], mouse anti-purified chicken villin (0258, 1:200; Immunotech), and mouse anti-CHT1 (MAB5514, 1:4000; Chemicon). For double-labeling immunofluorescence we used goat anti-ChAT (AB144P, 1:500 dilution; Chemicon) either with mouse anti-purified chicken villin (0258, 1:200; Immunotech) or with rabbit anti-TPRM5 (1:500-2000) [14]. Secondary antibodies were Cy3-conjugated donkey F(ab′)2 fragments directed against chicken IgY (1:2000; Dianova), FITC-conjugated donkey F(ab′)2 fragments directed against chicken IgY (1:800; Dianova), Cy3-conjugated donkey F(ab′)2 fragments directed against goat IgG (1:800; Merck Millipore), Cy3-conjugated anti-rabbit IgG from donkey (1:2000; Merck Millipore), Cy5-conjugated anti-rabbit IgG from donkey (1:800; Dianova), Texas Red®-dye-conjugated anti-goat IgG from donkey (1:200; Dianova), Cy3-conjugated anti-rat IgG from donkey (1:1000; Dianova), Cy3-conjugated anti-mouse IgG from donkey (1:1000; Dianova) and FITC-conjugated anti-mouse IgG from donkey (1:200; Dianova). Nuclei were labeled with 4′,6-diamidin-2-phenylindol (DAPI). All sections were rinsed and coverslipped with carbonate-buffered glycerol (pH 8.6). Sections were evaluated by epifluorescence microscopy (Zeiss Axioplan 2). Specificity of secondary reagents was validated by omission of primary antibodies.

3. Results

3.1. Primates

We previously described cholinergic UBC in human (*Homo sapiens*) urethra [13], and now investigated cynomolgus and common marmoset monkeys. Flask-like shaped cells positive for the brush cell marker villin were consistently observed in the epithelium of all urethral specimens, and ChAT-immunoreactive cells with comparable morphology in all but one sample from cynomolgus. The components of the taste transduction signaling cascade (α-gustducin, PLCβ2, TRPM5) were regularly detected in urethral epithelial cells of cynomolgus monkeys and common marmosets, albeit staining intensity for α-gustducin was weak in cynomolgus monkeys. Also, solitary urethral epithelial cells were weakly stained with PLCβ2 and TRPM5 antibodies in the marmoset (Fig. 2). In common marmoset monkeys, no gender diversity was noted.

3.2. Carnivora

Immunoreactivities for all five target proteins (villin, ChAT, α-gustducin, PLCβ2, TRPM5) were noted in epithelial cells with brush cell shape (flask-like, slender or triangular) in all canine and badger urethrae, with rather faint labeling for PLCβ2 and α-gustducin. Villin-immunolabeling was concentrated at the luminal surface (Fig. 2), likely corresponding to an apical tuft of microvilli from which brush cells have derived their name (reviewed in [4]). In feline (European shorthair) urethrae, TRPM5- and α-gustducin-immunoreactive cells were consistently observed, PLCβ2 and villin-positive cells in one of three samples. (Fig. 2). ChAT-immunolabeling was seen in large diameter axons in nerve fiber bundles in the urethral wall (Fig. 2), but neither in terminal nerve fibers innervating the urethral muscle layer nor in epithelial cells. In canine urethrae no gender diversity could be observed.

3.3. Artiodactyla

Among artiodactyla, cattle, red deer, and pigs were examined. α-Gustducin-positive cells with brush cell shape were detected in all bovine samples (N = 5), villin- and TRPM5-positive cells in 3/5 and PLCβ2-immunoreactive cells in 1/5 bovine urethrae (Fig. 3). In this species, the secondary anti-goat Ig antibody used for detection of the ChAT-antiserum raised in goat unspecifically bound to epithelial cells so that no conclusions about ChAT expression could be drawn. We included urethrae from six different pigs, three of each gender. TRPM5-, PLCβ2- and α-gustducin-positive cells were constantly detected, ChAT-positive cells were labeled in three of them. Staining of cholinergic cells was not limited to either gender. Villin-positive cells were found in 50% of the investigated samples, and labeling was nearly restricted to an apical spot (Fig. 3). We observed cholinergic cells in the urethral epithelium of all (N = 3) investigated red deer, and TRPM5-, PLCβ2-, gustducin- and villin-positive cells always in 2/3 samples (Fig. 3).

3.4. Perissodactyla

This taxonomic unit order was represented by horses in our study. TRPM5- as well as α-gustducin-positive cells with characteristic brush cell shape were detectable in all three equine samples, PLCβ2- and villin-positive epithelial cells, respectively, in two of them. ChAT-positive epithelial cells were not encountered. Few large diameter axons in nerve fiber bundles in the urethral wall displayed ChAT-immunolabeling (Fig. 3), but cholinergic terminals innervating urethral smooth muscle, which were evident by CHT1-immunoreactivity, were not labeled by the ChAT antibody (not shown).

3.5. Rodentia

Previously, we reported UBC in rats (*Rattus norvegicus domesticus*) and mice (*Mus musculus*) [13] and now extended our studies to guinea pigs and golden hamsters. We are aware of recently published phylogenetic analysis based on molecular data that guinea pigs are no rodents [25]. Still, here we used the classification of the tree of life web project [26], which places guinea pigs in the taxonomic unit rodentia. In both species, all target proteins were consistently detected by immunofluorescence in epithelial cells with brush cell morphology. PLCβ2-labeling

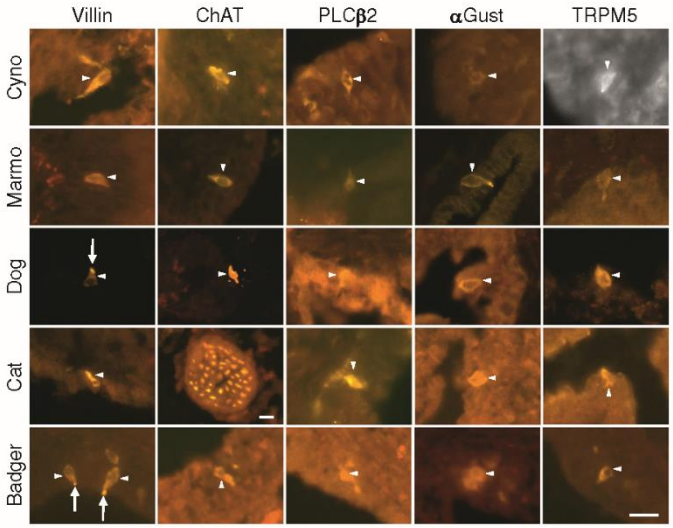

Fig. 2. Urethral brush cells in primates and carnivora. Urethral epithelial cells (*arrowhead*) with brush cell shape (flask-like, slender or triangular) of cynomolgus monkey (Cyno), common marmoset (Marmo), dog, and european badger are positive for ChAT, a characteristic brush cell marker (villin) and components of the canonical taste transduction cascade for sweet, bitter, and umami perception (PLCβ2, α-gustducin (αGust) and TRPM5). In several sections, connection of labeled cells to the urethral lumen is visible (villin: cynomolgus, dog, badger; α-gustducin: marmoset; TRPM5: dog, cat). In dog and badger, villin-immunolabeling is concentrated at the luminal surface (*arrow*), likely corresponding to an apical tuft of microvilli. Solitary urethral epithelial cells of cat are positive for villin, αGust, PLCβ2 and TRPM5. ChAT-immunolabeling was only seen in large diameter axons. TRPM5-immunolabeling in cynomolgus was detected with a Cy5-conjugated secondary antibody and, accordingly, recorded with an infrared-sensitive black-and-white camera. Scale bars represent 20 μm throughout, the scale in the lower right panel applies to all micrographs except for ChAT-labeling in cat.

intensities were relatively faint. Pronounced villin-labeling of a slender apical cell process was particularly evident in the guinea pig (Fig. 3).

3.6. Brush and chemosensory phenotype of cholinergic epithelial cells

As described above, immunohistochemical labeling efficiencies differed among species and antigens. Particularly in common marmosets and guinea pigs, labeling intensities obtained with ChAT, villin and TRPM5 antibodies were sufficient enough to perform double-labeling for ChAT and TRPM5 as well as for ChAT and villin, respectively. ChAT and TRPM5 antibodies stained practically identical cells in the epithelium (Fig. 4). Both ChAT- and villin-immunolabeling were less intense when FITC- instead of Cy3-conjugated secondary antisera were used. This was particularly pronounced for ChAT-immunolabeling, so that ChAT-immunoreactivity was visualized with Cy3- and villin-immunoreactivity with FITC-conjugated secondary antisera in double-labeling experiments. Under these conditions, villin-immunolabeling was often restricted to the apical pole of positive cells. With this antibody combination, colocalization was not nearly 1:1, and cells exhibiting only either of the immunoreactivities were also observed (Fig. 4).

4. Discussion

Including our previous study [13], we now identified cells with brush cell-like morphology and expression of chemosensory traits in the urethral epithelium of 14 species within Placentalia. Placentalia can be grossly grouped in Boreoeutheria, Afrotheria and Xenarthra [26]. The species from which samples were available for the present study all belong to five orders of the biggest of the magnorders, Boreoeutheria, covering both its superorders Euarchontoglires (or supraprimates) (here: primates, rodentia) and Laurasiatheria (here: carnivora, artio- and perissodactyla). A general consensus about time and mode of diversification of the Placentalia still has not been reached. Combining molecular sequence data with 4541 phenomic characters for fossil and living species led to the proposal that the crown clade Placentalia evolved after the Cretaceous-Paleogene (K-Pg) event 66 to 65 million years ago, which marks a significant extinction horizon [27,28]. According to this phylogenetic tree, Xenarthra, covering the two taxons Edentata (anteaters, sloths, armadillos) and Pholidota (pangolins), have first split from a common ancestor, and then Afrotheria (e.g. manatees, hyraxes and elephants) from Boreoeutheria in the first 200 to 400 thousand years after this K-Pg event [28]. Thus, it is likely that cholinergic chemosensory urethral brush cells evolved not later than about 64.5 million years ago.

Since identification of cholinergic chemosensory cells required immunohistochemistry, interspecies cross-reactivity of the antibodies and variation in tissue sampling, as it is unavoidable when samples are taken from the slaughterhouse, from veterinary autopsy and from hunted game, caused limitations of the present study. Accordingly, not all antigens were detected in all investigated samples of all species, and labeling intensities obtained with some antibodies were often weaker in particular species than in our previous study on mice with antibodies selected for reactivity with mouse proteins and standardized tissue processing [13]. Notably, alignment of the amino acid sequences used for immunization (when known) with published species-specific sequences retrieved from NCBI protein database (SI. 1) showed common stretches that potentially allow for antibody recognition (SI. 2-5). In two species (horse and cat), the ChAT antiserum failed to label urethral epithelial cells, albeit the structural brush cell protein villin and components of the taste transduction cascade were detected. Thus, either urethral chemosensory epithelial cells utilize another transmitter than acetylcholine in these species, or we obtained false negative labeling with the ChAT antiserum. Notably, thick preterminal axons of cholinergic α-motoneurons were recognized by the ChAT antiserum in both species, providing an internal positive control for the principal

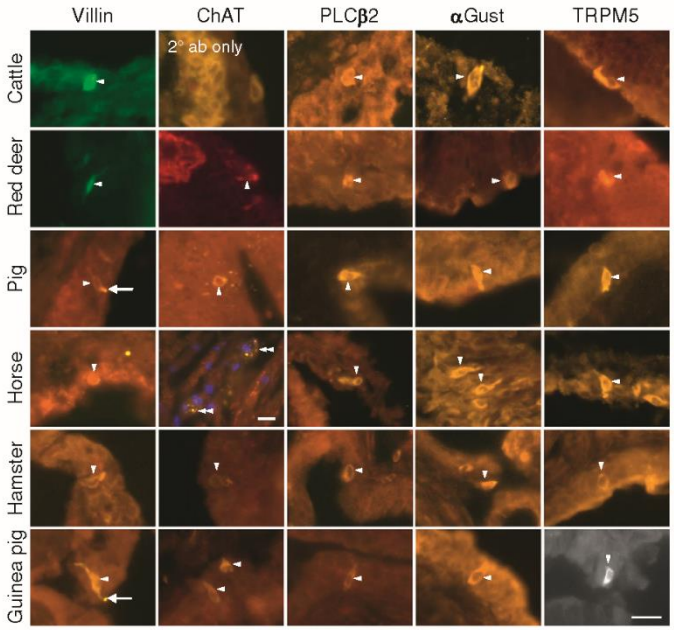

Fig. 3. Urethral brush cells in artiodactyla, perissodactyla and rodentia. Cattle, red deer, pig, golden hamster and guinea pig urethrae harbor epithelial cells (*arrowhead*) with brush cell shape (flask-like, slender or triangular). These cells are immunoreactive for ChAT in red deer, pig, hamster and guinea pig. In cattle, however, the Cy3-conjugated secondary antibody alone produced epithelial labeling, so that no conclusions about ChAT-immunoreactivity in the epithelium can be drawn. In all species, such cells are immunoreactive to villin, PLCβ2, α-gustducin (αGust) and TRPM5. In pig and guinea pig, villin-immunolabeling is concentrated at the luminal surface (*arrow*), likely corresponding to an apical tuft of microvilli. In the horse, ChAT-immunolabeling was only seen in large diameter axons in equine tissue (*doubled-arrowhead*, nuclei counterstained in blue with DAPI in this image). TRPM5-immunolabeling in guinea pig was detected with a Cy5-conjugated secondary antibody and, accordingly, recorded with an infrared-sensitive black-and-white camera. Scale bars represent 20 μm throughout, the scale in the lower right panel applies to all micrographs except for ChAT-labeling in horse.

suitability of this antiserum for its use in cat and horse. Although fine varicose terminals of cholinergic parasympathetic neurons innervating urethral smooth muscle bundles were not labeled by the ChAT antiserum in these species, they could be validated using another marker for cholinergic nerve terminals, i.e. CHT1 antiserum. Such discrepancy between successful ChAT-immunolabeling of central neurons and negative results obtained on cholinergic postganglionic autonomic neurons has been noted earlier, and expression of different ChAT isoforms (common versus peripheral) has been suggested. An alternative splice variant of ChAT is localized preferentially in peripheral nerve cells and fibers [29,30]. It still remains to be determined which ChAT variant is expressed by urethral brush cells and whether such molecular diversity might underlie the negative immunolabeling results in equine and feline urethral brush cells.

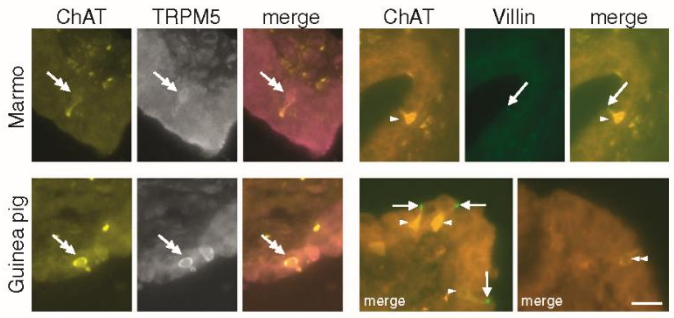

Fig. 4. Double-labeling of urethral brush cells in marmosets and guinea pigs. Urethrae of common marmosets (Marmo) and guinea pigs were double-labeled for Villin/ChAT or TRPM5/ChAT. ChAT-immunoreactivity was visualized with Cy3-, and villin-immunoreactivity with FITC-conjugated secondary antisera, and TRPM5-immunoreactivity with Cy5-conjugated secondary antisera. Cholinergic cells are positive for TRPM5 (*double-headed arrows*). Flask-shaped cells are immunoreactive for the brush cell marker villin (*arrows*) and ChAT (*arrowheads*). Villin-immunolabeling shows concentration of this microvillous protein at the apical cell pole. Another ChAT-positive cell is not villin-positive (*doubled arrowhead*). Scale bar represents 20 μm throughout.

In the murine urethra, there is evidence for the presence of subpopulations of urethral brush cells. Utilizing a reporter mouse strain expressing enhanced green fluorescent protein (eGFP) driven by the ChAT promotor, a nearly complete overlap was observed between ChAT-eGFP and TRPM5-immunolabeling, but various combinations of colocalization were observed between ChAT-eGFP and PLCβ2-immunoreactivity, and while all ChAT-eGFP-positive cells were villin-immunoreactive, there was an additional population of about equal size of villin-positive/ChAT-eGFP-negative cells [13].

The present double-labeling data have to be interpreted in view of the technical limitations of this multi-species study as discussed above. Nonetheless, the extensive colocalization of TRPM5- and ChAT-immunoreactivities allows the conclusion that cholinergic epithelial cells indeed express chemosensory traits. The only partial overlap with villin-immunoreactivity favors the existence of at least one additional population of brush cells (here defined by villin-immunoreactivity) which might use another sensor and signaling cascade than bitter/sweet/umami sensing cells and another signaling molecule than acetylcholine.

Conclusion

Epithelial cells with brush cell shape were immunolabeled in urethrae of all 11 placental mammals. Double-labeling immunofluorescence confirmed the cholinergic nature of villin- and chemosensory (TRPM5-positive) cells. These data indicate that cholinergic urethral brush cells are widespread throughout the mammalian kingdom and evolved not later than about 64.5 million years ago.

Acknowledgments

We thank L. Renno, T. Papadakis, M. Bodenbenner-Türich and K. Michael for technical assistance. We also like to thank M. Lottig (huntsmen), T. Schick (butcher) and all members of the Institute of Veterinary Pathology for providing us with animal tissue. Pathologists and technicians of the Pathology Unit of the German Primate Center as well as C. Curths (Fraunhofer ITEM) are thanked for organizing sampling of the nonhuman primates. This work was supported by the LOEWE Program of the State of Hesse (Non-neuronal Cholinergic Systems, project A5, to W.K. and T.B.) and the Deutsche Forschungsgemeinschaft grant TRP 152/1 (T.G. and V.C.).

Appendix A. Supplementary data

Supplementary data to this article can be found online at http://dx.doi.org/10.1016/j.intimp.2015.05.038.

References

[1] D. Hofer, D. Drenckhahn, Identification of brush cells in the alimentary and respiratory system by antibodies to villin and fimbrin, Histochemistry 98 (1992) 237–242.
[2] J. Rhodin, T. Dalhamn, Electron microscopy of the tracheal ciliated mucosa in rat, Z Zellforsch Mikrosk Anat 44 (1956) 345–412.
[3] L. Luciano, E. Reale, H. Ruska, Über eine glykogenhaltige Bürstenzelle im Rectum der Ratte, Z Zellforsch Mikrosk Anat 91 (1968) 153–158.
[4] A. Sbarbati, F. Osculati, A new fate for old cells: brush cells and related elements, J Anat 206 (2005) 349–358.
[5] T.E. Finger, B. Bottger, A. Hansen, K.T. Anderson, H. Alimohammadi, W.L. Silver, Solitary chemoreceptor cells in the nasal cavity serve as sentinels of respiration, Proc Natl Acad Sci U S A 100 (2003) 8981–8986.
[6] W. Lin, T. Ogura, R.F. Margolskee, T.E. Finger, D. Restrepo, TRPM5-expressing solitary chemosensory cells respond to odorous irritants, J Neurophysiol 99 (2008) 1451–1460.
[7] T. Ogura, K. Krosnowski, L. Zhang, M. Bekkerman, W. Lin, Chemoreception regulates chemical access to mouse vomeronasal organ: role of solitary chemosensory cells, PLoS One 5 (2010) e11924.
[8] M. Tizzano, B.D. Gulbransen, A. Vandenbeuch, T.R. Clapp, J.P. Herman, H.M. Sibhatu, et al., Nasal chemosensory cells use bitter taste signaling to detect irritants and bacterial signals, Proc Natl Acad Sci U S A 107 (2010) 3210–3215.
[9] G. Krasteva, B.J. Canning, T. Papadakis, W. Kummer, Cholinergic brush cells in the trachea mediate respiratory responses to quorum sensing molecules, Life Sci 91 (2012) 992–996.
[10] G. Krasteva, B.J. Canning, P. Hartmann, T.Z. Veres, T. Papadakis, C. Muhlfeld, et al., Cholinergic chemosensory cells in the trachea regulate breathing, Proc Natl Acad Sci U S A 108 (2011) 9478–9483.
[11] C.J. Saunders, M. Christensen, T.E. Finger, M. Tizzano, Cholinergic neurotransmission links solitary chemosensory cells to nasal inflammation, Proc Natl Acad Sci U S A 111 (2014) 6075–6080.
[12] G. Krasteva, W. Kummer, "Tasting" the airway lining fluid, Histochem Cell Biol 138 (2012) 365–383.
[13] K. Deckmann, K. Filipski, G. Krasteva-Christ, M. Fronius, M. Althaus, A. Rafiq, et al., Bitter triggers acetylcholine release from polymodal urethral chemosensory cells and bladder reflexes, Proc Natl Acad Sci U S A 111 (2014) 8287–8292.
[14] S. Kaske, G. Krasteva, P. Konig, W. Kummer, T. Hofmann, T. Gudermann, et al., TRPM5, a taste-signaling transient receptor potential ion-channel, is a ubiquitous signaling component in chemosensory cells, BMC Neurosci 8 (2007) 49.
[15] C.A. Perez, R.F. Margolskee, S.C. Kinnamon, T. Ogura, Making sense with TRP channels: store-operated calcium entry and the ion channel Trpm5 in taste receptor cells, Cell Calcium 33 (2003) 541–549.
[16] T. Hofmann, V. Chubanov, T. Gudermann, C. Montell, TRPM5 is a voltage-modulated and Ca(2+)-activated monovalent selective cation channel, Curr Biol 13 (2003) 1153–1158.
[17] S. Bhushan, H.C. Schuppe, S. Tchatalbachev, M. Fijak, W. Weidner, T. Chakraborty, et al., Testicular innate immune defense against bacteria, Mol Cell Endocrinol 306 (2009) 37–44.
[18] J.A. Roberts, Etiology and pathophysiology of pyelonephritis, Am J Kidney Dis 17 (1991) 1–9.
[19] L. Gautron, J.M. Rutkowski, M.D. Burton, W. Wei, Y. Wan, J.K. Elmquist, Neuronal and nonneuronal cholinergic structures in the mouse gastrointestinal tract and spleen, J Comp Neurol 521 (2013) 3741–3767.
[20] J.A. Eberle, P. Richter, P. Widmayer, V. Chubanov, T. Gudermann, H. Breer, Band-like arrangement of taste-like sensory cells at the gastric groove: evidence for paracrine communication, Front Physiol 4 (2013) 58.
[21] G. Krasteva, P. Hartmann, T. Papadakis, M. Bodenbenner, L. Wessels, E. Weihe, et al., Cholinergic chemosensory cells in the auditory tube, Histochem Cell Biol 137 (2012) 483–497.
[22] A.R. Panneck, A. Rafiq, B. Schutz, A. Soultanova, K. Deckmann, V. Chubanov, et al., Cholinergic epithelial cell with chemosensory traits in murine thymic medulla, Cell Tissue Res 358 (2014) 737–748.
[23] B. Schutz, I. Jurastow, S. Bader, C. Ringer, J. von Engelhardt, V. Chubanov, et al., Chemical coding and chemosensory properties of cholinergic brush cells in the mouse gastrointestinal and biliary tract, Front Physiol 6 (2015) 87.
[24] W. Kummer, K.S. Lips, U. Pfeil, The epithelial cholinergic system of the airways, Histochem Cell Biol 130 (2008) 219–234.
[25] A.M. D'Erchia, C. Gissi, G. Pesole, C. Saccone, U. Arnason, The guinea-pig is not a rodent, Nature 381 (1996) 597–600.
[26] Maddison DRaK-SSe, The tree of life Web project internet address, http://tolweb.org 2007.
[27] K.F. Kuiper, A. Deino, F.J. Hilgen, W. Krijgsman, P.R. Renne, J.R. Wijbrans, Synchronizing rock clocks of Earth history, Science 320 (2008) 500–504.
[28] M.A. O'Leary, J.I. Bloch, J.J. Flynn, T.J. Gaudin, A. Giallombardo, N.P. Giannini, et al., The placental mammal ancestor and the post-K-Pg radiation of placentals, Science 339 (2013) 662–667.
[29] I. Tooyama, H. Kimura, A protein encoded by an alternative splice variant of choline acetyltransferase mRNA is localized preferentially in peripheral nerve cells and fibers, J Chem Neuroanat 17 (2000) 217–226.
[30] Y. Nakanishi, I. Tooyama, O. Yasuhara, Y. Aimi, K. Kitajima, H. Kimura, Immunohistochemical localization of choline acetyltransferase of a peripheral type in the rat larynx, J Chem Neuroanat 17 (1999) 21–32.

THE FASEB JOURNAL • RESEARCH • www.fasebj.org

Muscarinic receptors 2 and 5 regulate bitter response of urethral brush cells *via* negative feedback

Klaus Deckmann,*,[1] Amir Rafiq,* Christian Erdmann,[†] Christian Illig,[†] Melanie Durschnabel,[†] Jürgen Wess,[‡] Wolfgang Weidner,[†] Thomas Bschleipfer,[§] and Wolfgang Kummer*

*Institute for Anatomy and Cell Biology and [†]Department of Urology, Pediatric Urology, and Andrology, Justus-Liebig-University Giessen, Giessen, Germany; [‡]Molecular Signaling Section, Laboratory of Bioorganic Chemistry, National Institute of Diabetes and Digestive and Kidney Diseases, Bethesda, Maryland, USA; and [§]Clinic of Urology, Andrology, and Pediatric Urology, Weiden Hospital/Clinics of Nordoberpfalz AG, Weiden, Germany

ABSTRACT: We have recently identified a cholinergic chemosensory cell in the urethral epithelium, urethral brush cell (UBC), that, upon stimulation with bitter or bacterial substances, initiates a reflex detrusor activation. Here, we elucidated cholinergic mechanisms that modulate UBC responsiveness. We analyzed muscarinic acetylcholine receptor (M1–5 mAChR) expression by using RT-PCR in UBCs, recorded $[Ca^{2+}]_i$ responses to a bitter stimulus in isolated UBCs of wild-type and mAChR-deficient mice, and performed cystometry in all involved strains. The bitter response of UBCs was enhanced by global cholinergic and selective M2 inhibition, diminished by positive allosteric modulation of M5, and unaffected by M1, M3, and M4 mAChR inhibitors. This effect was not observed in M2 and M5 mAChR-deficient mice. In cystometry, M5 mAChR-deficient mice demonstrated signs of detrusor overactivity. In conclusion, M2 and M5 mAChRs attenuate the bitter response of UBC *via* a cholinergic negative autocrine feedback mechanism. Cystometry suggests that dysfunction, particularly of the M5 receptor, may lead to such symptoms as bladder overactivity.—Deckmann, K., Rafiq, A., Erdmann, C., Illig, C., Durschnabel, M., Wess, J., Weidner, W., Bschleipfer, T., Kummer, W. Muscarinic receptors 2 and 5 regulate bitter response of urethral brush cells *via* negative feedback. FASEB J. 32, 000–000 (2018). www.fasebj.org

KEY WORDS: chemosensory cells · cholinergic · cystometry · overactive bladder syndrome

We have recently identified a novel cholinergic component in sensory control of bladder function, that is, a specialized cholinergic epithelial cell in the urethra, termed the urethral brush cell (UBC) (1, 2). UBCs are polymodal chemosensory cells that express both canonical bitter and umami receptors and their common downstream channel, transient receptor potential cation channel subfamily M member 5 (TRPM5). They respond to both bitter substances and glutamate with an increase in $[Ca^{2+}]_i$. Both stimuli represent a potential danger signal in the urethra as many bacterial products have bitter quality, and glutamate (umami) facilitates bacterial growth in urine. Accordingly, these cells also respond to heat-inactivated uropathogenic *Escherichia coli* (2). UBCs are cholinergic, release acetylcholine upon stimulation, and are approached by sensory nerve fibers that carry nicotinic acetylcholine receptors. Bitter application into the urethral lumen reflexively triggers enhanced detrusor activity, which has been interpreted as a protective reflex, as potential hazardous content is expelled from the urethra *via* micturition (2, 3).

In the course of these studies, we obtained first evidence of an autocrine cholinergic feedback mechanism that regulates the sensitivity of this system. Using knockout mice for all 5 known muscarinic acetylcholine receptor (mAChR) subtypes (M1–5), we have clarified the underlying receptors and demonstrate in cystometry in awake mice that the targeted deletion of the M5 receptor is associated with signs of overactivity.

Overactive bladder syndrome (OAB) is a common disorder that affects approximately 12–16% of the population in Western countries and millions of people worldwide (4, 5). OAB symptoms are urgency, with or without urinary incontinence, usually with frequency and nocturia, and OAB is often associated with involuntary contractions of the detrusor muscle, that is, detrusor overactivity (6). Antagonists of mAChRs are drugs of choice in OAB, originally based on the concept of inhibiting detrusor contraction, which is primarily mediated *via* acetylcholine

ABBREVIATIONS: ChAT, choline acetyltransferase; eGFP, enhanced green fluorescent protein; mAChR, muscarinic acetylcholine receptor; met, methoctramine hydrate; OAB, overactive bladder syndrome; TRPM5, transient receptor potential cation channel subfamily M member 5; UBC, urethral brush cell

[1] Correspondence: Institute for Anatomy and Cell Biology, Justus-Liebig-University Giessen, Aulweg 123, D-35385 Giessen, Germany. E-mail: klaus.deckmann@anatomie.med.uni-giessen.de

doi: 10.1096/fj.201700582R
This article includes supplemental data. Please visit *http://www.fasebj.org* to obtain this information.

(7); however, as mAChR blockers are effective in the bladder-filling phase during which no contractions occur, and because they do not impair physiologic voiding, a mode of action on the sensory component is currently favored, yet still not fully elucidated.

MATERIALS AND METHODS

Animals

The generation of M1–$5^{-/-}$ and M2/$3^{-/-}$ mice has been described previously (8–13). Corresponding wild-type mice were used as controls. Choline acetyltransferase [ChAT(BAC)-eGFP] mice that expressed enhanced green fluorescent protein (eGFP) in UBCs (2) and C57BL/6 mice were obtained from The Jackson Laboratory (Bar Harbor, ME, USA). All urodynamic experiments were performed with adult female mice (>14 wk). Experiments were conducted in accordance with the European Communities Council Directive of November 24, 1986 (86/609/EEC), and approved by the local authorities (Administration of Giessen, Germany; No. 571_M, 572_M, 574_M, A44-48/2011, V44/2008).

Cell isolation

Cell isolation was performed as described previously (2). Isolated UBCs were identified by either eGFP-fluorescence or labeled with a TRPM5 Ab (1:125; Abcam, Cambridge, United Kingdom), followed by FITC-conjugated donkey anti-rabbit IgG (1:125; EMD Millipore, Billerica, MA, USA). TRPM5 labeling and eGFP expression matched nearly 1:1 (2). For RT-PCR analysis, UBCs were isolated with the TRPM5 Ab and magnetic beads (Thermo Fisher Scientific, Waltham, MA, USA) that were coated with goat anti-rabbit IgG (H + L; PI65-6100; Thermo Fisher Scientific), followed by harvesting by magnetic cell separation (2).

RT-PCR

Total RNA from pooled isolated cells (n = 3 samples) was extracted by using an RNeasy Kit (Qiagen, Hilden, Germany) according to the manufacturer's protocol. RT-PCR was performed as described previously (primer sequences are given in Supplemental Table 1) (2).

Measurement of intracellular calcium concentration

Measurement of intracellular calcium concentration ($[Ca^{2+}]_i$) was performed as described previously (2). In brief, isolated cells were loaded with the fluorescent calcium indicator, Calcium Orange AM (0.01 $\mu g/\mu l$; Thermo Fisher Scientific), and plated on coverslips. $[Ca^{2+}]_i$ was analyzed with a confocal laser scanning microscope (LSM 710; Carl Zeiss, Jena, Germany) during continuous superfusion (2.5 ml/min). Fluorescence intensities at the start of the recording period were set arbitrarily at 100%. Test stimuli and concentrations were denatonium benzoate (25 mM; Molekula, Munich, Germany), mecamylamine hydrochloride (0.02 mM; Sigma-Aldrich, St. Louis, MO, USA), atropine sulfate (0.002 mM; Sigma-Aldrich), tropicamide (0.001 mM; Sigma-Aldrich), methoctramine hydrate (0.001 mM; Sigma-Aldrich), pirenzepine dihydrochloride (0.001 mM; Sigma-Aldrich), 4-DAMP (1,1-dimethyl-4-diphenylacetoxypiperidinium iodide; 0.001 mM; Sigma-Aldrich), and VU 0238429 (0.005 mM; Abcam).

Cystometric analysis

Cystometric analyses were performed as described elsewhere (14). In brief, animals were anesthetized with an injection of atropine/ketamine/xylazine (0.05/100/15 mg/kg, i.p.) and meloxicam (1.5 mg/kg). Intramedic PE-10 polyethylene tubing (Becton Dickinson, Franklin Lakes, NJ, USA) was then inserted in the dome of the bladder and tunneled subcutaneously to the neck. Three days later, cystometry was performed in conscious, freely moving mice. Saline (room temperature) was infused into the bladder at a rate of 1.5 ml/h. After a stabilization phase of 15–30 min, intravesical pressure and micturition were recorded continuously. We analyzed basal pressure level, maximum detrusor pressure during micturition, threshold pressure, bladder capacity, time interval between 2 pressure peaks, micturition interval, micturition volume, and postmicturition residual volume. Residual volume was measured by discontinuing the tube between animal and infusion pump after micturition. In this way, we were able to collect and weigh the saline that had remained in the bladder.

Statistical analysis

Student's paired/unpaired, 2-tailed Student's t test or 1-way factorial ANOVA followed by Dunnett's multiple comparison test was used to compare intracellular or δ maximum calcium concentration. Cytometric parameters between groups of mice was compared using 1-way factorial ANOVA, followed by Dunnett's multiple comparison test. Throughout, a value of $P < 0.05$ was considered significant.

RESULTS

Calcium response of UBCs upon repetitive bitter stimulation

Repetitive stimulation of isolated UBCs with the bitter stimulus, denatonium, led to repetitive increases in $[Ca^{2+}]_i$ in both ChAT(BAC)-eGFP and C57BL/6 mice, with a small decrease in the second response (significant only in C57BL/6 mice), which was indicative of a slight desensitization; however, the response to the second stimulus was significantly increased in the presence of a muscarinic/nicotinic blocker cocktail (atropine/mecamylamine), which indicated a cholinergic negative feedback mechanism (**Fig. 1*A–E, H***). This increase accounted for 42% in ChAT-eGFP and 44% in C57BL/6 mice compared with the immediately preceding stimulus, and, taking into account the slight loss of response that was observed at the second stimulus without receptor blockade, we observed a total increase of 47% in ChAT-eGFP and 60% in C57BL/6 mice (Supplemental Table 2). Because only 1–5 UBCs per coverslip were present in these preparations, lying approximately 100 μm apart from each other, this cholinergic negative feedback likely reflects autoinhibition rather than paracrine signaling. To identify whether this cholinergic negative feedback mechanism operates *via* muscarinic or nicotinic receptors, only one or the other of these inhibitors was used. The response, then, to the second stimulus was significantly increased only in the presence of atropine, but not in the presence of mecamylamine (Fig. 1*F–H*). This indicated a muscarinic

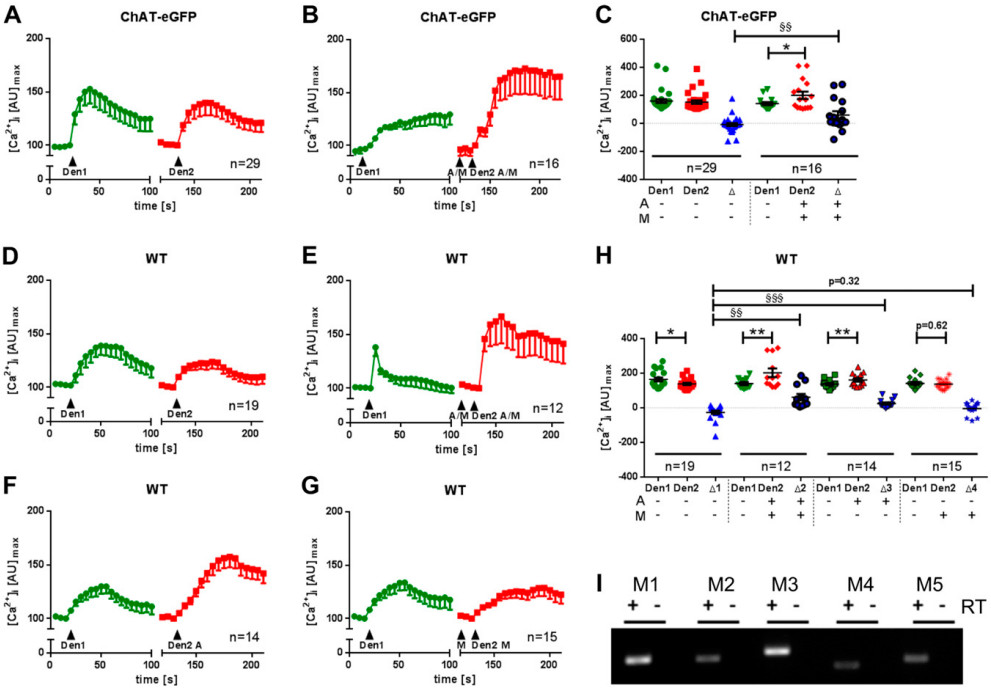

Figure 1. Negative cholinergic feedback in the calcium response of UBCs to bitter stimulation and expression of mAChRs. *A–H*) Recording of changes in Calcium Orange fluorescence of isolated UBCs during repetitive stimulation with denatonium (Den1 and Den2; 25 mM) with or without the addition of muscarinic (2 μM atropine) and nicotinic (20 μM mecamylamine) acetylcholine receptor blockers or a cocktail (A/M) of both between the 2 stimuli. All drugs were added under continuous flow in the chamber so that indicated concentrations were reached initially, then washed out. The *y*-axis depicts arbitrary units (AU) that correlate to $[Ca^{2+}]_i$. UBCs were isolated and identified by means of eGFP fluorescence from ChAT reporter mice or by binding to a TRPM5 Ab in the case of wild-type (WT; C57BL/6) mice. *A, B, D–G*) Shown are recordings over time (means ± SEM). *C, H*) Depicted are peak values after the first (Den1) and second stimulation (Den2) without or with blocker addition (A/M) between these 2 stimuli, analyzed with paired *t* test, and the difference between the peak responses under these conditions (Δ), analyzed with unpaired *t* test or 1-way factorial ANOVA followed by Dunnett's multiple comparisons test. *I*) RT-PCR, agarose gel, M1 (Chrm1; 198 bp), M2 (Chrm2; 193 bp), M3 (Chrm3; 222), M4 (Chrm4; 156), and M5 (Chrm5; 180). UBCs were isolated by using magnetic beads coated with TRPM5 Ab. $^{+/-}$ RT, aliquots were processed with/without reverse transcription. $^{*}P < 0.05$, $^{**}P < 0.01$, $^{\S\S}P < 0.01$, $^{\S\S\S}P < 0.001$.

feedback mechanism and led us to assess mAChR expression in UBCs.

Expression of mAChR in UBCs

RT-PCR revealed the expression of mRNAs that coded for all mAChRs in isolated UBCs (Fig. 1*I*). As previous immunohistochemical findings suggest heterogeneity within the UBC population (2), it seems likely that not all 5 mAChRs are simultaneously expressed within 1 cell.

Calcium response of UBCs to bitter in mAChR-deficient mice and selective pharmacologic intervention

Repetitive bitter stimulation in the absence and presence of cholinergic blockade was compared in mAChR-deficient mice. As in the corresponding wild-type (C57BL/6) mice, the second stimulus provoked a slightly smaller response without blockers, but an enhanced response in the presence of blockers with a significant difference between these responses in mice that lacked M1, M3, and M4 mAChRs (**Fig. 2*A, C, E***). The enhancing effect of cholinergic receptor blockade was not observed in UBCs from mice that lacked the M2 mAChR, either alone or in combination with the M3 mAChR, nor in M5 mAChR-deficient UBCs (Fig. 2*B, D, F*). Taking these differences in second responses in the absence or presence of cholinergic blockade as parameters, M2 and M5 mAChR-deficient UBCs were statistically different from wild-type mice, whereas those from other mAChR-deficient strains were not (Fig. 2*G*).

Acute pharmacologic inhibition of either M1 (pirenzepine), M3 (4-DAMP), or M4 receptors (tropicamide) had no impact on the response to subsequently applied denatonium, whereas M2 receptor inhibition

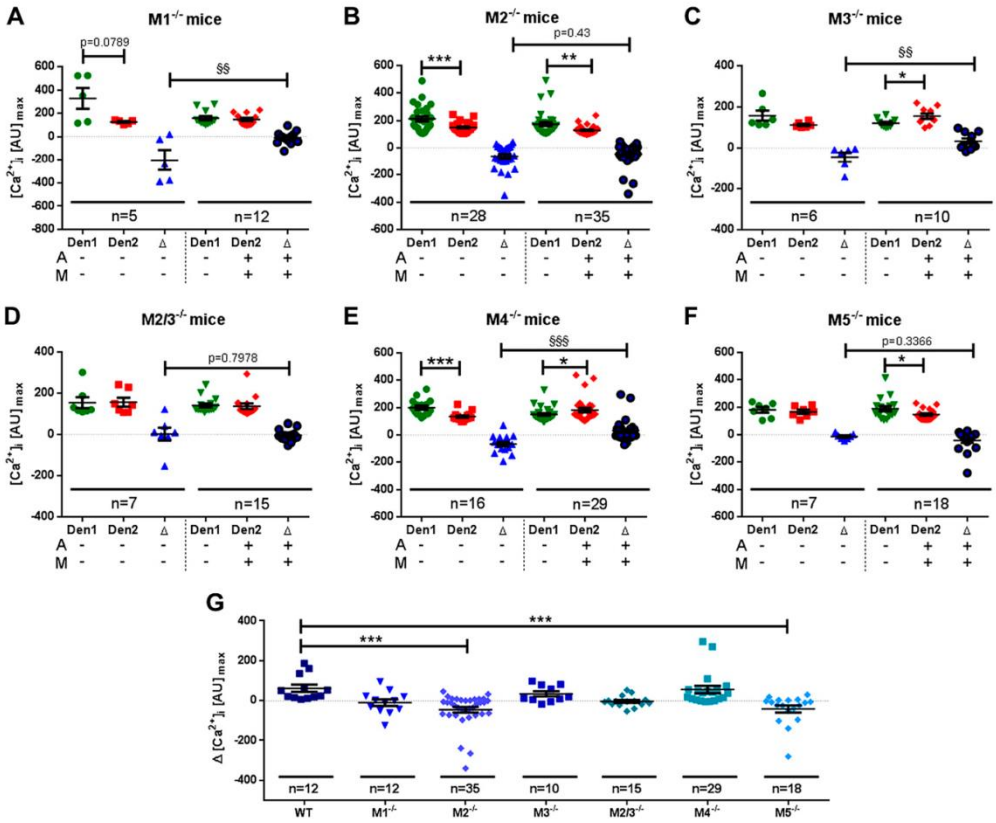

Figure 2. Impact of mAChR deficiency on the effect of cholinergic blockade on the calcium response of UBCs to bitter stimuli. *A–F*) UBCs were isolated and identified from M1–5 mAChR-deficient and M2/3 mAChR-deficient mice *via* TRPM5 Ab. UBCs were repetitively stimulated with denatonium (Den1 and Den2; 25 mM) with or without the addition of a cocktail (A/M) of muscarinic (2 μM atropine) and nicotinic (20 μM mecamylamine) acetylcholine receptor blockers between the 2 stimuli, and $[Ca^{2+}]_i$ was recorded as Calcium Orange fluorescence in arbitrary units (AU). Depicted are peak values after the first (Den1) and second stimulation (Den2) without or with blocker addition (A/M) between these 2 stimuli, analyzed with paired *t* test, and the difference between the peak responses under these conditions (Δ), analyzed with unpaired Student's *t* test. All drugs were added under continuous flow in the chamber so that indicated concentrations were reached initially, then washed out. *G*) A 1-way factorial ANOVA, followed by Dunnett's multiple comparison test was used to compare difference between peak responses under these conditions (Δ). $^{*}P < 0.05$, $^{**}P < 0.01$, $^{***}P < 0.001$, $^{§§}P < 0.01$, $^{§§§}P < 0.001$.

(methoctramine) alone fully mimicked the enhancing effect observed with the complete blocker cocktail. Conversely, positive allosteric modulation of the M5 mAChR (VU 238429) suppressed the response to subsequently applied denatonium (**Fig. 3**).

Urodynamic measurements in M1–5 mAChR-deficient mice

In all mouse strains, the basal pressure level recorded in transvesical cystometry was in the reported physiologic range between 10 and 25 cm H_2O (15, 16), with the lowest values observed in M2 $^{-/-}$, M2/3 $^{-/-}$, and M4 $^{-/-}$ mice (**Fig. 4**). We did not record a significant difference to wild-type mice in either parameter in M1 $^{-/-}$ and M4 $^{-/-}$ mice. M2 $^{-/-}$ mice demonstrated significantly lower threshold pressure, M3 $^{-/-}$ mice a significantly shorter peak-to-peak interval, and M2/3 $^{-/-}$ mice a significantly shorter peak-to-peak interval and lower peak and threshold pressure. Most parameters were altered in M5 $^{-/-}$ mice; significantly lowered micturition volume, bladder capacity, and shortened pressure peak-to-peak and micturition interval (Fig. 4).

DISCUSSION

Here, we demonstrate that the initial step of a bladder activity–enhancing reflex, that is, bitter activation of UBCs assessed by an increase in $[Ca^{2+}]_i$, is modulated by an

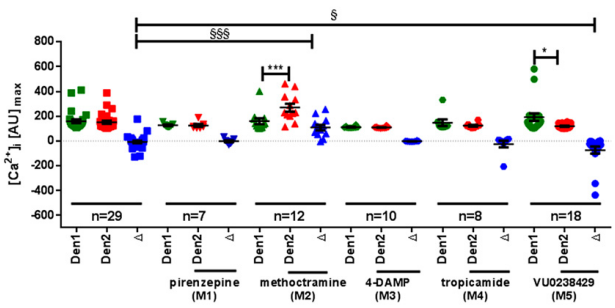

Figure 3. Impact of mAChR-selective pharmacologic intervention on the effect of cholinergic blockade on the calcium response of UBCs to bitter stimulus. We used the same technique and data presentation as in Fig. 2. All drugs were added under continuous flow in the chamber so that indicated concentrations were reached initially, then washed out. Initial concentrations of drugs were as follows: denatonium (Den1 and Den2; 25 mM), pirenzepine (0.001 mM; M1 receptor inhibitor), methoctramine (0.001 mM; M2 receptor inhibitor), 4-DAMP (0.001 mM; M3 receptor inhibitor), tropicamide (0.001 mM; M4 receptor inhibitor), and VU 0238429 (0.005 mM; positive allosteric modulator of the M5 receptor). A 1-way factorial ANOVA, followed by Dunnett's multiple comparison test was used to compare differences between peak responses under these conditions (Δ). $*P < 0.05$, $***P < 0.001$ (paired Student's t test), $^{§}P < 0.05$, $^{§§§}P < 0.001$.

autocrine cholinergic negative feedback loop as it is enhanced in the presence of a general cholinergic blocker cocktail. This situation differs from chemosensory lingual taste buds for which acetylcholine that is released from receptor cells enhances, rather than depresses, taste signaling *via* M3 mAChRs (17); however, in these rather complex sensory structures, the M3 receptor-mediated enhancement takes place at type III cells, which are considered to sense acidic substances, but not at type II cells that carry bitter and umami receptors (18), the receptors also expressed by UBCs (2).

In our approach, we unmasked the negative cholinergic feedback in UBCs by inhibiting all cholinergic receptors, thereby enhancing the response to the bitter stimulus, denatonium. Depending on the mode of calculation and mouse strain (ChAT-eGFP, C57BL/6), the average increase in response accounted for 42–60%. This is well in the range of increases in response to a blockade of autoinhibitory cholinergic feedback loops in peripheral cholinergic neurons that have been reported for rat myenteric plexus, rat heart, guinea pig trachea, mouse atrium, and mouse urinary bladder (19–22). This effect was lost in mice that lacked either M2 or M5 mAChRs. Accordingly, preferential M2 inhibition alone enhanced, and positive allosteric M5 modulation dampened, the bitter response. In contrast, this negative feedback loop was neither affected in mice with deficiency of any other muscarinic receptor (M1, M3, M4), nor could it be unmasked with M1-, M3-, and M4-preferring inhibitors. As UBCs are a rare cell type in the urethral epithelium, an entire murine urethra harbors approximately 380 (male) and 550 (female) UBCs (2), the paucity of available material precludes extensive dose-response curves in (ant)agonist experiments to determine K_d values, which limits the interpretation of data obtained with a single concentration. Still, the effects observed with the M2-preferring inhibitor and the M5-preferring allosteric modulator shall be ascribed to these and not to off-target effects on other mAChR subtypes, as inhibitors that preferentially address those did not demonstrate this effect. Hence, data from both inhibitor and knockout mice experiments revealed M2 and M5 receptors to be the crucial players (**Fig. 5**).

Autocrine negative feedback loops that operate *via* M2 receptors are commonly observed in cholinergic neurons, including striatal neurons (23), α-motoneurons (24), and postganglionic parasympathetic neurons (25). In parasympathetic cholinergic neurons, the M4 receptor can also serve as an autoreceptor that inhibits acetylcholine release, and it is the dominant, if not sole, receptor that confers this function in the mouse urinary bladder (19). Both M2 and M4 receptors typically act *via* $G_{i/o}$ proteins and the downstream inhibition of adenylate cyclase activity and voltage-activated Ca^{2+} channels (26), which fits to the inhibitory effect of the M2 receptor on the bitter stimulus increase in $[Ca^{2+}]_i$ that was observed in the present study.

The M5 receptor, however, is generally associated with an increase in $[Ca^{2+}]_i$ (26, 27), and, accordingly, enhances the activity of primary afferent terminals in the spinal cord, spinal glutamatergic interneurons, and somatodendrites of substantia nigra neurons (27, 28). This profile is in clear contrast to the dampening effect on stimulated $[Ca^{2+}]_i$ that was observed here in UBCs. Still, an M5 receptor–mediated inhibition of transmitter release that operates *via* a yet unresolved pathway has also been described for dopaminergic terminals in the striatum (27), so that the present finding of inhibitory M5 receptors is not unprecedented. The underlying signaling pathways still need to be identified.

We have previously demonstrated that urethral bitter stimulation markedly enhances detrusor activity during cystometric recordings with continuous bladder filling with saline through a reflex arc initiated by cholinergic (nicotinic) stimulation of sensory endings (2). Thus, factors that modulate the activation level of the initial sensor cell, UBCs, are expected to result in changes in the threshold setting of this reflex with an impact on bladder function. Then, in a simplistic model, the lack of the presently observed negative feedback, that is, deficiency of either M2 or M5 receptors, shall sensitize for enhanced detrusor activity. Of course, the overall outcome is determined not only by the threshold setting at the sensor cell, but also by the occurrence of muscarinic receptor subtypes along the entire pathway, including sensory neurons, spinal cord, parasympathetic neurons, and the bladder. This is particularly relevant for the M2 receptor, which, in addition to its role at UBCs, is prominently involved in sensory processing in the dorsal horn (28) and is abundantly expressed by the detrusor smooth muscle (29). The observed marked reduction in maximum detrusor pressure

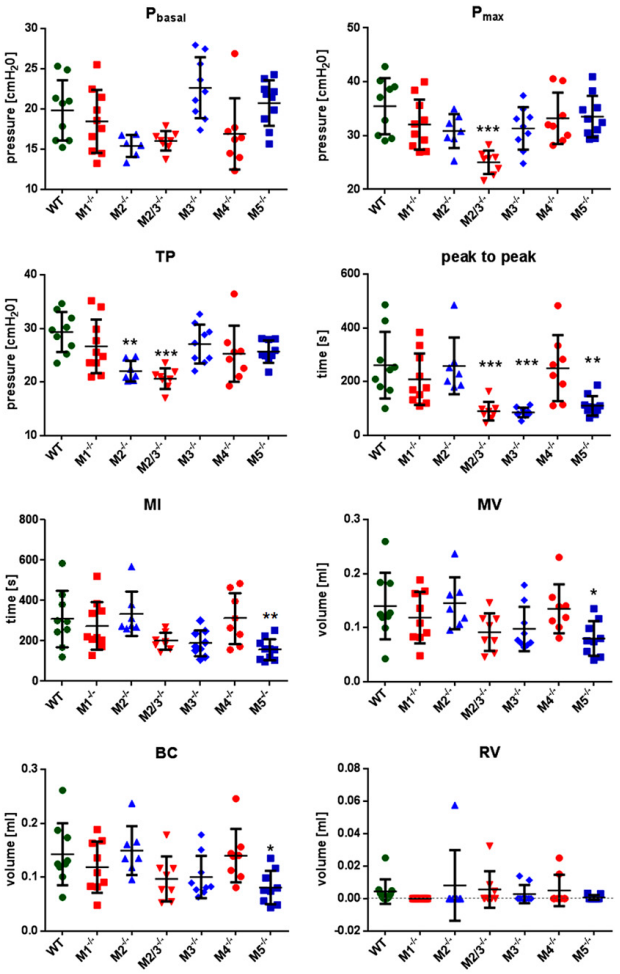

Figure 4. Urodynamic measurements in M1–5 mAChR-deficient mice. Cystometry was performed in conscious, freely moving mice. Saline (room temperature) was infused into the bladder at a rate of 1.5 ml/h. After a stabilization phase of 15–30 min, intravesical pressure and micturition were recorded continuously. We analyzed the basal pressure level (P_{base}), maximum detrusor pressure during micturition (P_{max}), threshold pressure (TP), bladder capacity (BC), time interval between 2 pressure peaks (PP), micturition interval (MI), micturition volume (MV), and residual volume (RV). A 1-way factorial ANOVA followed by Dunnett's multiple comparison test was used to compare cystometric parameters between groups of mice. $*P < 0.05$, $**P < 0.01$, $***P < 0.001$.

during micturition in the M2/M3 receptor double knockouts most likely reflects a direct effect at the detrusor, which is consistent with previous reports on single and double M2 and M3 receptor–deficient mice using cystometry and isolated bladders (15, 30, 31). Interference with the muscarinic regulation of ACh release from nerve terminals in the detrusor had no effect on cystometrically recorded parameters as mice with genetic deficiency of the M4 receptor, which mediates this function in the mouse bladder (19, 32), were indistinguishable from controls. Likewise, we did not observe functional alterations in deficiency of the M1 receptor, which facilitates the excitation of pelvic cholinergic neurons (33).

Of note, M5 receptor knockout animals exhibited the most extensive alterations in cystometry among the tested strains. Reduced bladder capacity and micturition volume, along with shortened micturition and pressure peak-to-peak intervals, are signs of overactivity that are compatible with the disinhibition of an activating input that originates from UBCs. Still, although its distribution is generally much more restricted than that of any other mAChR, it is not strictly limited to UBCs. In the mouse lumbar spinal cord, M5 receptor activation enhances glutamate release from afferent terminals (28, 34), which is also compatible with the observed phenotype in cystometry; however, with respect to bladder afferents, retrograde tracing experiments and RT-PCR analysis failed to detect M5 receptor expression in this specific population, despite readily detecting the M2, M3, and M4 subtypes (35), and the overall effect of mAChR activation on mouse bladder afferent neurons is inhibitory rather than excitatory (36). Lastly, M5 receptor mRNA is also expressed in the bladder wall, and the total binding of muscarinic

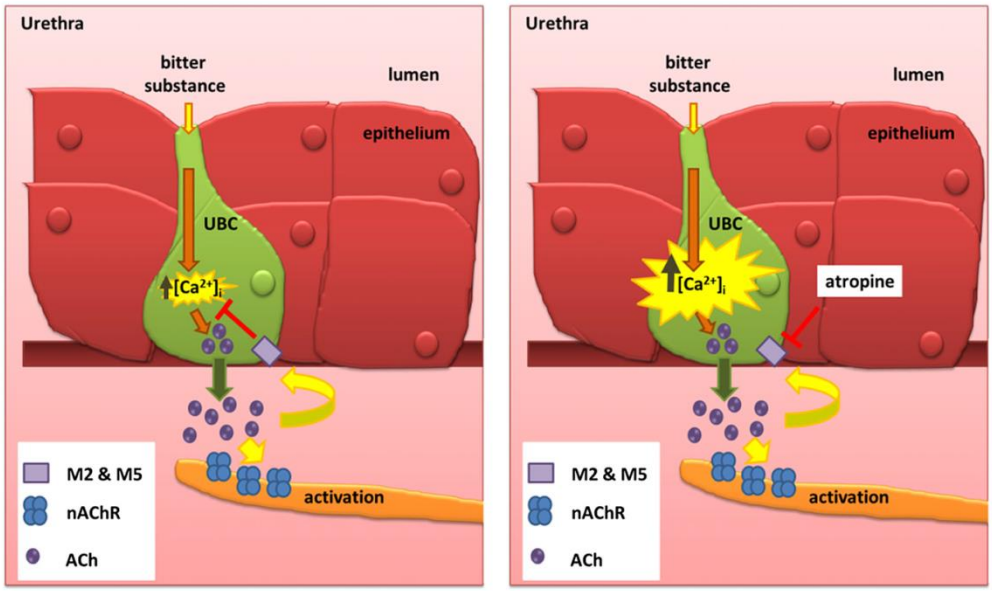

Figure 5. Schematic drawing of the hypothesized mechanism. The activation of a canonical taste transduction cascade in UBCs by a bitter stimulus leads to $[Ca^{2+}]_i$ increase followed by acetylcholine release. M2 and M5 mAChRs attenuate the bitter response of UBCs *via* a cholinergic negative autocrine feedback mechanism.

agonists is reduced in the bladder of M5 knockout mice (37, 38). The function of M5 receptors in the bladder is unknown; they neither play a role in regulating stimulus-induced ACh release from nerve terminals, nor do they have a role in cholinergic detrusor contraction (30, 32). Collectively, disinhibited UBCs seem to represent likely candidates to initiate signs of bladder overactivity in the general absence of M5 receptors, but cell type–specific deletion will be required to finally determine the crucial cellular element(s). In any case, these data are the first unraveling of a role for the M5 receptor in bladder physiology, and its activation may be considered and explored as a new line of intervention. The present study identifies a cholinergic autocrine negative feedback mechanism in the bitter response of UBCs, driven by the M2 and M5 muscarinic receptor subtypes. Cystometric recordings from awake mice, in which this mechanism is disturbed as a result of M5 receptor deficiency, revealed lowered micturition volume and enhanced frequency, which suggests that dysfunction of this system may lead to such symptoms as bladder overactivity.

ACKNOWLEDGMENTS

The authors thank M. Bodenbenner and K. Michael (Institute for Anatomy and Cell Biology, Justus-Liebig-University Giessen) for skillful technical assistance. This work was supported by the Hessian State Offensive for the Development of Scientific and Economic Excellence (LOEWE) (Non-neuronal Cholinergic Systems, Project A5; to W.K. and T.B.) and a University Hospital of Giessen and Marburg (UKGM)-Justus-Liebig-University (JLU)-Cooperation Grant (7/2016 GI to K.D.). The authors declare no conflicts of interest.

AUTHOR CONTRIBUTIONS

K. Deckmann, T. Bschleipfer, and W. Kummer designed the research, analyzed data, performed statistical analysis, obtained funding, and drafted the manuscript; K. Deckmann, A. Rafiq, C. Erdmann, C. Illig, and M. Durschnabel performed research; J. Wess and W. Weidner contributed administrative, technical, and material support; and W. Weidner and W. Kummer supervised work.

REFERENCES

1. Deckmann, K., Krasteva-Christ, G., Rafiq, A., Herden, C., Wichmann, J., Knauf, S., Nassenstein, C., Grevelding, C. G., Dorresteijn, A., Chubanov, V., Gudermann, T., Bschleipfer, T., and Kummer, W. (2015) Cholinergic urethral brush cells are widespread throughout placental mammals. *Int. Immunopharmacol.* **29**, 51–56
2. Deckmann, K., Filipski, K., Krasteva-Christ, G., Fronius, M., Althaus, M., Rafiq, A., Papadakis, T., Renno, L., Jurastow, I., Wessels, L., Wolff, M., Schütz, B., Weihe, E., Chubanov, V., Gudermann, T., Klein, J., Bschleipfer, T., and Kummer, W. (2014) Bitter triggers acetylcholine release from polymodal urethral chemosensory cells and bladder reflexes. *Proc. Natl. Acad. Sci. USA* **111**, 8287–8292
3. Kummer, W., and Deckmann, K. (2017) Brush cells, the newly identified gatekeepers of the urinary tract. *Curr. Opin. Urol.* **27**, 85–92
4. Irwin, D. E., Milsom, I., Hunskaar, S., Reilly, K., Kopp, Z., Herschorn, S., Coyne, K., Kelleher, C., Hampel, C., Artibani, W., and Abrams, P.

(2006) Population-based survey of urinary incontinence, overactive bladder, and other lower urinary tract symptoms in five countries: results of the EPIC study. *Eur. Urol.* **50**, 1306–1314; discussion 1314-1305
5. Milsom, I., Abrams, P., Cardozo, L., Roberts, R. G., Thüroff, J., and Wein, A. J. (2001) How widespread are the symptoms of an overactive bladder and how are they managed? A population-based prevalence study. *BJU Int.* **87**, 760–766
6. Abrams, P., Cardozo, L., Fall, M., Griffiths, D., Rosier, P., Ulmsten, U., Van Kerrebroeck, P., Victor, A., and Wein, A.; Standardisation Sub-Committee of the International Continence Society. (2003) The standardisation of terminology in lower urinary tract function: report from the standardisation sub-committee of the International Continence Society. *Urology* **61**, 37–49
7. Groen, J., Pannek, J., Castro Diaz, D., Del Popolo, G., Gross, T., Hamid, R., Karsenty, G., Kessler, T. M., Schneider, M., 't Hoen, L., and Blok, B. (2016) Summary of European Association of Urology (EAU) guidelines on neuro-urology. *Eur. Urol.* **69**, 324–333
8. Fisahn, A., Yamada, M., Duttaroy, A., Gan, J. W., Deng, C. X., McBain, C. J., and Wess, J. (2002) Muscarinic induction of hippocampal gamma oscillations requires coupling of the M1 receptor to two mixed cation currents. *Neuron* **33**, 615–624
9. Gomeza, J., Shannon, H., Kostenis, E., Felder, C., Zhang, L., Brodkin, J., Grinberg, A., Sheng, H., and Wess, J. (1999) Pronounced pharmacologic deficits in M2 muscarinic acetylcholine receptor knockout mice. *Proc. Natl. Acad. Sci. USA* **96**, 1692–1697
10. Gomeza, J., Zhang, L., Kostenis, E., Felder, C., Bymaster, F., Brodkin, J., Shannon, H., Xia, B., Deng, C., and Wess, J. (1999) Enhancement of D1 dopamine receptor-mediated locomotor stimulation in M4 muscarinic acetylcholine receptor knockout mice. *Proc. Natl. Acad. Sci. USA* **96**, 10483–10488
11. Struckmann, N., Schwering, S., Wiegand, S., Gschnell, A., Yamada, M., Kummer, W., Wess, J., and Haberberger, R. V. (2003) Role of muscarinic receptor subtypes in the constriction of peripheral airways: studies on receptor-deficient mice. *Mol. Pharmacol.* **64**, 1444–1451
12. Yamada, M., Lamping, K. G., Duttaroy, A., Zhang, W., Cui, Y., Bymaster, F. P., McKinzie, D. L., Felder, C. C., Deng, C. X., Faraci, F. M., and Wess, J. (2001) Cholinergic dilation of cerebral blood vessels is abolished in M5 muscarinic acetylcholine receptor knockout mice. *Proc. Natl. Acad. Sci. USA* **98**, 14096–14101
13. Yamada, M., Miyakawa, T., Duttaroy, A., Yamanaka, A., Moriguchi, T., Makita, R., Ogawa, M., Chou, C. J., Xia, B., Crawley, J. N., Felder, C. C., Deng, C. X., and Wess, J. (2001) Mice lacking the M3 muscarinic acetylcholine receptor are hypophagic and lean. *Nature* **410**, 207–212
14. Bschleipfer, T., Dannenmaier, A. K., Illig, C., Kreisel, M., Gattenlöhner, S., Langheinrich, A. C., Krombach, G. A., Weidner, W., and Kampschulte, M. (2015) Systemic atherosclerosis causes detrusor overactivity: functional and morphological changes in hyperlipoproteinemic apoE$^{-/-}$LDLR$^{-/-}$ mice. *J. Urol.* **193**, 345–351
15. Igawa, Y., Zhang, X., Nishizawa, O., Umeda, M., Iwata, A., Taketo, M. M., Manabe, T., Matsui, M., and Andersson, K. E. (2004) Cystometric findings in mice lacking muscarinic M2 or M3 receptors. *J. Urol.* **172**, 2460–2464
16. Andersson, K. E., Soler, R., and Füllhase, C. (2011) Rodent models for urodynamic investigation. *Neurourol. Urodyn.* **30**, 636–646
17. Dando, R., and Roper, S. D. (2012) Acetylcholine is released from taste cells, enhancing taste signalling. *J. Physiol.* **590**, 3009–3017
18. Mori, Y., Eguchi, K., Yoshii, K., and Ohtubo, Y. (2016) Selective expression of muscarinic acetylcholine receptor subtype M3 by mouse type III taste bud cells. *Pflugers Arch.* **468**, 2053–2059
19. Zhou, H., Meyer, A., Starke, K., Gomeza, J., Wess, J., and Trendelenburg, A. U. (2002) Heterogeneity of release-inhibiting muscarinic autoreceptors in heart atria and urinary bladder: a study with M2- and M4-receptor-deficient mice. *Naunyn Schmiedebergs Arch. Pharmacol.* **365**, 112–122
20. Wessler, I., and Werhand, J. (1990) Evaluation by reverse phase HPLC of [^{3}H]acetylcholine release evoked from the myenteric plexus of the rat. *Naunyn Schmiedebergs Arch. Pharmacol.* **341**, 510–516
21. Bognar, I. T., Beinhauer, B., Kann, P., and Fuder, H. (1990) Different muscarinic receptors mediate autoinhibition of acetylcholine release and vagally-induced vasoconstriction in the rat isolated perfused heart. *Naunyn Schmiedebergs Arch. Pharmacol.* **341**, 279–287
22. Kilbinger, H., Schneider, R., Siefken, H., Wolf, D., and D'Agostino, G. (1991) Characterization of prejunctional muscarinic autoreceptors in the guinea-pig trachea. *Br. J. Pharmacol.* **103**, 1757–1763
23. Mohr, F., Krejci, E., Zimmermann, M., and Klein, J. (2015) Dysfunctional presynaptic M2 receptors in the presence of chronically high acetylcholine levels: data from the PRiMA knockout mouse. *PLoS One* **10**, e0141136
24. Oliveira, L., Timóteo, M. A., and Correia-de-Sá, P. (2002) Modulation by adenosine of both muscarinic M1-facilitation and M2-inhibition of [^{3}H]acetylcholine release from the rat motor nerve terminals. *Eur. J. Neurosci.* **15**, 1728–1736
25. Fryer, A. D., and Maclagan, J. (1984) Muscarinic inhibitory receptors in pulmonary parasympathetic nerves in the guinea-pig. *Br. J. Pharmacol.* **83**, 973–978
26. Wess, J. (1996) Molecular biology of muscarinic acetylcholine receptors. *Crit. Rev. Neurobiol.* **10**, 69–99
27. Foster, D. J., Gentry, P. R., Lizardi-Ortiz, J. E., Bridges, T. M., Wood, M. R., Niswender, C. M., Sulzer, D., Lindsley, C. W., Xiang, Z., and Conn, P. J. (2014) M5 receptor activation produces opposing physiological outcomes in dopamine neurons depending on the receptor's location. *J. Neurosci.* **34**, 3253–3262
28. Chen, S. R., Chen, H., Yuan, W. X., Wess, J., and Pan, H. L. (2014) Differential regulation of primary afferent input to spinal cord by muscarinic receptor subtypes delineated using knockout mice. *J. Biol. Chem.* **289**, 14321–14330
29. Chess-Williams, R. (2002) Muscarinic receptors of the urinary bladder: detrusor, urothelial and prejunctional. *Auton. Autacoid Pharmacol.* **22**, 133–145
30. Matsui, M., Motomura, D., Fujikawa, T., Jiang, J., Takahashi, S., Manabe, T., and Taketo, M. M. (2002) Mice lacking M2 and M3 muscarinic acetylcholine receptors are devoid of cholinergic smooth muscle contractions but still viable. *J. Neurosci.* **22**, 10627–10632
31. Ehlert, F. J., Griffin, M. T., Abe, D. M., Vo, T. H., Taketo, M. M., Manabe, T., and Matsui, M. (2005) The M2 muscarinic receptor mediates contraction through indirect mechanisms in mouse urinary bladder. *J. Pharmacol. Exp. Ther.* **313**, 368–378
32. Takeuchi, T., Yamashiro, N., Kawasaki, T., Nakajima, H., Azuma, Y. T., and Matsui, M. (2008) The role of muscarinic receptor subtypes in acetylcholine release from urinary bladder obtained from muscarinic receptor knockout mouse. *Neuroscience* **156**, 381–389
33. Sculptoreanu, A., Yoshimura, N., de Groat, W. C., and Somogyi, G. T. (2001) Protein kinase C is involved in M1-muscarinic receptor-mediated facilitation of L-type Ca^{2+} channels in neurons of the major pelvic ganglion of the adult male rat. *Neurochem. Res.* **26**, 933–942
34. Chen, S. R., Chen, H., Yuan, W. X., Wess, J., and Pan, H. L. (2010) Dynamic control of glutamatergic synaptic input in the spinal cord by muscarinic receptor subtypes defined using knockout mice. *J. Biol. Chem.* **285**, 40427–40437
35. Nandigama, R., Bonitz, M., Papadakis, T., Schwantes, U., Bschleipfer, T., and Kummer, W. (2010) Muscarinic acetylcholine receptor subtypes expressed by mouse bladder afferent neurons. *Neuroscience* **168**, 842–850
36. Daly, D. M., Chess-Williams, R., Chapple, C., and Grundy, D. (2010) The inhibitory role of acetylcholine and muscarinic receptors in bladder afferent activity. *Eur. Urol.* **58**, 22–28; discussion 31-22
37. Ito, Y., Oyunzul, L., Seki, M., Fujino Oki, T., Matsui, M., and Yamada, S. (2009) Quantitative analysis of the loss of muscarinic receptors in various peripheral tissues in M1-M5 receptor single knockout mice. *Br. J. Pharmacol.* **156**, 1147–1153
38. Bschleipfer, T., Weidner, W., Kummer, W., and Lips, K. S. (2012) Does bladder outlet obstruction alter the non-neuronal cholinergic system of the human urothelium? *Life Sci.* **91**, 1082–1086

Received for publication June 23, 2017.
Accepted for publication December 26, 2017.

frontiers in Cell and Developmental Biology

ORIGINAL RESEARCH
published: 15 August 2018
doi: 10.3389/fcell.2018.00089

ENaC in Cholinergic Brush Cells

*Chrissy Kandel[1], Patricia Schmidt[1], Alexander Perniss[1], Maryam Keshavarz[1], Paul Scholz[2], Sabrina Osterloh[2], Mike Althaus[3], Wolfgang Kummer[1] and Klaus Deckmann[1]**

[1] Institute for Anatomy and Cell Biology, Justus-Liebig-University Giessen, Giessen, Germany, [2] Department of Cell Physiology, Ruhr-University Bochum, Bochum, Germany, [3] School of Natural and Environmental Sciences, Newcastle University, Newcastle upon Tyne, United Kingdom

Cholinergic polymodal chemosensory cells in the mammalian urethra (urethral brush cells = UBC) functionally express the canonical bitter and umami taste transduction signaling cascade. Here, we aimed to determine whether UBC are functionally equipped for the perception of salt through ENaC (epithelial sodium channel). Cholinergic UBC were isolated from ChAT-eGFP reporter mice (ChAT = choline acetyltransferase). RT-PCR showed mRNA expression of ENaC subunits *Scnn1a*, *Scnn1b*, and *Scnn1g* in urethral epithelium and isolated UBC. *Scnn1a* could also be detected by next generation sequencing in 4/6 (66%) single UBC, two of them also expressed the bitter receptor Tas2R108. Strong expression of *Scnn1a* was seen in some urothelial umbrella cells and in 65% of UBC (30/46 cells) in a *Scnn1a* reporter mouse strain. Intracellular [Ca^{2+}] was recorded in isolated UBC stimulated with the bitter substance denatonium benzoate (25 mM), ATP (0.5 mM) and NaCl (50 mM, on top of 145 mM Na^+ and 153 mM Cl^- baseline in buffer); mannitol (150 mM) served as osmolarity control. NaCl, but not mannitol, evoked an increase in intracellular [Ca^{2+}] in 70% of the tested UBC. The NaCl-induced effect was blocked by the ENaC inhibitor amiloride (IC_{50} = 0.47 μM). When responses to both NaCl and denatonium were tested, all three possible positive response patterns occurred in a balanced distribution: 42% NaCl only, 33% denatonium only, 25% to both stimuli. A similar reaction pattern was observed with ATP and NaCl as test stimuli. About 22% of the UBC reacted to all three stimuli. Thus, NaCl evokes calcium responses in several UBC, likely involving an amiloride-sensitive channel containing α-ENaC. This feature does not define a new subpopulation of UBC, but rather emphasizes their polymodal character. The actual function of α-ENaC in cholinergic UBC—salt perception, homeostatic ion transport, mechanoreception—remains to be determined.

Keywords: chemosensory cells, cholinergic, ENaC, urethra, urethral brush cells, salt

OPEN ACCESS

Edited by:
Cesare Indiveri,
University of Calabria, Italy

Reviewed by:
Vito De Pinto,
Università degli Studi di Catania, Italy
Diego Alvarez de la Rosa,
Universidad de La Laguna, Spain

****Correspondence:***
Klaus Deckmann
klaus.deckmann@anatomie.med.uni-giessen.de

Specialty section:
This article was submitted to Cellular Biochemistry, a section of the journal Frontiers in Cell and Developmental Biology

Received: *29 March 2018*
Accepted: *25 July 2018*
Published: *15 August 2018*

Citation:
Kandel C, Schmidt P, Perniss A, Keshavarz M, Scholz P, Osterloh S, Althaus M, Kummer W and Deckmann K (2018) ENaC in Cholinergic Brush Cells. Front. Cell Dev. Biol. 6:89. doi: 10.3389/fcell.2018.00089

INTRODUCTION

Bitter, sweet, umami, salty, sour, and fatty are the six recognized taste qualities detected by taste buds (Chaudhari and Roper, 2010). In type II sensory cells in the oropharyngeal taste buds, bitter, sweet, and umami perception is mediated by the canonical taste transduction signaling cascade, including G protein-coupled taste receptors, the taste-specific G protein α-gustducin, phospholipase Cβ2 (PLCβ2), and the transient potential receptor cation channel subfamily M member 5 (TRPM5) (Chaudhari and Roper, 2010). Other classes of G protein-coupled receptors respond to short- and long-chain fatty acids (Chaudhari and Roper, 2010).

In contrast, acid (protons) and salt (sodium chloride) are monitored by ion channels, directly leading to depolarization of the taste cell. Nonselective cation channels formed by polycystic kidney disease 2-like 1 protein (PKD2L1) and polycystic kidney disease 2-like 3 protein (PKD1L3) were proposed as candidates for sour taste receptors (Huang et al., 2006; Ishimaru et al., 2006; Lopezjimenez et al., 2006; Chaudhari and Roper, 2010). An ion channel that is long been thought to mediate salt perception is the amiloride-sensitive epithelial sodium channel, ENaC (Heck et al., 1984; Avenet and Lindemann, 1988; Lindemann et al., 1998; Lin et al., 1999; Lindemann, 2001; Chandrashekar et al., 2010). It is predominantly expressed in epithelial cells of the colon, lung, kidney, sweat and salivary glands, where it is a major regulator of sodium absorption and, thereby, essential for fluid homeostasis (Duc et al., 1994; McDonald et al., 1995; Garty and Palmer, 1997). ENaC is also expressed in the urothelium (Carattino et al., 2005; Du et al., 2007; Birder et al., 2010; Birder and Andersson, 2013). The canonical heteromeric ion channel consists of three subunits (α, β, γ) (Canessa et al., 1994b), encoded by the genes *Scnn1a*, *Scnn1b*, and *Scnn1c*. A fourth δ-subunit with distinct characteristics was identified and the presence of this subunit changes the biophysical characteristics as well as molecular regulation of this ion channel. Mice, however, lack a functional gene for this subunit and its physiological function remains unclear (Giraldez et al., 2012; Wichmann et al., 2018). ENaC is a constitutively active ion channel. Still, its expression, membrane abundance and open probability are tightly regulated by extrinsic and intrinsic factors. These include hormones, intracellular kinases and intramembrane lipids, as well as the extracellular sodium concentration, pH and mechanical stimuli (Chraïbi and Horisberger, 2002; Althaus et al., 2007; Baines, 2013; Kleyman et al., 2018). The ion conductivity of αβγ-ENaC is limited to monovalent cations ($Li^+ > Na^+ > K^+$) (Kellenberger and Schild, 2002).

Extraoral chemosensory cells, monitoring the composition of the mucosal lining fluid, have been described in the respiratory, gastrointestinal and urogenital tract. Like type II taste cells, they express the canonical taste transduction signaling cascade (taste receptors, α-gustducin, PLCβ2, TRPM5) (Höfer et al., 1996; Höfer and Drenckhahn, 1998; Finger et al., 2003; Krasteva et al., 2011, 2012; Deckmann et al., 2014; Schütz et al., 2015). They respond to bitter substances and bacterial products with a release of acetylcholine and initiate avoidance reflexes, thereby apparently serving as sentinels situated at entrances into the body (Finger and Kinnamon, 2011; Lee and Cohen, 2015; Deckmann and Kummer, 2016). These cholinergic epithelial cells also express villin, a structural protein of microvilli. Such cells have originally been termed "brush cells" in the respiratory tract, and this term has also been adopted to the villin-positive, cholinergic chemosensory cells of the urethra (urethral brush cells = UBC) (Deckmann et al., 2014, 2015). In line with the sentinel concept, UBC respond to heat-inactivated uropathogenic *Escherichia coli* and are connected to sensory nerve fibers (Deckmann et al., 2014). Bitter application into the urethral lumen reflexively triggers enhanced detrusor activity, which has been interpreted as a protective reflex, as potential hazardous content is expelled from the urethra through micturition (Deckmann et al., 2014; Kummer and Deckmann, 2017).

Most cholinergic UBC are polymodal chemosensory cells, responding both to bitter substances and to glutamate with an increase in intracellular calcium concentration ($[Ca^{2+}]_i$) (Deckmann et al., 2014). This discriminates them from type II taste bud cells, which are generally responsive either to bitter, representing an aversive stimulus, or to umami, an attractive stimulus (Nelson et al., 2001; Chaudhari and Roper, 2010). At the urethral mucosa, both stimuli represent a potential danger signal, since many bacterial products have bitter quality and glutamate (umami) facilitates bacterial growth in urine. Here, we aimed to determine whether their polymodal properties extend beyond taste receptor mediated qualities, focusing upon the perception of salt.

MATERIALS AND METHODS

Animals

Mice expressing enhanced green fluorescent protein (eGFP) under the control of the promoter of the acetylcholine synthesizing enzyme, choline acetyltransferase, (ChAT-eGFP; B6.Cg-Tg(RP23-268L19-EGFP)2Mik/J; Stock No. 007902) were obtained from Jackson Laboratory (Bar Habor, ME, USA). Mice expressing tdTomato, a bright red fluorescent protein, under the control of the promotor of *Scnn1a*, the coding gene sequence of α-ENaC (*Scnn1a*/tdTomato; Guy et al., 2015) were kindly provided by J. Guy and J. Staiger (Institute for Neuroanatomy, University Medical Center Goettingen, Georg-August-University Goettingen, Germany). This study was carried out in accordance with the recommendations of European Communities Council Directive of 24th November 1986 (86/609/EEC). The protocol was approved by the local authorities (Animal Welfare Officer at the University of Giessen and the Committee for Animal Welfare, Dept. V54, Regierungspräsidium Giessen, Germany; reference no. 572_M).

Cell Isolation

Cell isolation was performed as described previously (Deckmann et al., 2014). In brief: Urethrae were dissected, cut into small pieces, and enzymatically digested in dispase (2 mg/mL; Sigma-Aldrich/Merck, Darmstadt, Germany) and trypsin/PBS (1:1, Invitrogen, Carlsbad, CA, USA). After mechanical dissociation, cells were separated through a cell strainer (pore size 70 μm; BD Bioscience, Franklin Lakes, NJ, USA). The ChAT promotor is constitutively active in cholinergic chemosensory cells (Tallini et al., 2006). Hence, UBC constitutively express eGFP which served to sort them via FACS and to identify them with a fluorescence microscope.

RT-PCR

Total RNA from dissected urethra or pooled isolated cells ($n = 4$ samples, sorting based on ChAT-eGFP expression by FACS; BD

Abbreviations: AU, arbitrary units; ChAT, choline acetyltransferase; Den, denatonium benzoate; eGFP, enhanced green fluorescent protein; ENaC, epithelial sodium channel; $[Ca^{2+}]_i$, intracellular calcium concentration; TRPM5, transient receptor potential cation channel subfamily M member 5; UBC, urethral brush cell.

FASCARIA III cell sorter, settings and analysis were performed with a BD FACSDiva v6.1.3; BD Bioscience, Franklin Lakes, NJ, USA) was extracted using the Qiagen RNeasy Micro Kit (Qiagen, Hilden, Germany) according to the manufacturer's protocol. Extracted total RNA from kidney was used as positive control. RT-PCR was performed as described previously (primer sequences: **Table S1**; Deckmann et al., 2014).

Next Generation Sequencing

Next generation sequencing was performed as described elsewhere (Scholz et al., 2016). In brief: isolated single eGFP-positive cells were identified, picked and transferred to a PCR tube using a combined confocal laser-scanning/patch-clamp setup (Leica TCS SP5, Leica Microsystems/Luigs-Neumann, Wetzlar/Ratingen, Germany). Cell lysis, cDNA generation and amplification were performed using the Sigma SeqPlex RNA Amplification Kit (Sigma-Aldrich/Merck, Darmstadt, Germany). For library preparation, the Illumina Nextera XT DNA sample preparation protocol (Part # 15031942 Rev. C) was used. Samples run together with a 2 × 75 bp read length using the MiSeq Reagent Kit v3 (150 cycles) and the Illumina MiSeq Desktop Sequencer (Illumina, San Diego, CA, USA). The sequencing reads were aligned to the mm9 reference genome and transcriptome using TopHat2 (2.0.9). The TopHat output files were saved in BAM format and evaluated by Cuffdiff2 (2.1.1). All samples were compared and evaluated in one calculation cycle, allowing the algorithm to estimate the Fragments Per Kilobase Million (FPKM) values at the transcript level resolution and to control for variability across the replicate libraries.

Immunohistochemistry and Whole-Mount Immunostaining

Specimen preparations and analyses were performed as described previously (Krasteva et al., 2011). In brief: urethrae used for immunohistochemistry ($N = 3$) and gall bladders used for whole-mount immunostaining ($N = 2$) were fixed using transcardiac perfusion with Zamboni solution (2% paraformaldehyde/15% saturated picric acid in 0.1 M phosphate buffer, pH 7.4). Fixed organs were dissected, washed in 0.1 M phosphate buffer (0.1 M NaH_2PO_4; 0.1 M Na_2HPO_4), and either incubated overnight in 18% sucrose in 0.1 M phosphate buffer and frozen in liquid nitrogen or mounted on a block of silicon elastomer using insect pins. Primary antibody was applied to 4–18 tissue sections from every individual animal. Primary antibodies were chicken anti-RFP (NBP1-97371, 1:200 dilution; Novus Biologicals, Littleton, CO, USA) and rabbit anti-TPRM5 (1:2,000) (Kaske et al., 2007). Secondary antibodies were goat-anti rabbit Ig conjugated to Alexa 488 (1:500; Thermo Fisher Scientific Inc. Waltham, MA, USA) and donkey-anti chicken Ig conjugated to Cy3 (1:2,000; Dianova, Hamburg, Germany). Nuclei were labeled with 4′,6-diamidino-2-phenylindol (DAPI; 1 μg/ml; Sigma-Aldrich/Merck, Darmstadt, Germany). All sections were rinsed and coverslipped with carbonate-buffered glycerol (pH 8.6). Sections were evaluated by epifluorescence microscopy (Axioplan 2, Zeiss, Wetzlar, Germany) or with a confocal laser scanning microscope (LSM 710, Zeiss, Wetzlar, Germany). Specificity of secondary reagents was validated by omission of primary antibodies.

Measurement of Intracellular Calcium Concentration

Measurement of intracellular calcium concentration ($[Ca^{2+}]_i$) was performed as described previously (Deckmann et al., 2014). In brief: Isolated cells were loaded with the fluorescent calcium indicator Calcium Orange® AM (0.01 μg/μL; Thermo Fisher Scientific Inc., Waltham, MA, USA) and plated on coverslips. $[Ca^{2+}]_i$ was analyzed with a confocal laser scanning microscope (LSM 710 with ZEN 2010 B SP1, Zeiss, Wetzlar, Germany). Lasers and filters were: eGFP: excitation with Argon laser at 488 nm; recording of emission at 495–553 nm with optical filters MBS-488/561/633; Calcium Orange: excitation with DPSS561-10 laser at 561 nm; recording of emission at 566-683 nm with optical filters MBS-558/561. Regions of interest were selected manually and fluorescence intensities at the start of the recording period were set arbitrarily at 100%. Test stimuli and concentrations were denatonium benzoate (25 mM; Molekula, Munich, Germany), ATP (0.5 mM; Sigma-Aldrich/Merck, Darmstadt, Germany) and NaCl (1–150 mM; Carl Roth, Karlsruhe, Germany), and inhibitors and controls included the osmolarity control mannitol (1–150 mM; Sigma-Aldrich/Merck, Darmstadt, Germany) and the ENaC inhibitor amiloride (0.01–100 μM; Sigma-Aldrich/Merck, Darmstadt, Germany). All recordings were done during continuous superfusion with Tyrode III buffer (NaCl 130 mM; HEPES 10 mM; glucose 10 mM; KCl 5 mM; $MgCl_2$ 1 mM; $CaCl_2$ 8 mM; sodium pyruvate 10 mM; $NaHCO_3$ 5 mM; 2.5 mL/min; 37°C). Stimuli were added under continuous flow of Tyrode III into the chamber, so that indicated concentrations were reached initially and then washed out. Since baseline concentration of Na^+ in the buffer was 145 mM, the total concentration after addition of 1–150 mM ranged from 146 to 295 mM.

Statistical Analysis

Data were analyzed for normal distribution by the Kolmogorov-Smirnov test. Multiple comparison analysis was performed by Kruskal-Wallis test followed by Dunn's Multiple Comparison Test. $P \leq 0.05$ were regarded as statistically significant. Analyses were performed by GraphPad Prism 5 (GraphPad Software Inc., La Jolla, CA, USA).

RESULTS AND DISCUSSION

RT-PCR revealed mRNA expression of the ENaC subunits *Scnn1a*, *Scnn1b*, and *Scnn1g* in the urethral epithelium (**Figure 1A**) and in pooled isolated UBC (**Figure 1B**). Next generation sequencing (NGS) of six isolated single eGFP-positive cells showed a heterogeneous expression pattern of *Scnn1a, b, g* (**Figure 2**). *Scnn1a* was detected in 4/6 cells (66.6%), *Scnn1b* and *Scnn1g* only in 1/6 cells. Canonical ENaC is composed of the α-, β-, and γ-subunit (Canessa et al., 1994a), but the ENaC α-subunit alone is able to

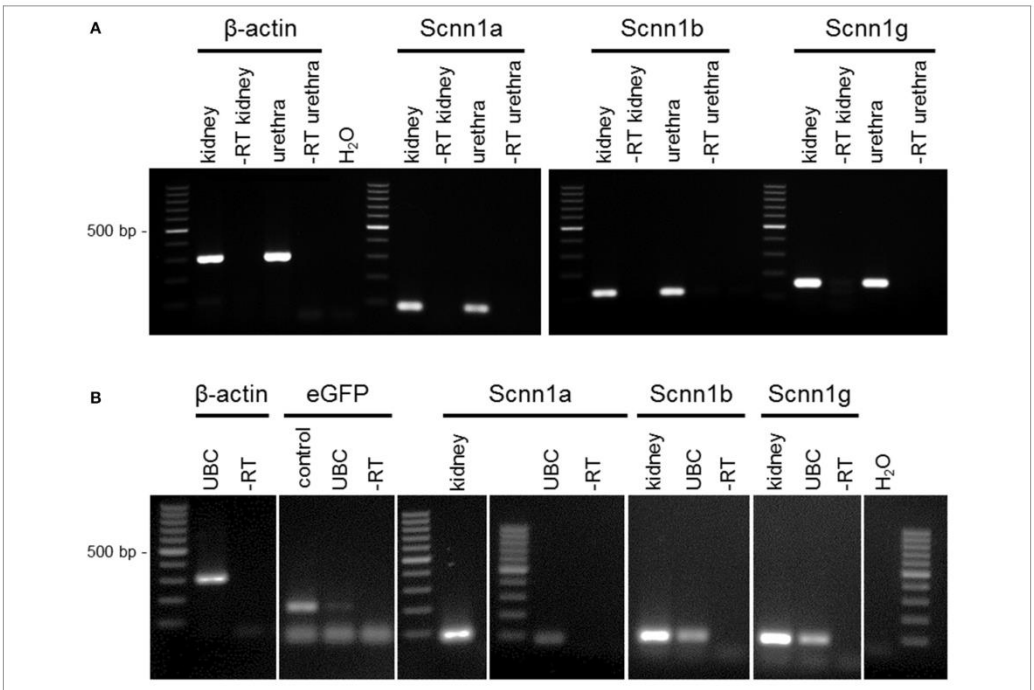

FIGURE 1 | RT-PCR of urethral epithelium and isolated UBC. **(A)** RT-PCR of urethral epithelium. **(B)** RT-PCR of UBC. Cells were isolated and sorted based on ChAT-eGFP expression by flow cytometry; agarose gel; α-ENaC (*Scnn1a*; 82 bp), β-ENaC (*Scnn1b*; 115 bp), γ-ENaC (*Scnn1g*; 150 bp), β-actin (300 bp), eGFP (180 bp); ± RT = aliquots processed with/without reverse transcription; kidney = positive control; H_2O = water control.

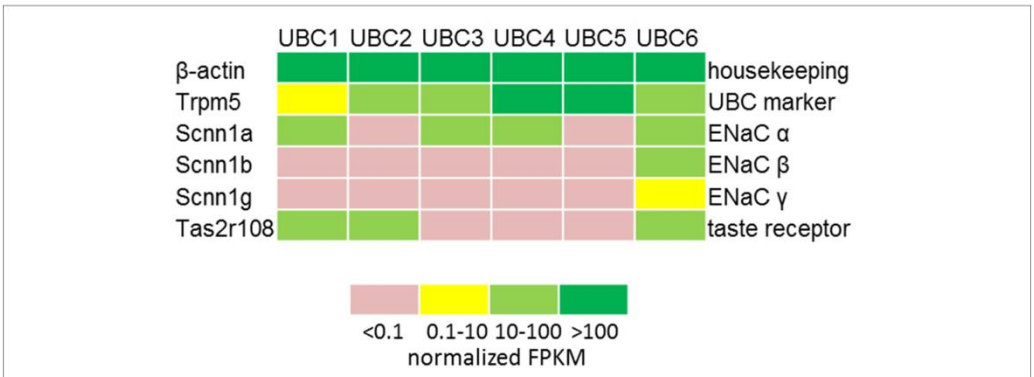

FIGURE 2 | Expression of ENAC genes and markers of chemosensory cells in single UBC determined by NGS. Heatmap displaying the detection levels as normalized FPKM in GFP-positive UBC. FPKM, Fragments Per Kilobase Million.

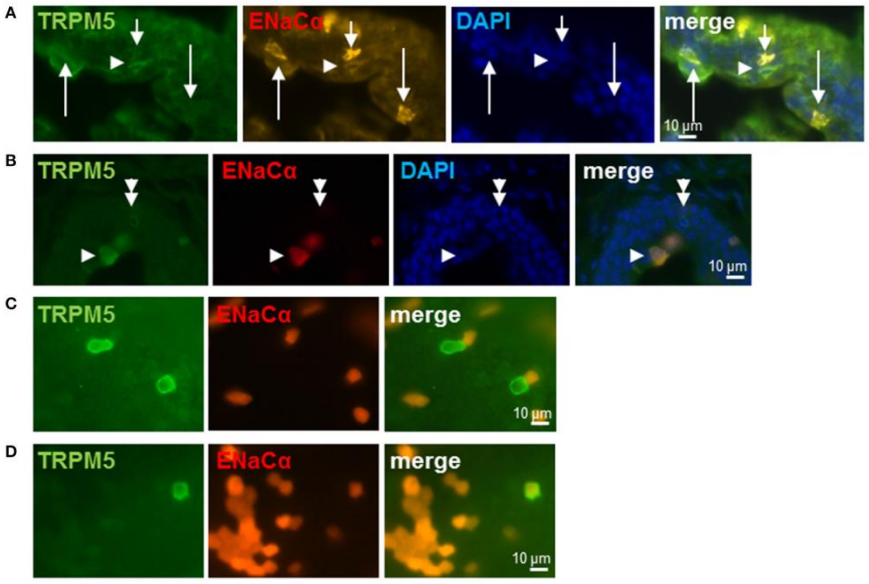

FIGURE 3 | Brush cells express ENaCα. **(A,B)** Urethra; frozen sections: *Scnn1a*/tdTomato (orange or red), TRPM5-immunoreactivity (green) and cell nuclei (DAPI; blue). Several epithelial cells express α-ENaC only (*arrows* in **A**). At least two of them (*long arrows* in **A**) are urothelial umbrella cells as judged by their shape and position. *Arrowheads* point to α-ENaC (orange) and TRPM5 (green) double-positive cells, the *doubled arrowhead* points to a TRPM5-immunoreactive cell that does not express α-ENaC. **(C,D)** Gall bladder; whole-mount: *Scnn1a*/tdTomato (red) and TRPM5 (green). **(C)** Selected cells show no co-localization of α-ENaC and TRPM5. **(D)** Selected TRPM5-immunoreactive cell shows co-localization of α-ENaC and TRPM5.

form amiloride-sensitive homomers *in vitro* (Canessa et al., 1994b).

To further validate *Scnn1a* expression in cholinergic UBC, urethral tissue sections of a *Scnn1a* reporter mouse strain were labeled for cholinergic UBC. In view of often experienced methodological problems in detecting ChAT by immunohistochemistry in peripheral cells, we set out to establish a technically more reliable marker for immunohistochemical detection of cholinergic UBC. Villin-antibodies, an often used marker for brush cells in general, appeared not suitable for this purpose as there is a considerable number of villin-positive but ChAT- and TRPM5-negative slender epithelial cells in the murine urethra, in addition to the villin/ChAT/TRPM5-positive cells (Deckmann et al., 2014). These two phenotypes represent truly different cell populations, since genetic ablation of the transcription factor Skn-1a/Pou2f3 selectively prevents the development of TRPM5-positive (i.e., cholinergic UBC) but not of villin-positive but TRPM5-negative urethral cells (Yamashita et al., 2017).

We used TRPM5-immunolabeling as a marker for cholinergic UBC in *Scnn1a*-tdTomato reporter mice. In these mice, strong expression of *Scnn1a* was observed in several cells of the urethral epithelium (**Figures 3A,B**). Among them were umbrella cells, which build up the luminal lining in the proximal parts of the urethra being covered with an urothelium and which can be readily identified by virtue of their position and morphology. This is in line with the previously reported ENaCα-immunoreactivity at the luminal membrane of umbrella cells in the rat urinary bladder (Smith et al., 1998) and functional investigation of this cell type (McCloskey et al., 2017). Notably, this cell layer did not consistently express tdTomato with positive and negative umbrella cells occurring in a mosaic pattern (**Figure 3A**). Although heterogeneity of umbrella cells with respect to other characteristics such as uroplakin expression has also been reported in select localizations such as the human ureter (Riedel et al., 2005), this labeling pattern might reflect incomplete expression of tdTomato in potentially *Scnn1a*-expressing cells. To test for this possibility, we looked for tdTomato expression in the gall bladder whose mucosal surface is known for homogeneous ENaCα expression (Li et al., 2016). In two gall bladder whole-mount preparations, strong tdTomato expression was observed in epithelial cells covering only about 21% (case 1: 26.8%, case 2: 16.0%) of the mucosal surface whereas nearly 80% remained unlabeled (**Figures 3C,D**). Gall bladder whole-mounts were also incubated with TRPM5-antibody in order to label cholinergic chemosensory brush cells that are also present in this epithelium (Schütz et al., 2015).

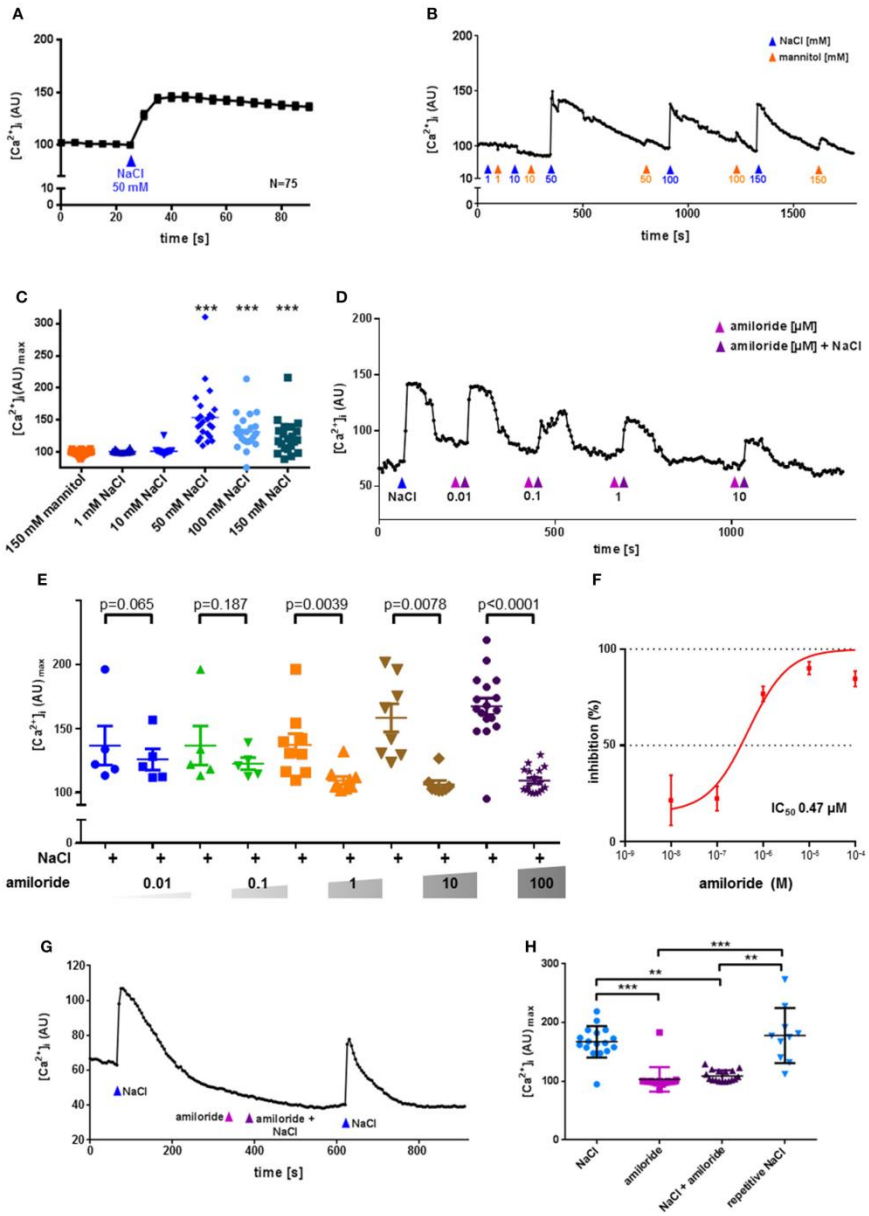

FIGURE 4 | UBC response to NaCl is ENaC dependent and not an osmolarity effect. Urethral epithelial cells of ChAT-eGFP reporter mice were isolated and UBC were identified due to eGFP fluorescence. Experiments were performed during continuous superfusion with Tyrode III buffer containing 145 mM Na^+. NaCl, mannitol and *(Continued)*

FIGURE 4 | amiloride were added under continuous flow of Tyrode III into the chamber, so that indicated concentrations were reached initially and then washed out. In case of NaCl, concentration changes on top of the baseline of concentrations in Tyrode III are indicated. Thus, the total sodium concentration after addition of 1–150 mM ranged from 146 to 295 mM. Y-Axis depicts arbitrary units (AU) of Calcium Orange® fluorescence recorded by confocal laser scanning microscopy, correlating to $[Ca^{2+}]_i$. **(A)** NaCl evokes an increase in $[Ca^{2+}]_i$; shown are mean and SEM. **(B)** Representative recording of changes in Calcium Orange® fluorescence in a single cholinergic (eGFP$^+$) UBC in response to increasing concentrations of NaCl (blue arrowhead) and mannitol (orange arrowhead). **(C)** Depicted are peak values after stimulation with mannitol (150 mM, $N = 22$) and NaCl (1 mM, $N = 22$; 10 mM, $N = 22$, 50 mM, $N = 24$, 100 mM, $N = 23$; 150 mM, $N = 21$); $^*P < 0.05$, $^{**}P < 0.01$, $^{***}P < 0.001$ compared to mannitol 150 mM, Kruskall-Wallis test followed by Dunn's Multiple Comparison Test. **(D)** Representative recording of changes in Calcium Orange® fluorescence in a single cholinergic (eGFP$^+$) UBC in response to NaCl (50 mM) in absence and presence of increasing concentrations of amiloride (0.01–10 μM). **(E)** Depicted are peak values after application of NaCl (50 mM) in absence and presence of increasing concentrations of amiloride (0.01 μM, $N = 5$; 0.1 μM, $N = 5$; 1 μM, $N = 9$; 10 μM, $N = 8$; 100 μM, $N = 17$), p-values were calculated by, Kruskal-Wallis test and are indicated in the figure. **(F)** Dose-inhibition curve of amiloride in UBC. $IC_{50} = 0.47$ μM. **(G)** Representative recording of changes in Calcium Orange® fluorescence in a single cholinergic (eGFP$^+$) UBC in response to NaCl (50 mM) in absence and presence of amiloride (0.1 mM). **(H)** Depicted are peak values after application of NaCl (50 mM, $N = 17$), amiloride (0.1 mM, $N = 17$), NaCl (50 mM) together with amiloride (0.1 mM, $N = 17$), and repetitive NaCl (50 mM, $N = 10$); $^*P < 0.05$, $^{**}P < 0.01$, $^{***}P < 0.001$, Kruskal-Wallis test followed by Dunn's Multiple Comparison Test.

Two out of 69 TRPM5-positive cells expressed *Scnn1a*-tdTomato (**Figures 3C,D**).

Among non-umbrella cells with nuclei located in deeper layers of the urethral epithelium, we detected co-localization of TRPM5-immunoreactivity and *Scnn1a*-tdTomato signal (30 of 46 TRPM5-positive cells, 65%, $N = 3$ animals) (**Figures 3A,B**) as well as TRPM5-positive cells without *Scnn1a*-tdTomato signal (**Figure 3B**). These observations support our findings in RT-PCR experiments and single cell sequencing that a subpopulation of UBC expresses α-ENaC.

Functionally, application of NaCl evoked significant increases in $[Ca^{2+}]_i$ in 70% of the isolated cholinergic UBC. At concentrations of 50, 100, and 150 mM NaCl, but not at 1 or 10 mM, significant increases in $[Ca^{2+}]_i$ were observed (**Figures 4A–C**). There was a tendency toward a decline in the evoked increase in $[Ca^{2+}]_i$ with increasing NaCl concentration. To test for a possible osmolarity effect, increasing concentrations of mannitol were administered alternating with corresponding concentrations of NaCl (**Figure 4B**). Since mannitol had no stimulatory effect upon $[Ca^{2+}]_i$ even at 150 mM (**Figure 4B**), the observed reaction of UBC to 50 mM NaCl, which was used for further characterization of polymodality, is not an osmolarity effect. Amiloride, an ENaC inhibitor that also suppresses salt perception in type I taste cells of the taste buds (Vandenbeuch et al., 2008), fully blocked the $[Ca^{2+}]_i$ response in UBC to NaCl (50 mM) with an IC_{50} of 0.47 μM (**Figures 4D–F**). Even at the highest concentration used (100 μM), the inhibitory effect of amiloride was reversible upon wash-out (**Figures 4G,H**). Thus, the NaCl-induced increase in $[Ca^{2+}]_i$ in UBC is amiloride-sensitive. This, however, does not seem to involve the canonical αβγ-ENaC which was shown to detect low concentrations of sodium in taste receptor cells of fungiform papillae in mice (Chandrashekar et al., 2010). First, only 1/6 UBC expressed all three ENaC subunits detected by NGS. Second, activity of mouse αβγ-ENaC appears to be maximal at 60 mM extracellular sodium (Sheng et al., 2004), a concentration which is below the stimuli used in the present study (≥50 mM NaCl added to Tyrode III). Third, this response to the NaCl stimulus was sensitive to amiloride, whereas baseline $[Ca^{2+}]_i$ in UBC (in the presence of 145 mM Na^+ in Tyrode III) was not (**Figure 4G**). Fourth, even though this study used calcium-imaging and this does not directly measure ENaC-activity, the IC_{50} for the observed inhibition of the calcium signal by amiloride is above that reported for inhibition of mouse αβγ-ENaC (0.1 μM) (Ahn et al., 1999). This might suggest an alternative amiloride-sensitive cation channel containing the ENaC α-subunit. Recently, it was shown that α-ENaC can assemble with alternative ion channels such as the acid sensing ion channel 1 (Jeggle et al., 2015), which may form a non-selective cation channel (Trac et al., 2017). The expression of acid sensing ion channels in UBC was, however, low and inconsistent (**Figure S1**). Alternatively, α-ENaC can form homomeric ion channels *in vitro* (Canessa et al., 1994b). Their physiological function, however, remains to be proven *in vivo*.

Irrespective of the molecular composition of the amiloride-sensitive sodium conductance in UBC, exposure to high concentrations of NaCl might trigger a membrane depolarization which may stimulate calcium-influx via voltage-gated calcium channels and subsequent release of acetylcholine. UBC showed consistent expression of α-subunits of the L-type voltage-gated calcium channels $Ca_v1.2$ (*Cacna1d*), $Ca_v1.3$ (*Cacna1d*), and Cav2.3 (*Cacnac1e*) (**Figure S2**). Furthermore, there was strong expression of the auxiliary subunit β4 (*Cacnb4*) in 5/6 cells. The auxiliary β-subunits are generally important for membrane expression and the β4-subunit seems to determine subcellular membrane-localization in polarized cells (Campiglio and Flucher, 2015). Voltage-gated calcium channels thus represent promising targets for the coupling of NaCl-induced membrane depolarization to acetylcholine release in UBC.

The physiological meaning of salt responsiveness of cholinergic UBC remains uncertain. In adult C57BL/6J mice, urinary sodium concentration is around 150 mM, similar to our 145 mM baseline in Tyrode buffer, and can significantly increase during water deprivation or high-salt intake (Li et al., 2012). During such conditions, cholinergic UBC may thus be exposed to sodium concentrations which trigger calcium responses as shown in this study. UBC are interpreted as sentinels of the lower urinary tract equipped for monitoring the mucosal surface for potential hazardous content, especially bacterial products (Deckmann et al., 2014; Deckmann and Kummer, 2016; Kummer and Deckmann, 2017). Threatening bacterial infections, however, are usually not connected to increased salt concentrations. Thus, α-ENaC may here serve other functions than monitoring luminal NaCl concentration. Canonical ENaC holds a key position in maintaining electrolyte

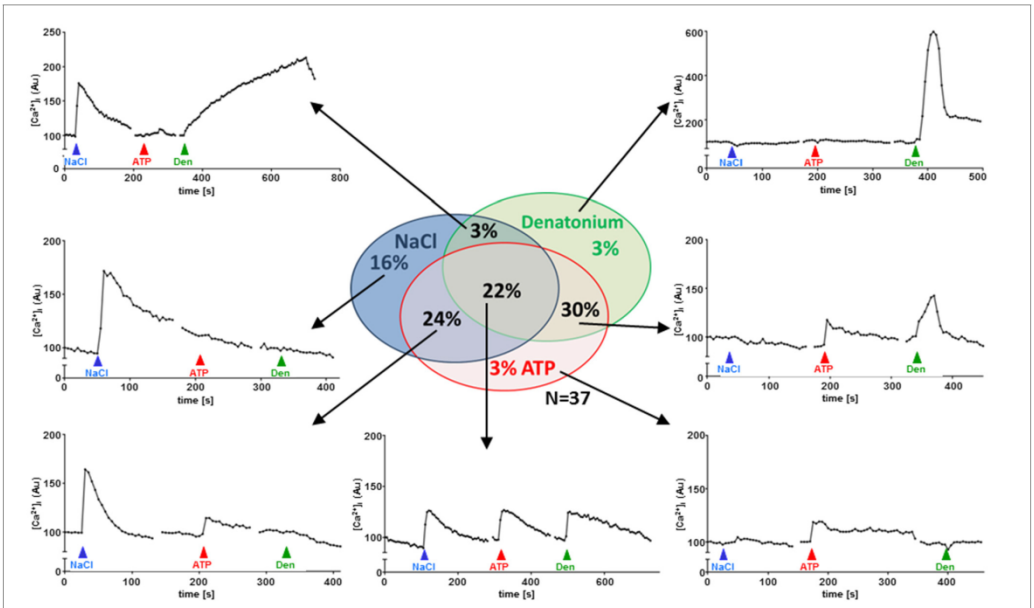

FIGURE 5 | UBC responses to NaCl, ATP and denatonium. Sequential stimulation with NaCl (50 mM on top of baseline concentrations in Tyrode), ATP (0.5 mM) and denatonium (25 mM); sequence of stimuli was changed between experiments ($N = 37$). Graphs show representative recordings of changes in Calcium Orange® fluorescence in single cholinergic (eGFP$^+$) UBC. Experiments were performed during continuous superfusion with Tyrode III buffer Stimuli were added under continuous flow of Tyrode III into the chamber, so that indicated concentrations were reached initially and then washed out. Y-Axis depicts arbitrary units (AU) of Calcium Orange® fluorescence.

and water homeostasis, e.g., concentration of primary urine in the kidney (Kellenberger and Schild, 2002). Given the low number of cholinergic UBC in the urethra and their minimal exposure to the luminal surface, this function appears rather unlikely for this particular cell type. However, ENaC is also a mechanosensitive ion channel, reacting to shear stress (Althaus et al., 2007; Guo et al., 2016). This opens the possibility that ENaC-subunit carrying UBC may be involved in sensing urine flow in the urethra. Notably, as mechanical strain affects the entire epithelium and is not restricted to the luminal membrane, it will reach UBC without a clear connection to the luminal surface ("closed type," see **Figure 3B** and Deckmann and Kummer, 2016). Cholinergic UBC are connected to sensory nerve fibers and, reflexively, initiate micturition in response to a bitter stimulus in the urethral lumen (Deckmann et al., 2014). This has been interpreted as a protective reflex in that potentially hazardous content will be flushed out (Deckmann et al., 2014; Kummer and Deckmann, 2017). Voiding efficiency is augmented by sensory feedback from the urethra, where flow sensors are physiologically well characterized but not yet defined anatomically (Todd, 1964; Peng et al., 2008; Danziger and Grill, 2015). Thus, mechanosensitivity of cholinergic UBC may serve to augment the reflex response they have initiated.

To test for polymodal properties, cholinergic UBC were successively exposed to NaCl and ATP ($N = 90$; 70% responded to NaCl), to NaCl and denatonium ($N = 36$; 67% responded to NaCl), and to all three stimuli ($N = 37$; 65% responded to NaCl, **Figure 5**). When responses to both NaCl and denatonium were tested on 36 UBC, all three possible response patterns occurred in a balanced distribution (**Figure 5**): 42% NaCl only, 33% denatonium only, 25% both stimuli. These percentages are roughly reflected by the (immuno)histochemical (65% of UBC expressing *Scnn1a*-tdTomato signal) and by the NGS data with 4/6 cells (67%) expressing *Scnn1a*, and 2 of them (33%) expressing additionally a known receptor for denatonium, i.e., Tas2r108 (**Figure 2**). Of course, the small total number of cholinergic UBC subjected to NGS ($N = 6$) precludes a systematic quantitative analysis.

We have previously shown that a substantial number of denatonium-responsive UBC also reacts to monosodium glutamate (Deckmann et al., 2014). In terms of oropharyngeal gustation, these substances reflect an aversive (denatonium: bitter) and an attractive (monosodium glutamate: umami) stimulus, and, accordingly, are perceived by distinct cell populations, which still are considered as subtypes of type II taste cells (Chaudhari and Roper, 2010). The present data show

an even broader diversity of UBC properties in that some of them share features also with type I cells of taste buds, expressing ENaC and being responsive to NaCl (Vandenbeuch et al., 2008). These findings further substantiate the polymodal character of cholinergic UBC. As far as further distinctive criteria are missing, we interpret the multiple combinations of responsiveness to various chemosensory stimuli and gene expression of related signaling components as phenotypic variation of a broadly tuned, polymodal chemosensory cell rather than defining multiple, clearly separated cell types.

CONCLUSION

In sum, we could show that a fraction of cholinergic UBC expresses α-ENaC and responds to the salty stimulus NaCl in an amiloride-sensitive manner. This feature does not define a new subpopulation of UBC, but rather emphasizes their polymodal character.

AUTHOR CONTRIBUTIONS

KD designed research and performed statistical analysis. KD, CK, PatS, PauS, MK, and SO performed research and analyzed data. KD and WK obtained funding. KD, WK, AP, and MA drafted the manuscript. Work was supervised by WK and KD.

FUNDING

This work was supported by a University Hospital of Giessen and Marburg (UKGM)-Justus-Liebig-University (JLU)-Cooperation Grant (# 7/2016 GI to KD), the German Research Foundation (KU 688/8-1 to WK), and the Else Kröner-Fresenius-Stiftung (2016_A90 to KD).

ACKNOWLEDGMENTS

We thank M. Bodenbenner, T. Eiffert, and K. Michael for skillful technical assistance as well as the FACS Core Facility of the University of Giessen for technical support. We also thank J. Staiger and J. Guy for providing material.

SUPPLEMENTARY MATERIAL

The Supplementary Material for this article can be found online at: https://www.frontiersin.org/articles/10.3389/fcell.2018.00089/full#supplementary-material

REFERENCES

Ahn, Y. J., Brooker, D. R., Kosari, F., Harte, B. J., Li, J., Mackler, S. A., et al. (1999). Cloning and functional expression of the mouse epithelial sodium channel. *Am. J. Physiol.* 277, F121–F129. doi: 10.1152/ajprenal.1999.277.1.F121

Althaus, M., Bogdan, R., Clauss, W. G., and Fronius, M. (2007). Mechano-sensitivity of epithelial sodium channels (ENaCs): laminar shear stress increases ion channel open probability. *FASEB J.* 21, 2389–2399. doi: 10.1096/fj.06-7694com

Avenet, P., and Lindemann, B. (1988). Amiloride-blockable sodium currents in isolated taste receptor cells. *J. Membr. Biol.* 105, 245–255. doi: 10.1007/BF01871001

Baines, D. (2013). Kinases as targets for ENaC regulation. *Curr. Mol. Pharmacol.* 6, 50–64. doi: 10.2174/18744672112059990028

Birder, L., and Andersson, K. E. (2013). Urothelial signaling. *Physiol. Rev.* 93, 653–680. doi: 10.1152/physrev.00030.2012

Birder, L., De Groat, W., Mills, I., Morrison, J., Thor, K., and Drake, M. (2010). Neural control of the lower urinary tract: peripheral and spinal mechanisms. *Neurourol. Urodyn.* 29, 128–139. doi: 10.1002/nau.20837

Campiglio, M., and Flucher, B. E. (2015). The role of auxiliary subunits for the functional diversity of voltage-gated calcium channels. *J. Cell. Physiol.* 230, 2019–2031. doi: 10.1002/jcp.24998

Canessa, C. M., Merillat, A. M., and Rossier, B. C. (1994a). Membrane topology of the epithelial sodium channel in intact cells. *Am. J. Physiol.* 267, C1682–C1690.

Canessa, C. M., Schild, L., Buell, G., Thorens, B., Gautschi, I., Horisberger, J. D., et al. (1994b). Amiloride-sensitive epithelial Na^+ channel is made of three homologous subunits. *Nature* 367, 463–467.

Carattino, M. D., Sheng, S., and Kleyman, T. R. (2005). Mutations in the pore region modify epithelial sodium channel gating by shear stress. *J. Biol. Chem.* 280, 4393–4401. doi: 10.1074/jbc.M413123200

Chandrashekar, J., Kuhn, C., Oka, Y., Yarmolinsky, D. A., Hummler, E., Ryba, N. J., et al. (2010). The cells and peripheral representation of sodium taste in mice. *Nature* 464, 297–301. doi: 10.1038/nature08783

Chaudhari, N., and Roper, S. D. (2010). The cell biology of taste. *J. Cell Biol.* 190, 285–296. doi: 10.1083/jcb.201003144

Chraïbi, A., and Horisberger, J. D. (2002). Na self inhibition of human epithelial Na channel: temperature dependence and effect of extracellular proteases. *J. Gen. Physiol.* 120, 133–145. doi: 10.1085/jgp.20028612

Danziger, Z. C., and Grill, W. M. (2015). Dynamics of the sensory response to urethral flow over multiple time scales in rat. *J. Physiol.* 593, 3351–3371. doi: 10.1113/JP270911

Deckmann, K., Filipski, K., Krasteva-Christ, G., Fronius, M., Althaus, M., Rafiq, A., et al. (2014). Bitter triggers acetylcholine release from polymodal urethral chemosensory cells and bladder reflexes. *Proc. Natl. Acad. Sci. U.S.A.* 111, 8287–8292. doi: 10.1073/pnas.1402436111

Deckmann, K., Krasteva-Christ, G., Rafiq, A., Herden, C., Wichmann, J., Knauf, S., et al. (2015). Cholinergic urethral brush cells are widespread throughout placental mammals. *Int. Immunopharmacol.* 29, 51–56. doi: 10.1016/j.intimp.2015.05.038

Deckmann, K., and Kummer, W. (2016). Chemosensory epithelial cells in the urethra: sentinels of the urinary tract. *Histochem. Cell Biol.* 146, 673–683. doi: 10.1007/s00418-016-1504-x

Du, S., Araki, I., Mikami, Y., Zakoji, H., Beppu, M., Yoshiyama, M., et al. (2007). Amiloride-sensitive ion channels in urinary bladder epithelium involved in mechanosensory transduction by modulating stretch-evoked adenosine triphosphate release. *Urology* 69, 590–595. doi: 10.1016/j.urology.2007.01.039

Duc, C., Farman, N., Canessa, C. M., Bonvalet, J. P., and Rossier, B. C. (1994). Cell-specific expression of epithelial sodium channel alpha, beta, and gamma subunits in aldosterone-responsive epithelia from the rat: localization by in situ hybridization and immunocytochemistry. *J. Cell Biol.* 127, 1907–1921. doi: 10.1083/jcb.127.6.1907

Finger, T. E., Bottger, B., Hansen, A., Anderson, K. T., Alimohammadi, H., and Silver, W. L. (2003). Solitary chemoreceptor cells in the nasal cavity serve as sentinels of respiration. *Proc. Natl. Acad. Sci. U.S.A.* 100, 8981–8986. doi: 10.1073/pnas.1531172100

Finger, T. E., and Kinnamon, S. C. (2011). Taste isn't just for taste buds anymore. *F1000 Biol. Rep.* 3:20. doi: 10.3410/B3-20

Garty, H., and Palmer, L. G. (1997). Epithelial sodium channels: function, structure, and regulation. *Physiol. Rev.* 77, 359–396. doi: 10.1152/physrev.1997.77.2.359

Giraldez, T., Rojas, P., Jou, J., Flores, C., and Alvarez De La Rosa, D. (2012). The epithelial sodium channel delta-subunit: new notes for an old song. *Am. J. Physiol. Renal. Physiol.* 303, F328–F338. doi: 10.1152/ajprenal.00116.2012

Guo, D., Liang, S., Wang, S., Tang, C., Yao, B., Wan, W., et al. (2016). Role of epithelial Na+ channels in endothelial function. *J. Cell Sci.* 129, 290–297. doi: 10.1242/jcs.168831

Guy, J., Wagener, R. J., Mock, M., and Staiger, J. F. (2015). Persistence of functional sensory maps in the absence of cortical layers in the somsatosensory cortex of reeler mice. *Cereb. Cortex* 25, 2517–2528. doi: 10.1093/cercor/bhu052

Heck, G. L., Mierson, S., and Desimone, J. A. (1984). Salt taste transduction occurs through an amiloride-sensitive sodium transport pathway. *Science* 223, 403–405. doi: 10.1126/science.6691151

Höfer, D., and Drenckhahn, D. (1998). Identification of the taste cell G-protein, alpha-gustducin, in brush cells of the rat pancreatic duct system. *Histochem. Cell Biol.* 110, 303–309. doi: 10.1007/s004180050292

Höfer, D., Puschel, B., and Drenckhahn, D. (1996). Taste receptor-like cells in the rat gut identified by expression of alpha-gustducin. *Proc. Natl. Acad. Sci. U.S.A.* 93, 6631–6634. doi: 10.1073/pnas.93.13.6631

Huang, A. L., Chen, X., Hoon, M. A., Chandrashekar, J., Guo, W., Trankner, D., et al. (2006). The cells and logic for mammalian sour taste detection. *Nature* 442, 934–938. doi: 10.1038/nature05084

Ishimaru, Y., Inada, H., Kubota, M., Zhuang, H., Tominaga, M., and Matsunami, H. (2006). Transient receptor potential family members PKD1L3 and PKD2L1 form a candidate sour taste receptor. *Proc. Natl. Acad. Sci. U.S.A.* 103, 12569–12574. doi: 10.1073/pnas.0602702103

Jeggle, P., Smith, E. S., Stewart, A. P., Haerteis, S., Korbmacher, C., and Edwardson, J. M. (2015). Atomic force microscopy imaging reveals the formation of ASIC/ENaC cross-clade ion channels. *Biochem. Biophys. Res. Commun.* 464, 38–44. doi: 10.1016/j.bbrc.2015.05.091

Kaske, S., Krasteva, G., Konig, P., Kummer, W., Hofmann, T., Gudermann, T., et al. (2007). TRPM5, a taste-signaling transient receptor potential ion-channel, is a ubiquitous signaling component in chemosensory cells. *BMC Neurosci.* 8:49. doi: 10.1186/1471-2202-8-49

Kellenberger, S., and Schild, L. (2002). Epithelial sodium channel/degenerin family of ion channels: a variety of functions for a shared structure. *Physiol. Rev.* 82, 735–767. doi: 10.1152/physrev.00007.2002

Kleyman, T. R., Kashlan, O. B., and Hughey, R. P. (2018). Epithelial $Na^{(+)}$ channel regulation by extracellular and intracellular factors. *Annu. Rev. Physiol.* 80, 263–281. doi: 10.1146/annurev-physiol-021317-121143

Krasteva, G., Canning, B. J., Hartmann, P., Veres, T. Z., Papadakis, T., Muhlfeld, C., et al. (2011). Cholinergic chemosensory cells in the trachea regulate breathing. *Proc. Natl. Acad. Sci. U.S.A.* 108, 9478–9483. doi: 10.1073/pnas.1019418108

Krasteva, G., Canning, B. J., Papadakis, T., and Kummer, W. (2012). Cholinergic brush cells in the trachea mediate respiratory responses to quorum sensing molecules. *Life Sci.* 91, 992–996. doi: 10.1016/j.lfs.2012.06.014

Kummer, W., and Deckmann, K. (2017). Brush cells, the newly identified gatekeepers of the urinary tract. *Curr. Opin. Urol.* 27, 85–92. doi: 10.1097/MOU.0000000000000361

Lee, R. J., and Cohen, N. A. (2015). Taste receptors in innate immunity. *Cell. Mol. Life Sci.* 72, 217–236. doi: 10.1007/s00018-014-1736-7

Li, Q., Kresge, C., Bugde, A., Lamphere, M., Park, J. Y., and Feranchak, A. P. (2016). Regulation of mechanosensitive biliary epithelial transport by the epithelial $Na^{(+)}$ channel. *Hepatology* 63, 538–549. doi: 10.1002/hep.28301

Li, X. C., Shao, Y., and Zhuo, J. L. (2012). AT1a receptor signaling is required for basal and water deprivation-induced urine concentration in AT1a receptor-deficient mice. *Am. J. Physiol. Renal. Physiol.* 303, F746–F756. doi: 10.1152/ajprenal.00644.2011

Lin, W., Finger, T. E., Rossier, B. C., and Kinnamon, S. C. (1999). Epithelial Na^+ channel subunits in rat taste cells: localization and regulation by aldosterone. *J. Comp. Neurol.* 405, 406–420. doi: 10.1002/(SICI)1096-9861(19990315)405:3<406::AID-CNE10>3.0.CO;2-F

Lindemann, B. (2001). Receptors and transduction in taste. *Nature* 413, 219–225. doi: 10.1038/35093032

Lindemann, B., Barbry, P., Kretz, O., and Bock, R. (1998). Occurrence of ENaC subunit mRNA and immunocytochemistry of the channel subunits in taste buds of the rat vallate papilla. *Ann. N.Y. Acad. Sci.* 855, 116–127. doi: 10.1111/j.1749-6632.1998.tb10553.x

Lopezjimenez, N. D., Cavenagh, M. M., Sainz, E., Cruz-Ithier, M. A., Battey, J. F., and Sullivan, S. L. (2006). Two members of the TRPP family of ion channels, Pkd1l3 and Pkd2l1, are co-expressed in a subset of taste receptor cells. *J. Neurochem.* 98, 68–77. doi: 10.1111/j.1471-4159.2006.03842.x

McCloskey, K. D., Vahabi, B., and Fry, C. H. (2017). Is electrolyte transfer across the urothelium important? ICI-RS 2015. *Neurourol. Urodyn.* 36, 863–868. doi: 10.1002/nau.23085

McDonald, F. J., Price, M. P., Snyder, P. M., and Welsh, M. J. (1995). Cloning and expression of the beta- and gamma-subunits of the human epithelial sodium channel. *Am. J. Physiol.* 268, C1157–C1163. doi: 10.1152/ajpcell.1995.268.5.C1157

Nelson, G., Hoon, M. A., Chandrashekar, J., Zhang, Y., Ryba, N. J., and Zuker, C. S. (2001). Mammalian sweet taste receptors. *Cell* 106, 381–390. doi: 10.1016/S0092-8674(01)00451-2

Peng, C. W., Chen, J. J., Cheng, C. L., and Grill, W. M. (2008). Role of pudendal afferents in voiding efficiency in the rat. *Am. J. Physiol. Regul. Integr. Comp. Physiol.* 294, R660–R672. doi: 10.1152/ajpregu.00270.2007

Riedel, I., Liang, F. X., Deng, F. M., Tu, L., Kreibich, G., Wu, X. R., et al. (2005). Urothelial umbrella cells of human ureter are heterogeneous with respect to their uroplakin composition: different degrees of urothelial maturity in ureter and bladder? *Eur. J. Cell Biol.* 84, 393–405.doi: 10.1016/j.ejcb.2004.12.011

Scholz, P., Kalbe, B., Jansen, F., Altmueller, J., Becker, C., Mohrhardt, J., et al. (2016). Transcriptome analysis of murine olfactory sensory neurons during development using single cell RNA-Seq. *Chem. Senses* 41, 313–323. doi: 10.1093/chemse/bjw003

Schütz, B., Jurastow, I., Bader, S., Ringer, C., Von Engelhardt, J., Chubanov, V., et al. (2015). Chemical coding and chemosensory properties of cholinergic brush cells in the mouse gastrointestinal and biliary tract. *Front. Physiol.* 6:87. doi: 10.3389/fphys.2015.00087

Sheng, S., Bruns, J. B., and Kleyman, T. R. (2004). Extracellular histidine residues crucial for Na^+ self-inhibition of epithelial Na^+ channels. *J. Biol. Chem.* 279, 9743–9749. doi: 10.1074/jbc.M311952200

Smith, P. R., Mackler, S. A., Weiser, P. C., Brooker, D. R., Ahn, Y. J., Harte, B. J., et al. (1998). Expression and localization of epithelial sodium channel in mammalian urinary bladder. *Am. J. Physiol.* 274, F91–F96. doi: 10.1152/ajprenal.1998.274.1.F91

Tallini, Y. N., Shui, B., Greene, K. S., Deng, K. Y., Doran, R., Fisher, P. J., et al. (2006). BAC transgenic mice express enhanced green fluorescent protein in central and peripheral cholinergic neurons. *Physiol. Genomics* 27, 391–397. doi: 10.1152/physiolgenomics.00092.2006

Todd, J. K. (1964). Afferent impulses in the pudendal nerves of the cat. *Q. J. Exp. Physiol. Cogn. Med. Sci.* 49, 258–267. doi: 10.1113/expphysiol.1964.sp001730

Trac, P. T., Thai, T. L., Linck, V., Zou, L., Greenlee, M., Yue, Q., et al. (2017). Alveolar nonselective channels are ASIC1a/alpha-ENaC channels and contribute to AFC. *Am. J. Physiol. Lung Cell. Mol. Physiol.* 312, L797–L811. doi: 10.1152/ajplung.00379.2016

Vandenbeuch, A., Clapp, T. R., and Kinnamon, S. C. (2008). Amiloride-sensitive channels in type I fungiform taste cells in mouse. *BMC Neurosci.* 9:1. doi: 10.1186/1471-2202-9-1

Wichmann, L., Vowinkel, K. S., Perniss, A., Manzini, I., and Althaus, M. (2018). Incorporation of the delta-subunit into the epithelial sodium channel (ENaC) generates protease-resistant ENaCs in Xenopus laevis. *J. Biol. Chem.* 293, 6647–6658. doi: 10.1074/jbc.RA118.002543

Yamashita, J., Ohmoto, M., Yamaguchi, T., Matsumoto, I., and Hirota, J. (2017). Skn-1a/Pou2f3 functions as a master regulator to generate Trpm5-expressing chemosensory cells in mice. *PLoS ONE* 12:e0189340. doi: 10.1371/journal.pone.0189340

Conflict of Interest Statement: The authors declare that the research was conducted in the absence of any commercial or financial relationships that could be construed as a potential conflict of interest.

Cell and Tissue Research
https://doi.org/10.1007/s00441-021-03424-9

REGULAR ARTICLE

Development of epithelial cholinergic chemosensory cells of the urethra and trachea of mice

Alexander Perniss[1] · Patricia Schmidt[1] · Aichurek Soultanova[1] · Tamara Papadakis[1] · Katja Dahlke[2] · Anja Voigt[3] · Burkhard Schütz[4] · Wolfgang Kummer[1] · Klaus Deckmann[1]

Received: 17 June 2020 / Accepted: 24 January 2021

Abstract
Cholinergic chemosensory cells (CCC) are infrequent epithelial cells with immunosensor function, positioned in mucosal epithelia preferentially near body entry sites in mammals including man. Given their adaptive capacity in response to infection and their role in combatting pathogens, we here addressed the time points of their initial emergence as well as their postnatal development from first exposure to environmental microbiota (i.e., birth) to adulthood in urethra and trachea, utilizing choline acetyltransferase (ChAT)-eGFP reporter mice, mice with genetic deletion of MyD88, toll-like receptor-2 (TLR2), TLR4, TLR2/TLR4, and germ-free mice. Appearance of CCC differs between the investigated organs. CCC of the trachea emerge during embryonic development at E18 and expand further after birth. Urethral CCC show gender diversity and appear first at P6-P10 in male and at P11-P20 in female mice. Urethrae and tracheae of MyD88- and TLR-deficient mice showed significantly fewer CCC in all four investigated deficient strains, with the effect being most prominent in the urethra. In germ-free mice, however, CCC numbers were not reduced, indicating that TLR2/4-MyD88 signaling, but not vita-PAMPs, governs CCC development. Collectively, our data show a marked postnatal expansion of CCC populations with distinct organ-specific features, including the relative impact of TLR2/4-MyD88 signaling. Strong dependency on this pathway (urethra) correlates with absence of CCC at birth and gender-specific initial development and expansion dynamics, whereas moderate dependency (trachea) coincides with presence of first CCC at E18 and sex-independent further development.

Keywords Brush cells · Tuft cells · Innate immunity · Toll-like receptors · MyD88 · Solitary chemosensory cells · Chemosensation

Introduction

Referring to their apical brush or tuft of stiff microvilli, identified in ultrastructural studies, a group of rare solitary epithelial cells has been initially termed brush or tuft cells (Rhodin and Dalhamn 1956; Sbarbati and Osculati 2005). Meanwhile, structural, histochemical, and single cell sequencing data revealed several unique characteristics defining distinct cell populations within and among organs (Deckmann et al. 2014; Krasteva et al. 2011; Montoro et al. 2018; Nadjsombati et al. 2018; Yamamoto et al. 2018). One of them is characterized by the expression of the acetylcholine synthesizing enzyme, choline acetyltransferase (ChAT), and the expression of the taste transduction signaling cascade, including the taste-specific G protein α-gustducin (GNAT3), phospholipase Cβ2 (PLCβ2), and the transient potential receptor cation channel subfamily M (melanostatin) member 5 (TRPM5). Such cholinergic

Alexander Perniss and Patricia Schmidt contributed equally to this work.

✉ Klaus Deckmann

[1] Institute for Anatomy and Cell Biology, German Center for Lung Research (DZL), Excellence Cluster Cardiopulmonary Institute (CPI), Justus-Liebig-University Giessen, Giessen, Germany

[2] Department of Gastroenterology, Infectious Diseases and Rheumatology, Charité Universitätsmedizin Berlin, Campus Benjamin Franklin, Berlin, Germany

[3] Max Rubner Laboratory, German Institute of Human Nutrition (DIfE), Nuthetal, Germany

[4] Institute of Anatomy and Cell Biology, Philipps-University, Marburg, Germany

Published online: 22 February 2021

chemosensory cells (CCC) have been identified in the upper airways (Saunders et al. 2014; Tizzano et al. 2011), the vomeronasal organ (Ogura et al. 2010), the auditory tube (Krasteva et al. 2012b), the trachea (Krasteva et al. 2011), the conjunctiva (Wiederhold et al. 2015), the gastro-intestinal tract including the gall bladder (Schutz et al. 2015), the urethra (Deckmann et al. 2014), and the thymus (Panneck et al. 2014). All cells of this category are closely related, even though there are organ-specific characteristics (Deckmann and Kummer 2016; Finger and Kinnamon 2011; Nadjsombati et al. 2018; O'Leary et al. 2019).

Their function is only partially identified. They utilize elements of the canonical taste transduction cascade to respond to potentially harmful substances including bacterial products (Deckmann et al. 2014; Finger et al. 2003; Krasteva et al. 2012a; Ogura et al. 2011; Saunders et al. 2014; Sbarbati et al. 2009; Tizzano et al. 2010) and helminths (Gerbe et al. 2016; Howitt et al. 2016; Nadjsombati et al. 2018; von Moltke et al. 2016). Upon activation, CCC initiate protective mechanisms like reflex inhibition of inspiratory activity (Krasteva et al. 2011; Tizzano et al. 2010) or stimulation of micturition (Deckmann et al. 2014), initiation of neurogenic inflammation (Saunders et al. 2014), and triggering type 2 immune responses (Bankova et al. 2018; Gerbe et al. 2016; Howitt et al. 2016; Nadjsombati et al. 2018; von Moltke et al. 2016). Accordingly, they have been attributed with a sentinel function and are regarded as crucial elements of the mucosal innate immune system (Krasteva and Kummer 2012; Kummer and Deckmann 2017; Middelhoff et al. 2017; Schneider et al. 2019; Tizzano and Finger 2013).

The transcription factor Skn-1a/Pou2f3 is required for CCC development, and its genetic deletion results in their absence in several organs (Ohmoto et al. 2013; Yamashita et al. 2017). Unlike taste cells in the taste buds, neither development nor maintenance of nasal CCC is dependent on intact innervation (Gulbransen et al. 2008). In postnatal life, CCC do undergo turnover like the surrounding epithelium, as initially demonstrated for the nose (Gulbransen and Finger 2005), and respond dynamically to challenges. While tracheal CCC have been described as "a stable population in a dynamic epithelium" under unchallenged conditions (Saunders et al. 2013), they increase markedly in numbers after exposure to house dust mites or mold in a leukotriene-dependent manner (Bankova et al. 2018). Severe infection with H1N1 influenza virus even provokes de novo appearance of solitary chemosensory cells (cholinergic traits not investigated in this study) in the murine distal lung, whereas such cells are not present in uninfected lungs (Rane et al. 2019). In the intestine, their number increases vastly in response to helminth and protozoan infection (Gerbe et al. 2016; Howitt et al. 2016; Nadjsombati et al. 2018; Schneider et al. 2018; von Moltke et al. 2016). At least in the intestine, CCC not only increase in numbers during infection but are also necessary for helminth clearance. Mice lacking TRPM5 remain infected with *Nippostrongylus brasiliensis*, whereas wildtype mice expel this helminth within 2 weeks (Nadjsombati et al. 2018). Given their adaptive capacity in response to infection and their role in combatting pathogens, we addressed the time points of their initial emergence as well as their postnatal development from first exposure to environmental microbiota (i.e., birth) to adulthood, utilizing ChAT-eGFP reporter mice and focusing upon tracheal, urethral, and, to a lesser extent, thymic CCC. The necessity of direct contact to living microbiota for the development of CCC was assessed by using germ-free mice. Since these mice are still exposed, e.g., via the food, to bacterial products and bacterial remains capable of triggering innate immune responses by activating toll-like receptors (TLRs), we also included MyD88 (myeloid differentiation primary response 88) knockout (KO) mice in this study. MyD88 is involved in downstream signaling of all TLRs, except TLR3, as well as the interleukin-1-receptor (Wang et al. 2014). As genetic loss of MyD88 indeed resulted in lower CCC numbers, we further included TLR2 and TLR4 single- and double-deficient mice to narrow down the spectrum of signaling pathways potentially being involved. TLR2 and TLR4 were chosen because of their well-known importance in the recognition of bacterial lipopeptides and lipoteichoic acids of Gram-positive bacteria in the case of TLR2 (Irvine et al. 2013) and lipopolysaccharides of Gram-negative bacteria in the case of TLR4 (Park et al. 2009).

Material and methods

Animals

ChAT-eGFP (B6.Cg-Tg(RP23-268L19-EGFP)2Mik/J; Stock No. 007902) mice were obtained from Jackson Laboratory (Bar Habor, ME, USA). A second ChAT-eGFP mouse strain (von Engelhardt et al. 2007) was exclusively used to assess CCC appearance during embryonic development. Mice were housed in the animal facilities of the Justus-Liebig-University Giessen or the Philipps-University Marburg under specific-pathogen-free (SPF) conditions (10 h dark, 14 h light), with free access to food and water.

Germ-free mice (C57BL/6N; germ-free; > 12 weeks) were obtained from the gnotobiotic animal facility of the German Institute of Human Nutrition, Potsdam-Rehbruecke, Germany. Gnotobiotic mice were maintained in positive-pressure isolators. Mice were housed individually in polycarbonate cages on irradiated wood chips (25 kGy) at 22 ± 2 °C and a relative humidity of 55 ± 5% on a 12 h light-dark cycle. All mice had unrestricted access to irradiated (50 kGy) experimental diets and autoclaved water throughout the experiment. Control mice (C57BL/6N, same

sex and age as germ-free mice; SPF) were obtained from Jackson Laboratory and housed at the animal facility of the Justus-Liebig-University Giessen in individually ventilated cages under SPF conditions. TLR2-KO (C57BL/10ScSn-TLR2^{tm1}), TLR4-def (C57BL/10ScN-TLR4 (spontaneous deletion of the *Trl4* gene)), and TLR2-KO/TLR4-def (C57BL10ScN-TLR4/TLR2^{tm1}) and corresponding wildtypes (TLR-WT; C57BL/10ScSn) were also obtained from the animal facility of the German Institute of Human Nutrition, Potsdam-Rehbruecke, Germany; all investigated mice of this strains were > 12 weeks old. These mice were bred as described previously (Heimesaat et al. 2007).

Tissues from MyD88-KO mice (B6.129-Myd88^{tm1}Aki; > 12 weeks) and corresponding wildtypes (MyD88-WT; litter mates of MyD88-KO mice) were obtained from two independent sources. The strain originally generated by Adachi et al. (1998) was bred and provided by Rainer Glauben, Charite Berlin, and by Axel Pagenstecher, Philipps-University Marburg.

This study was carried out in accordance with the recommendations of European Communities Council Directive of 24th November 1986 (86/609/EEC). The protocol was approved by the local authorities, i.e., Regierungspräsidium Giessen, Germany (reference no. 572_M, 571_M, 557_AZ, Ex-15–2018), the Office for Agriculture, Ecology, and Regional Planning of the State of Brandenburg (Germany) according to §8.1 Animal Welfare Act (approval number: 23-2347-6-2009 and 23-2347-24-2010), and the Landesamt für Gesundheit und Soziales (LAGESO), Berlin (approval number T0294/10).

3R statement

In this study, more than 450 tissue specimens were collected, investigated, and analyzed. In order to adhere to the 3R principle (reduction, replacement, and refinement in animal experiments principle (Russell and Burch 1959)) the number of animals used for this study was kept to a minimum by taking multiple organs (urethra, trachea, thymus) from the same animal and by taking specimens from animals that have been sacrificed for other purposes.

Immunohistochemistry and whole-mount immunostaining

Organs used for immunohistochemistry and whole-mount immunostaining were either freshly dissected and fixed by immersion or taken from animals fixed by transcardiac perfusion with 4% paraformaldehyde (in 0.1 M phosphate buffer, pH 7.4; both purchased from Carl Roth, Karlsruhe, Germany) or Zamboni solution (2% paraformaldehyde/15% saturated picric acid; Merck, Darmstadt, Germany, in 0.1 M phosphate buffer, pH 7.4), preceded by a flush with vascular rinsing solution (Forssmann et al. 1977). Organs were washed in 0.1 M phosphate buffer and embedded in paraffin (Paraplast Plus®, Leica, Nussloch, Germany) or incubated overnight in 18% sucrose (Carl Roth, Karlsruhe, Germany) in 0.1 M phosphate buffer, embedded in Tissue-Tek® O.C.T.™ Compound (Sakura Finetek Germany GmbH, Staufen, Germany) and frozen in liquid nitrogen. For immunostainings, tissue sections or whole-mounts of investigated strains were processed simultaneously with corresponding controls, e.g., wildtypes. Primary antibody was applied to 4–18 tissue sections (frozen 10 µm or paraffin 5 µm) from every organ. At least three animals per experimental setup were analyzed. For whole-mount immunostainings of tracheae, the trachea was dissected from the larynx to the bifurcation and the trachealis muscle was cut longitudinally. For whole-mount immunostainings of urethrae, the whole urethra was taken and cut longitudinally. The tracheae and urethrae were opened and fixed flat on a silicon elastomer (Dow Corning, Midland, MI, USA) with insect needles (Fiebig-Lehrmittel, Berlin, Germany). Specimens were permeabilized with 0.3% Triton X 100 (Carl Roth, Karlsruhe, Germany) for 2 h; unspecific protein binding sites were saturated by incubation with 4% horse serum (PAA Laboratories Inc., Pasching, Austria) and 1% bovine serum albumin (Sigma Aldrich/Merck, Darmstadt, Germany) in 0.005 M phosphate buffer for 2 h. Samples were incubated in primary and secondary antibodies overnight each, rinsed, post-fixed for 10 min in 4% paraformaldehyde, and mounted in Mowiol (Sigma Aldrich/Merck, Darmstadt, Germany) containing 4′,6-diamidino-2-phenylindol (DAPI, 1 µg/ml, Sigma Aldrich/Merck, Darmstadt, Germany).

To investigate prenatal development of CCC, embryos of ChAT-eGFP mice (von Engelhardt et al. 2007) were harvested at specified embryonic stages (E12, $N = 4$; E14, $N = 5$; E16, $N = 8$; E18, $N = 6$) and shortly after birth (P0, $N = 3$), which were determined by fertilization. After extraction, embryos were sacrificed, fixed by immersion with Zamboni solution, cut into halves, and embedded in paraffin. Embryos were sectioned (5 µm), and every 10th section was stained with H.E. or Giemsa for orientation. Every second section harboring tracheal epithelium was immunostained and analyzed.

Primary antibodies were chicken-anti-GFP (green fluorescent protein, NB100-1614, 1:4000 dilution; Novus Biologicals, Centennial, USA), goat-anti-ChAT (AB144P, 1:250 dilution; Merck Millipore/Merck, Darmstadt, Germany), rabbit-anti-DCAMKL1 (Serine/threonine-protein kinase DCLK1 (Doublecortin-like kinase 1)), ab31704 (1:2000 dilution; Abcam, Cambridge, UK), and rabbit-anti-TPRM5 (1:4000–8000 (Kaske et al. 2007)).

Secondary antibodies were donkey-anti-chicken IgG conjugated to fluorescein isothiocyanate (FITC; 703-095-155; 1:800; Dianova, Hamburg, Germany), donkey-anti-rabbit

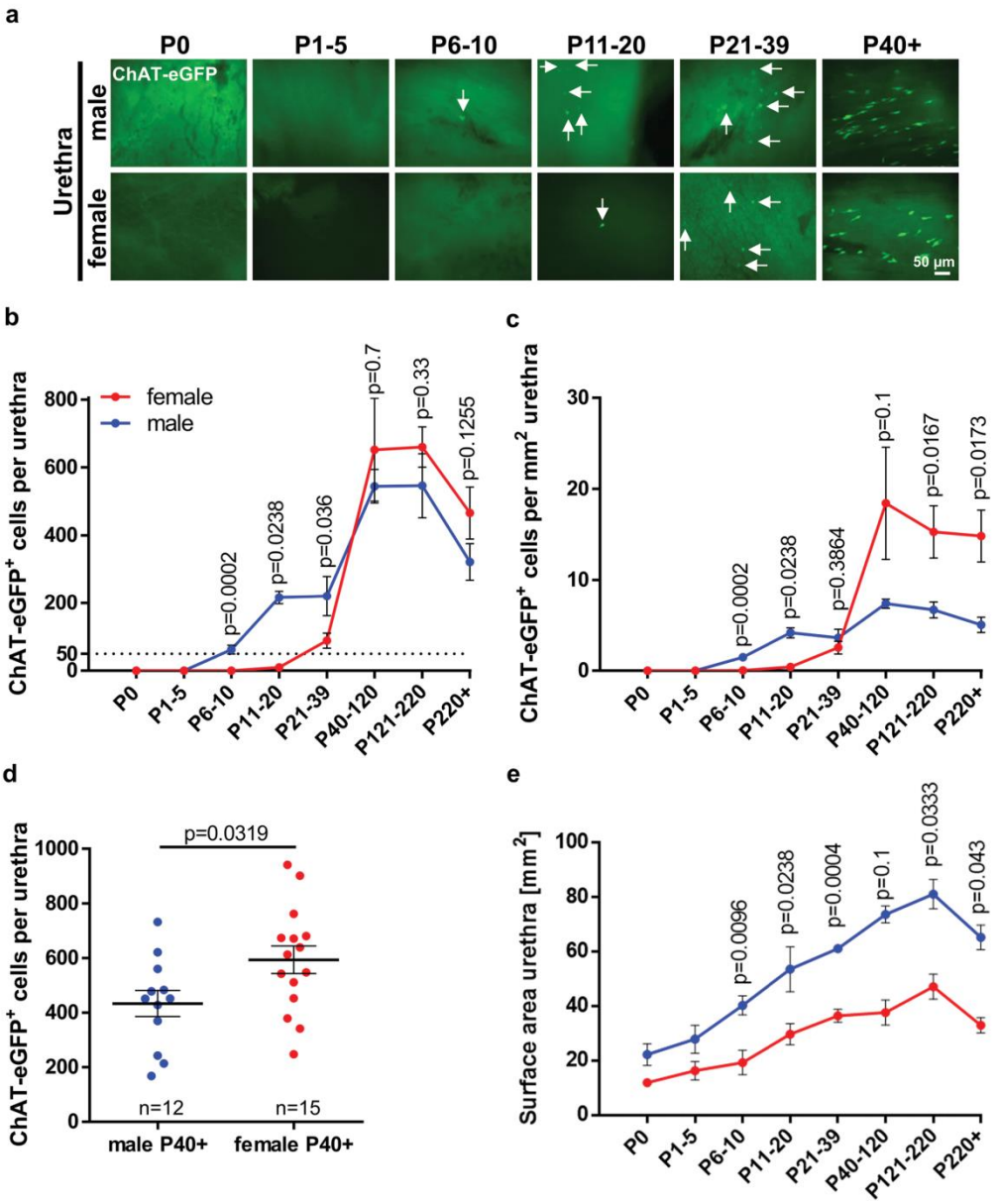

IgG conjugated to Cyanine 3 (Cy3; 2567112; 1:2000; Merck Millipore/Merck, Darmstadt, Germany), donkey-anti-rabbit IgG Alexa 488 (A21206; 1:500; Thermo Fisher Scientific Inc., Waltham, MA, USA), donkey-anti-goat IgG Alexa 488 (A11055; 1:1000; Thermo Fisher Scientific Inc., Waltham, MA, USA), and donkey-anti-goat IgG Cy3 (AP180C;

◂**Fig. 1** Postnatal development of CCC in the urethra. **a** Immunofluorescence using tissue from ChAT-eGFP mice, eGFP signal was antibody enhanced, representative images of female and male urethrae at different time points during postnatal development; arrows mark ChAT-eGFP-positive urethral CCC. **a** and **b** Quantitative analysis of ChAT-eGFP-positive cells per urethra **b** and per mm^2 **c** using whole-mount preparations in female and male mice at different time points during development; male: P0 $N = 5$; P1-5 $N = 8$; P6-10 $N = 17$; P11-20 $N = 3$; P21-39 $N = 6$; P40-120 $N = 3$; P121-220 $N = 3$; P250+ $N = 6$; female: P0 $N = 3$; P1-5 $N = 4$; P6-10 $N = 6$; P11-20 $N = 6$; P21-39 $N = 9$; P40-120 $N = 3$; P121-220 $N = 7$; P220+ $N = 5$. Dashed line marks cell count of 50 cells per urethra. **d** Numbers of ChAT-eGFP-positive cells per urethra in animals P40+, cumulative data of the three oldest age groups depicted in **b**; **e** Surface area of male and female urethrae used for generating **c**. **b**–**e** Graphs depict means and SEM. Blue: males, red: females. P-values were calculated with Mann-Whitney test

1:16,000; Merck Millipore/Merck, Darmstadt, Germany). Specificity of secondary reagents was validated by omission of primary antibodies.

CCC number in ChAT-eGFP mice was assessed by enhancement of endogenous eGFP signal with antibodies against eGFP. In C57BL/6N-mice, MyD88-KO mice, TLR-KO mice, TLR-def mice, and corresponding wildtypes, all not carrying the ChAT-eGFP reporter, CCC numbers were assessed by TRPM5-, ChAT-, or DCAMKL1-immunolabeling. To evaluate the degree of co-localization of ChAT-eGFP expression and TRPM5-immunoreactivity in CCC, the TRPM5-antibody was applied to whole-mounts (trachea and urethra) from ChAT-eGFP mice.

Sections and whole-mounts were evaluated by epifluorescence microscopy (Axioplan 2, Zeiss, Oberkochen, Germany) or with a confocal laser scanning microscope (LSM 710, Zeiss, Oberkochen, Germany). Overlay images were created using ImageJ (https://imagej.nih.gov/ij). For evaluation of cell numbers in tracheae and urethrae, we used whole-mount preparations and counted all positive cells in the organ manually or interactively using an ImageJ cell counter plug-in. Counting of a data set was performed by the same person to exclude experimenter dependent bias.

Surface area of trachea and urethra was calculated using ImageJ, except for adult tracheae of germ-free, control mice, MyD88-KO and MyD88-WT. In these cases, 8 pictures at × 10 magnification were taken along tracheal whole-mounts as illustrated in Supplementary Fig. 1a and used to evaluate CCC number per square millimeter. The number of CCC in TLR-deficient mice and corresponding wildtypes was evaluated using frozen or paraffin sections; here, the number of positive cells per millimeterbasal lamina was calculated utilizing the software Axiovision (Zeiss, Oberkochen, Germany) in case of the trachea (at least 10 longitudinal sections per animal were analyzed) or positive cells per section for the urethra (on average 25 sections per animal) were counted. To investigate appearance of CCC in thymi of different ages, at least 6 sections per animal ($N = 3$, mixed sexes) were analyzed.

Statistical analysis

Data were analyzed by Mann-Whitney test or Kruskal-Wallis test with GraphPad Prism 7 (GraphPad Software Inc., La Jolla, CA, USA). $P \leq 0.05$ were regarded as statistically significant.

Results

Sexual dimorphism of postnatal urethral CCC development

The time course of urethral CCC appearance showed a sexual dimorphism in ChAT-eGFP mice (Fig. 1). In male mice, urethral CCC appeared first between P6 and P10. In female mice, urethral CCC appeared first between P11 and P20. In both sexes, maximum urethral CCC numbers were reached between P40 and P220 and declined thereafter (Fig. 1b and c). Male mice had significantly higher absolute CCC numbers and CCC density per surface area than females in the periods P6–10, P11–20, and P21–39. In older animals (P40+), however, urethral CCC were more abundant in female mice (Fig. 1b, c, d; Supplementary Fig. 2). This gender difference was particularly pronounced in urethral CCC density, since the total urethral surface area was about 1.8 times larger in males than in females (Fig. 1e).

CCC of the trachea appear already during embryonic development

In ChAT-eGFP mice (von Engelhardt et al. 2007), CCC could not be detected within the tracheal epithelium at E12, E14, and E16. They appeared first at E18 in 5 of 6 investigated tracheae (Fig. 2), albeit in rare occurrence compared with pups sacrificed directly after birth (P0) (Figs. 2 and 3). Postnatal development was quantified in ChAT-eGFP (B6.Cg-Tg(RP23-268L19-EGFP)2Mik/J) mice. The number and density of tracheal CCC increased considerably until P78 (from 54 at P0 to 3950 cells at P78, Fig. 3a–c and Supplementary Fig. 1b and 3). In contrast to the urethra, no gender difference could be observed (Fig. 3b, c; Supplementary Fig. 1c). In tracheal whole-mount preparations of adult mice, about 89% of the cells labeled with TRPM5 antibody were also ChAT-eGFP-positive (Fig. 3d; Supplementary Fig. 3). In neonatal animals (P0-P2), however, only 45% of cells were double-positive ($p < 0.0004$, Mann-Whitney test). This co-localization increased further to 65% at P33 (Fig. 3e and f). The number of cells only positive for eGFP was extremely low in the tracheal epithelium throughout all ages.

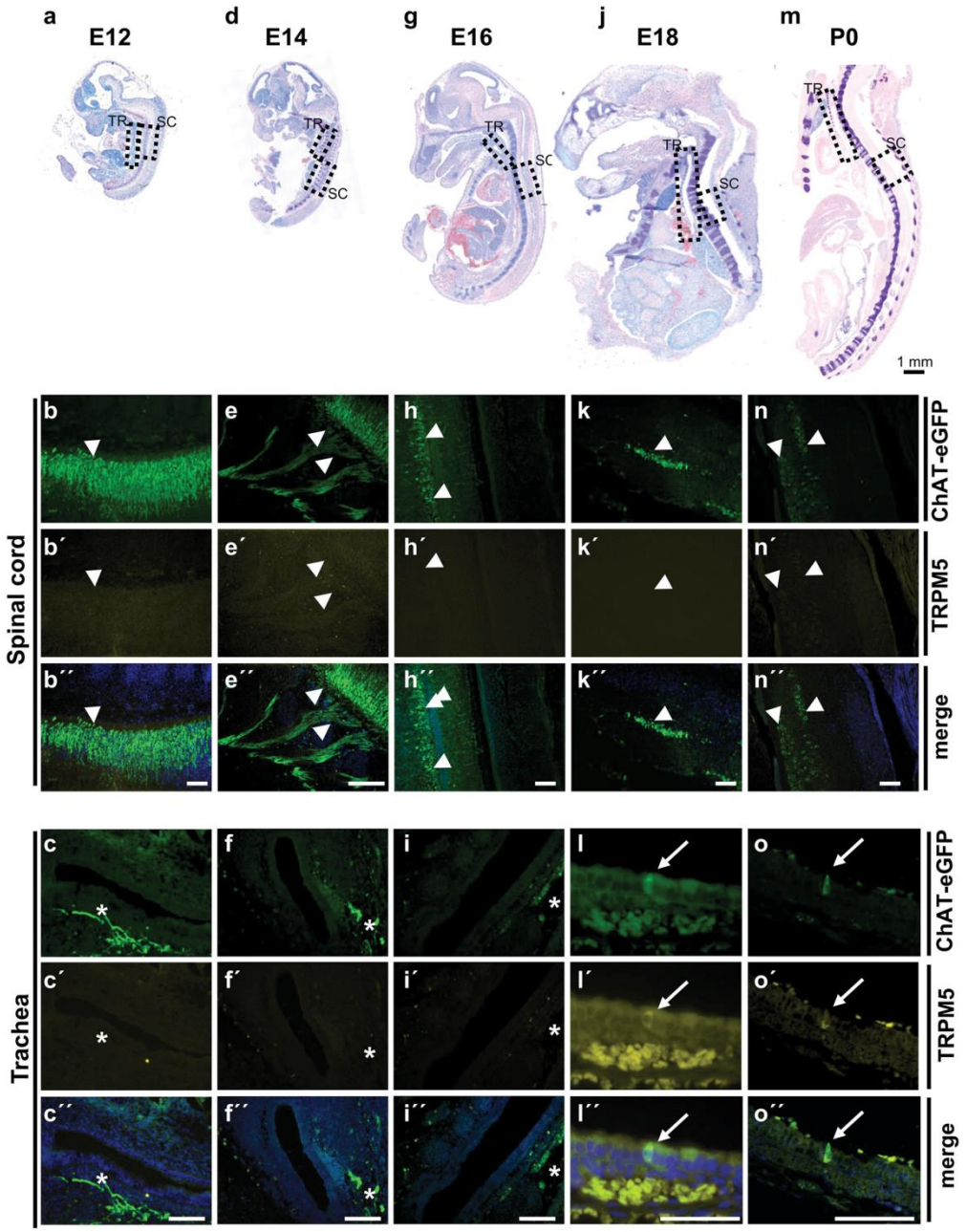
a
E12
d
E14
g
E16
j
E18
m
P0
TR
SC
1 mm
Spinal cord
Trachea
ChAT-eGFP
TRPM5
merge

◂**Fig. 2** Prenatal and perinatal development of tracheal CCC. Giemsa-stained paraffin sections from ChAT-eGFP mice (von Engelhardt et al. 2007) at distinct developmental stages with corresponding immunofluorescence images of trachea and spinal cord **a**–**c** E12 ($N = 4$), **d**–**f** E14 ($N = 5$), **g**–**i** E16 ($N = 8$), (j–l) E18 ($N = 6$), and (m–o) P0 ($N = 3$). Dashed boxes highlight locations where according immunofluorescence images of trachea (TR; **b**, **e**, **h**, **k**, and **n**) and spinal cord (SC; **c**, **f**, **i**, **l**, and **o**) were taken from adjacent sections double-labeled for TRPM5 and GFP; arrows mark ChAT-eGFP- and TRPM5-positive tracheal CCC at E18 and P0; arrowheads mark ChAT-eGFP-positive neurons; asterisks mark ChAT-eGFP-positive nerve fibers below the tracheal epithelium. Scale bar depicts 100 µm in the immunofluorescence images and 1 mm in Giemsa-stained overview images

TLR2/TLR4 and MyD88 deficiencies impair postnatal CCC expansion

We could not detect any urethral CCC in tissue sections from MyD88-KO mice stained with TRPM5 antibody (Supplementary Fig. 4a and b) and, hence, proceeded with whole-mount preparations using both TRPM5 and ChAT antibodies. TRPM5 antibody staining of urethral whole-mounts of adult ChAT-eGFP mice revealed about 99% congruency of ChAT-eGFP expression and TRPM5-immunolabeling antibody, justifying the use of TRPM5 antibody as a surrogate marker for urethral CCC (Supplementary Fig. 4c). Double staining of urethral whole-mount preparations from MyD88-KO mice and corresponding wildtypes with TRPM5 and ChAT antibodies also confirmed the near total coexistence of both signals (Fig. 4a and b). The total number of urethral CCC was significantly reduced by 69% in MyD88-KO mice compared with corresponding wildtypes (Fig. 4c). Since MyD88 is involved in downstream signaling of most TLRs (except TLR3), we reasoned that TLRs might be involved in the development of urethral CCC. We focused on TLR2 and TLR4 because of their importance in recognizing cell wall components of uropathogenic Gram-positive and -negative bacteria, respectively (Irvine et al. 2013; Park et al. 2009). Urethral sections from TLR2-KO, TLR4-def, and TLR2-KO/TLR4-def mice all showed significant reduction of TRMP5-immunoreactive cells by 88%, 88%, and 74%, respectively, when compared with corresponding wildtypes. However, no significant differences between the TLR-KO strains could be observed (Fig. 4d).

In tracheal whole-mount preparations, the congruency of staining with TRPM5 and ChAT antibodies was not 100%. $TRPM5^+/ChAT^-$ cells occurred in addition to double-labeled ($TRPM5^+/ChAT^+$) cells (Fig. 5a and b). Nevertheless, both stainings revealed significantly fewer CCC in MyD88-KO mice than in corresponding wildtypes (TRPM5: reduction by 36%, ChAT: reduction by 33%; Fig. 5c and d). Comparable results were also obtained with antibodies against DCAMKL1, another CCC marker, applied on TLR2-KO, TLR4-def, and TLR2-KO/TLR4-def tracheal sections (reduction of CCC by 47%, 29%, and 42%, respectively; Fig. 5e). DCAMKL1 was validated as a marker for CCC in tracheal whole-mount preparations of ChAT-eGFP mice, showing DCAMKL1-immunoreactivity in about 92% of all GFP-positive cells (Supplementary Fig. 5).

CCC develop independent of living microbiota

To determine whether the presence of living microbiota has impact on the development of CCC, germ-free C57BL/6 N mice were investigated. Selection of investigated time points was guided by the preceding experiments on urethrae of ChAT-eGFP mice, showing initial appearance and average cell count of about 50 cells per urethra on P7 in male and P33 in female mice, and highest numbers in both sexes in mice older than P100 (Fig. 1b). TRPM5-immunolabeling was utilized to investigate postnatal development of urethral CCC in germ-free versus SPF mice (Fig. 6a and b). Significantly more TRPM5-positive urethral CCC were counted on P7 in germ-free male mice, compared with SPF-housed C57BL/6 N mice (Fig. 6c; Supplementary Fig. 6a), but neither in P33 female mice (Fig. 6e; Supplementary Fig. 6c) nor in adult (P100+) mice of either sex (Fig. 6d, f; Supplementary Fig. 6b, d). In the trachea, we could not detect any difference in cell number between germ-free and SPF-housed control mice, neither in young (P7 [male] and P33 [female]), nor in adult mice (both genders) (Fig. 7).

Thymic CCC

In the course of our studies, we obtained some qualitative observations on thymic CCC. They were present already at birth (Supplementary Fig. 7), in adult MyD88-KO and TLR2/4-deficient mice (Supplementary Fig. 8), and in thymi of germ-free mice at the investigated time points, i.e., P7, P33, and P100+ (Supplementary Fig. 9).

Discussion

The present data reveal a perinatal appearance and postnatal expansion of CCC with distinct organ-specific onset in development, sexual dimorphism, and dependency on pattern recognition receptor signaling. This time course of development renders a significant role of this cell type in intrauterine organ development unlikely, and rather points towards an onset of function in postnatal life. Accordingly, mucosal CCC are generally considered as sentinels monitoring luminal content for potentially harmful substances, predominantly of microbial origin (Deckmann and Kummer 2016; Finger and Kinnamon 2011; Krasteva and Kummer 2012;

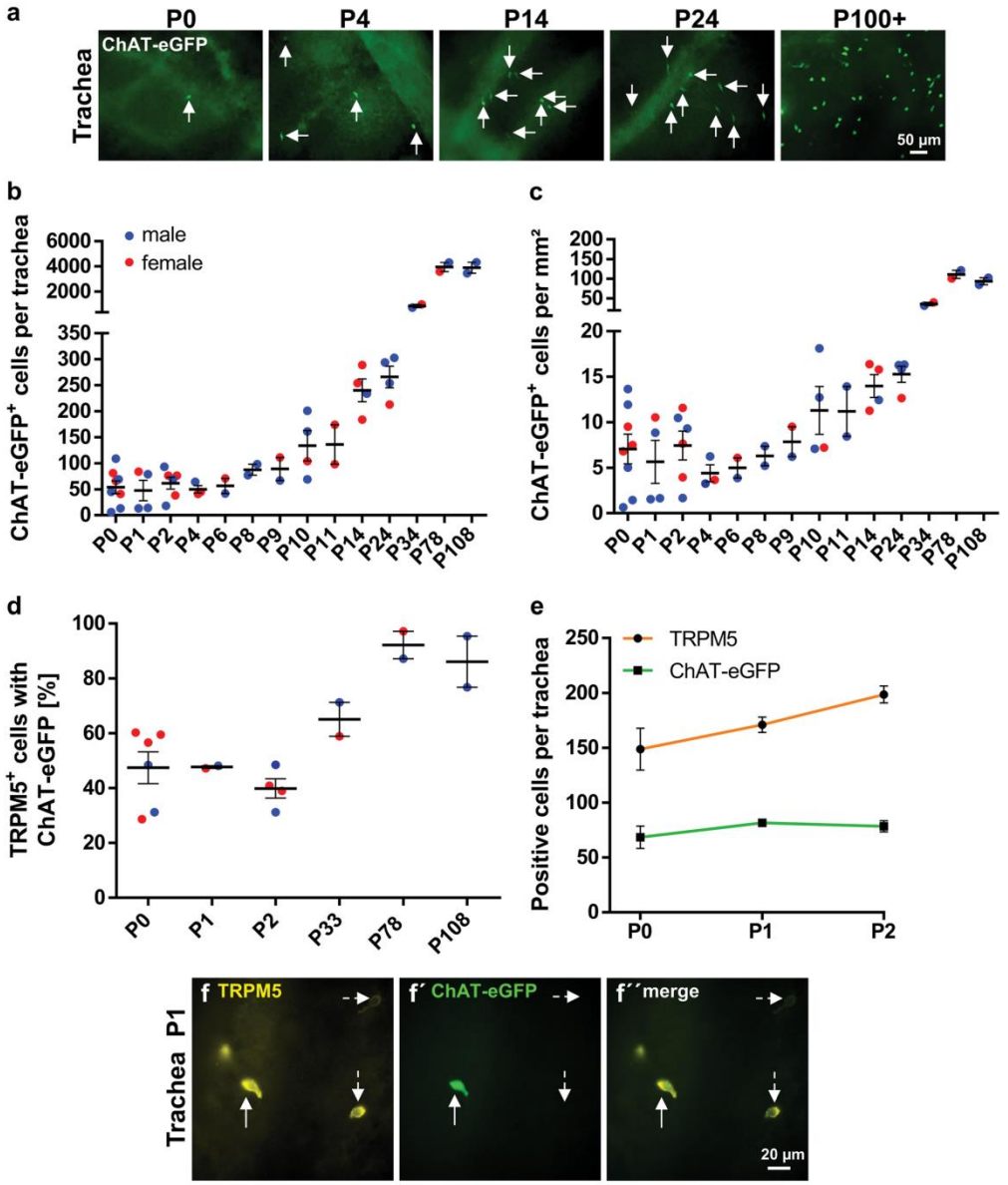

Kummer and Deckmann 2017; Schneider et al. 2019; Ting and von Moltke 2019; Tizzano and Finger 2013), to which exposure begins after birth. The present data also indicate at least a modulating and enhancing influence of the developing microbiota on the postnatal population dynamics of CCC, albeit microbiota are not an absolute requirement for the occurrence of CCC. This conclusion is based on our experiments with MyD88-KO

◂**Fig. 3** Postnatal development of CCC in the trachea. **a** Immunofluorescence with GFP antibody using tissue from ChAT-eGFP mice, representative images of tracheae at different time points during postnatal development; arrows point to ChAT-eGFP-positive tracheal CCC. GFP-positive cells were counted in tracheal whole-mount preparations; absolute numbers are given in **b**, cell number per mm^2 is shown in **c**. **d** Percentage of TRPM5-positive cells which also were positive for ChAT-eGFP from same animals as in **b** and **c**. **e** Total number of TRPM5- and ChAT-eGFP-positive cells at P0–P2 from same animals as in **b** and **c** ($N = 2$–6 each time point). **f** Representative immunofluorescence pictures with antibodies against TRPM5 and GFP of a tracheal whole-mount from an one day old ChAT-eGFP animal; dashed arrows mark a TRPM5 single-positive cell; solid arrows mark a TRPM5 and ChAT-eGFP double-positive cell. Graphs depict mean and SEM; **b**–**d** all data points depicted in scatter plots. Blue: males, red: females

and TLR-deficient mice. TLR2 and TLR4 are necessary for the detection of lipopeptides from bacterial origin and lipoteichoic acids or lipopolysaccharides from Gram-positive bacteria or Gram-negative bacteria, respectively, (Irvine et al. 2013; Park et al. 2009), and MyD88 is an essential downstream component of all TLR signaling except TLR3 (Wang et al. 2014). Genetic deletion of either of these components essentially reduced the number of CCC in the urethra and, to a lesser extent, in the trachea.

Likewise, MyD88 is also required for the induction of ChAT expression in lymphocytes (Reardon et al. 2013). Gnotobiotic mice are still exposed to TLR agonists, e.g., through their food and bedding material, and MyD88 expression was even found to be enhanced in the intestine of gnotobiotic mice compared with SPF mice (Yamamoto et al. 2012). This is consistent with our observation of generally unreduced and even enhanced numbers of CCC in male P7 urethra. These findings demonstrate that CCC development is independent of viability-associated

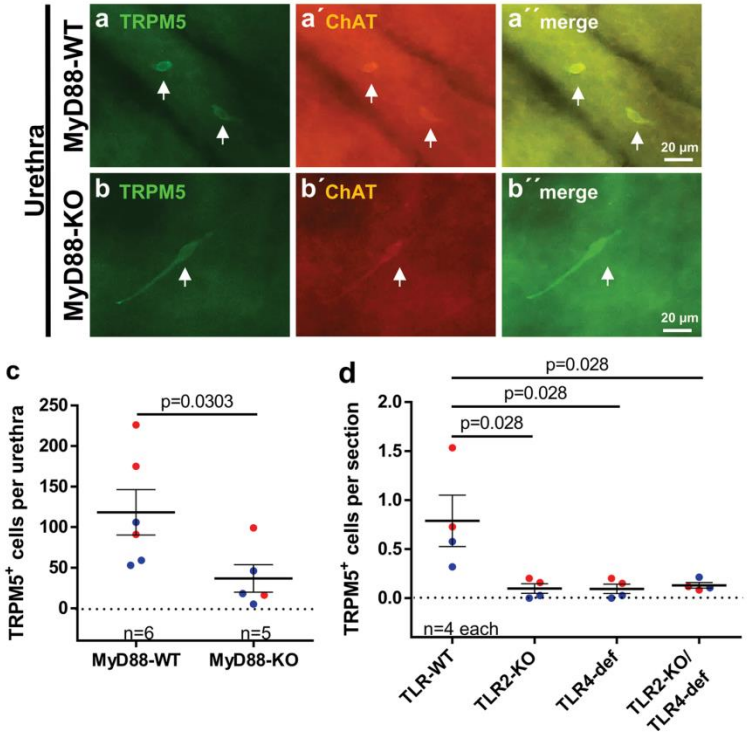

Fig. 4 Urethral CCC in MyD88-KO, TLR2-KO, TLR4-def, and TLR2-KO/TLR4-def mice. **a** and **b** Representative pictures of TRPM5 and ChAT double-labeled CCC (arrows) in urethral whole-mounts of MyD88-WT **a** and MyD88-KO **b** mice; all examples taken from P100+ mice. **c** Quantitative analysis of TRPM5-positive cells per urethra counted at whole-mount preparations as shown in **a** and **b**. **d** Number of TRPM5-positive cells in urethral tissue sections of TLR2-KO, TLR4-def, TLR2-KO/TLR4-def, and TLR-WT mice. Each data point represents the average number of cells from 20 sections from one animal. Bars and whiskers depict mean and SEM. Blue: males, red: females. All investigated animals were adult (> 12 weeks). *P* values were calculated with Mann-Whitney test

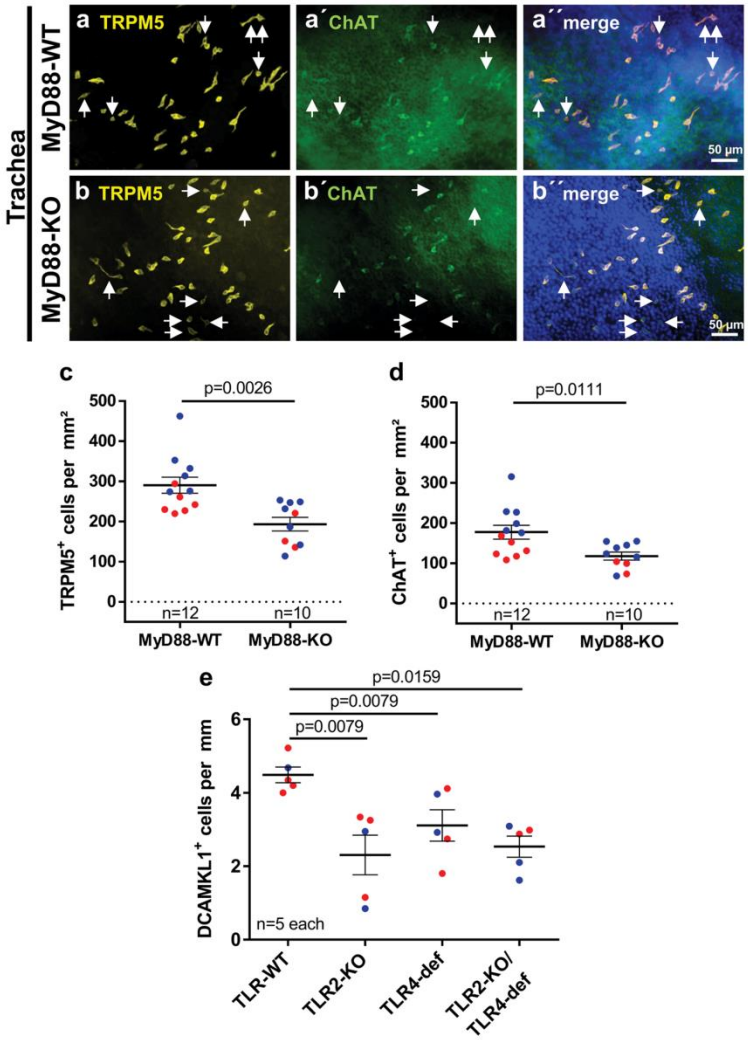

Fig. 5 Tracheal CCC in MyD88-KO, TLR2-KO, TLR4-def, and TLR2-KO/TLR4-def mice. **a** and **b** Double-labeling immunofluorescence of tracheal whole-mounts of MyD88-WT **a** and MyD88-KO **b** mice with antibodies against TRPM5 (yellow) and ChAT (green). Double-labeled cells dominate, single-labeled CCC ($TRPM5^+$/$ChAT^-$) are marked with arrows. **c** and **d** Densities of TRPM5-positive cells **c** and ChAT-positive cells **c** counted from whole-mounts as shown in **a** and **b**. **e** Number of DCAMKL1-positive cells per mm of basal lamina in tracheal tissue sections of TLR2-KO, TLR4-def, TLR2-KO/TLR4-def, and TLR-WT mice. Each data point represents a single animal analyzed with an average number of 20 single sections. Bars and whiskers depict mean and SEM. Blue: males, red: females. All investigated animals were adult (> 12 weeks). *P* values were calculated with Mann-Whitney test

pathogen-associated molecular patterns (vita PAMPs, (Sander et al. 2011)), but controlled by TLR2/4 signaling.

Although genetic deletion of TLR2, TLR4, TLR2/4, or MyD88 led to significantly reduced CCC numbers in the trachea, still more than 50% of CCC remained, pointing towards a CCC-inducing stimulus independent of pattern recognition signaling. This notion is supported by the presence of low basal numbers of CCC at birth (P0),

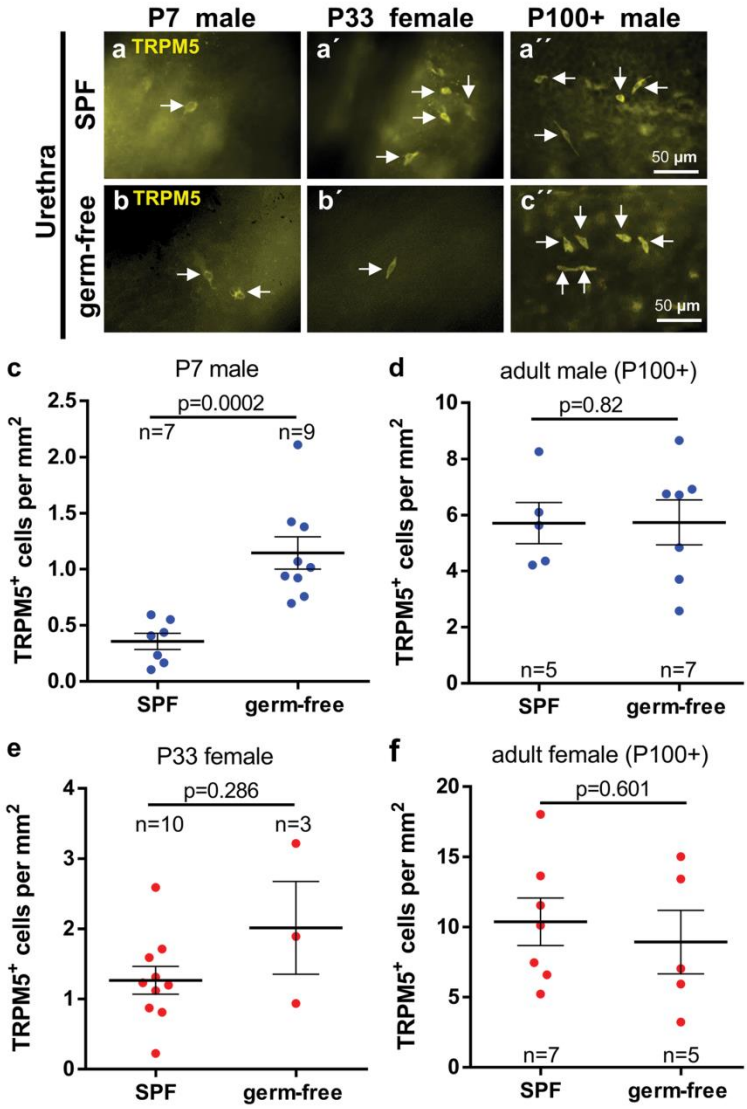

Fig. 6 Postnatal development of urethral CCC in germ-free versus SPF mice. **a** and **b** Representative immunofluorescence pictures, TRPM5-immunolabeling of urethral whole-mounts of SPF **a** and germ-free **b** mice. **c**–**f** Quantitative analysis of whole-mounts shown in **a** and **b**. Bars and whiskers depict mean and SEM. Blue: males, red: females. All investigated animals were adult (> 12 weeks). *P* values were calculated with Mann-Whitney test

prior to microbial contact. In line with our findings, early occurrence of chemosensory cells in the murine tracheal epithelium has also been described in TRPM5-GFP (P5, earlier time points not investigated; Saunders et al. 2013) and Tas2R131-GFP reporter mice (P3, earlier time points not investigated; Voigt et al. 2015). Similarly,

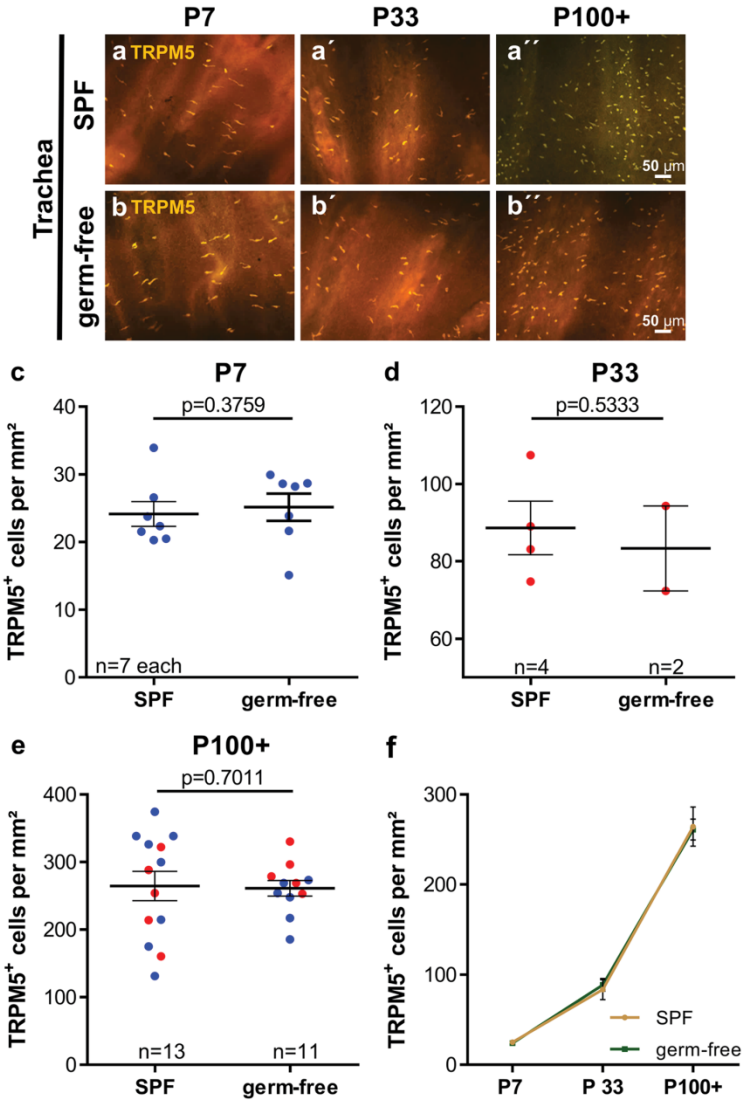

Fig. 7 Postnatal development of tracheal CCC in germ-free versus SPF mice. **a** and **b** Representative immunofluorescence pictures, TRPM5-immunolabeling of tracheal whole-mounts. **c**–**e** Quantitative analysis of whole-mounts shown in **a** and **b**, **f** visualization of data shown in **c**–**e** over time. Graphs depict means and SEM. Blue: males, red: females. All investigated animals were adult (> 12 weeks). *P* values were calculated with Mann-Whitney test

we observed considerable numbers of CCC, albeit not quantified, in the thymic medulla of MyD88-KO, TLR2-KO/TLR4-def, and germ-free mice. They were also present at birth, consistent with the observation of Tas2R131-GFP$^+$ and GNAT3-immunoreactive cells in the thymus at P3 (Voigt et al. 2015).

In contrast, genetic deletion of TLR2, TLR4, or MyD88 drastically reduced CCC numbers in the urethra by 69–88% compared with corresponding wildtypes and this coincided with lack of urethral CCC at birth. This strongly suggests that postnatal contact to TLR2/4 agonists, derived from the microbiome under physiological conditions, is required for CCC development in the urethra. MyD88 expression is regulated by estrogens (Zheng et al. 2006), and the downstream signaling proteins of the TLR4-MyD88 pathway, Bruton tyrosine kinase (BTK), and IL-1 receptor associated kinase (IRAK)1 are encoded by the X-chromosome (Spolarics 2007) with the consequence of higher IRAK1 levels in umbilical cord blood of female neonates compared with males (O'Driscoll et al. 2017). This has been considered one of the causes of sex-specific responses to infection and subsequent immunological advantage in female neonates (O'Driscoll et al. 2017). Notably, we also observed gender-specific differences in the first postnatal appearance of urethral CCC, which is also governed by TLR2/4-MyD88 signaling. It is tempting to assume a causal relationship, but this still needs to be experimentally addressed, in particular, since higher IRAK1 levels in females would predict earlier appearance of UCCC in females rather than in males. Consistent with this hypothesis, postnatal appearance and gender-specific developmental dynamics have also been reported for a closely related cell type, the brush cell of the rat common bile duct. It can be first detected by scanning electron microscopy at 4 weeks after birth and, thereafter, shows a remarkable increase in numbers, with a gender specific difference in time, i.e., between 8 and 12 weeks in the male and between 10 and 14 weeks in the female (Iseki 1991).

Collectively, our data show a marked postnatal expansion of CCC populations with distinct organ-specific features, including the relative impact of TLR2/4-MyD88 signaling. Strong dependency on this pathway (urethra) correlates with absence of CCC at birth and gender-specific initial development and expansion dynamics, whereas moderate dependency (trachea) coincides with presence of first CCC at E18 and sex-independent further development.

Supplementary information The online version contains supplementary material available at https://doi.org/10.1007/s00441-021-03424-9.Acknowledgements We thank Martin Bodenbenner, Theresa Eiffert, and Stefanie Demgensky for skillful technical assistance. We thank Rainer Glauben, Charite Berlin, and Axel Pagenstecher, Philipps-University Marburg, for providing the MyD88-knockout animals. We thank Vladimir Chubanov and Thomas Gudermann, Ludwig-Maximilian-University Munich, for providing TRPM5 antibody. We also thank Claudia Dames, Charite Berlin, for organizational assistance.

Author contribution AP and KD (Klaus Deckmann) designed research and performed statistical analysis. AP, KD, PS, AS, BS, and TP performed research and analyzed data. AV and DK (Katja Dahlke) designed animals. KD, AS, and WK obtained funding. KD, AP, PS, and WK drafted the manuscript. Work was supervised by WK and KD.

Funding Open Access funding enabled and organized by Projekt DEAL. This work was supported by a University Hospital of Giessen and Marburg (UKGM)-Justus-Liebig-University (JLU)-Cooperation Grant (# 7/2016 GI to KD), the German Research Foundation (SFB-TR84; project A6 to WK), SCHU1259/10-1 to BS, the German Center for Lung Research (DZL ALI-1.1 to WK) the Excellence Cluster Cardiopulmonary Institute (CPI, EXC 147 to WK), a Young Researcher Grant of the Faculty of Medicine, JLU Giessen (to AS), and the Else Kröner-Fresenius-Stiftung (2016_A90 to KD).

Declarations

Conflict of interest The authors declare that they have no conflict of interest.

References

Adachi O, Kawai T, Takeda K, Matsumoto M, Tsutsui H, Sakagami M, Nakanishi K, Akira S (1998) Targeted disruption of the MyD88 gene results in loss of IL-1- and IL-18-mediated function. Immunity 9:143–150

Bankova LG, Dwyer DF, Yoshimoto E, Ualiyeva S, McGinty JW, Raff H, von Moltke J, Kanaoka Y, Frank Austen K, Barrett NA (2018) The cysteinyl leukotriene 3 receptor regulates expansion of IL-25-producing airway brush cells leading to type 2 inflammation. Sci Immunol 3

Deckmann K, Filipski K, Krasteva-Christ G, Fronius M, Althaus M, Rafiq A, Papadakis T, Renno L, Jurastow I, Wessels L, Wolff M, Schutz B, Weihe E, Chubanov V, Gudermann T, Klein J, Bschleipfer T, Kummer W (2014) Bitter triggers acetylcholine release from polymodal urethral chemosensory cells and bladder reflexes. Proc Natl Acad Sci U S A 111:8287–8292

Deckmann K, Kummer W (2016) Chemosensory epithelial cells in the urethra: sentinels of the urinary tract. Histochem Cell Biol 146:673–683

Finger TE, Bottger B, Hansen A, Anderson KT, Alimohammadi H, Silver WL (2003) Solitary chemoreceptor cells in the nasal cavity serve as sentinels of respiration. Proc Natl Acad Sci U S A 100:8981–8986

Finger TE, Kinnamon SC (2011) Taste isn't just for taste buds anymore. F1000 Biol Rep 3:20

Forssmann WG, Ito S, Weihe E, Aoki A, Dym M, Fawcett DW (1977) An improved perfusion fixation method for the testis. Anat Rec 188:307–314

Gerbe F, Sidot E, Smyth DJ, Ohmoto M, Matsumoto I, Dardalhon V, Cesses P, Garnier L, Pouzolles M, Brulin B, Bruschi M, Harcus Y, Zimmermann VS, Taylor N, Maizels RM, Jay P (2016) Intestinal epithelial tuft cells initiate type 2 mucosal immunity to helminth parasites. Nature 529:226–230

Gulbransen BD, Clapp TR, Finger TE, Kinnamon SC (2008) Nasal solitary chemoreceptor cell responses to bitter and trigeminal stimulants in vitro. J Neurophysiol 99:2929–2937

Gulbransen BD, Finger TE (2005) Solitary chemoreceptor cell proliferation in adult nasal epithelium. J Neurocytol 34:117–122

Heimesaat MM, Fischer A, Siegmund B, Kupz A, Niebergall J, Fuchs D, Jahn HK, Freudenberg M, Loddenkemper C, Batra A, Lehr HA, Liesenfeld O, Blaut M, Gobel UB, Schumann RR, Bereswill S (2007) Shift towards pro-inflammatory intestinal bacteria aggravates acute murine colitis via Toll-like receptors 2 and 4. PLoS One 2:e662

Howitt MR, Lavoie S, Michaud M, Blum AM, Tran SV, Weinstock JV, Gallini CA, Redding K, Margolskee RF, Osborne LC, Artis D, Garrett WS (2016) Tuft cells, taste-chemosensory cells, orchestrate parasite type 2 immunity in the gut. Science 351:1329–1333

Irvine KL, Hopkins LJ, Gangloff M, Bryant CE (2013) The molecular basis for recognition of bacterial ligands at equine TLR2, TLR1 and TLR6. Vet Res 44:50

Iseki S (1991) Postnatal development of the brush cells in the common bile duct of the rat. Cell Tissue Res 266:507–510

Kaske S, Krasteva G, Konig P, Kummer W, Hofmann T, Gudermann T, Chubanov V (2007) TRPM5, a taste-signaling transient receptor potential ion-channel, is a ubiquitous signaling component in chemosensory cells. BMC Neurosci 8:49

Krasteva G, Canning BJ, Hartmann P, Veres TZ, Papadakis T, Muhlfeld C, Schliecker K, Tallini YN, Braun A, Hackstein H, Baal N, Weihe E, Schutz B, Kotlikoff M, Ibanez-Tallon I, Kummer W (2011) Cholinergic chemosensory cells in the trachea regulate breathing. Proc Natl Acad Sci U S A 108:9478–9483

Krasteva G, Canning BJ, Papadakis T, Kummer W (2012) Cholinergic brush cells in the trachea mediate respiratory responses to quorum sensing molecules. Life Sci 91:992–996

Krasteva G, Hartmann P, Papadakis T, Bodenbenner M, Wessels L, Weihe E, Schutz B, Langheinrich AC, Chubanov V, Gudermann T, Ibanez-Tallon I, Kummer W (2012) Cholinergic chemosensory cells in the auditory tube. Histochem Cell Biol 137:483–497

Krasteva G, Kummer W (2012) "Tasting" the airway lining fluid. Histochem Cell Biol 138:365–383

Kummer W, Deckmann K (2017) Brush cells, the newly identified gatekeepers of the urinary tract. Curr Opin Urol 27:85–92

Middelhoff M, Westphalen CB, Hayakawa Y, Yan KS, Gershon MD, Wang TC, Quante M (2017) Dclk1-expressing tuft cells: critical modulators of the intestinal niche? Am J Physiol Gastrointest Liver Physiol 313:G285–G299

Montoro DT, Haber AL, Biton M, Vinarsky V, Lin B, Birket SE, Yuan F, Chen S, Leung HM, Villoria J, Rogel N, Burgin G, Tsankov AM, Waghray A, Slyper M, Waldman J, Nguyen L, Dionne D, Rozenblatt-Rosen O, Tata PR, Mou H, Shivaraju M, Bihler H, Mense M, Tearney GJ, Rowe SM, Engelhardt JF, Regev A, Rajagopal J (2018) A revised airway epithelial hierarchy includes CFTR-expressing ionocytes. Nature 560:319–324

Nadjsombati MS, McGinty JW, Lyons-Cohen MR, Jaffe JB, DiPeso L, Schneider C, Miller CN, Pollack JL, Nagana Gowda GA, Fontana MF, Erle DJ, Anderson MS, Locksley RM, Raftery D, von Moltke J (2018) Detection of Succinate by Intestinal Tuft Cells Triggers a Type 2 Innate Immune Circuit. Immunity 49(33–41):e37

O'Driscoll DN, De Santi C, McKiernan PJ, McEneaney V, Molloy EJ, Greene CM (2017) Expression of X-linked Toll-like receptor 4 signaling genes in female vs. male neonates. Pediatr Res 81:831–837

O'Leary CE, Schneider C, Locksley RM (2019) Tuft cells-systemically dispersed sensory epithelia integrating immune and neural circuitry. Annu Rev Immunol 37:47–72

Ogura T, Krosnowski K, Zhang L, Bekkerman M, Lin W (2010) Chemoreception regulates chemical access to mouse vomeronasal organ: role of solitary chemosensory cells. PLoS One 5:e11924

Ogura T, Szebenyi SA, Krosnowski K, Sathyanesan A, Jackson J, Lin W (2011) Cholinergic microvillous cells in the mouse main olfactory epithelium and effect of acetylcholine on olfactory sensory neurons and supporting cells. J Neurophysiol 106:1274–1287

Ohmoto M, Yamaguchi T, Yamashita J, Bachmanov AA, Hirota J, Matsumoto I (2013) Pou2f3/Skn-1a is necessary for the generation or differentiation of solitary chemosensory cells in the anterior nasal cavity. Biosci Biotechnol Biochem 77:2154–2156

Panneck AR, Rafiq A, Schutz B, Soultanova A, Deckmann K, Chubanov V, Gudermann T, Weihe E, Krasteva-Christ G, Grau V, del Rey A, Kummer W (2014) Cholinergic epithelial cell with chemosensory traits in murine thymic medulla. Cell Tissue Res 358:737–748

Park BS, Song DH, Kim HM, Choi BS, Lee H, Lee JO (2009) The structural basis of lipopolysaccharide recognition by the TLR4-MD-2 complex. Nature 458:1191–1195

Rane CK, Jackson SR, Pastore CF, Zhao G, Weiner AI, Patel NN, Herbert DR, Cohen NA, Vaughan AE (2019) Development of solitary chemosensory cells in the distal lung after severe influenza injury. Am J Physiol Lung Cell Mol Physiol

Reardon C, Duncan GS, Brustle A, Brenner D, Tusche MW, Olofsson PS, Rosas-Ballina M, Tracey KJ, Mak TW (2013) Lymphocyte-derived ACh regulates local innate but not adaptive immunity. Proc Natl Acad Sci U S A 110:1410–1415

Rhodin J, Dalhamn T (1956) Electron microscopy of the tracheal ciliated mucosa in rat. Z Zellforsch Mikrosk Anat 44:345–412

Russell WMS, Burch RL (1959) The principles of humane experimental technique. Anim Welf Wheathampstead

Sander LE, Davis MJ, Boekschoten MV, Amsen D, Dascher CC, Ryffel B, Swanson JA, Muller M, Blander JM (2011) Detection of prokaryotic mRNA signifies microbial viability and promotes immunity. Nature 474:385–389

Saunders CJ, Christensen M, Finger TE, Tizzano M (2014) Cholinergic neurotransmission links solitary chemosensory cells to nasal inflammation. Proc Natl Acad Sci U S A 111:6075–6080

Saunders CJ, Reynolds SD, Finger TE (2013) Chemosensory brush cells of the trachea. A stable population in a dynamic epithelium. Am J Respir Cell Mol Biol 49:190–196

Sbarbati A, Osculati F (2005) A new fate for old cells: brush cells and related elements. J Anat 206:349–358

Sbarbati A, Tizzano M, Merigo F, Benati D, Nicolato E, Boschi F, Cecchini MP, Scambi I, Osculati F (2009) Acyl homoserine lactones induce early response in the airway. Anat Rec (Hoboken) 292:439–448

Schneider C, O'Leary CE, Locksley RM (2019) Regulation of immune responses by tuft cells. Nat Rev Immunol

Schneider C, O'Leary CE, von Moltke J, Liang HE, Ang QY, Turnbaugh PJ, Radhakrishnan S, Pellizzon M, Ma A, Locksley RM (2018) A metabolite-triggered tuft cell-ILC2 circuit drives small intestinal remodeling. Cell 174(271–284):e214

Schutz B, Jurastow I, Bader S, Ringer C, von Engelhardt J, Chubanov V, Gudermann T, Diener M, Kummer W, Krasteva-Christ G, Weihe E (2015) Chemical coding and chemosensory properties of cholinergic brush cells in the mouse gastrointestinal and biliary tract. Front Physiol 6:87

Spolarics Z (2007) The X-files of inflammation: cellular mosaicism of X-linked polymorphic genes and the female advantage in the host response to injury and infection. Shock 27:597–604

Ting HA, von Moltke J (2019) The immune function of tuft cells at gut mucosal surfaces and beyond. J Immunol 202:1321–1329

Tizzano M, Cristofoletti M, Sbarbati A, Finger TE (2011) Expression of taste receptors in solitary chemosensory cells of rodent airways. BMC Pulm Med 11:3

Tizzano M, Finger TE (2013) Chemosensors in the nose: guardians of the airways. Physiol (Bethesda) 28:51–60

Tizzano M, Gulbransen BD, Vandenbeuch A, Clapp TR, Herman JP, Sibhatu HM, Churchill ME, Silver WL, Kinnamon SC, Finger TE (2010) Nasal chemosensory cells use bitter taste signaling to detect irritants and bacterial signals. Proc Natl Acad Sci U S A 107:3210–3215

Voigt A, Hubner S, Doring L, Perlach N, Hermans-Borgmeyer I, Boehm U, Meyerhof W (2015) cre-mediated recombination in Tas2r131 cells-A unique way to explore bitter taste receptor function inside and outside of the taste system. Chem Senses 40:627–639

von Engelhardt J, Eliava M, Meyer AH, Rozov A, Monyer H (2007) Functional characterization of intrinsic cholinergic interneurons in the cortex. J Neurosci 27:5633–5642

von Moltke J, Ji M, Liang HE, Locksley RM (2016) Tuft-cell-derived IL-25 regulates an intestinal ILC2-epithelial response circuit. Nature 529:221–225

Wang JQ, Jeelall YS, Ferguson LL, Horikawa K (2014) Toll-like receptors and cancer: MYD88 mutation and inflammation. Front Immunol 5:367

Wiederhold S, Papadakis T, Chubanov V, Gudermann T, Krasteva-Christ G, Kummer W (2015) A novel cholinergic epithelial cell with chemosensory traits in the murine conjunctiva. Int Immunopharmacol

Yamamoto M, Yamaguchi R, Munakata K, Takashima K, Nishiyama M, Hioki K, Ohnishi Y, Nagasaki M, Imoto S, Miyano S, Ishige A, Watanabe K (2012) A microarray analysis of gnotobiotic mice indicating that microbial exposure during the neonatal period plays an essential role in immune system development. BMC Genomics 13:335

Yamamoto Y, Ozawa Y, Yokoyama T, Nakamuta N (2018) Immunohistochemical characterization of brush cells in the rat larynx. J Mol Histol 49:63–73

Yamashita J, Ohmoto M, Yamaguchi T, Matsumoto I, Hirota J (2017) Skn-1a/Pou2f3 functions as a master regulator to generate Trpm5-expressing chemosensory cells in mice. PLoS One 12:e0189340

Zheng R, Pan G, Thobe BM, Choudhry MA, Matsutani T, Samy TS, Kang SC, Bland KI, Chaudry IH (2006) MyD88 and Src are differentially regulated in Kupffer cells of males and proestrus females following hypoxia. Mol Med 12:65–73

Chemosensory epithelial cells in the urethra: sentinels of the urinary tract

Klaus Deckmann & Wolfgang Kummer

Histochemistry and Cell Biology

ISSN 0948-6143
Volume 146
Number 6

Histochem Cell Biol (2016) 146:673-683
DOI 10.1007/s00418-016-1504-x

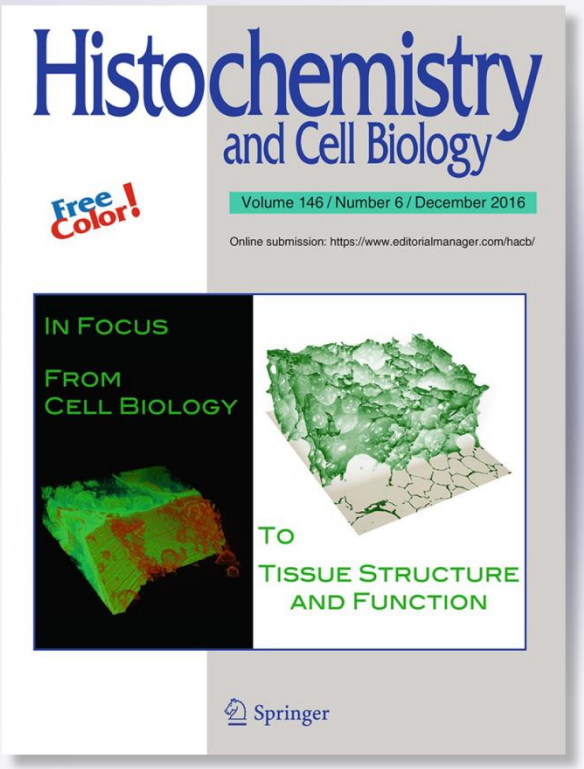

Springer

Histochem Cell Biol (2016) 146:673–683
DOI 10.1007/s00418-016-1504-x

REVIEW

Chemosensory epithelial cells in the urethra: sentinels of the urinary tract

Klaus Deckmann[1] · **Wolfgang Kummer**[1]

Accepted: 21 September 2016 / Published online: 29 September 2016

Abstract A peculiar cell type of the respiratory and gastrointestinal epithelia, originally termed "brush cell" or "tuft cell" by electron microscopists because of its apical tuft of microvilli, utilizes the canonical bitter taste transduction cascade known from oropharyngeal taste buds to detect potential hazardous compounds, e.g. bacterial products. Upon stimulation, this cell initiates protective reflexes and local inflammatory responses through release of acetylcholine and chemokines. Guided by the understanding of these cells as sentinels, they have been newly discovered at previously unrecognized anatomical locations, including the urethra. Solitary cholinergic urethral cells express canonical taste receptors and are polymodal chemosensors for certain bitter substances, glutamate (umami) and uropathogenic *Escherichia coli*. Intraurethral bitter stimulation triggers cholinergic reflex activation of bladder detrusor activity, which is interpreted as cleaning flushing of the urethra. The currently known scenario suggests the presence of at least two more urethral chemosensory cell types: non-cholinergic brush cells and neuroendocrine serotonergic cells. The potential implications are enormous and far reaching, as these cells might be involved in monitoring and preventing ascending urinary tract infection and triggering of inappropriate detrusor activity. However, although appealing, this is still highly speculative, since the actual number of distinct chemosensory cell types needs to be finally clarified, as well as their embryological origin, developmental dynamics, receptor equipment, modes of signalling to adjacent nerve fibres and other cells, repertoire of chemo- and cytokines, involvement in pathogenesis of diseases and many other aspects.

Keywords Chemosensory · Brush cell · Acetylcholine · Bitter · Neuroendocrine · Urethra

This review is dedicated to Detlev Drenckhahn who provided first experimental evidence for a chemosensory function of brush cells by discovering their expression of the taste-specific G-protein α-gustducin.

✉ Wolfgang Kummer
wolfgang.kummer@anatomie.med.uni-giessen.de

[1] Institute for Anatomy and Cell Biology, Justus-Liebig-University Giessen, Aulweg 123, 35385 Giessen, Germany

Introduction

The urethra connects the urinary bladder with the body's exterior and passes urine during micturition. In men, most of its length also constitutes the final pathway of semen during ejaculation. In general perception, this pure passive transport function is more or less the only task the urethra is serving, and this organ does not receive particular attention in research and in clinical medicine. This view is simplistic as the urethra is not just a one-way road for urine and semen but may also allow for ascent of bacteria into the urinary tract (Chromek 2015). Due to the anatomical neighbourhood to the perineum, microbial pressure is enormous, and urinary tract infections are among the most common bacterial infections worldwide (Foxman 2010; Wagenlehner et al. 2012). Thus, appropriate measures have to been taken to prevent ascending infection, and they include flushing through micturition, trapping of bacteria by mucus and secretion of immunoglobulin A, lysozyme, cathelicidin, defensins, and other antimicrobial proteins and peptides (Holstein et al. 1991; Parr et al. 1992; Kunin et al. 2002; Porter et al. 2005; Chromek 2015). Effective initiation and coordination of these effector mechanisms requires continuous monitoring of the mucosal surface for

the presence of pathogenic bacteria and hazardous compounds in general. Recent years have shown that, beyond long- and well-known pathogen detection systems such as toll-like receptors, chemosensory mechanisms originally characterized in the chemical senses of taste and smell also contribute to this mucosal surveillance (Finger et al. 2003; Margolskee et al. 2007; Gulbransen et al. 2008; Lin et al. 2008; Ogura et al. 2010; Tizzano et al. 2010; Krasteva et al. 2011; Lee et al. 2012; Deckmann et al. 2014). In particular, canonical bitter taste receptors have been linked to detection of bacterial products such as homoserine lactones serving as quorum-sensing molecules in *Pseudomonas aeruginosa* (Tizzano et al. 2010; Krasteva et al. 2011, 2012a; Lee et al. 2012).

These mechanisms have been initially unravelled in the respiratory tract where they have been ascribed to a rare, specialized epithelial cell type that originally had been recognized purely on the basis of its characteristic ultrastructure. Rhodin and Dalhamn (1956) were the first to describe by electron microscopy a rare cell type in the rat tracheal epithelium with no cilia but brush-like processes, which led them to designate this cell as "brush cell". Cells with similar, although not fully identical ultrastructure have been observed in various parts of the upper airways and in the gastrointestinal tract (Luciano et al. 1981; Luciano and Reale 1990; Höfer and Drenckhahn 1992, 1996; Hansen and Finger 2008; Krasteva et al. 2012b).

Owing both to historical reasons and to distinct morphological features, alternative terms to designate these cells are in use, and the preferential use differs among anatomical location. In the intestine, "tuft" or "tufted cells" are widely used, highlighting the stiff microvilli which are also characteristic for the "brush cells" of the trachea (Isomaki 1973; Howitt et al. 2016). In the nose, these microvilli appear less straight, and since 2003 the term "solitary chemosensory cells" is preferred (Monteiro-Riviere and Popp 1984; Finger et al. 2003). First evidence for a chemosensory function of these cells arose from the immunohistochemical detection of the taste-specific G-protein α-gustducin in these cells (Höfer et al. 1996; Finger et al. 2003), and about a decade later it became clear that they detect bacterial products via the bitter taste transduction cascade and induce protective local and systemic reflexes in the respiratory tract such as reduction of respiratory rate, local neurogenic inflammation and secretion of antimicrobial peptides (Tizzano et al. 2010; Krasteva et al. 2011, 2012a; Saunders et al. 2014; Lee et al. 2014). Hence, these cells are now interpreted as sentinels monitoring the mucosal surface for the presence of potentially hazardous compounds, in particular of pathogenic microbial origin (Finger and Kinnamon 2011; Krasteva and Kummer 2012; Lee and Cohen 2014), a model that was hypothesized earlier by Sbarbati and Osculati before experimental proof had been provided (Sbarbati and Osculati 2006). Such sentinel cells are particularly frequent at anatomical entry sites such as the nose (entrance into the entire respiratory tract) (Gulbransen et al. 2008), tuba auditiva (to middle ear) (Krasteva et al. 2012b), nasal opening of the vomeronasal duct (Ogura et al. 2010), bile and pancreatic duct (from gut to liver and pancreas) (Weyrauch and Schnorr 1976; Luciano and Reale 1979; Luciano et al. 1981; Höfer and Drenckhahn 1992; Schütz et al. 2015).

These data point towards a general principle of placing chemosensory sentinel cells near the opening of tubular systems to the outer environment or internal body surfaces with bacterial colonization. On this background, it might be anticipated that a similar cellular system surveils the urinary tract. Early immunohistological studies utilizing marker antibodies directed against characteristic structural proteins of brush cell microvilli (villin, fimbrin) failed to identify such cells in various organs of the urinary and genital tract, but the urethra, the immediate connection to the outer body surface, was not included in this investigation (Höfer and Drenckhahn 1992). A reinvestigation of the urinary tract in the light of the sentinel concept led to the identification of the hitherto not recognized urethral brush cell (Deckmann et al. 2014), and we here will focus on this urethral chemosensory cell and its relationship to the still enigmatic so-called urethral neuroendocrine cell.

Chemosensation via canonical taste receptors

Cells of the oropharyngeal taste buds respond to five basic taste qualities: sweet, salty and umami are annotated as valuable, bitter and sour as potentially harmful. G-protein-coupled receptors of the taste receptor families (TasR) are responsible for detection of sweet, umami and bitter. The Tas1R family consists of only three members (Tas1R1–Tas1R3), and Tas1R2/Tas1R3 heterodimers constitute a receptor for sweet compounds, whereas Tas1R1/Tas1R3 heterodimers are umami (e.g. glutamate) receptors (Nelson et al. 2001, 2002; Zhang et al. 2003; Zhao et al. 2003). A broad range of chemically diverse substances is potentially harmful if ingested, and a range of receptors is required to cover this spectrum. Accordingly, there are about 40 receptors of the Tas2R family, depending on species, and their activation finally results in bitter taste (Adler et al. 2000; Chandrashekar et al. 2000; Matsunami et al. 2000; Bachmanov and Beauchamp 2007). It has to be mentioned that both for naturally occurring sugars and for glutamate alternative receptor configurations have been identified (Lindemann 2001; Damak et al. 2003; Maillet et al. 2015; Kim et al. 2003). Their role in the present context of chemosensation in epithelial defence mechanism yet needs to be elucidated, so that they are not further described here. Taste receptors of both families share the downstream signalling

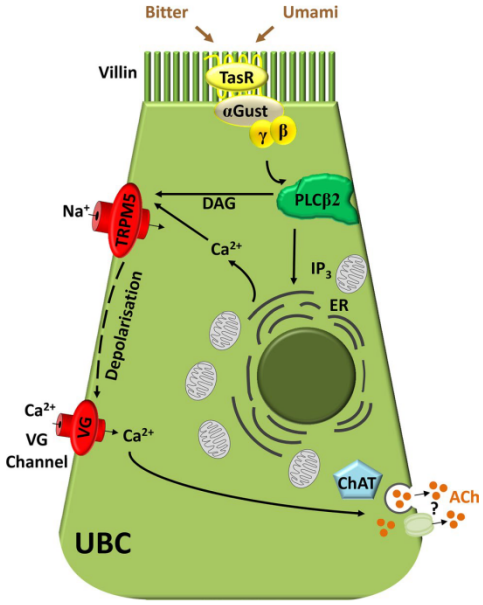

Fig. 1 Elements of the taste transduction cascade in a cholinergic urethral brush cell (UBC). Taste receptors (TasR) are anticipated at the apical microvilli with the structural protein villin, often serving as brush cell marker. Subsequent events involve activation of phospholipase $C_{\beta 2}$ (PLCβ2) via β,γ G-protein subunits, formation of inositol-tris-phosphate (IP_3) and diacylglycerol (DAG) with subsequent release of calcium from the endoplasmic reticulum (ER) and opening of the monovalent cation channel TRPM5, resulting in depolarization with opening of voltage-gated (VG) calcium channels, finally triggering acetylcholine (ACh) release, either via vesicular exocytosis or through hemichannels. αGust = G-protein α-subunit α-gustducin; *ChAT* choline acetyltransferase

cascade (Fig. 1). A characteristic, albeit not the only G-protein coupled to TasR is α-gustducin (McLaughlin et al. 1992; Glendinning et al. 2005; Tizzano et al. 2008; Chaudhari and Roper 2010). Further signalling involves activation of a specific isoform of phospholipase C, i.e. PLCβ2 (Zhang et al. 2003; Chaudhari and Roper 2010), with subsequent formation of inositol-tris-phosphate, release of calcium from the endoplasmic reticulum and opening of the monovalent cation channel TRPM5 (transient receptor potential cation channel subfamily M member 5). This results in depolarization of the cell, triggering transmitter release (Fig. 1). In the taste bud, these receptors and signalling cascades are expressed by the so-called Type II taste cells, which release ATP as their primary transmitter via hemichannels rather than vesicular exocytosis (Finger et al. 2005; Huang et al. 2007; Chaudhari and Roper 2010; Taruno et al. 2013; Vandenbeuch et al. 2015).

All these components of the canonical taste transduction cascade have been identified in brush cells/solitary chemosensory cells/tuft cells in the respiratory and gastrointestinal tract, and inhibition of either PLCβ2 or TRPM5, and genetic deletion of TRPM5 attenuated the cells' response to bitter stimuli and resulted in loss of intestinal worm clearance in a helminth infection model, respectively (Gulbransen et al. 2008; Ogura et al. 2010; Tizzano et al. 2010; Saunders et al. 2014; Howitt et al. 2016). Hence, it can be assumed that the receptors and transduction mechanisms acting in extra-oral chemosensory cells are largely, if not fully, identical to those originally described in Type II cells of taste buds. While ATP is the primary transmitter of Type II cells of taste buds, respiratory and gastrointestinal chemosensory cells express the acetylcholine (ACh) synthesizing enzyme choline acetyltransferase (ChAT) and act upon neighbouring sensory nerve terminals and other cells via cholinergic signalling (Krasteva et al. 2011; Ogura et al. 2011; Saunders et al. 2014).

The cholinergic urethral brush cell: a polymodal chemosensor

Based on the sentinel concept of cholinergic chemosensory epithelial cells residing at openings of mucosal organs to the outer body surface, the urethra was intentionally screened for their occurrence utilizing reporter mice expressing enhanced green fluorescent protein (eGFP) under the control of the ChAT promoter. ChAT-eGFP-positive cells with slender, often flask-like shape with long processes were identified in the urethra and the terminal portions of glandular ducts near their opening into the urethra, but neither further upstream in the urinary tract (bladder, ureter, renal pelvis) nor in the acinar regions of the associated glands (prostate lobes, seminal vesicles, urethral, preputial and clitoridal glands) (Deckmann et al. 2014). These cells displayed villin-immunoreactivity with particular prominent labelling at the apical cell pole, and electron microscopy revealed microvilli protruding into the lumen and some lateral microvilli (Deckmann et al. 2014), all being characteristics of brush cells (Höfer and Drenckhahn 1992). Thus, the name cholinergic "urethral brush cell" (UBC) has been proposed for this newly recognized cell entity (Deckmann et al. 2014). All of these cells were TRPM5-immunoreactive (Fig. 2a); 73 % (female) to 83 % (male) were PLCβ2-immunoreactive and α-gustducin-immunoreactivity varied largely depending on anatomical location. In the female urethra, a quarter of ChAT-eGFP-positive epithelial cells was α-gustducin-immunoreactive; in the male penile urethra and in the diverticle double-positive cells accounted for about 50 %; while only 10 % of cholinergic cells in the pelvic urethra were α-gustducin-immunoreactive (Deckmann et al. 2014). It remains to be

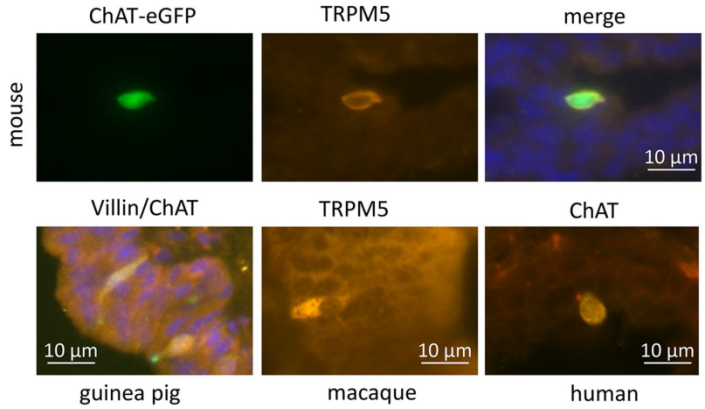

Fig. 2 Urethral cholinergic brush cells. **a** Immunoreactivity to the monovalent cation channel TRPM5 in a cell expressing eGFP under the control of the ChAT promoter. In the merged image, nuclei are also labelled with DAPI. **b** Immunoreactivities to the brush cell marker protein villin, to TRPM5 and to the acetylcholine synthesizing enzyme ChAT are also found in solitary urethral epithelial cells in the guinea pig, macaque monkey (*Callithrix jacchus*) and human, respectively. In the merged image of villin (*green*) and ChAT (*orange*) double-labelling of the guinea pig urethra, pronounced villin-labelling is seen at the luminal aspect, probably reflecting the tuft of microvilli

determined whether these incomplete colocalization patterns define distinct cell types or reflect certain functional cellular states or different sensitivities of the immunohistochemical labelling.

This cell is not unique to the mouse but occurs widespread throughout placental mammals. Solitary epithelial cells with this immunophenotype were also detected in other rodents (rat, golden hamster and guinea pig—with respect to classification of the guinea pig we here adhere to the tree of life project; Maddison 2007), carnivores (dog, badger), artiodactyla (pig, deer) and primates (*Macaca fascicularis*, *Callithrix jacchus*, *Homo sapiens*) (Fig. 2b). These data indicate that cholinergic UBC evolved not later than about 64.5 million years ago (Deckmann et al. 2015).

RT-PCR analysis of pooled murine cholinergic UBC, isolated by means of an antibody targeting an extracellular domain of TRPM5, revealed expression of the taste receptors Tas1R1 and Tas1R3 but not Tas1R2, suggesting responsiveness to umami. Indeed, glutamate but not the artificial sweetener saccharin evoked an increase in intracellular [Ca^{2+}]. Among bitter receptors, expression of Tas2R108, but neither of Tas2R105 nor of Tas2R119 was noted, suggesting responses to certain but not all bitter stimuli. Accordingly, the Tas2R108 ligand denatonium dose dependently evoked rises in intracellular [Ca^{2+}], whereas cycloheximide, a Tas2R108 ligand, did not. These responses to tastants were sensitive to the TRPM5 inhibitor triphenylphosphine oxide, indicating involvement of the canonical taste transduction cascade. Much in favour of a physiological role as sentinel for pathogenic bacteria, cholinergic UBC also responds to heat-inactivated uropathogenic *Escherichia coli*, the most common cause of urinary tract infection, with increase in intracellular [Ca^{2+}] (Deckmann et al. 2014).

In oropharyngeal taste buds, segregation of receptors for the different taste qualities to separate cell types is commonly considered as the basis for taste coding. In general, cells of the taste buds are classified as glial-like Type I cells, receptor (Type II) cells and presynaptic (Type III) cells. Sour stimuli are perceived by Type III cells, sweet, umami and bitter by Type II cells, and it is still not clear which of these cell types senses salt taste (Roper 2013, 2015). Albeit all Tas1R- and Tas2R-expressing cells in taste buds are classified as Type II cells, this is a heterogeneous population. Tas1R and Tas2R are usually not coexpressed in Type II cells (Adler et al. 2000; Ohmoto et al. 2008), and 83 % of Type II cells respond to only a single taste quality in murine vallate papillae (Tomchik et al. 2007). Still, there are cells that do respond to multiple chemical stimuli (Gilbertson et al. 2001; Caicedo et al. 2002; Tomchik et al. 2007).

Much in contrast, the vast majority (86 %) of cholinergic UBC responded both to monosodium glutamate (umami) and to denatonium (a bitter stimulus), thereby exhibiting polymodal sensitivity (Deckmann et al. 2014). This is particularly noteworthy since in oropharyngeal gustation bitter is an aversive stimulus, reflecting potential hazardous compounds, and umami is a rewarding stimulus, since it

represents energy uptake. Accordingly, taste receptor cells responding to both bitter and an appetitive stimuli (sweet) are rare (Caicedo et al. 2002). There is reason to assume, however, that glutamate (umami) reflects a potentially dangerous situation on the mucosal lining of the urethra. It facilitates bacterial growth in urine (Aubron et al. 2012), production of the virulence factor pyocyanin by *Pseudomonas aeruginosa* is dependent on the availability of glutamate (Polisetti et al. 2016) and glutamate metabolism is positively linked to biofilm formation by *Pseudomonas aeruginosa* (Xu et al. 2015) and to the pathogenic potential of *Proteus mirabilis* in the urinary tract (Pearson et al. 2011). Thus, polymodality broadens the spectrum of potentially hazardous compounds to be detected by cholinergic UBC.

Acetylcholine is a para- and autocrine messenger in urethral chemosensation

In line with the expression of the ACh synthesizing enzyme ChAT by urethral chemosensory cells, the bitter stimulus denatonium evokes ACh release from isolated urethral epithelial cells in sufficient quantities to raise intracellular [Ca^{2+}] in cells neighbouring ChAT-eGFP-negative cells due to cholinergic receptor activation (Deckmann et al. 2014). Instillation of denatonium into the urethral lumen of rats results in drastic increase in bladder detrusor activity, and this reflex is largely, but not completely, depressed by concomitant instillation of the nicotinic ACh receptor inhibitor, mecamylamine. It is highly likely that this urethrovesical reflex involves initial recognition by cholinergic chemosensory cells, cholinergic transmission to adjacent sensory nerve fibres carrying nicotinic ACh receptors with the α3-subunit, which have been shown to approach these chemosensory cells, and reflex activation of the sacral parasympathetic outflow to the urinary bladder. Notably, the nicotinic blocker mecamylamine did not fully abrogate the reflex response, which might indicate cotransmission utilizing another transmitter in addition to acetylcholine and/or involvement of other, non-cholinergic chemosensory cells yet to be identified. In essence, the intraluminal presence of a potential hazardous compound in the urethra triggers micturition, which can be interpreted as a cleaning flushing (Deckmann et al. 2014). This classical reflex involving the central nervous system appears to be the urinary counterpart for bitter tastant-induced apnoea or reduction in breathing rate after intranasal and intratracheal application, respectively (Tizzanao et al. 2010; Krasteva et al. 2011). In case of the urinary tract, flushing may help to eliminate the content from the urethra; in the airways, reduced respiratory activity shall prevent or minimize further ingression.

In addition to these classical reflex loops, further local responses induced by stimulation of cholinergic chemosensory cells have been identified in the upper airways. Bitter stimuli and the *Pseudomonas* quorum-sensing molecule 3-oxo-C12-homoserine lactone evoke a local neurogenic inflammation by cholinergic activation of peptidergic sensory nerve fibres which in turn release the neuropeptide substance P, resulting in mast cell degranulation and plasma leakage from postcapillary venules (Saunders et al. 2014). Intranasal application of bitter substances also causes swelling of the vomeronasal duct at its opening into the nasal cavity, probably due to neurogenic inflammation, thereby limiting access of fluid into this organ. This effect requires TRPM5 and cholinergic transmission (Ogura et al. 2010), again in line with a crucial role of cholinergic chemosensory cells serving a sentinels.

Solitary chemosensory cells further contribute to innate immunity through nerve-independent local reactions that may not involve cholinergic signalling. In human sinonasal epithelial cultures, stimulation of bitter receptors on chemosensory cells activates a calcium wave that propagates through gap junctions to the surrounding respiratory epithelial cells and triggers release of antimicrobial peptides (Lee et al. 2014). In the gut, tuft cells, which are known to be cholinergic and chemosensory (Höfer et al. 1996; Höfer and Drenckhahn 1996; Schütz et al. 2015), release interleukin-25 (IL-25) to activate innate lymphoid cells type 2 which in turn triggers goblet and tuft cell hyperplasia in the course of helminth infection (von Moltke et al. 2016; Howitt et al. 2016; Gerbe et al. 2016). Tuft cell-deficient mice are no longer capable to clear the gut from the helminth *Nippostrongylus brasiliensis*, highlighting the importance of the sentinel function of these chemosensory cells (Gerbe et al. 2016). In the light of these data obtained at other organ systems, it appears likely that urethral cholinergic chemosensory cells serve also more functions than triggering a flushing micturition, e.g. initiation of local inflammatory responses both through cholinergic activation of neurogenic inflammation and through cytokine release. Yet, these hypotheses still require experimental validation.

The cholinergic urethral brush cell is not alone: Are there other "brush" cells?

In cat and horse, cells with immunoreactivity to villin and to the components of the canonical taste transduction cascade (α-gustducin, PLCβ2, TRPM5) have not been successfully labelled with ChAT antisera which might indicate that, if this lack of immunolabelling does not simply reflect technical problems, urethral chemosensory cells utilize other transmitters in some mammalian species (Deckmann et al. 2015).

In the mouse, the initial approach to search for potential chemosensory sentinel cells in the urinary tract involved a reporter mouse strain with labelled cholinergic (ChAT

expressing) cells, and subsequent functional studies used either this ChAT-eGFP expression or surface expression of TRPM5 for cell isolation and identification (Deckmann et al. 2014). These studies have revealed important information on this population of cholinergic chemosensory cells, but it shall not be forgotten that another cell population has been newly identified in parallel, i.e. villin-immunoreactive but ChAT-eGFP- and TRPM5-negative cells, which is at least as frequent as villin/ChAT/TRPM5-positive cells (Deckmann et al. 2014). Their overall shape is very similar to that of cholinergic chemosensory cells and does not serve as a distinctive criterion. Based on the expression of the marker protein villin, it is tempting to designate them as "non-cholinergic brush cells", but this would imply to assume a chemosensory function for which there is no direct functional evidence at the time. At current, the knowledge on this cell population is minimal, and further tools will be needed to conduct selective functional studies to elucidate their role.

What about the structurally long-known "neuroendocrine cell" of the urethra?

In the mouse, double-labelling with appropriate marker antibodies confirmed that urethral cholinergic brush cells, villin-positive but ChAT-negative cells, and endocrine cells represent distinct entities (Deckmann et al. 2014) (Fig. 3). Solitary endocrine cells in the urethral epithelium have first been described by Feyrter using classical staining—here they appeared light which led him to coin the term "clear cells" (in German: "Helle Zellen")—and silver impregnation techniques in the human urogenital tract (Feyrter 1951a, b). Much like the just recently discovered UBC, he never observed them in the ureter or renal pelvis, and only in women he noted some of these cells in the urinary bladder (Feyrter 1951a). In humans, they are also found in associated glands (urethral, prostate, bulbourethral) and are particularly increased in prostate cancer (Feyrter 1951a, b; Amorino and Parsons 2004; Dorff et al. 2011; Heinrich et al. 2011). In the rat, they are lacking from the glandular body itself but are present in the ducts of the seminal vesicles and the ventral and lateral prostate, and less frequent in the ducts of the coagulating gland, dorsal prostate and bulbourethral gland while being absent in the deferent duct (Aumüller et al. 2012), thereby closely mimicking the distribution of cholinergic brush cells in the murine urinary tract (Deckmann et al. 2014).

Urethral endocrine cells produce serotonin (Hakanson et al. 1974; Fetissof et al. 1983; di Sant'Agnese and de Mesy Jensen 1987; Hanyu et al. 1987), and immunoreactivities to the peptide hormones somatostatin and cholecystokinin have been reported (Vittoria et al. 1992; Czaja et al. 1996). Accordingly, their basal cytoplasm is loaded with

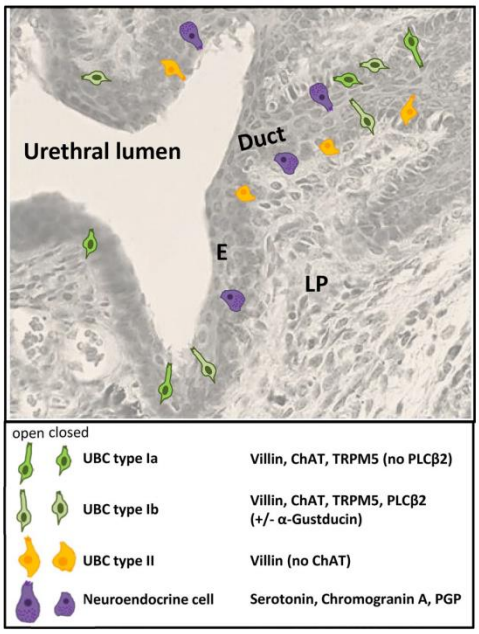

Fig. 3 Potential chemosensory epithelial cell types in the urethra and ducts of urethral glands, an original haematoxylin–eosin-stained section is taken as background image. Chemosensory properties are validated for cholinergic urethral brush cells (UBS type I), which may be subdivided into subpopulations (Ia and Ib) according to expression of phospholipase $C_{\beta 2}$ (PLCβ2). A chemosensory function of non-cholinergic solitary villin-expressing cells (UBC type II) and serotonergic neuroendocrine cells with basal dense core vesicles may be anticipated, yet has to be validated. *E* epithelium, *LP* lamina propria, *PGP* protein gene product 9.5

secretory dense core vesicles, the typical amine and peptide hormone storing organelle, and they express chromogranin A, a characteristic dense core vesicle protein (Dixon et al. 1973; Casanova et al. 1974; Fetissof et al. 1983; di Sant'Agnese and de Mesy Jensen 1987; Hanyu et al. 1987; Aumüller et al. 2012). In the gastrointestinal tract, several distinct endocrine cell types exist and can be easily distinguished by the size and morphology of their dense core vesicles. In human urethral endocrine–paracrine cells, there is a wide range of granule morphology, but many intermediates have been observed forming a continuum between the extremes, so that the presence of truly distinct cellular populations has been questioned (di Sant'Agnese and de Mesy Jensen 1984). Vesicles and histochemically demonstrable serotonin are often concentrated in long processes ramifying within the epithelium and projecting towards the basal lamina, so that paracrine actions are generally

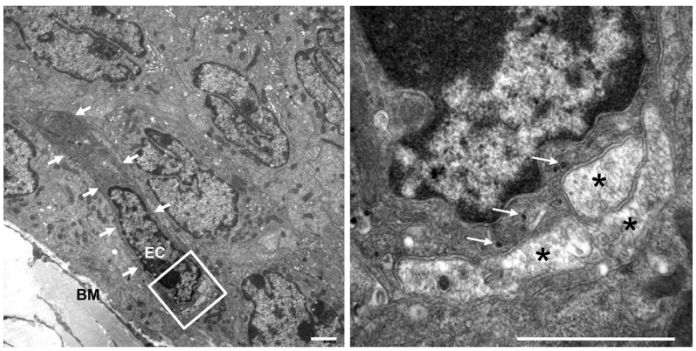

Fig. 4 Female mouse urethra, electron microscopy. An elongated endocrine cell (EC) is oriented horizontally to the basal membrane (BM), *short arrows* indicate their outlines. The *boxed area* is shown at higher magnification in the right panel, depicting dense core vesicles (*long arrows*) in the cytoplasm of the endocrine cells next to extensive contacts to nerve terminals (*asterisks*) which contain clear vesicles. Membrane specializations between the endocrine cell and the nerve terminals are not evident. *Scale bar* 1 µm in both panels

assumed (di Sant'Agnese and de Mesy Jensen 1987; Hanyu et al. 1987). Serotonin stimulates smooth muscle contraction in the urethra (Mbaki and Ramage 2008; Fan et al. 2013), but it remains to be determined whether this effect indeed can be evoked by serotonin release from endocrine cells.

Albeit there is no direct evidence for a systemic endocrine function of these cells, the term "endocrine" cells rather than "paracrine" cells is established and widely used. Quite often, they are even called "neuroendocrine" cells, mainly based on the production of serotonin, the presence of large dense core vesicles with chromogranin A and expression of proteins typically found in neurons such as protein gene product 9.5 (Aumüller et al. 2012; Deckmann et al. 2014). It has to be stressed, however, that these markers are often, but not consistently expressed together in solitary flask-like cells in the epithelium. In the human ejaculatory duct, for example, potential neuroendocrine cells are immunoreactive to protein gene product 9.5 but not to chromogranin A while various patterns of coexistence were observed in the prostate (Aumüller et al. 1999). There are currently no published full reports providing evidence that they originate from the neuroectoderm. According to first data published as abstract, those in the prostate might have a mixed origin with some of them deriving from the neural crest (Szczyrba et al. 2014).

The dense core vesicles allow to identifying urethral endocrine cells in the electron microscope without further specific labelling, so that their ultrastructure and their relationship to neighbouring cells are relatively well known. They have extensive, but non-synaptic contact with large nerve endings with numerous vesicles (Fig. 4). Since autonomic efferent nerve fibres have not been seen penetrating the basal lamina and entering the epithelium, these nerve endings are generally considered as sensory (Dixon et al. 1973; Aumüller et al. 2012). Of course, this prompts the speculation that, in addition to possible paracrine effects, neural reflexes might be initiated by serotonin release from neuroendocrine cells, in analogy to nicotinic activation of an urethrovesical reflex via cholinergic brush cells.

The key question yet to be solved, however, is: What are the appropriate stimuli that trigger serotonin and peptide release from urethral endocrine cells? A general assumption is that these cells sense chemical or physicochemical (e.g. pH, osmotic pressure, flow) stimuli from the urethral lumen and respond by basolateral mediator release. In line with this assumption, Fujita has included them into his concept of "receptor-secretory paraneurons" which operates to a large extent with analogies from other organ systems (Fujita et al. 1988). In the gastrointestinal tract, there is a large number of endocrine cell types disseminated in the epithelium which regulate motility, secretion and metabolism. Commonly, they secrete hormones in response to luminal chemical stimuli, and receptors known from oropharyngeal gustation are involved in these chemosensory processes (Margolskee et al. 2007; Breer et al. 2012; Meyer-Gerspach et al. 2014; Latorre et al. 2016). However, this cannot be translated one-to-one to other mucosal surfaces which harbour singly occurring endocrine cells. In human airways, for example, neuroendocrine cells express olfactory rather than taste receptors (Gu et al. 2014), and the receptor repertoire of other endocrine cell populations, including urethral, yet remains to be determined. Thus, it is tempting to assume a chemosensory function of some type for urethral neuroendocrine cells, but despite being known for now 65 years there is still no firm evidence for their function.

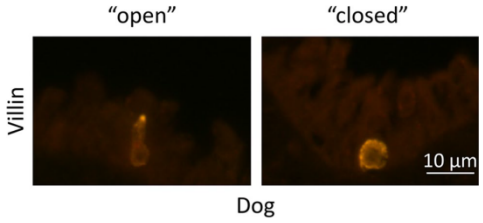

Fig. 5 Dog urethra immunolabelled for villin. In the *left panel*, a connection of the cell to the lumen is seen, which is taken as criterion to classify this cell as "open". Villin-immunoreactivity is particularly prominent at this apical cell pole. In the *right panel*, no connection of the cell to the lumen is seen, which is taken as criterion to classify this cell as "closed"

Open or closed?

In the gastrointestinal epithelium, some endocrine cells clearly reach the lumen with an apical process and are called "open" endocrine cells, whereas, at least judged from light microscopical preparations, others do not have contact to the lumen and are called "closed" endocrine cells (Fujita et al. 1988). This terminology has also been adopted to the urethra where closed neuroendocrine cells appear to dominate numerically (di Sant'Agnese and de Mesy Jensen 1984). It has been hypothesized that urethral neuroendocrine cells of the open and closed type are functionally different with open cells serving as chemosensors and closed cells as mechanosensors (Fujita et al. 1988). The same considerations may apply to cholinergic and non-cholinergic brush cells which also not always have microscopically visible contact to the epithelial surface (Fig. 5) and sometimes appear to be oriented rather horizontally within the epithelial layer (Deckmann et al. 2014).

Electron microscopy revealed bundles of microvilli at the apical cell pole of both endocrine and brush cells that extended into enlarged intercellular spaces or small intraepithelial cavities with unclear connection to the luminal surface (Dixon et al. 1973; Deckmann et al. 2014). It is likely that such cells might have been classified as "closed" when seen in light microscopical preparations. Still, other than typical basal epithelial cells, they have a clear apico-basal polarization since the apical cell area carrying the microvillus bundles is demarcated by occludens junctions between these cells and their neighbours (Dixon et al. 1973; Deckmann et al. 2014). It also has to be considered that, in other pseudostratified epithelia (epididymis, trachea), advanced labelling and imaging methods have revealed that basally located cells, which were traditionally considered as having no contact to the luminal surface, indeed can have extremely thin processes reaching the apical side of the epithelium. Notably, these thin processes were identified as sensors of intraluminal stimuli (Shum et al. 2008). Thus, it might be worth re-evaluating the concept of "closed" endocrine and brush cells.

Conclusion

The last 6 years have seen exciting breakthroughs in the field of chemosensory epithelial cells. In several organ systems, it is now well established that cells previously characterized just structurally utilize canonical taste receptors and signalling cascades for surveillance of the mucosal surface to initiate appropriate defence responses. Just as in classical chemical senses, taste and smell, this chemosensation is designed to detect substances coming from outside rather than monitoring the bodies' internal milieu. Guided by the understanding of these cells as sentinels, they even have been newly discovered at anatomical locations where their presence had been unknown so far, and this includes the urethra. The scenario as known so far suggests the presence of at least three chemosensory cells in the urethral epithelium, i.e. cholinergic brush cells (which might be even subdivided), non-cholinergic brush cells and neuroendocrine cells. The potential implications are enormous and far reaching, as these cells might be involved in monitoring and preventing ascending urinary tract infection and triggering of inappropriate detrusor activity, which might contribute to the common disorder known as overactive bladder, but a clear emphasis has to be put on "potential" implications. The actual number of distinct chemosensory cell types still needs to be finally clarified, as well as their embryological origin, developmental dynamics, receptor equipment, modes of signalling to adjacent nerve fibres and other cells, repertoire of chemo- and cytokines, involvement in pathogenesis of diseases and many other aspects. Thus, although undoubtedly a significant progress has been made, the bulk of work still has to be done.

Funding Our studies reviewed here were supported by the State of Hesse (LOEWE Research Focus *Non-neuronal Cholinergic Systems*).

Compliance with ethical standards

Conflict of interest The authors declare that they have no conflict of interest.

References

Adler E, Hoon MA, Mueller KL, Chandrashekar J, Ryba NJ, Zuker CS (2000) A novel family of mammalian taste receptors. Cell 100(6):693–702

Amorino GP, Parsons SJ (2004) Neuroendocrine cells in prostate cancer. Crit Rev Eukaryot Gene Expr 14(4):287–300. doi:10.1615/CritRevEukaryotGeneExpr.v14.i4.40

Aubron C, Huet O, Ricome S, Borderie D, Pussard E, Leblanc PE, Bouvet O, Vicaut E, Denamur E, Duranteau J (2012) Changes in urine composition after trauma facilitate bacterial growth. BMC Infect Dis 12:330. doi:10.1186/1471-2334-12-330

Aumüller G, Renneberg H, Leonhardt M, Lilja H, Abrahamsson PA (1999) Localization of protein gene product 9.5 immunoreactivity in derivatives of the human Wolffian duct and in prostate cancer. Prostate 38(4):261–267

Aumüller G, Doll A, Wennemuth G, Dizeyi N, Abrahamsson PA, Wilhelm B (2012) Regional distribution of neuroendocrine cells in the urogenital duct system of the male rat. Prostate 72(3):326–337. doi:10.1002/pros.21437

Bachmanov AA, Beauchamp GK (2007) Taste receptor genes. Annu Rev Nutr 27:389–414. doi:10.1146/annurev.nutr.26.061505.111329

Breer H, Eberle J, Frick C, Haid D, Widmayer P (2012) Gastrointestinal chemosensation: chemosensory cells in the alimentary tract. Histochem Cell Biol 138(1):13–24. doi:10.1007/s00418-012-0954-z

Caicedo A, Kim KN, Roper SD (2002) Individual mouse taste cells respond to multiple chemical stimuli. J Physiol 544(Pt 2):501–509

Casanova S, Carrado F, Vignoli G (1974) Endocrine-like cells in the epithelium of the human male urethra. J Submicrol Cytol 6:435–438

Chandrashekar J, Mueller KL, Hoon MA, Adler E, Feng L, Guo W, Zuker CS, Ryba NJ (2000) T2Rs function as bitter taste receptors. Cell 100(6):703–711

Chaudhari N, Roper SD (2010) The cell biology of taste. J Cell Biol 190(3):285–296. doi:10.1083/jcb.201003144

Chromek M (2015) The role of the antimicrobial peptide cathelicidin in renal diseases. Pediatr Nephrol 30(8):1225–1232. doi:10.1007/s00467-014-2895-3

Czaja K, Sienkiewicz W, Vittoria A, Costagliola A, Cecio A (1996) Neuroendocrine cells in the female urogenital tract of the pig, and their immunohistochemical characterization. Acta Anat (Basel) 157(1):11–19

Damak S, Rong M, Yasumatsu K, Kokrashvili Z, Varadarajan V, Zou S, Jiang P, Ninomiya Y, Margolskee RF (2003) Detection of sweet and umami taste in the absence of taste receptor T1r3. Science 301(5634):850–853. doi:10.1126/science.1087155

Deckmann K, Filipski K, Krasteva-Christ G, Fronius M, Althaus M, Rafiq A, Papadakis T, Renno L, Jurastow I, Wessels L, Wolff M, Schütz B, Weihe E, Chubanov V, Gudermann T, Klein J, Bschleipfer T, Kummer W (2014) Bitter triggers acetylcholine release from polymodal urethral chemosensory cells and bladder reflexes. Proc Natl Acad Sci USA 111(22):8287–8292. doi:10.1073/pnas.1402436111

Deckmann K, Krasteva-Christ G, Rafiq A, Herden C, Wichmann J, Knauf S, Nassenstein C, Grevelding CG, Dorresteijn A, Chubanov V, Gudermann T, Bschleipfer T, Kummer W (2015) Cholinergic urethral brush cells are widespread throughout placental mammals. Int Immunopharmacol 29(1):51–56. doi:10.1016/j.intimp.2015.05.038

di Sant'Agnese PA, De Mesy Jensen KL (1984) Endocrine-paracrine cells of the prostate and prostatic urethra: an ultrastructural study. Hum Pathol 15(11):1034–1041

di Sant'Agnese PA, de Mesy Jensen KL (1987) Endocrine-paracrine (APUD) cells of the human female urethra and paraurethral ducts. J Urol 137(6):1250–1254

Dixon JS, Gosling JA, Ramsdale DR (1973) Urethral chromaffin cells. A light and electron microscopic study. Z Zellforsch Mikrosk Anat 138(3):397–406

Dorff TB, Liu SV, Xiong S, Cai J, Hawes D, Pinski J (2011) Ethnic differences in neuroendocrine expression in prostate cancer tissue. Anticancer Res 31(11):3897–3901

Fan WJ, Li YT, Chen JJ, Chen SC, Lin YS, Kou YR, Peng CW (2013) Sexually dimorphic urethral activity in response to pharmacological activation of 5-HT1A receptors in the rat. Am J Physiol Renal Physiol 305(9):F1332–F1342. doi:10.1152/ajprenal.00261.2013

Fetissof F, Dubois MP, Arbeille-Brassart B, Lanson Y, Boivin F, Jobard P (1983) Endocrine cells in the prostate gland, urothelium and Brenner tumors. Immunohistological and ultrastructural studies. Virchows Arch B Cell Pathol Incl Mol Pathol 42(1):53–64

Feyrter F (1951a) Über das urogenitale Helle-Zellen-System des Menschen. Z Mikrosk Anat Forsch 57(3):324–344

Feyrter F (1951b) Zur Pathologie des urogenitalen Helle-Zellen-Systems. Virchows Arch Pathol Anat Physiol Klin Med 320(6):564–576

Finger TE, Kinnamon SC (2011) Taste isn't just for taste buds anymore. F1000 Biol Rep 3:20. doi:10.3410/B3-20

Finger TE, Bottger B, Hansen A, Anderson KT, Alimohammadi H, Silver WL (2003) Solitary chemoreceptor cells in the nasal cavity serve as sentinels of respiration. Proc Natl Acad Sci USA 100(15):8981–8986. doi:10.1073/pnas.1531172100

Finger TE, Danilova V, Barrows J, Bartel DL, Vigers AJ, Stone L, Hellekant G, Kinnamon SC (2005) ATP signaling is crucial for communication from taste buds to gustatory nerves. Science 310(5753):1495–1499. doi:10.1126/science.1118435

Foxman B (2010) The epidemiology of urinary tract infection. Nat Rev Urol 7(12):653–660. doi:10.1038/nrurol.2010.190

Fujita T, Kanno T, Kobayashi S (1988) The paraneuron. Springer, Heidelberg

Gerbe F, Sidot E, Smyth DJ, Ohmoto M, Matsumoto I, Dardalhon V, Cesses P, Garnier L, Pouzolles M, Brulin B, Bruschi M, Harcus Y, Zimmermann VS, Taylor N, Maizels RM, Jay P (2016) Intestinal epithelial tuft cells initiate type 2 mucosal immunity to helminth parasites. Nature 14; 529(7585):226–230. doi: 10.1038/nature16527

Gilbertson TA, Boughter JD Jr, Zhang H, Smith DV (2001) Distribution of gustatory sensitivities in rat taste cells: whole-cell responses to apical chemical stimulation. J Neurosci 21(13):4931–4941

Glendinning JI, Bloom LD, Onishi M, Zheng KH, Damak S, Margolskee RF, Spector AC (2005) Contribution of alpha-gustducin to taste-guided licking responses of mice. Chem Senses 30(4):299–316. doi:10.1093/chemse/bji025

Gu X, Karp PH, Brody SL, Pierce RA, Welsh MJ, Holtzman MJ, Ben-Shahar Y (2014) Chemosensory functions for pulmonary neuroendocrine cells. Am J Respir Cell Mol Biol 50(3):637–646. doi:10.1165/rcmb.2013-0199OC

Gulbransen BD, Clapp TR, Finger TE, Kinnamon SC (2008) Nasal solitary chemoreceptor cell responses to bitter and trigeminal stimulants in vitro. J Neurophysiol 99(6):2929–2937. doi:10.1152/jn.00066.2008

Hakanson R, Larsson LI, Sjoberg NO, Sundler F (1974) Amine-producing endocrine-like cells in the epithelium of urethra and prostate of the guinea-pig. A chemical, fluorescence histochemical, and electron microscopic study. Histochemie 38(3):259–270

Hansen A, Finger TE (2008) Is TrpM5 a reliable marker for chemosensory cells? Multiple types of microvillous cells in the main olfactory epithelium of mice. BMC Neurosci 9:115. doi:10.1186/1471-2202-9-115

Hanyu S, Iwanaga T, Kano K, Fujita T (1987) Distribution of serotonin-immunoreactive paraneurons in the lower urinary tract of dogs. Am J Anat 180(4):349–356. doi:10.1002/aja.1001800405

Heinrich E, Trojan L, Friedrich D, Voss M, Weiss C, Michel MS, Grobholz R (2011) Neuroendocrine tumor cells in prostate

cancer: evaluation of the neurosecretory products serotonin, bombesin, and gastrin—impact on angiogenesis and clinical follow-up. Prostate 71(16):1752–1758. doi:10.1002/pros.21392
Höfer D, Drenckhahn D (1992) Identification of brush cells in the alimentary and respiratory system by antibodies to villin and fimbrin. Histochemistry 98(4):237–242
Höfer D, Drenckhahn D (1996) Cytoskeletal markers allowing discrimination between brush cells and other epithelial cells of the gut including enteroendocrine cells. Histochem Cell Biol 105(5):405–412
Höfer D, Püschel B, Drenckhahn D (1996) Taste receptor-like cells in the rat gut identified by expression of alpha-gustducin. Proc Natl Acad Sci USA 93(13):6631–6634
Holstein AF, Davidoff MS, Breucker H, Countouris N, Orlandini G (1991) Different epithelia in the distal human male urethra. Cell Tissue Res 264(1):23–32
Howitt MR, Lavoie S, Michaud M, Blum AM, Tran SV, Weinstock JV, Gallini CA, Redding K, Margolskee RF, Osborne LC, Artis D, Garrett WS (2016) Tuft cells, taste-chemosensory cells, orchestrate parasite type 2 immunity in the gut. Science 351(6279):1329–1333. doi:10.1126/science.aaf1648
Huang YJ, Maruyama Y, Dvoryanchikov G, Pereira E, Chaudhari N, Roper SD (2007) The role of pannexin 1 hemichannels in ATP release and cell-cell communication in mouse taste buds. Proc Natl Acad Sci USA 104(15):6436–6441. doi:10.1073/pnas.0611280104
Isomaki AM (1973) A new cell type (tuft cell) in the gastrointestinal mucosa of the rat. A transmission and scanning electron microscopic study. Acta Pathol Microbiol Scand A: Suppl 240:1–35
Kim MR, Kusakabe Y, Miura H, Shindo Y, Ninomiya Y, Hino A (2003) Regional expression patterns of taste receptors and gustducin in the mouse tongue. Biochem Biophys Res Commun 312(2):500–506
Krasteva G, Kummer W (2012) "Tasting" the airway lining fluid. Histochem Cell Biol 138(3):365–383. doi:10.1007/s00418-012-0993-5
Krasteva G, Canning BJ, Hartmann P, Veres TZ, Papadakis T, Mühlfeld C, Schliecker K, Tallini YN, Braun A, Hackstein H, Baal N, Weihe E, Schütz B, Kotlikoff M, Ibanez-Tallon I, Kummer W (2011) Cholinergic chemosensory cells in the trachea regulate breathing. Proc Natl Acad Sci USA 108(23):9478–9483. doi:10.1073/pnas.1019418108
Krasteva G, Canning BJ, Papadakis T, Kummer W (2012a) Cholinergic brush cells in the trachea mediate respiratory responses to quorum sensing molecules. Life Sci 91(21–22):992–996. doi:10.1016/j.lfs.2012.06.014
Krasteva G, Hartmann P, Papadakis T, Bodenbenner M, Wessels L, Weihe E, Schütz B, Langheinrich AC, Chubanov V, Gudermann T, Ibanez-Tallon I, Kummer W (2012b) Cholinergic chemosensory cells in the auditory tube. Histochem Cell Biol 137(4):483–497. doi:10.1007/s00418-012-0911-x
Kunin CM, Evans C, Bartholomew D, Bates DG (2002) The antimicrobial defense mechanism of the female urethra: a reassessment. J Urol 168(2):413–419
Latorre R, Huynh J, Mazzoni M, Gupta A, Bonora E, Clavenzani P, Chang L, Mayer EA, De Giorgio R, Sternini C (2016) Expression of the bitter taste receptor, T2R38, in enteroendocrine cells of the colonic mucosa of overweight/obese vs. lean subjects. PLoS One 11(2):e0147468. doi:10.1371/journal.pone.0147468.eCollection2016
Lee RJ, Cohen NA (2014) Sinonasal solitary chemosensory cells "taste" the upper respiratory environment to regulate innate immunity. Am J Rhinol Allergy 28(5):366–373. doi:10.2500/ajra.2014.28.4077
Lee RJ, Xiong G, Kofonow JM, Chen B, Lysenko A, Jiang P, Abraham V, Doghramji L, Adappa ND, Palmer JN, Kennedy DW, Beauchamp GK, Doulias PT, Ischiropoulos H, Kreindler JL, Reed DR, Cohen NA (2012) T2R38 taste receptor polymorphisms underlie susceptibility to upper respiratory infection. J Clin Invest 122(11):4145–4159. doi:10.1172/JCI64240
Lee RJ, Kofonow JM, Rosen PL, Siebert AP, Chen B, Doghramji L, Xiong G, Adappa ND, Palmer JN, Kennedy DW, Kreindler JL, Margolskee RF, Cohen NA (2014) Bitter and sweet taste receptors regulate human upper respiratory innate immunity. J Clin Invest 124(3):1393–1405. doi:10.1172/JCI72094
Lin W, Ogura T, Margolskee RF, Finger TE, Restrepo D (2008) TRPM5-expressing solitary chemosensory cells respond to odorous irritants. J Neurophysiol 99(3):1451–1460. doi:10.1152/jn.01195.2007
Lindemann B (2001) Receptors and transduction in taste. Nature 413(6852):219–225. doi:10.1038/35093032
Luciano L, Reale E (1979) A new morphological aspect of the brush cells of the mouse gallbladder epithelium. Cell Tissue Res 201(1):37–44
Luciano L, Reale E (1990) Brush cells of the mouse gallbladder. A correlative light- and electron-microscopical study. Cell Tissue Res 262(2):339–349
Luciano L, Castellucci M, Reale E (1981) The brush cells of the common bile duct of the rat. This section, freeze-fracture and scanning electron microscopy. Cell Tissue Res 218(2):403–420
Maddison DR, Schulz KS (2007) (eds) The tree of life web project. http://tolweb.org
Maillet EL, Cui M, Jiang P, Mezei M, Hecht E, Quijada J, Margolskee RF, Osman R, Max M (2015) Characterization of the binding site of aspartame in the human sweet taste receptor. Chem Senses 40(8):577–586. doi:10.1093/chemse/bjv045
Margolskee RF, Dyer J, Kokrashvili Z, Salmon KS, Ilegems E, Daly K, Maillet EL, Ninomiya Y, Mosinger B, Shirazi-Beechey SP (2007) T1R3 and gustducin in gut sense sugars to regulate expression of Na+-glucose cotransporter 1. Proc Natl Acad Sci USA 104(38):15075–15080. doi:10.1073/pnas.0706678104
Matsunami H, Montmayeur JP, Buck LB (2000) A family of candidate taste receptors in human and mouse. Nature 404(6778):601–604. doi:10.1038/35007072
Mbaki Y, Ramage AG (2008) Investigation of the role of 5-HT2 receptor subtypes in the control of the bladder and the urethra in the anaesthetized female rat. Br J Pharmacol 155(3):343–356. doi:10.1038/bjp.2008.273
McLaughlin SK, McKinnon PJ, Margolskee RF (1992) Gustducin is a taste-cell-specific G protein closely related to the transducins. Nature 357(6379):563–569. doi:10.1038/357563a0
Meyer-Gerspach AC, Wolnerhanssen B, Beglinger C (2014) Gut sweet taste receptors and their role in metabolism. Front Horm Res 42:123–133. doi:10.1159/000358321
Monteiro-Riviere NA, Popp JA (1984) Ultrastructural characterization of the nasal respiratory epithelium in the rat. Am J Anat 169(1):31–43. doi:10.1002/aja.1001690103
Nelson G, Hoon MA, Chandrashekar J, Zhang Y, Ryba NJ, Zuker CS (2001) Mammalian sweet taste receptors. Cell 106(3):381–390
Nelson G, Chandrashekar J, Hoon MA, Feng L, Zhao G, Ryba NJ, Zuker CS (2002) An amino-acid taste receptor. Nature 416(6877):199–202. doi:10.1038/nature726
Ogura T, Krosnowski K, Zhang L, Bekkerman M, Lin W (2010) Chemoreception regulates chemical access to mouse vomeronasal organ: role of solitary chemosensory cells. PLoS One 5(7):e11924. doi:10.1371/journal.pone.0011924
Ogura T, Szebenyi SA, Krosnowski K, Sathyanesan A, Jackson J, Lin W (2011) Cholinergic microvillous cells in the mouse main olfactory epithelium and effect of acetylcholine on olfactory sensory neurons and supporting cells. J Neurophysiol 106(3):1274–1287. doi:10.1152/jn.00186.2011
Ohmoto M, Matsumoto I, Yasuoka A, Yoshihara Y, Abe K (2008) Genetic tracing of the gustatory and trigeminal neural pathways

originating from T1R3-expressing taste receptor cells and solitary chemoreceptor cells. Mol Cell Neurosci 38(4):505–517. doi:10.1016/j.mcn.2008.04.011

Parr MB, Ren HP, Russell LD, Prins GS, Parr EL (1992) Urethral glands of the male mouse contain secretory component and immunoglobulin A plasma cells and are targets of testosterone. Biol Reprod 47(6):1031–1039

Pearson MM, Yep A, Smith SN, Mobley HL (2011) Transcriptome of Proteus mirabilis in the murine urinary tract: virulence and nitrogen assimilation gene expression. Infect Immun 79(7):2619–2631. doi:10.1128/IAI.05152-11

Polisetti S, Baig NF, Morales-Soto N, Shrout JD, Bohn PW (2016) Spatial mapping of pyocyanin in pseudomonas aeruginosa bacterial communities using surface enhanced raman scattering. Appl Spectrosc. doi:10.1177/0003702816654167

Porter E, Yang H, Yavagal S, Preza GC, Murillo O, Lima H, Greene S, Mahoozi L, Klein-Patel M, Diamond G, Gulati S, Ganz T, Rice PA, Quayle AJ (2005) Distinct defensin profiles in Neisseria gonorrhoeae and Chlamydia trachomatis urethritis reveal novel epithelial cell-neutrophil interactions. Infect Immun 73(8):4823–4833

Rhodin J, Dalhamn T (1956) Electron microscopy of the tracheal ciliated mucosa in rat. Z Zellforsch Mikrosk Anat 44(4):345–412

Roper SD (2013) Taste buds as peripheral chemosensory processors. Semin Cell Dev Biol 24(1):71–79. doi:10.1016/j.semcdb.2012.12.002

Roper SD (2015) The taste of table salt. Pflugers Arch 467(3):457–463. doi:10.1007/s00424-014-1683

Saunders CJ, Christensen M, Finger TE, Tizzano M (2014) Cholinergic neurotransmission links solitary chemosensory cells to nasal inflammation. Proc Natl Acad Sci USA 111(16):6075–6080. doi:10.1073/pnas.1402251111

Sbarbati A, Osculati F (2006) Allelochemical communication in vertebrates: kairomones, allomones and synomones. Cells Tissues Organs 183(4):206–219. doi:10.1159/000096511

Schütz B, Jurastow I, Bader S, Ringer C, von Engelhardt J, Chubanov V, Gudermann T, Diener M, Kummer W, Krasteva-Christ G, Weihe E (2015) Chemical coding and chemosensory properties of cholinergic brush cells in the mouse gastrointestinal and biliary tract. Front Physiol 6:87. doi:10.3389/fphys.2015.00087

Shum WW, Da Silva N, McKee M, Smith PJ, Brown D, Breton S (2008) Transepithelial projections from basal cells are luminal sensors in pseudostratified epithelia. Cell 135(6):1108–1117. doi:10.1016/j.cell.2008.10.020

Szczyrba J, Niesen A, Wagner M, Wandernoth P, Aumüller G., Wennemuth G (2014) A subset of neuroendocrine cells of the prostate derives from the neural crest. 109th Annual Meeting of the Anatomische Gesellschaft, Salzburg. doi:10.13140/2.1.3502.9765

Taruno A, Vingtdeux V, Ohmoto M, Ma Z, Dvoryanchikov G, Li A, Adrien L, Zhao H, Leung S, Abernethy M, Koppel J, Davies P, Civan MM, Chaudhari N, Matsumoto I, Hellekant G, Tordoff MG, Marambaud P, Foskett JK (2013) CALHM1 ion channel mediates purinergic neurotransmission of sweet, bitter and umami tastes. Nature 495(7440):223–226. doi:10.1038/nature11906

Tizzano M, Dvoryanchikov G, Barrows JK, Kim S, Chaudhari N, Finger TE (2008) Expression of Galpha14 in sweet-transducing taste cells of the posterior tongue. BMC Neurosci 9:110. doi:10.1186/1471-2202-9-110

Tizzano M, Gulbransen BD, Vandenbeuch A, Clapp TR, Herman JP, Sibhatu HM, Churchill ME, Silver WL, Kinnamon SC, Finger TE (2010) Nasal chemosensory cells use bitter taste signaling to detect irritants and bacterial signals. Proc Natl Acad Sci USA 107(7):3210–3215. doi:10.1073/pnas.0911934107

Tomchik SM, Berg S, Kim JW, Chaudhari N, Roper SD (2007) Breadth of tuning and taste coding in mammalian taste buds. J Neurosci 27(40):10840–10848. doi:10.1523/JNEUROSCI.1863-07.2007

Vandenbeuch A, Anderson CB, Kinnamon SC (2015) Mice lacking pannexin 1 release ATP and respond normally to all taste qualities. Chem Senses 40(7):461–467. doi:10.1093/chemse/bjv034

Vittoria A, Cocca T, La Mura E, Cecio A (1992) Immunocytochemistry of paraneurons in the female urethra of the horse, cattle, sheep, and pig. Anat Rec 233(1):18–24. doi:10.1002/ar.1092330104

von Moltke J, Ji M, Liang HE, Locksley RM (2016) Tuft-cell-derived IL-25 regulates an intestinal ILC2-epithelial response circuit. Nature 529(7585):221–225. doi:10.1038/nature16161

Wagenlehner FM, Cek M, Naber KG, Kiyota H, Bjerklund-Johansen TE (2012) Epidemiology, treatment and prevention of healthcare-associated urinary tract infections. World J Urol 30(1):59–67. doi:10.1007/s00345-011-0757-1

Weyrauch KD, Schnorr B (1976) Die Feinstruktur des Epithels des Ductus pancreaticus major des Schafes. Acta Anat 96:232–247

Xu Z, Islam S, Wood TK, Huang Z (2015) An integrated modeling and experimental approach to study the influence of environmental nutrients on biofilm formation of pseudomonas aeruginosa. Biomed Res Int. 2015:506782. doi:10.1155/2015/506782

Zhang Y, Hoon MA, Chandrashekar J, Mueller KL, Cook B, Wu D, Zuker CS, Ryba NJ (2003) Coding of sweet, bitter, and umami tastes: different receptor cells sharing similar signaling pathways. Cell 112(3):293–301

Zhao GQ, Zhang Y, Hoon MA, Chandrashekar J, Erlenbach I, Ryba NJ, Zuker CS (2003) The receptors for mammalian sweet and umami taste. Cell 115(3):255–266

Aus Lizenzgrüden ist dieser Artikel hier nicht enthalten:

REVIEW

Brush cells, the newly identified gatekeepers of the urinary tract

Wolfgang Kummer and Klaus Deckmann

Kummer, Wolfgang; Deckmann, Klaus. Brush cells, the newly identified gatekeepers of the urinary tract. Current Opinion in Urology 27(2):p 85-92, March 2017. DOI: 10.1097/MOU.0000000000000361

8 Eidesstattliche Erklärung

Ich erkläre hiermit an Eides statt, dass ich die vorliegende Habilitationsschrift über „**Die Entdeckung und Charakterisierung der urethralen cholinergen chemosensorischen Zelle“** selbständig angefertigt und mich anderer Hilfsmittel als der in ihr angegebenen nicht bedient habe, insbesondere, dass alle Entlehnungen aus anderen Schriften mit Angabe der betreffenden Schrift gekennzeichnet sind.

Ich versichere, nicht die Hilfe einer kommerziellen Habilitations- oder Promotionsvermittlung in Anspruch genommen zu haben.

Gießen, den 13. Dezember 2021

_____

Klaus Deckmann

9 Danksagung

Die Grundlage der vorliegenden Arbeit wurde von Januar 2012 bis Dezember 2021 am Institut für Anatomie und Zellbiologie der Justus-Liebig-Universität Gießen angefertigt.

Mein ganz besonderer Dank gilt Herrn Prof. Wolfgang Kummer für die sehr gute Unterstützung und Betreuung während meiner Habilitation.
Außerdem danke ich meiner ganzen Arbeitsgruppe für die sehr gute Zusammenarbeit. Hierbei ist insbesondere Herr Martin Bodenbenner-Türich, Frau Tamara Papadakis, Frau Silke Wiegand und Frau Theresa Eiffert zu danken.
Ich möchte auch Frau Prof. Gabriela Krasteva-Christ und Frau Dr. Katharina Filipski für die Vorarbeiten dieser Arbeit danken.
Ich danke auch Herrn Prof. Thomas Bschleipfer.
Des Weiteren bedanke ich mich bei Frau Chrissy Kandel, Frau Patricia Schmidt und Herrn Alexander Perniss, die zum Gelingen dieser Arbeit maßgeblich beigetragen haben.
Bei allen Kooperationspartnern möchte ich mich für die erfolgreiche Zusammenarbeit bedanken.
Nicht zuletzt möchte ich mich bei allen Mitarbeitern unseres Instituts für das angenehme Arbeitsklima und die gegenseitige Unterstützung bedanken.

Außerdem gilt mein Dank meiner Frau Désirée, meinem Sohn Lukas, meinem Hund Junior und meinen Eltern für alles was sie für mich getan haben.

DANKE.